University of Ljubljana
Faculty of Health Sciences

5TH 2021 SOCRATIC LECTURES

SOCRATIC LECTURES

5TH INTERNATIONAL MINISYMPOSIUM, LJUBLJANA, 16. APRIL 2021

PEER REVIEWED PROCEEDINGS

EDITED BY: VERONIKA KRALJ-IGLIČ

FACULTY OF HEALTH SCIENCES, UNIVERSITY OF LJUBLJANA

Socratic lectures
5th International Minisymposium, Ljubljana, April 16., 2021
Peer Reviewed Proceedings
Edited by Prof. Veronika Kralj-Iglič, Ph.D.
Reviewers: Prof. Rok Vengust, M.D., Ph.D., Karin Schara, M.D., Ph. D.
Published by: University of Ljubljana, Faculty of Health Sciences
Design and photos: Anna Romolo, Matevž Tomaževič, Veronika Kralj-Iglič
Image on the front page: Matevž Tomaževič

Publication is available online in PDF format at:
https://www.zf.uni-lj.si/images/stories/datoteke/Zalozba/Sokratska_5.pdf

Ljubljana, 2021

Kataložni zapis o publikaciji (CIP) pripravili v Narodni in univerzitetni knjižnici v Ljubljani
COBISS.SI-ID 69120259
ISBN 978-961-7112-05-4 (PDF)

The members of the Organizing Committee of Socratic Lectures: Kralj Iglič Veronika, Vauhnik Renata, Stražar Klemen, Kristan Anže, Prelovšek Anita

Program

Socratic Symposium April 16, 2021, 16:00 – 20:00 (Ljubljana time)

Plenary lecture

16:00 – 16:45 Soeballe Kjeld, Aarhus University Hospital, Aarhus, Denmark: Surgical treatment of acetabular dysplasia

16:45 –16:50 Weiss Silvius Leopold: Fantasia. Guitar: **Masi Giovanni**

16:50 - 17:00 Break

Parallel Sections

Section 1: Emergent Problems in Orthopaedics and Traumatology

organized and moderated by **Stražar Klemen** and **Kristan Anže**, University Medical Centre Ljubljana, Ljubljana, Slovenia

17:00-17:25 Spasovski Duško, Banjica Clinics, Belgrade, Serbia: Operative treatment of hip dysplasia

17:25-17:50 Skala-Rosenbaum Jiri, University Medical Centre Prague, Czech Republik: Femur malrotation after trochanteric fracture: incedence and concequences

17:50-18:15 Stražar Klemen, University Medical Centre Ljubljana, Ljubljana, Slovenia: Limits of hip arthroscopy

18:15-18.20 Break

18:20-18:45 Atul Kamath, Cleveland Clinic, Cleveland, U.S.A., Role of hip preservation in 2021

18:45-18.55 Kristan Anže, University Medical Centre Ljubljana, Ljubljana, Slovenia, Influence of implant placement and of reduction of trochanteric fractures type A2 on mobility of the patient after healing of the fracture and on probability of mechanical failures

18:55-19:05 Šarler Taras, University Medical Centre Ljubljana, Ljubljana, Slovenia, Anatomic and kinematic planning of arthroscopic femoroacetabular osteoplasty

19:05-19:15 Jug Marko, University Medical Centre Ljubljana, Ljubljana, Slovenia, Spinal cord injury and decompression- a question of time and pressure

19:15-19:25 Ambrožič Miha, Kovačič Ladislav: University Medical Centre Ljubljana, Ljubljana, Slovenia, Platelet-rich plasma injection following arthroscopic rotator cuff repair - Is there any benefit?

19:25-19:35 Tomaževič Matevž, University Medical Centre Ljubljana, Ljubljana, Slovenia, The effect of stress distribution in artificial hip joint on the dislocation of the hip endoprosthesis

19:35-19:45 Zore Anderj Lenart, University Medical Centre Ljubljana, Ljubljana, Slovenia, Computer assistance in periacetabular osteotomy

Section 2: Emergent Problems in Physiotherapy

organized and moderated by **Vauhnik Renata** and **Rugelj Darja**, University of Ljubljana, Faculty of Health Sciences

17:00-17:30 Daniel Munoz Garcia, University La Salle, Madrid, Spain, Prior cortical activity differences during an action observation plus motor imagery task related to motor performance of a coordinated multi-lmb complex task.

17:30-18:00 Alon Wolf, Technion, Israel Institute of Technology, Faculty of Mechanical Engineering, Haifa, Israel, Biomechanics: When science and engineering meet sport

18:00-18:30 Carmen Belen Martinez Cepa, Juan Carlos Zuil Escobar, Rocio Palomo, University CEU San Pablo, Madrid, Spain, Action observation therapy combined with mirror therapy in children with unilateral cerebral palsy: randomized controlled trial protocol and feasibility study

18:30 - 18:45 Darja Rugelj, University of Ljubljana, Faculty of Health Sciences, Ljubljana, Slovenia: Postural sway on inclined surfaces

18:45-19:00 Renata Vauhnik, University of Ljubljana, Faculty of Health Sciences, Ljubljana, Slovenia: Can we decrease knee anterior laxity?

19:00-19:15 Marko Vidovič, University of Ljubljana, Faculty of Health Sciences, Ljubljana, Slovenia: Increasing hand dexterity through the use of various somatosensory stimuli such as vibration, electrical stimulation, and textured materials

19:15-19:30 Helena Žunko, University of Ljubljana, Faculty of Health Sciences, Ljubljana, Slovenia: Ankle dorisflexion range of motion measurement tools

19:30-19:45 Maja Petrič, University of Ljubljana, Faculty of Health Sciences, Ljubljana, Slovenia: The effect of yoga and stabilization exercises on trunk muscle endurance and flexibility in healthy adults

Section 3: Free topics

organized and moderated by **Prelovšek Anita**

17:00-17:45 Muršič Rajko, University of Ljubljana, Faculty of Philosophy, Ljubljana, Slovenia: Creativity and music - essential elements in human development

17:45-18:45 Paliska Nelfi, Music School Koper, Koper, Slovenia, Mozart's travels to Italy

18:45-19:15 Gala Kušej Nina, Protocol of Republic of Slovenia, Music and protocol

19:15-19:30 Pečan Irenej, Jeran Marko, University of Ljubljana, Faculty of Health Sciences, Ljubljana, Slovenia: Step into the Future by Bauman Moscow State Technical University & Russian Youth Engineering Society.

19:30 - 19:45 Ipavec Marija, Government of Republic of Slovenia, 42 years of experience with above-knee prosthesis.

20:00 Closing Ceremony with Cultural program.

Chopin Frederic: Variations on the theme by Giaccomo Rossini; flute: **Prelovšek Anita**

Editorial

In the academic year 2020/2021 the Socratic Lectures were organized twice: in December, with co-production of the Ves4us consortium, and in April. This was a reflection of the decision of the Medical Faculty to reorganize the performance of the optional courses into the "package" form, to be completed in November or in June. The course "Biomechanics of joints" was completed in the first semester and as the Socratic Lectures have always been the final event of the course, the symposium was organized in December 2020. The original timing of the course Special biomechanics for students of the 1st year of Orthotics and Prosthetics at the Faculty of Health Sciences remained the same (February –April) and ended with Socratic Lectures as the final event in April.

The online form of the symposium enabled participation of world top professionals and scientists. Following the inspiring plenary lecture given by prof. Kjeld Soeballe from Aarhus University Hospital, Aarhus, Denmark**,** the symposium featured tree sections: Emergent problems in Orthopaedics and Traumatology, Emergent problems in Physiotherapy and Free topics. The members of the organizing committee were prof. Veronika Kralj-Iglič, prof. Klemen Stražar, prof. Anže Kristan, prof. Renata Vauhnik, prof. Darja Rugelj and dr. Anita Prelovšek. Cultural program was performed by dr. Anita Prelovšek on the flute and by Giovanni Masi on the guitar.

Anita Prelovšek, PhD, studied flute in Ljubljana, Slovenia and in Trieste, Italy and finished postgraduate studies in France. She is a free-lance artist and performs worldwide. Also she completed postgraduate study of Musicology at the University of Ljubljana, Faculty of Philosophy. Her choice in Socratic Lectures was Variations on a Theme of Rossini in E major for flute by Frederic Chopin.

Giovanni Masi (2002) studied guitar at the musical high school P.E. Imbriani, Avellino, Italy under the guidance of Mº Gianluca Allocca and currently attends the specialized guitar course at the D. Cimarosa Conservatory, Avellino, under the guidance of Mº Lucio Matarazzo. He is performing publicly since he was 14 years old and has won over 20 national and international competitions. At Socratic Lectures he performed Fantasia by Silvius Leopold Weiss (1687-1750).

An addition to the present issue were photographs taken by Matevž Tomaževič in Namibia shortly after the symposium. He participated at the symposium with a contribution which was a subject of his PhD that took place a day before the symposium.

The April Socratic Lectures was a meaningful event that will remain in the memories of the participants (the joint section was attended by approximately 120 participants), in particular the students.

Veronika Kralj-Iglič, Anna Romolo

Contents


5TH
2021
SOCRATIC
LECTURES

Research

How can we influence the mobility of the patients and probability of mechanical failures in trochanteric fractures type A2?

Kristan Anže*
Department of Traumatology, University Medical Centre Ljubljana, Ljubljana, Slovenia
*anze.kristan@kclj.si

Abstract
In the first part of this paper, we are discussing the influence of reduction and implant placement on position of the healed trochanteric fracture AO/OTA A2 and how it influences the walking ability after healing. In the second part we are analysing factors which can be influenced during the surgery and can lead to mechanical failure and reoperation in these fractures.

1. Introduction

Fracture of the proximal femur in elderly patients can be a devastating event which might lead to disability and even death. Half of elderly patients can regain preinjury walking ability, and level of returning to preinjury activities is between 60 and 70%. The functional outcome is multifactorial, and it is not related just to operative technique, however failure of internal fixation guarantees poor outcome [1,2].

The position of the trochanteric fracture after healing is related to intraoperative reduction and placement of the implants. Some authors have proposed non-anatomical reduction with the position of proximal fragment more medial and anterior to the shaft to prevent excessive secondary movements caused by typical posteromedial comminution [3].

Mechanical failure of osteosynthesis in trochanteric fractures is present in up to 30 % of the cases. It is influenced by fracture type, fracture geometry, age of the patient, fracture reduction, placement of the implant, bone quality etc. [4,5].

The goals of our study were to analyse the surgery-related factors that lead to mechanical failures and to determine what is the influence of position of united fracture on functional outcome.

2. Patients and methods

We retrospectively reviewed patients which were treated in our institution in one year period for trochanteric fractures AO 31 A2. All patients were operated with sliding hip screw (DHS; DePuy Synthes) or intramedullary nail for proximal femur (PFNA; DePuy Synthes).

In given period, 176 patients met the inclusion criteria. After strict exclusion criteria we included 92 patients in the study.

Basic patient's characteristic (gender, age, ASA score, mobility) before the injury and on last follow up were extracted from medical documentation.

On the plain radiographs of the pelvis and hips in two standard radiographic views (AP and lateral) on the first postoperative day (before starting physiotherapy) and on the last follow up we evaluated: degree of osteoporosis on the contralateral femoral neck region (according to Singh index (SI) from 1 (no osteoporosis) to 6 (severe osteoporosis)); the position of the fracture (according to anterior cortical support (ACS) in lateral view, medial cortical support (MCS) in AP (according to Chang criteria [3]), and neck – shaft angle (NSA)) (**Table 1, Figure 1**); the quality of fixation - implant placement (tip to apex distance (TAD) and Parker index; mechanical failure (cut-out, breakage of the fixation material, neck – shaft collapsed for more than 10^{o} and main proximal fragments slided for more than 10 mm).

In first part of the study the groups were divided according to the position of proximal fragment after six months. In group A the patients had all tested reduction parameters (NSA, MCS, ACS) in satisfying position (anatomical or positive) and in group B patients had at least on parameter rated considered as unsatisfactory (negative). In the second part the patients were divided in the groups according to absence (group A) or presence of fixation failure (group B).

Table 1. Reduction criteria according to Chang.

reduction parameter	anatomical	positive	negative
NSA	125° – 137°	> 137°	< 125°
MCS	anatomical	medial to the shaft	lateral to the shaft
ACS	anatomical	anterior to the shaft	posterior to the shaft

NSA: neck-shaft angle, MCS: medial cortical support, ACS: anterior cortical support.

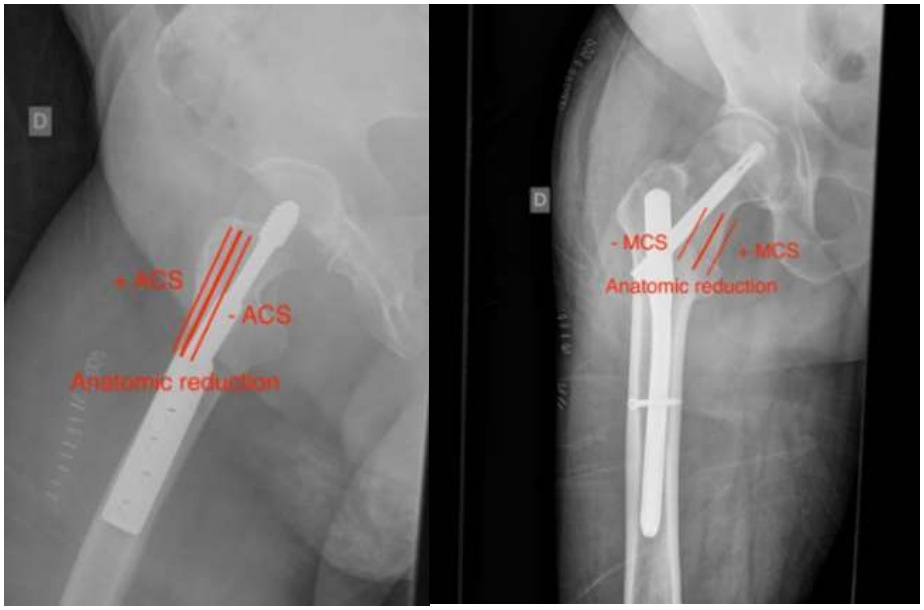

Figure 1. Reduction criteria according to Chang. If proximal fragment is anteriorly to the shaft, ACS it is positive (+ACS), if it is posteriorly to the shaft, ACS is negative (-ACS). If proximal fragment is medial to the shaft, MCS is positive (+MCS) if it is lateral to the shaft, MCS is negative (-MCS).

3. Results

In first part we divided our patients in two groups according to position of united fractures (Group A – good position; group B – unsatisfying). We had equal number of patients in both groups (46). They did not differ in basic patients' characteristics, degree of osteoporosis, type of implant used or placement.

The only significant difference was in reduction parameters during the surgery, which got worse during the healing (**Table 2**).

Table 2. Comparison of groups A and B in reduction parameters after the surgery and six months later (in statistical probability of the t-test pertaining to the difference between the groups)

reduction	A vs. B (op)	A vs. B (6m)	A (op) vs. A (6m)	B (op) vs. B (6m)
NSA	0.074	0.003	0.290	0.719
MCS	0.057	< 0.001	0.014	0.002
ACS	0.001	< 0.001	0.076	0.435

A: group A, B: group B, op: immediately after the surgery, 6m: six months after the surgery, NSA: neck-shaft angle, MCS: medial cortical support, ACS: anterior cortical support.

These differences influence the mobility level after healing. In both groups the mobility was worse after the healing of the fracture comparing to the preinjury level. But in group B the difference was bigger. (**Table 3**) [6]. We found statistically significant difference in mobility between Group A and Group B determined 6 months after the surgery (p = 0.029).

Table 3. Comparing mobility level before injury and six months after the surgery for groups A and B.

mobility	Group A n (%)	Group A 6m n (%)	p	Group B n (%)	Group B 6m n (%)	p
no assistance	31 (67.4%)	16 (34.8%)		25 (54.3%)	5 (10.9%)	
assistance	15 (32.6%)	28 (60.8%)	0.006	21 (45.7%)	37 (80.4)	<0,001
wheelchair	0 (0%)	2 (4.4%)		0 (0%)	4 (8.7%)	

n: number of patients, p: p-value - statistical probability, op: postoperatively, 6m: six months after the surgery

In the second part of the study, we compared patients with mechanical failure (group B) to those with uneventful healing (group A). In group B there were 30 % of all operated patients. Less frequent was most catastrophic event of cut-out which happened in 4.2% of our patients, followed by neck – shaft collapse (for more than 10^{o}) in 8.3 %. The most frequent was excessive sliding of main proximal fragments (for more than 10 mm) - in 16.7%. There were no cases of breakage of osteo-synthetic material in our series. The only difference between groups at the surgery was reduction in MCS. At follow up, the differences were significant in all parameters except NSA and TAD (**Table 4**) [7].

Table 4. Comparison of groups A and B in reduction parameters after the surgery and six months later. Probability pertaining to the difference between the groups, calculated by the t-test is given.

Parameter	A vs. B (OP)	A vs. B (FU)
NSA	0.860	0.892
MCS	0.006*	< 0.001*
ACS	0.246	0.001*
TAD	0.546	0.092
PIAP	0.213	0.029*
PIL	0.828	0.015*

A: group A, B: group B, OP: immediately after the surgery, FU: last follow up, NSA: neck-shaft angle, MCS: medial cortical support, ACS: anterior cortical support, TAD: tip to apex distance, PIAP: Parker index in anteroposterior projection, PIL: Parker index in lateral projection, *: statistically significant.

4. Conclusions

In our study we clearly showed the influence of unsatisfactory position of the proximal fragment on walking ability of patients with trochanteric fracture type A2 after half a year. With retrograde analysis from the known outcome, we were able to show decisive influence of anterior cortical support on final position of proximal fragment. The parameters which were controlled in anteroposterior projections were less important, however more attention during surgery should be put on anterior cortical support in the future.

Regarding mechanical failure we can conclude that reduction in AP view is the most important prognostic factor for mechanical failure of A2 trochanteric fractures. However the effects of NSA, ACS and the position of the implant should be considered in the future. Knowing that the proximal fragment is a three-dimensional structure, it is not possible to strictly divide ACS, MCS and NSA when judging the quality of reduction. In future studies, more attention must be devoted to rotational malalignment of the proximal fragment itself. Its relation to the shaft of the femur would give some additional information on position of the fracture (NSA, MCS and ACS) and on its influence on mechanical failure and functional outcome.

References

1. Shah MR, Aharonoff GB, Wolinsky P, Zuckerman JD, Koval KJ. Outcome afterhip fracture in individuals ninety years of age and older. J Orthop Trauma.2001; 15(1):34–39. doi: 10.1097/00005131-200101000-00007
2. Koval KJ, Skovron ML, Aharonoff GB, Zuckerman JD. Predictors of functional recovery after hip fracture in the elderly. Clin Orthop Relat Res. 1998; 348:22–28.
3. Chang SM, Zhang YQ, Du SC, Ma Z, Hu SJ, Yao XZ, et al. Anteromedial cortical support reduction in unstable pertrochanteric fractures: a comparison of intra-operative fluoroscopy and post-operative three-dimensional computerized tomography reconstruction. Int Orthop. 2018; 42(1):183-189. doi: 10.1007/s00264-017-3623-y
4. Hsueh KK, Fang CK, Chen CM, Su YP, Wu HF, Chiu FY. Risk factors in cutout of sliding hip screw in intertrochanteric fractures: an evaluation of 937 patients. Int Orthop. 2010; 34(8):1273-1276. doi: 10.1007/s00264-009-0866-2
5. Ye KF, Xing Y, Sun C, Cui ZY, Zhou F, Ji HQ, Guo Y, Lyu Y, Yang ZW, Hou GJ, Tian Y, Zhang ZS. Loss of the posteromedial support: a risk factor for implant failure after fixation of AO 31-A2 intertrochanteric fractures. Chin Med J (Engl). 2020; 5;133(1):41-48. doi: 10.1097/CM9.0000000000000587
6. Kristan A, Benulič Č, Jaklič M. Influence of reduction and implant placement on mechanical failure in A2 type of trochanteric fractures. AOTT. 2021 in revision.
7. Kristan A, Benulič Č, Jaklič M. Reduction of trochanteric fractures in lateral view is significant predictor for radiological and functional result after six months. Injury. 2021; S0020-1383(21)00141-8. doi: 10.1016/j.injury.2021.02.038

Research

The effect of stress distribution in artificial hip joint on the dislocation of the hip endoprosthesis

Tomaževič Matevž[1,*], Cimerman Matej[1], Kralj Iglič Veronika[2].
[1]University Medical Centre Ljubljana, Department of Traumatology, Ljubljana, Slovenia
[2]University of Ljubljana, Faculty of Health Sciences, Laboratory of Clinical Biophysics, Ljubljana, Slovenia
*matevz.tomazevic@kclj.si

Abstract
Dislocation after hip arthroplasty is still a major concern. Recent study of the volumetric wear of the cup has suggested that stresses studied in a one-legged stance model could predispose arthroplasty dislocation. The aim of this work was to study whether biomechanical parameters of contact stress distribution in total hip arthroplasty during a neutral hip position can predict a higher possibility of the arthroplasty dislocating. Biomechanical parameters were determined using 3-dimensional mathematical models of the one-legged stance within the HIPSTRESS method. Geometrical parameters were measured from standard anteroposterior X-ray images of the pelvis and proximal femora. Fifty-five patients subjected to total hip arthroplasty that later suffered dislocation of the head and, for comparison, 95 total hip arthroplasties that were functional at least 10 years after the implantation, were included in the study. Arthroplasties that suffered dislocation had on average a 6% higher resultant hip force than the control group (p=0.004), 11% higher peak stress on the load-bearing area (p=0.001) and a 50% more laterally positioned stress pole (p=0.026), all parameters being less favorable in the group of unstable arthroplasties. There was no statistically significant difference in the hip gradient index or in the functional angle of the weight bearing. Our study showed that arthroplasties that show a tendency to push the head out of the cup in the representative body position - the one-legged stance - are prone to dislocation. An unfavorable resultant hip force, peak stress on the load bearing and laterally positioned stress pole are predictors of arthroplasty dislocation.

1. Introduction

Based on patient reported outcome measures, hip arthroplasty is the most successful elective surgical procedure [1]. Today more than 95% of arthroplasties survive more than 10 years [2,3]. Some total hip arthroplasties (THAs) nevertheless fail and revision surgery is needed. Hip dislocation after THA is the second most common cause of revision surgery [2]. The reported rate of revision due to dislocation after primary THA is 2-4 % in the first six months [4] and increases to 6% after 20 years [5]. After revision surgery, the dislocation rate levels at 5.4% in the first year after the operation [6]. Dislocation studies of THA have been performed based on component positioning, with an emphasis on cup orientation [7-10], the effect of artificial head size [5,11,12] and impingement as causes of a prosthesis head dislocation [13-15]. More than 50 % of dislocations occur when the cup is in the so-called safe zone position [10]. A larger femoral head diameter increases the range of motion before the prosthesis neck impinges on the acetabulum liner, which causes the prosthesis to dislocate [5,11,16]. Despite the careful positioning of THA components, dislocations still occur. The question arises as to whether THA changes the geometry of the hip in such a way to affect the biomechanical parameters in the joint, forcing the hip to dislocate at the edge of the motion range.

The HIPSTRESS method was developed to calculate biomechanical parameters in the hip considering pelvis and femur anatomy [17,18].

The HIPSTRESS method demonstrates that linear wear occurs in the direction of the stress pole [19,20] and that it is proportional to the peak stress on the weight bearing area[19]. Because of this effect, the volumetric wear on the cup is less for a larger abduction angle of the cup [21], since the head partly migrates out of the socket [21]. On the other hand, it has been shown that this could be unfavorable in terms of dislocation [21].

The aim of this work was that check whether biomechanical parameters (higher peak stress, more lateral position of stress pole and less negative stress gradient index) are predictors for dislocation of a THA. To test this hypothesis, we compared the biomechanical parameters of a THA population that had suffered dislocation and a THA population that did not dislocate at least 10 years post-operatively.

2. Methods

The study was designed as a retrospective individual case control study, level of evidence 3B. It was approved by Slovene National Medical Ethics Committee letter No.: 110/04/15. Anteroposterior (AP) X-ray images of the hip and pelvic skeleton of patients that had undergone THA were used to measure geometrical parameters relevant for a determination of biomechanical parameters within the HIPSTRESS method. X-ray images of patients that had suffered dislocation of hip arthroplasties were included in the study group. Patients were chosen from the emergency department database based on a diagnosis of hip dislocation, ICD S73.0. Patients admitted to the Emergency Department, University Clinical Center Ljubljana from November 2012 until September 2015 were included. Images were downloaded from the Impax server and coded. Eighty-one patients with a diagnosis of

dislocation of the hip joint were gathered. Exclusion criteria were patients that had suffered hip dislocation due to high energy trauma (17 patients), patients with whom dislocation had occurred due to material breakage of the hip prosthesis (2 patients), patients where the contours of the femur or pelvis were not clearly visible on the X-ray image (1 patient) and patients with partial endoprosthesis (6 patients). X-ray images taken immediately after reduction of the dislocation were used for analysis. After excluding the patients with the exclusion criteria, 55 patients remained in the study group. Twenty-five (41%) of them had already undergone hip arthroplasty on the contralateral hip.

Standard X-ray images of the hip and pelvis taken at the Emergency Department, University Medical Center Ljubljana were assumed to have an average magnification of 115% and the size of the prosthesis head was estimated by rounding to 28mm, 32mm or 36 mm using software developed for preoperative planning at the Department of Traumatology, University Medical Center Ljubljana. Twenty-six (47%) hips in the study group with THA had a femoral head diameter of 28 mm, 12 (22%) had a femoral head diameter of 32 mm and 17 (31%) had a femoral head diameter of 36 mm. On average, the radius of the prosthesis head was 15.67 mm ± 1.75 mm.

To define the control group, we examined X-ray images of 311 patients who had undergone total hip arthroplasty (THA) at the Orthopedic Hospital Valdoltra, Slovenia. The first available X-ray images or THA with whole pelvis (in terms of date) were taken from the Impax server at the hospital. Inclusion criteria were an X-ray image of the pelvis and proximal femora after implantation, no event of hip dislocation or septic or aseptic loosening and regular follow-up for at least 10 years. Patients who had undergone any revision procedure during that time were also excluded. Ninety-four hips (54 (63%) right and 35 (37%) left) of 77 patients that met the inclusion criteria (45 female and 32 male) were included in the analysis. Sixty-nine of them also had a prosthesis on the contralateral side. The average age of the patients included at the time of implantation was 59.6 years. There were 79 (84%) THA with a femoral head diameter of 28mm, 2 (2%) of them had a femoral head diameter of 32 mm and 13 (14%) had a femoral head diameter of 36mm.

For biomechanical evaluation, three-dimensional mathematical models of an adult human hip within the HIPSTRESS method were used [18,22]. The models are described in detail elsewhere (see for example ref. [22]) so only a brief description will be given here. The method consists of two mathematical models: one for determination of the resultant hip force in the representative body position for everyday activities [23], i.e., the one-legged stance (24), and the other for determination of contact hip stress distribution [17]. The model for resultant hip force is based on force and torque equilibrium equations [18,24]. The model describes a system composed of two segments: the loaded leg and the rest of the body. It includes 9 effective muscle forces, the weight of the segments and the intersegment force (the resultant hip force). The reference muscle attachment points are obtained from measurements performed on a cadaver and then re-scaled for the individual hip considered. Since the X-ray image is two-dimensional, data in the third dimension are taken to be equal to the reference values. The model for force uses as input the geometrical parameters of

pelvis and proximal femur: pelvic width (*C*) and height (*H*), inter-hip distance (*l*) and the position of the muscle attachment point on the greater trochanter (*x,z*) (**Figure 1**). Stress integrated over the load-bearing area yields the resultant hip force **R** = ∫ *p* **dA,** where *p* is stress and **dA** is the area element. The calculations and procedures have been explained previously [19,22,25,26].

HIPSTRESS models use hip and pelvis geometric parameters as input data: inter-hip distance (*l*), height of the pelvis (*H*), horizontal distance from the prosthesis head center to the lateral edge of the pelvis (*C*), position of the greater trochanter relative to the prosthesis head center in the coordinate system of the femur (distances *z* and *x*) and abduction angle. The geometrical parameters were determined using CorelDRAW Graphics Suite X7, 2015, Ottawa, Canada, by two blinded measurers. HIPSTRESS software (26) was used for calculation of the biomechanical parameters. (**Figure 1**). Previous studies [28-32] have indicated that the peak stress on the load-bearing area p_{max} is a useful biomechanical parameter. If the stress pole is located inside the load bearing area, p_{max} is equal to the value of the stress at the pole. If the stress pole lies outside the load-bearing area, contact stress is highest at the point of the load-bearing area that is closest to the pole,

$$p_{max} = p_0 \cos(\pi/2 - \vartheta_{abd} - \Theta_{pole}) \quad , \qquad (1)$$

where p_0 is the value of stress at its pole, ϑ_{abd} is the abduction angle of the prosthesis cup and Θ_{pole} is the angle of the stress pole (**Figure 1**). Another indicator of the stress distribution is the gradient of stress, represented by its value at the lateral rim of the cup G_p (Eq. (2)) [21,33]

$$G_p = - p_0 \cos(\pi - \vartheta_{abd} - \Theta_{pole})/r \quad , \qquad (2)$$

where *r* is the radius of the articular surface. If the pole of stress distribution lies outside the load-bearing area (i.e., if $\Theta_{pole} > \pi/2 - \vartheta_{abd}$), then G_p is positive, stress attains its highest value at the lateral rim and falls off rapidly in the medial direction, while the corresponding weight bearing area is small [34]. Such a distribution represents dysplastic hips [34]. If, however, the pole of stress distribution lies inside the load–bearing area (if $\Theta_{pole} < \pi/2 - \vartheta_{abd}$), then stress reaches its peak within the weight bearing area, which is consequently larger and G_p is negative [34]. The functional angle of load bearing ϑ_f is defined as

$$\vartheta_f = (\pi - \vartheta_{abd} - \Theta_{pole}) \quad . \qquad (3)$$

In relation to dislocation, high resultant hip force and high peak stress are unfavorable. However, a high gradient index and more laterally positioned pole are expected to represent an even greater risk of dislocation, since the head is pushed more laterally each time the leg is loaded.

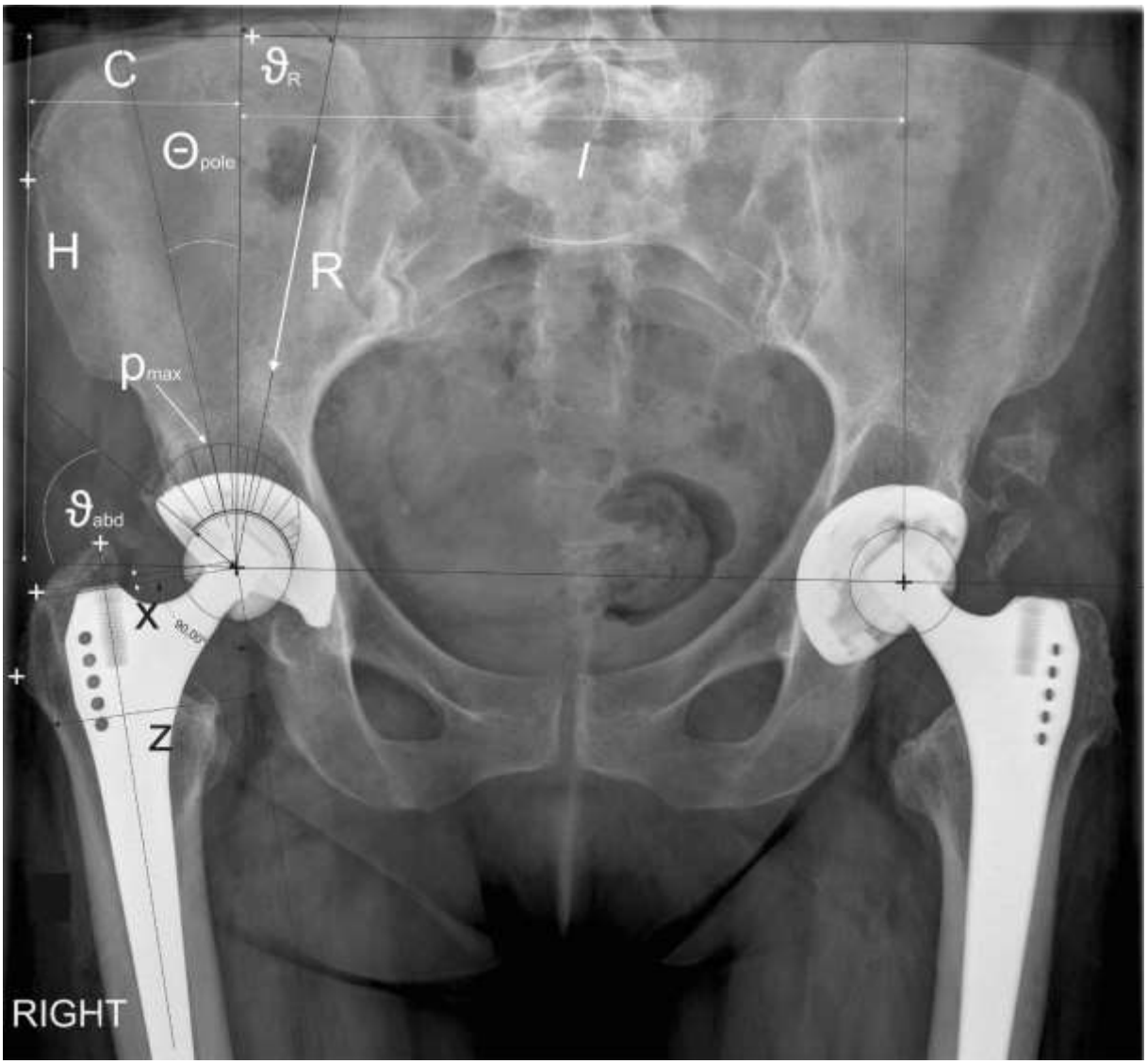

Figure 1. Geometric and biomechanical parameters within the HIPSTRESS models that are used for calculation of stress distribution in a right artificial hip. *R* resultant hip force; p_{max} peak stress on the load bearing area; θ_{pole} angle of the stress pole; ϑ_{abd} abduction angle; ϑ_R angle of the resultant hip force; *C* horizontal distance between the center of the prosthesis head and the most lateral point on the iliac crest; *H* vertical distance between the center of the prosthesis head and the highest point on the iliac crest; *x* vertical distance between the center of the prosthesis head and the point on the greater trochanter in the direction of the femur; *z* distance between the center of the prosthesis head and the point on the greater trochanter perpendicular to the femur axis; *l* distance between the centers of the femoral heads [27].

The peak stress p_{max} is proportional to r^{-2}, while the hip stress gradient index G_p is proportional to r^{-3} [17,34]. Since different sizes of prosthesis heads were involved, the effect of the femoral head size on biomechanical parameters was eliminated by multiplying p_{max} by r^2 and G_p by r^3. The resultant hip force, peak stress and stress gradient index are also proportional to body weight W_b. Since the body weight was unknown, its effect was eliminated by normalizing the respective parameters by W_b. The normalized biomechanical parameters R/W_B, $p_{max}r^2/W_b$, G_pr^3/W_b, ϑ_f and Θ_{pole} express the geometry of the pelvis and

the proximal femur and the geometry and position of the arthroplasty's elements (but not the size of the artificial head).
Statistical analysis of the biomechanical parameters between the two groups was done using the Student T - test. If the p value was ≤ 0.05, the difference between these two groups was significant. The statistical power (1-β) of the result was taken as sufficient when the power was >80%. Statistical analysis was done using Microsoft Excel 2010 (14.0.7188.5000, Microsoft Corporation, Santa Rosa, California, USA). The power of the statistics was calculated using a statistics power calculator on the internet: http://clincalc.com/Stats/Power.aspx

3. Results

Normalized resultant hip force R/W_b and normalized peak stress $p_{max.}r^2/W_b$ were considerably and statistically significantly less favorable in the study group than in the control group, with sufficient statistical power. The position of the stress pole was more lateral in the study group. The difference was statistically significant but with somewhat deficient statistical power (**Table 1**). The normalized stress gradient index $G_{p.}r^3/W_b$ and functional angle of load bearing showed no statistically significant difference, although it was less negative and smaller (which is unfavorable) in the study group.
There was a considerable and statistically significant difference in parameters *x* (distance between the center of the prosthesis head and the point on the greater trochanter in the direction of the femur axis) and *C* (horizontal distance between the center of the prosthesis head and the most lateral point of the iliac crest) between the study and control groups (**Table 2**). Higher *x* and *C* indicate less favorable biomechanical parameters in the study group. The difference between the abduction angles in the study group and control group was minute, which explains the lack of statistical significance of the difference in the functional angle of weight bearing (**Table 1**).

Table 1. Comparison of biomechanical parameters of the hips with THA in the study and control group.

Average ± SD	Study group (55 THA)	Control group (94 THA)	Difference (%)	p	Power (1-β)
R/W_b	mean 2.71 (SD 0.36)*	mean 2.54 (SD 0.32)	6.3	0.004	89.9%
$p_{max}*r^2/W_b$	mean 152.11 (SD 37.04)*	mean 135.32 (SD 21.42)	11.0	0.001	92.7%
G_p*r^3/W_b	mean -828287.70 (SD 413381.01)*	mean -871926.04 (SD 220240.41)	-5.27	0.400	10.9%
ϑ_f (°)	mean 129.13 (SD 17.57)	mean 132.90 (SD 13.60)	-2.9	0.146	39.5%
θ_{pole} (°)	mean 5.77 (SD 9.71)*	mean 2.86 (SD6.08)	50.0	0.026	62.9%

R/W_b, resultant hip force normalized by body weight; $p_{max}*r^2/W_b$; effect of pelvis geometry on peak stress on the load bearing area normalized by body weight; G_p*r^3/W_b; effect of pelvic geometry on the peak hip gradient index; ϑ_f (°), functional angle of the load bearing; θ_{pole} (°), position of the stress pole.
(*) An asterisk denotes a value with higher risk for dislocation.

Table 2. Comparison of geometrical parameters of the hips with THA in the study group and control group

Average ± SD	Study group (55 THA)	Control group (94 THA)	Difference (%)	P	Power (1-β)
H (mm)	mean 136.80 (SD 13.53)	mean 133.78 (SD11.18)	2.2	0.144	40.6%
z (mm)	mean 56.73 (SD 8.71)	mean 59.18 (SD 6.73)	-4.3	0.057	56.3%
x (mm)	mean 14.77 (SD 8.69)*	mean 7.81 (SD 5.34)	47.1	0.000	100%
C (mm)	mean 59.58 (SD 8.87)*	mean 55.52 (SD 9.22)	6.8	0.010	84.8%
l (mm)	mean 179.61 (SD 11.15)	mean 177.13 (SD 10.26)	1.38	0.169	10.9%
ϑ_{abd} (°)	mean 45.10 (SD9.12)	mean 44.24 (SD 7.97)	1.9	0.547	14.5%

H (mm), vertical distance between the center of the prosthesis head and the highest point on the iliac crest; *z* (mm), distance between the center of the prosthesis head and the point on the greater trochanter perpendicular to the femur axis; *x* (mm), vertical distance between the center of the prosthesis head and the point on the greater trochanter in the direction of the femur; *C* (mm), horizontal distance between the center of the prosthesis head and the most lateral point on the iliac crest; *l* (mm), horizontal distance between the right and left center of the femoral head; ϑ_{abd} (°), abduction angle.
(*) An asterisk denotes a value with a higher risk of dislocation.

4. Discussion

Our study proved that contact stress distribution on the prosthesis head is a predictor of arthroplasty dislocation.

It is shown above (**Table 1**) that THA that had suffered dislocation had a less favorable distribution of contact stress (given by its peak value and the position of the pole), which pushed the artificial head more laterally than in the case of prostheses that were functional at least 10 years post-operatively. A previous study had shown that the head migrates in the direction of the stress pole [19]. This process changes the shape of the interface between the head and the cup and contributes to the development of a lever that leads to dislocation. In contrast to the previous study, there were no significant differences in the abduction angle of the actebulum, but the acetabulum was positioned more medial in the study group than in the control group.

Dislocation of the hip joint after THA is one of the major side complications (2% - 4% after primary total hip arthroplasty) [2,35] and its causes have been studied previously [5,7-16,35-38]**.** Among procedure related factors, the measured parameters of component positions, a cup inclination out of the range of 40° ± 10°, a cup anteversion of less than 10° or more than 35°, a stem anteversion out of the range of 14.8° ± 6,01° and a height of hip rotation center outside the range of 2.16 mm ± 9.11 mm, increased the risk of dislocation [8,9,36]. The artificial head size, leg length discrepancy and acetabular inclination were all studied in two separate studies and it was found that these are not statistically important factors predicting dislocation of the femoral head [7,39] On the other hand, in a study by Berry [5], a smaller size of the prosthesis head was shown to be related to a higher dislocation rate of THA. In a study by Forde et al. (2018) [7], it was reported that if the femoral offset was at least 3 mm greater than on the contralateral side, the risk of dislocation was lower [7]. Offset is expressed in the HIPSTRESS model by parameter z. A larger z is biomechanically favorable, since it implies a lower resultant force and larger angle of inclination, which consequently means lower peak stress, a more medial location of the pole, a smaller gradient index and a larger functional angle of weight bearing [22]. Our results additionally pointed out the importance of position of the acetabulum in the pelvis in the mediolateral direction.

In a study by Rijavec et al. (2015) [21] that considered the effect of cup inclination on predicted contact stress-induced volumetric wear in THA, stress distribution was proposed as a relevant factor connected to the probability of dislocation of the artificial head. Our results show that normalized stress was indeed considerably and statistically significantly less favorable in the study group. The position of the pole was statistically significantly less favorable in the study group, while the difference in gradient index $G_p.r^3/W_b$, albeit showing a less favorable configuration in the study group, was not statistically significant. Since three of the parameters were on average less favorable in the study group, our results support the proposed hypothesis.

Our study and control groups had a different distribution of artificial head sizes and we focused on the effect of the geometry of the pelvis and the proximal femur and the

inclination of the artificial cup. We therefore chose biomechanical parameters that were independent of the artificial head size.

Preoperative planning is advised before implantation of an artificial hip and is usually done [40]. Optimization of the choice and position of prosthesis elements using simulation with a mathematical model could be included in preoperative planning. Simulation of postoperative biomechanical parameters would be useful in planning the configuration of prostheses, especially in demographic groups in which hips are more vulnerable to dislocation, or in revision cases. In cases in which preoperative planning predicted an arthroplasty prone to dislocation, the surgeon could decide on another implant configuration.

Our results showed that the shape of the pelvis and proximal femur after total hip arthroplasty impacted on a less favorable stress distribution in the representative everyday activity, the one-legged stance, in prostheses that had suffered dislocation. Although the hip does not dislocate during the one-legged stance, these hips had higher stress, accumulated more laterally, than arthroplasties that were functional for at least 10 years. The more lateral position of the stress pole could remodel the joint and predispose dislocation during other activities.

Acknowledgements

The authors thank the Slovenian Research Agency for grant P3-0388.

References

1. Finalised Patient Reported Outcome Measures (PROMs) in England for Hip and Knee Replacement Procedures (April 2017 to March 2018). Available at: https://digital.nhs.uk/data-and-information/publications/statistical/patient-reported-outcome-measures-proms/hip-and-knee-replacement-procedures---april-2017-to-march-2018
2. Ferguson RJ, Palmer AJ, Taylor A, Porter ML, Malchau H, Glyn-Jones S. Hip replacement. The Lancet. 2018; 392(10158):1662–1671. doi: 10.1016/S0140-6736(18)31777-X
3. Annual reports from The Swedish Hip Arthroplasty Register · Svenska höftprotesregistret. 2018. Available at https://shpr.registercentrum.se/shar-in-english/annual-reports-from-the-swedish-hip-arthroplasty-register/p/rkeyyeElz
4. Goel A, Lau EC, Ong KL, Berry DJ, Malkani AL. Dislocation rates following primary total hip arthroplasty have plateaued in the medicare population. J Arthroplasty. 2015; 30(5):743–746. doi: 10.1016/j.arth.2014.11.012
5. Berry DJ. Effect of femoral head diameter and operative approach on risk of dislocation after primary total hip arthroplasty. J Bone Joint Surg Am. 2005; 87(11):2456. doi: 10.2106/JBJS.D.02860

6. Badarudeen S, Shu AC, Ong KL, Baykal D, Lau EC, Malkani AL. Complications after revision total hip arthroplasty in the medicare population. J Arthroplasty. 2017; 32(6):1954–1958. doi: 10.1016/j.arth.2017.01.037
7. Forde B, Engeln K, Bedair H, Bene N, Talmo C, Nandi S. Restoring femoral offset is the most important technical factor in preventing total hip arthroplasty dislocation. J Orthop. 2018; 15(1):131–133. doi: 10.1016/j.jor.2018.01.026
8. Lewinnek GE, Lewis JL, Tarr R, Compere CL, Zimmerman JR. Dislocations after total hip-replacement arthroplasties. J Bone Joint Surg. 1978; 60(2):217–220.
9. Yoon Y-S, Hodgson AJ, Tonetti J, Masri BA, Duncan CP. Resolving inconsistencies in defining the target orientation for the acetabular cup angles in total hip arthroplasty. Clin Biomech. 2008; 23(3):253–259. doi: 10.1016/j.clinbiomech.2007.10.014
10. Abdel MP, von Roth P, Jennings MT, Hanssen AD, Pagnano MW. What safe zone? The vast majority of dislocated THAs are within the Lewinnek safe zone for acetabular component position. Clin Orthop. 2016; 474(2):386–391. doi: 10.1007/s11999-015-4432-5
11. Kluess D, Martin H, Mittelmeier W, Schimtz K-P, Bader R. Influence of femoral head size on impingement, dislocation and stress distribution in total hip replacement. Med Eng Phys. 2007; 29(4):465–471. doi: 10.1016/j.medengphy.2006.07.001
12. Bunn A, Colwell CW, D'Lima DD. Effect of head diameter on passive and active dynamic hip dislocation. J Orthop Res. 2014; 32(11):1525–1531. doi: 10.1002/jor.22659. Epub 2014 Jun 24
13. Nadzadi ME, Pedersen DR, Yack HJ, Callaghan JJ, Brown TD. Kinematics, kinetics, and finite element analysis of commonplace maneuvers at risk for total hip dislocation. J Biomech. 2003; 36(4):577–591. doi: 10.1016/s0021-9290(02)00232-4
14. Elkins JM, Kruger KM, Pedersen DR, Callaghan JJ, Brown TD. Edge-loading severity as a function of cup lip radius in metal-on-metal total hips – a finite element analysis. J Orthop Res Off Publ Orthop Res Soc. 2012; 30(2):169–177. doi: 10.1002/jor.21524
15. Scifert CF, Brown TD, Lipman JD. Finite element analysis of a novel design approach to resisting total hip dislocation. Clin Biomech. 1999; 14(10):697–703. doi: 10.1016/s0268-0033(99)00054-6
16. Tanino H, Harman MK, Banks SA, Hodge WA. Association between dislocation, impingement, and articular geometry in retrieved acetabular polyethylene cups. J Orthop Res. 2007; 25(11):1401–1407. doi: 10.1002/jor.20410
17. Ipavec M, Brand RA, Pedersen DR, Mavčič B, Kralj-Iglič V, Iglič A. Mathematical modelling of stress in the hip during gait. J Biomech. 1999; 32(11):1229–1235. doi: 10.1016/s0021-9290(99)00119-0
18. Iglič A, Srakar F, Antolic V. Influence of the pelvic shape on the biomechanical status of the hip. Clin Biomech. 1993; 8(4):223–224. doi: 10.1016/0268-0033(93)90019-E
19. Košak R, Kralj-Iglič V, Iglič A, Daniel M. Polyethylene wear is related to patient-specific contact stress in THA. Clin Orthop. 2011; 469(12):3415–3422. doi: 10.1007/s11999-011-2078-5

20. Košak R, Antolič V, Pavlovčič V, Kralj-Iglič V, Milošev I, Vidmar G, idr. Polyethylene wear in total hip prostheses: the influence of direction of linear wear on volumetric wear determined from radiographic data. Skeletal Radiol. 2003; 32(12):679–686. doi 10.1007/s00256-003-0685-2
21. Rijavec B, Košak R, Daniel M, Kralj-IgliČ V, Dolinar D. Effect of cup inclination on predicted contact stress-induced volumetric wear in total hip replacement. Comput Methods Biomech Biomed Engin. 2015; 18(13):1468–1473. doi: 10.1080/10255842.2014.916700
22. Kralj-Iglič V. Validation of Mechanical Hypothesis of hip Arthritis Development by HIPSTRESS Method. V: Chen Q, urednik. Osteoarthritis - Progress in Basic Research and Treatment [Internet]. InTech; 2015; doi: 10.5772/59976
23. Debevec H, Pedersen DR, Iglič A, Daniel M. One-legged stance as a representative static body position for calculation of hip contact stress distribution in clinical studies. J Appl Biomech. 2010; 26(4):522–525. doi: 10.1123/jab.26.4.522
24. Iglič A, Srakar F, Antolič V, Kralj-Iglič V, Batagelj V. Mathematical analysis of Chiari osteotomy. Acta Orthop Iugosl. 1990; 20:35–39.
25. Kralj-Iglič V, Dolinar D, Ivanovski M, List I, Daniel M. Role of Biomechanical Parameters in Hip Osteoarthritis and Avascular Necrosis of Femoral Head. V: Naik GR, urednik. Applied Biological Engineering - Principles and Practice [Internet]. InTech; 2012. doi: 10.5772/30159
26. Iglič A, Kralj-Iglič V, Daniel M, Maček-Lebar A. Computer determination of contact stress distribution and size of weight bearing area in the human hip joint. Comput Methods Biomech Biomed Engin. 2002; 5(2):185–192. doi: 10.1080/10255840290010300
27. Tomaževič M, Kaiba T, Kurent U, Trebše R, Cimerman M, Kralj-Iglič V. Hip stress distribution - Predictor of dislocation in hip arthroplasties. A retrospective study of 149 arthroplasties. PLOS ONE. 2019; 14(11):e0225459. doi: 10.1371/journal.pone.0225459
28. Mavčič B, Pompe B, Antolič V, Daniel M, Iglič A, Kralj-Iglič V. Mathematical estimation of stress distribution in normal and dysplastic human hips. J Orthop Res. 2002; 20(5):1025–1030. doi: 10.1016/S0736-0266(02)00014-1
29. Mavčič B, Iglič A, Kralj-Iglič V, Brand RA, Vengust R. Cumulative hip contact stress predicts osteoarthritis in DDH. Clin Orthop. 2008; 466(4):884–891. doi: 10.1007/s11999-008-0145-3
30. Kralj M, Mavčič B, Antolič V, Iglič A, Kralj-Iglič V. The Bernese periacetabular osteotomy: clinical, radiographic and mechanical 7–15-year follow-up of 26 hips. Acta Orthop. 2005; 76(6):833–840. doi: 10.1080/17453670510045453
31. Recnik G, Kralj-Iglič V, Iglič A, Antolič V, Kramberger S, Vengust R. Higher peak contact hip stress predetermines the side of hip involved in idiopathic osteoarthritis. Clin Biomech. 2007; 22(10):1119–1124. doi: 10.1016/j.clinbiomech.2007.08.002

32. Recnik G, Vengust R, Kralj-Iglič V, Vogrin M, Krajnc Z, Kramberger S. Association between sub-clinical acetabular dysplasia and a younger age at hip arthroplasty in idiopathic osteoarthritis. J Int Med Res. 2009. https://doi.org/10.1177/147323000903700541
33. Pompe B, Daniel M, Sochor M, Vengust R, Kralj-Iglic V, Iglic A. Gradient of contact stress in normal and dysplastic human hips. Med Eng Phys. 2003; 25(5):379–385. doi: 10.1016/s1350-4533(03)00014-6
34. Pompe B, Antolic V, Iglic A, Jaklic A, Kralj-Iglic V, Mavcic B. How should dysplastic human hips be evaluated? Cell Mol Biol Lett. 2002; 7(1):144–146.
35. Dargel J, Oppermann J, Brüggemann G-P, Eysel P. Dislocation following total hip replacement. Dtsch Ärztebl Int. 2014; 111(51–52):884–890. doi: 10.3238/arztebl.2014.0884
36. Kim Y-H, Choi Y, Kim J-S. Influence of Patient-, design-, and surgery-related factors on rate of dislocation after primary cementless total hip arthroplasty. J Arthroplasty. 2009; 24(8):1258–1263. doi: 10.1016/j.arth.2009.03.017
37. Sikes CV, Lai LP, Schreiber M, Mont MA, Jinnah RH, Seyler TM. Instability after total hip arthroplasty. J Arthroplasty. 2008; 23(7):59–63. doi: 10.1016/j.arth.2008.06.032
38. Soong M, Rubash HE, Macaulay W. Dislocation after total hip arthroplasty. J Am Acad Orthop Surg. 2004; 12(5):314–321. doi: 10.5435/00124635-200409000-00006
39. Brennan MSA, Khan F, Kiernan C, Queally JM, McQuillan J, Gormley IC, et al., Dislocation of primary total hip arthroplasty and the risk of redislocation: Hip Int. 2018. doi: 10.5301/HIP.2012.9747
40. Eggli S, Pisan M, Müller ME. The value of preoperative planning for total hip arthroplasty. J Bone Joint Surg Br. 1998; 80(3):382–390. doi: 10.1302/0301-620x.80b3.7764

Review

Limits of hip arthroscopy

Stražar Klemen[1,2,*]

[1]University Medical Centre Ljubljana, Department for Orthopaedic Surgery, Ljubljana, Slovenia
[2]University of Ljubljana, Faculty of Medicine, Chair of Orthopaedics, Ljubljana, Slovenia
klemen.strazar@kclj.si

Abstract

Hip arthroscopy has been popularized in the last 15 years and numerous indications have been introduced. Most common indication for hip arthroscopy is femoroacetabular impingement with its consequent pathology, chondral and labrum lesions. Preoperatively, it is essential to define all morphological abnormalities that need to be corrected. Most of these pathologies represent risk for later osteoarthritis. The risk becomes significant when treatment is substantially delayed. According to clinical studies, hip arthroscopy is contraindicated in advance osteoarthritis and in moderate to severe acetabular dysplasia if it is not combined with corrective osteotomy. Author presents limits of hip arthroscopy according to his own clinical experience and the evidence from the literature.

1. Introduction

In 2003, Ganz and coworkers from Bern (Switzerland) defined two basic types of femoroacetabular impingement (FAI), the acetabular type – pincer and the femoral type – CAM [1]. Correlation between developmental morphological abnormalities and intraarticular lesions, i.e. focal chondral injury and labrum tear, was described. Knowledge about FAI together with simultaneous technical progress instantly popularized hip arthroscopy. In the following years, several indications for hip arthroscopy were introduced with FAI remaining far most common among them. It has been verified that most of indications for hip arthroscopy present significant risk for later development of osteoarthritis (OA). Limits of hip arthroscopy have been tested in patients with different degrees of OA and with developmental disorders different from FAI, the acetabular dysplasia in particular [2]. Various combinations of morphological abnormalities have been described and importance to thoroughly study each single case prior surgery has been stressed. Recently, computer science has been introduced in hip arthroscopy [3]. First, kinematic planning from CT based 3D models of the joint has been implemented. Second, surgical execution can be supported by intraoperative navigation based on preoperative plan. Third, end result of surgical correction can be studied by using postoperative CT based 3D models. According to clinical experience of experts and increased evidence from the literature, limits of hip arthroscopy have been set. Furthermore, arthroscopy has been suggested for treatment of pertrochanteric pathology and for recently described extraarticular causes of impingement, e.g. ischiofemoral or subspinal impingement [4].

2. Limits of hip arthroscopy for treatment of FAI

During arthroscopy, enlarged field of view enables to observe minor surface abnormalities but limits overall perception of the joint geometry on the other hand. The later limitation is the reason why surgical reshaping in case of FAI (osteoplasty) is technically demanding. Under-resection of CAM deformity has been found the most common reason for revision hip arthroscopy [5]. Intraoperative navigation has been suggested to improve surgical accuracy but it is still in developing phase [3] (**Figure 1**). Not all severe and complex combined deformities of the hip with mechanical impingement, e.g. post-Perthes deformity, could be treated by arthroscopy alone [6]. Combined arthroscopic and open approach is advocated in many instances. According to publications and our clinical experience patient's age over 45 years present risk factor for worse final outcome after arthroscopic treatment of FAI due to more global involvement of the joint and OA in particular [7]. Adjustment of activities may temporarily improve symptoms although long-term conservative treatment of FAI is not recommended [8]. It was suggested to restore labrum function, to treat focal chondral lesions and to restore joint anatomy before the pathology advances in OA. According to clinical studies, it is recommended to perform hip arthroscopy for CAM FAI not later than 1.5 year after first symptoms [8]. Best results of treatment of patients with FAI can be expected

in young patient with pure mechanical symptoms in the groin especially during sitting or during dynamic activities with hips in flexion.

A B

Figure 1. Intraoperative navigation during arthroscopic osteoplasty of the femoral head (patient with CAM FAI deformity); setting in operating room (A), surgical navigation (B)

3. Limited role of hip arthroscopy in acetabular dysplasia

In acetabular dysplasia, constant increased hip stress has been found responsible for increase incidence of early OA changes [9]. Epidemiological studies have shown that patients with moderate to severe acetabular dysplasia (CE angle < 20°) have 50% of chance to get dysplastic hip replaced before age 55 due to OA [10]. Unfortunately, these patients do not profit from arthroscopy alone even in cases of isolated labrum lesion (**Figure 2**). There was significant risk found for postoperative instability and subjective worsening when hip capsulotomy/capsulectomy was performed on dysplastic hips [11]. In borderline dysplasia (CE angle 20 - 25°) patient may report up to 5 years of subjective improvement if labrum is preserved and plication of capsule is performed [11]. Majority of symptomatic patients with acetabular dysplasia have labrum tears or focal chondral lesions. The only long-term solution in this patients is periacetabular osteotomy (PAO) [3]. According to author's personal communication with prof Soeballe K and based on Danish PAO registry only 20% of patients who undergo PAO needs additional arthroscopy. Despite limited evidence for this, some hip centers prefer one or two stage combined arthroscopy and PAO. According to author's own experience rupture of ligamentum capitis femoris represent additional negative prognostic factor in this patients if arthroscopy is considered.

A B C

Figure 2. Moderate acetabular dysplasia (A) treated by arthroscopy. Subluxation 8 months after arthroscopy (B). Hip replaced by endoprosthesis 2 years after arthroscopy.

4. Advanced osteoarthritis – contraindication for hip arthroscopy

Unfavorable result or even progression of symptoms can be expected when advanced hip OA is treated arthroscopically (**Figure 3**). According to ISHA (International Society for Hip Arthroscopy) arthroscopy is contraindicated in Tönnis II or higher degree of hip OA or when joint space is less than 2 mm wide or its width is less than 50% in comparison with contralateral healthy hip. Pain at rest and during the night is commonly seen in patients with advanced OA. Another hint that hip OA is in its advanced stage are progressive decrease of ROM and positive provocative tests other then FADIR, e.g. FABER and log-roll tests.

Figure 3. Arthroscopy of the osteoarthritic hip. To predict the outcome of treatment, the degree of OA should be estimated prior surgery.

5. Conclusion and future of hip arthroscopy

Hip preservation surgery is becoming more complex and demands thorough knowledge about wide spectrum of intra- and extra-articular causes for symptoms and functional disability. As some pathologies are good indications for arthroscopy others are better solved with open approach. Surgeons are already forced to gain skills in both arthroscopic and open surgery. In the future, limits of hip arthroscopy as well as indications for open preservation surgery will be further clarified. Optimum short- and long-term functional result remains the ultimate goal of individualized approach. Technical advances in computer assistance will most probably change clinical praxis substantially.

References

1. Ganz R, Parvizi J, Beck M, Leunig M, Nötzli H, Siebenrock KA.(2003) Femoroacetabular impingement: a cause for osteoarthritis of the hip. Clin Orthop Relat Res. 2003; 417:112–120. doi: 10.1097/01.blo.0000096804.78689.c2
2. Seijas R, Ares O, Sallent A, Cuscó X, Álvarez-Díaz P, Tejedor R, Cugat R. Hip arthroscopy complications regarding surgery and early postoperative care: retrospective study and review of literature. Musculoskelet Surg. 2017; 101(2):119–131. doi: 10.1007/s12306-016-0444-x

3. Stražar K. Computer assistance in hip preservation surgery-current status and introduction of our system. Int Orthop. 2021; 45(4):897-905. doi: 10.1007/s00264-020-04788-3
4. Perets I, Rybalko D, Mu BH, Friedman A, Morgenstern DR, Domb BG. Hip Arthroscopy: extra-articular Procedures. Hip Int. 2019; 29(4):346-354. doi: 10.1177/1120700019840729
5. Mansor Y, Perets I, Close MR, Mu BH, Domb BG. In search of the spherical femoroplasty: cam overresection leads to inferior functional scores before and after revision hip arthroscopic surgery. Am J Sports Med. 2018; 46(9):2061–2071. doi: 10.1177/0363546518779064
6. Goyal T, Barik S, Gupta T. Hip Arthroscopy for sequelae of Legg-Calve-Perthes Disease: a systematic review. Hip Pelvis. 2021; 33(1):3-10. doi: 10.5371/hp.2021.33.1.3
7. Elwood R, El-Hakeem O, Singh Y, Shoman H, Weiss O, Khanduja V. Outcomes and rate of return to play in elite athletes following arthroscopic surgery of the hip. Int Orthop. 2021; doi: 10.1007/s00264-021-05077-3
8. Larson CM, Giveans RM, Taylor M. Does arthroscopic FAI correction improve function with radiographic arthritis? Clin Orthop Relat Res. 2011; 469(6):1667-1676. doi: 10.1007/s11999-010-1741-6
9. Mavcic B, Iglic A, Kralj-Iglic V, Brand RA, Vengust R. Cumulative hip contact stress predicts osteoarthritis in DDH. Clin Orthop Relat Res. 2008; 466(4):884–891. doi: 10.1007/s11999-008-0145-3
10. Manek NJ, Lane NE. Osteoarthritis: current concepts in diagnosis and management. Am Fam Physician. 2000; 61(6):1795-1804. PMID: 10750883.
11. Maldonado DR, Perets I, Mu BH, Ortiz-Declet V, Chen AW, Lall AC, Domb BG. Arthroscopic capsular plication in patients with labral tears and borderline dysplasia of the hip: analysis of risk factors for failure. Am J Sports Med. 2018; 46(14):3446–3453. doi: 10.1177/0363546518808033

Research

Spinal cord injury and decompression- a question of time and pressure

Jug Marko [1,*]
[1]University Medical Centre Ljubljana, Department of Traumatology, Ljubljana, Slovenia
*jugmarko74@gmail.com

Abstract
Traumatic spinal cord injury (tSCI) is a devastating event, which often results in permanent neurologic disability. Current treatment strategies are limited and focused on secondary injury mitigation. Early decompression of the injured spinal cord and blood pressure augmentation represent current treatment options, but controversies persist regarding the ideal timing for decompression and the value of targeted blood pressure. In addition, other factors as degree of spinal canal compromise (SCC) and severity of injury may influence nerologic outcome.
Here were present the results of our previuos work regarding the effects of the timing of decompression, SCC and severity of injury on neurological recovery in a cohort of subsequent patients with cervical tSCI. In addition, we present the preliminary results of intraspinal pressure monitoring in patients with cervical spinal cord injury to help blood pressure management and the its effect on spinal cord perfusion pressure.
The optimal timing for surgical decompression to achieve a significant neurologic recovery in our cohort was within 4 h of injury (95% CI: 4-9 h). Increasing the time from injury to decompression or the degree of SCC significantly reduced the chances of significant neurologic improvement. Injury severity was a marginally significant predictor of neurologic recovery due to the strong correlation with SCC. Intraspinal pressure monitoring helped blood pressure management in achieving the target spinal cord perfusion pressure.
Our results show that patients with cervical tSCI should undergo surgical decompression as soon as possible, preferably in the first hours after injury and that increasing levels of spinal cord compression and severity of injury reduce the chances of neurologic recovery. Intraspinal pressure monitoring after decompression offers the possibility for individual spinal cord perfusion pressure management.

1. Introduction

Traumatic spinal cord injury (tSCI) is a devastating event, which often results in permanent neurologic disability. Current treatment strategies are limited and focused on secondary injury mitigation [1]. Early decompression of the injured spinal cord and blood pressure augmentation represent current treatment options, but controversies persist regarding the ideal timing for decompression and the value of targeted blood pressure. In addition, other factors as severity of spinal canal compromise (SCC) and severity of injury may influence nerologic outcome. The result of decompression is a drop in intraspinal pressure (ISP) and better spinal cord perfusion, but spinal cord perfusion pressure (SCPP) my not only be compromised by spinal cord compression due to bony fragments and hematoma, but also due to intrinsic oedema in the noncompliant dural space [1-3]. On the other hand, SCPP not only depends on ISP but also on mean arterial blood pressure (MAP)[4]. Therefore, continuous invasive mean arterial pressure (MAP) monitoring and management to prevent hypotension and a target MAP between 85 and 90 mm Hg is suggested for at least 5-7 days after injury [4]. However, the ideal MAP depends on ISP and ISP monitoring could help in MAP management. In the present paper the effects of the timing of decompression, SCC and severity of injury on neurological recovery in a cohort of subsequent patients with cervical tSCI are presented. In addition, intraspinal pressure monitoring was introduced to help blood pressure management and its effect on spinal cord perfusion pressure is presented [5].

2. Methods

A prospective cohort study was conducted to evaluate the effect of timing of decompression, degree of spinal canal compromise and severity of injury in a cohort of consecutive patients with acute cervical tSCI and fracture or dislocation of the subaxial cervical spine operated on within the first 24 h in our institution. To allow the comparison of a potential two AIS-grade improvement only patients presenting with overall ASIA Impairment Scale (AIS) grades A–C were enrolled. The degree of SCC was assessed on a midsagital T2-weighted MRI and re-examined after surgery with CT scan. The time of SD was defined as the time from injury to successful SD. Patients were neurologically reevaluated 6 months after injury. Analyses were exploratory and performed using R environment. Comparisons between groups were made by Mann-Whitney or Fisher exact tests. Receiver operating characteristic (ROC) curve was used to determine the optimal cut-point for the time from injury to SD in which a maximal gain in significant neurologic recovery is achieved [2]. In a later cohort of patients with cervical tSCI in addition to SD a pressure probe was inserted in the subarachnoid space and ISP was monitored in the first week in the ICU and the effect of ISP on blood pressure management was evaluated [2].

3. Outcome

The optimal time window for SD to achieve a neurologic recovery of at least two AIS grades in our cohort of 67 patients was within 4 h of injury (bootstrapped 5 h) (95% bootstrap CI: 4h, 9h). The association between neurologic recovery and time to SD, degree of SCC, and injury severity is presented in **Figure 1** [2]. Increasing the delay from injury to SD or increasing the degree of SCC before SD (controlling for other variables in the model) lowered the chances of a neurologic improvement of at least two AIS grades. There was also a tendency towards a lower probability of an at least two AIS grades neurologic recovery for AIS A patients, although it was not statistically significant [2]. The ISP was successfully monitored for one week in seven patients. ISP monitoring revealed a patient specific pattern of ISP dynamics with ISP ranging from 5 to 30 mm Hg significantly influencing MAP management (**Figure 2**).

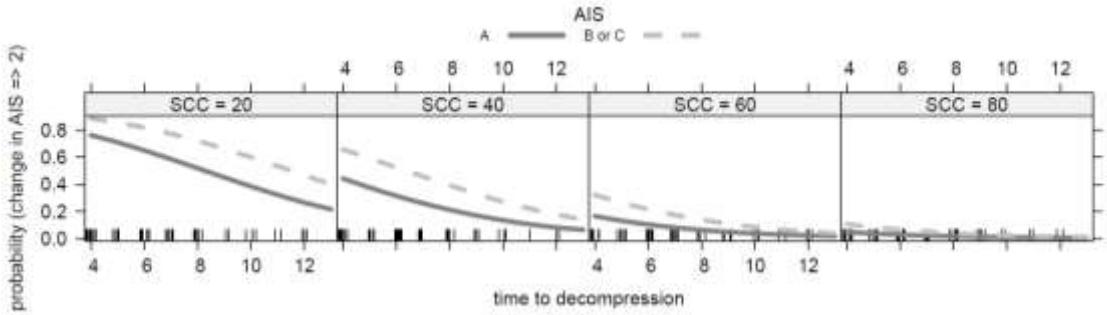

Figure 1. Plot of the estimated effects for different times to surgical decompression (SD), spinal canal compromise (SCC) before decompression and spinal cord injury severity (AIS A vs. AIS B or AIS C) at presentation on neurologic recovery of at least two AIS grades [2]). (AIS- ASIA Impairment Scale)

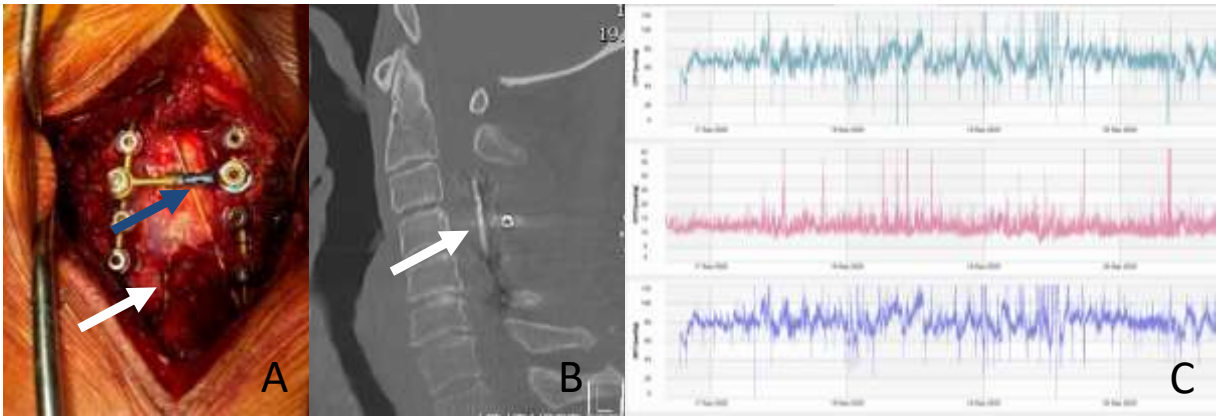

Figure 2. ISP monitoring in a patient with cervical spinal cord injury and posterior decompression and fusion. A: Intraopretaive picture of epidural (blue arrow) and intradural probe (white arrow); B: CT showing intradural probe (white arrow); C: Recordings of SCPP, ISP and MAP (ICP =ISP, CPP=SCPP, ART= MAP).

4. Discussion

Our results suggest that the first 4 to 9 h of cervical tSCI represent a window of opportunity for SD with the best chances for neurologic recovery entailing at least two AIS grades 6 months after injury. In addition to the SD timing, the degree of SCC was found to be a significant predictor of neurological recovery, with high degrees of SCC resulting in worse neurologic outcome in spite of decompression in the first hours after injury. In this view, we can assume there are patients whose severe primary injury and/or high degree of SCC make them unresponsive for significant neurologic recovery even to ultra-early SD, with degrees of SCC higher than 60% consistent with complete cervical tSCI at admission and the follow-up in our cohort [2]. This may be the result of more prominent local swelling of the spinal cord reported in patients with complete compared to patients with incomplete tSCI [6-9] leading to a devastating injury with higher SCC, which renders patients unresponsive to ultra-early SD. Interestingly, the preliminary data of ISP monitoring revealed a gradual elevation in the ISP profile in most patients after SD, but different the levels of maximal and prevalent ISP within the cohort suggesting a patient specific ISP profile, which resulted better management of MAP and SCPP. Surprisingly, our results suggest that the completeness of injury at admission, especially in the elderly, is not necessarily linked with elevated ISP. However, despite ISP monitoring results in improved SCPP due to better blood pressure regulation, the effect on neurologic recovery still has to be evaluated in further studies.

5. Conclusions

Our results show that patients with cervical tSCI should undergo surgical decompression as soon as possible, preferably in the first hours after injury and that increasing levels of spinal cord compression and severity of injury reduce the chances of neurologic recovery. Intraspinal pressure monitoring after decompression offers the possibility for individual spinal cord perfusion pressure management.

Acknowledgements

I thank Fajko F. Bajrović and Nataša Kejžar for scientific support.

References

1. Ahuja CS, Badhiwala JH, Fehlings MG. "Time is spine": the importance of early intervention for traumatic spinal cord injury. Spinal Cord. 2020; 58(9):1037-1039. doi: 10.1038/s41393-020-0477-8
2. Jug M, Kejžar N, Cimerman M, Bajrović FF. Window of opportunity for surgical decompression in patients with acute traumatic cervical spinal cord injury. J Neurosurg Spine, 2019; 27:1-9. doi: 10.3171/2019.10.SPINE19888

3. Jug M, Kejžar N, Vesel M, Al Mawed S, Dobravec M, Herman S, Bajrović FF. Neurological recovery after traumatic cervical spinal cord injury is superior if surgical decompression and instrumented fusion are performed within 8 hours versus 8 to 24 hours after injury: A Single center experience. J Neurotrauma. 2015; 32(18):1385-1392. doi: 10.1089/neu.2014.3767
4. Saadoun S, Chen S, Papadopoulos MC. Intraspinal pressure and spinal cord perfusion pressure predict neurological outcome after traumatic spinal cord injury. J Neurol Neurosurg Psychiatry. 2017; 88(5):452–453. doi: 10.1136/jnnp-2016-314600
5. Saadeh YS, Smith BW, Joseph JR, Jaffer SY, Buckingham MJ, Oppenlander ME, Szerlip NJ, Park P. The impact of blood pressure management after spinal cord injury: a systematic review of the literature. Neurosurg Focus. 2017; 43(5):E20. doi: 10.3171/2017.8.FOCUS17428
6. Mihai G, Nout YS, Tovar CA, Miller BA, Schmalbrock P, Bresnahan JC, et al. Longitudinal comparison of two severities of unilateral cervical spinal cord injury using magnetic resonance imaging in rats. J Neurotrauma. 2008; 25:1-18. doi: 10.1089/neu.2007.0338
7. Rutges JPHJ, Kwon BK, Heran M, Ailon T, Street JT, Dvorak MF, et al. A prospective serial MRI study following acute traumatic cervical spinal cord injury. Eur Spine J. 2017; 26:2324-2332. doi: 10.1007/s00586-017-5097-4
8. Shabani S, Kaushal M, Budde M, Kurpad SN, et al. Correlation of magnetic resonance diffusion tensor imaging parameters with American Spinal Injury Association score for prognostication and long-term outcomes. Neurosurg Focus. 2019; 46(3):E2. doi: 10.3171/2018.12.FOCUS18595
9. Miyanji F, Furlan JC, Aarabi B, Arnold PM, Fehlings MG, et al. Acute cervical traumatic spinal cord injury: MR imaging findings correlated with neurologic outcome--prospective study with 100 consecutive patients. Radiology. 2007; 243:820-827. doi: 10.1148/radiol.243306058

Research

Platelet-rich plasma injection following arthroscopic rotator cuff repair: Is there any benefit?

Ambrožič Miha[1], Kovačič Ladislav[2]
*University Clinical Centre Ljubljana, Clinical Department of Traumatology, Ljubljana, Slovenia
*marko.ambrozic@kclj.si

Abstract

Rotator cuff repair remains a non-negligible source of iterative ruptures after reconstruction and disappointing functional results, especially in degenerative tendons with poor healing potential. Autologous platelet-rich plasma (PRP) has been used to improve tendon healing and potentially reduce the incidence of subsequent tendon re-tears. Objective of this work is to investigate recent literature for differences in re-tear rates and patient-reported outcomes (PROMs), after augmentation of arthroscopic rotator cuff repair with PRP. A systematic search of online databases PubMed, Google Scholar and Cochrane Library was conducted, in accordance with the PRISMA guidelines, from the 20th of February until 22nd of March. Prospective randomised clinical studies, comparing PROMs and structural results after rotator cuff augmentation with PRP, were included. Articles published in the last five years were taken into account. Only level of evidence 1 and 2 studies were considered. The search strategy ultimately identified 10 randomised control studies (RCTs), eligible for inclusion. A number of different, yet established PROMs, and imaging techniques were applied. Groups were equally divided into PRP-augmented groups and control groups. Two studies showed reduced pain levels in short-term outcomes, one study outlined better results in PROMs and one study displayed significantly better strength in PRP groups. Two level 1 studies and one level 2 study showed significantly less re-tear rates in PRP groups. Other investigated studies gave no significant difference in results, for either group. There is still no clear evidence in recent literature, to support routine use of PRP in arthroscopic rotator cuff repair. Radiological results and PROMs have displayed a trend towards less re-tears and better early functional outcomes (with reduced pain), in PRP groups. Standardisation of PRP preparation and application has been advocated.

1. Introduction

Rotator cuff tear is one of the most common shoulder conditions, that drives patients to seek treatment [1]. Its increase in incidence is due to tendon degeneration with increasing age in population, which leads to pain and functional limitation. The gold standard for treatment is arthroscopic repair when conventional treatment fails [2]. Even though this procedure is highly effective, concerns still exist about the demanding postoperative rehabilitation and the risk of tear recurrence; no particular surgical technique has showed superiority in regard to rotator cuff tendon structure healing [3]. Functional outcomes have been correlated with postoperative integrity of the rotator cuff [4]. The incidence of re-tears following rotator cuff repair has been reported to be as high as 80% to 90% in the radiology literature and as high as 57% in the orthopaedic literature [5,6], with mean re-tear rates still remaining close to 30% [7,8]. Re-tear rates have been reported higher in degenerative cuff (advanced age), large tears and fatty infiltration of rotator cuff muscles [2,9]. Tendon re-tears may be due to a specific re-injury at repair site but may also reflect incomplete or failed primary healing after surgery [4,10]. Because of significant rate of re-tears, different techniques were developed in order to improve fixation strength. A double-row repair and anchors with stronger suture material and greater pull-out strength were introduced [11,12]. Whilst mechanical problems were addressed, the optimal biologic environment for healing still remained a problem. For these reasons, new biological strategies, use of so - called ortobiologic substances, such as autologous plasma serum and mesenchymal stem cells (MSCs) [13], has been proposed to overcome these drawbacks [14]. The improvement and quickening of the repair mechanisms of the tendon would thus reduce the rate of post-surgical recurrence, and enhance long-term shoulder functionality after arthroscopic repair [15]. One of broadly used ortobiologic preparations has become platelet-rich plasma (PRP) [13]. PRP is an autologous blood product acquired from part of plasma fraction, created via centrifugation of whole blood. By definition it has a platelet concentration above physiological levels (2-5 times that of a normal value) [16]. It has gained wide popularity in sports medicine, orthopaedics and traumatology, but it's clinical efficacy in rotator cuff healing is still unclear.

PRP is basically a blood-derived plasma suspension containing high concentration of platelets. Although the initial focus on platelets centred on their role in coagulation, it was soon discovered that platelets harbour over 1,100 proteins, including growth factors (GFs), such as such as platelet-derived growth factor (PDGF), transforming growth factor – beta (TGF - β) and vascular endothelial growth factor (VEGF); immune system messengers, enzymes, and other bioactive compounds, that are involved in various aspects of tissue repair [17–19]. The administered platelets also synthesize additional cytokines and bioactive compounds, which coincide with the inflammatory and repair process of the tendon [20–22]. Supra-physiological levels of GFs can therefore theoretically stimulate resolution of chronic pathological processes in tissues, that don't have a rich blood supply, like tendons, ligaments and cartilage [16]. While the mechanism and effect of PRP has been demonstrated

in vitro by different studies [23], clear clinical benefit has yet to be proven. Since the beginning of PRP's use, a number of different preparations have been developed and administered in an attempt to augment the repair. A larger portion of diversity comes with a preparation of different cell ratio (pure platelet-rich plasma or P-PRP, leukocyte-platelet-rich plasma or L-PRP). PRP can also be applied as liquid (with or without calcium-based cascade activation) or can be implanted as a solid matrix, in the form of platelet-rich fibrin (PRF). Similarly to PRP, two forms of PRF exist, regarding their cell ratio: pure platelet-rich fibrin (P-PRF) and leukocyte-rich fibrin (L-PRF). The four types of preparations of PRP were described in one of the first classifications, by Ehrenfest et al [24]. PRF differs from PRP, in that blood is collected without the use of anticoagulant or activator and is immediately centrifuged and administered. In PRP, calcium chloride has an activating role in order to start fibrinogen polymerisation. It allows an increased platelet degranulation [25]. If PRP is created in the absence of anticoagulant (citrate dextrose-A or citrate phosphate dextrose), the resulting PRP product is subject to the normal clotting cascade, and, thus, consideration must be given to the time between blood draw and PRP injection.

This review will outline the current evidence for the novel frontier in the management of rotator cuff disease, with PRP augmentation of arthroscopic surgical repair, and its effect on functional result and re-tear rates.

2. Methods

A systematic review of literature was conducted in accordance with the PRISMA guidelines using the three major online database sources: PubMed, Cochrane Library and Google Scholar. Articles published in English were considered for eligibility. Only primary research was considered for review. Data-base search started on 20th of February 2021 and ended on the 22nd of March 2021. Time frame was set for the last 5 years (January 2015 - December 2020). No other search strategies were employed. Data was extracted uniformly, and gathered in Microsoft Excel 2021, version 16.47.1. Search words for Google Scholar were set as: »rotator cuff + plasma«; for PubMed as: rotator cuff AND plasma (only clinical trials and randomised clinical trials were included); and for Cochrane library as: rotator cuff, repair, plasma. Search platforms included in Cochrane library were PubMed, Embase, CT.gov, CINAHIL, ICTRP.

Inclusion criteria: prospective clinical study with level of evidence 1 or 2, arthroscopically repaired rotator cuff tendon, imaging control after a period of time, for evaluation of repair integrity, at least one acknowledged internationally used patient-reported outcome measure. Studies had to compare one group with PRP augmentation after arthroscopic reconstruction (any kind or form of PRP) and control group with only arthroscopically reconstructed tendon, without augmentation. Timing of PRP application was not considered (intraoperatively or delayed).

Exclusion criteria: conservative treatment, augmentation with other substrate than PRP, any pathology other than full-thickness rotator cuff tendon rupture, any form of research other than prospective clinical study (meta-analyses, review articles, case reports and case-control

studies, technique descriptions, letters to editors, expert opinion, in-vitro studies, animal research, etc.) were excluded. Non-English papers were not evaluated.

3. Results

Google scholar: 170 published articles were gathered. After reviewing only the titles of studies, 73 were eliminated, mostly due to type of treatment (conservative). After reading through abstracts, another 30 were eliminated for various reasons. We ended up with 7 prospective randomised studies. PubMed: 19 articles met inclusion criteria. Duplicated articles from Google Scholar were excluded. After reviewing titles and abstracts, only 8 studies remained, mainly because of conservative treatment for rotator cuff tears. Cochrane library: 42 articles were found. Duplicated articles from Google Scholar and PubMed were excluded. After reviewing titles and abstracts of remaining articles, 4 articles were left. 16 articles were marked as duplicated. From 170 published studies we ended up with 18, potentially eligible studies. 2 studies were later identified as biomechanical studies and were excluded. Another 2 studies were excluded because of eligibility problems (not able to retrieve full text). After thoroughly reviewing remaining studies, we excluded 4 studies, that weren't appraised as level of evidence 1 or 2. In the end, 10 eligible randomised control studies (RCTs) were appraised for analysis [20,21,26–33] (**Table 1, Table 2**).

Surgical repair was done arthroscopically in all included studies. Unless mentioned specifically, subacromial decompression and tenotomy (or tenodesis) of the long head of biceps tendon was done, when deemed necessary by the surgeon. When applying PRP at the site of the repair, saline was removed from the shoulder, thus applying PRP in a relatively dry manner and minimising the so-called »washout effect«. When delayed application was used, it was done under ultrasound control at the site of tendon repair [21,27,31]. Pure-PRP or LP-PRP (leukocyte-poor PRP) was used in research by D'Ambrosi, Pandey, Ebert, Flury, Zhang and Malavolta ; LP-PRP gel was used in a research by Jo [34]; L-PRP (leukocyte-rich PRP) was used in research by Snow [27], PRPFM (PRP in fibrin matrix) was used in research by Walsh [29].

Table 1: Study characteristics and patient reported outcome measures results.

Author	Title	Ref	Research design	LoE	Population Size of tear	Type of treatment and number of patients	Outcome measures	Follow-up	Conclusion
D'Ambrosi et al	Platelet-rich plasma supplementation in arthroscopic repair of full-thickness rotator cuff tears: a randomised clinical trial.	Musculoskelet Surg 2016	RCT, double-blinded	1	40 patients 20 PRP : 20 NA 40-75 years of age Degenerative full-thickness SSP tear, grade C2-C3 (Snyder classification)	arthroscopic (single-row) biceps tenotomy in all cases pure PRP intraop. appl.	DASH: PRP vs NA (p > 0,05) Constant: PRP vs NA (p > 0,05) VAS: 2.5 +/- 1.9 (PRP) vs 5.3 +/- 2.1 NA at 1 week, 1.5 PRP vs 3.2 at 1 month (p < 0,05)	VAS for 1 month Constant and Dash at 6 months	Reduction in pain in short-term follow-up, no differences in PROMs
Malavolta et al	Clinical and structural evaluations of rotator cuff repair with and without added platelet-rich plasma at 5-year follow-up	Am J Sports Med 2018	RCT, double-blinded	2	51 patients 26 PRP : 25 NA Complete SSP tears, retraction less than 3 cm	arthroscopic (single-row), acromioplasty L-PRP intraop. appl.	UCLA (p > 0,05) Constant (p > 0,05) VAS (p > 0,05)	6, 12, 24, 60 months	No differences in PROMs
Pandey et al	Does application of moderately concentrated platelet-rich plasma improve clinical and structural outcome after arthroscopic repair of medium-sized to large rotator cuff tear? A randomized controlled trial	J Shoulder Elbow Surg 2018	RCT double-blinded	2	102 patients 52 PRP : 50 NA Full-thickness Medium (1-3cm) to large (3-5 cm) posterosuperior RC tear (Cofield class.)	arthroscopic (single-row) pure PRP intraop. appl.	VAS (p < 0,05) Constant (p < 0,05 at 12 and 24 months) UCLA (p < 0,05 at 6, 12, 24 months) ASES (p > 0,05)	VAS for 1, 3, and 6 months Constant and UCLA 6, 12, 24 months	Reduction in pain in short-term follow-up and better PROMs (Constant and UCLA)
Ebert et al	A midterm evaluation of postoperative platelet-rich plasma injections on arthroscopic supraspinatus repair	AJSM 2017	RCT	1	60 patients initially 27 PRP : 28 NA (PRP applied 7 and 14 days after surgery) Only SSP, full-thickness tear, < 20 mm AP wide	arthroscopic (double-row) pure PRP intraop. appl.	strength (Constant subscale): p = 0,008 for PRP group quickDASH, OSS, VAS: p > 0,05	3,5 years (range from 36-51 moths)	Strength measurement better in PRP group, other scores no additional benefit
Flury et al	Does pure platelet-rich plasma affect postoperative clinical outcomes after arthroscopic rotator cuff repair? A randomized control trial.	AJSM PreView 2018	RCT triple-blinded	1	120 patients 60 PRP: 60 NA (ropivacaine) After attrition 51:51 Isolated SSP tendon rupture	arthroscopic (double-row) pure PRP delayed 7 and 14 days	OSS (primary endpoint; 30.7 vs 32.9, p = 0.221) Constant ASES quickDASH EuroQol5 pain diary, VAS	3, 6, 24 months	No differences in PROMs, Smoking as a significant effect modifier (in OSS)
Jo et al	Platelet-rich plasma for arthroscopic repair of medium to large rotator cuff tears. A randomised control trial	AJSM 2015	RCT	1	74 patients 37 PRP : 37 NA 45 – 85 years of age medium to large rupture (1-5 cm)	arthroscopic (double-row) PRP gel intraop. appl.	Constant ASES SPADI SST VAS results in all p > 0,05	3 months	No significant differences in PROMs
Wang et al	Do postoperative platelet-rich plasma injections accelerate early tendon healing and functional recovery after arthroscopic supraspinatus repair? A randomised control trial	AJSM PreView 2015	RCT	1	60 patients 30 PRP : 30 NA full-thickness SSP tears < 20 mm in active individual	arthroscopic (double-row) pure PRP delayed 7 and 14 days	OSS quickDASH Short form-12 Active range of motion (goniometer) Isokinetic strength all values had p > 0,05	6, 12, 16 weeks	No significant differences in PROMs
Snow et al	The effect of delayed injection of leukocyte-rich platelet-rich plasma (LR-PRP) following rotator cuff repair on patient function: a randomised double-blind trial	Arthroscopy 2019	RCT, double-blind	2	87 patients 40 PRP : 47 NA full-thickness tear from 1-5 cm	arthroscopic (single/double-row) L-PRP delayed between 10 to 14 days	Constant ASES WORC DASH p > 0,05 at all check points	1 year	No significant differences in PROMs
Walsh et al	Platelet-rich plasma in fibrin matrix to augment rotator cuff repair: a prospective, single-blinded, randomized study with 2-year follow-up	J Shoulder Elbow 2018	RCT, single-blinded	2	76 patients PRPFM 28 : NA 41 full-thickness SSP and/or ISP tear 40-80 years of age	arthroscopic (double-row) PRPFM intraop. appl.	WORC SST strength test dynamometer VAS p > 0,05 at all check points	8 and 24 months	No significant differences in functional outcomes, level of pain or strength
Zhang et al	The effect of platelet-rich plasma on arthroscopic double-row rotator cuff repair: a clinical study with 12 month follow-up	Acta Orthop Traumatol Turc 2016	RCT	1	60 patients 30 PRP : 30 NA full-thickness, more than 1 cm	arthroscopic (double-row) pure-PRP intraop. appl.	DASH Constant VAS active movements in forward flexion and rotations all measures p > 0,05	6 and 12 months	No significant differences in PROMs

LoE-level of evidence, NA- non-augmentated, SSP – supraspinatus, RC – rotator cuff, AP – anteroposterior, PROMs – patient-reported outcome measures, OSS – Oxford Shoulder Score, Constant – Constant-Murley Score, SST – Simple Shoulder Test, UCLA – University of California-Los Angeles score, ASES – The American Shoulder and Elbow Surgeons score, VAS – visual analogue scale, SPADI – Shoulder Pain and Disability Index, US – ultrasound, MRI – magnetic resonance imaging, WORC – Western Ontario, Rotator Cuff score, CSA – cross-sectional area

Table 2: Imaging results with retear rates and complications.

Author	Type of imaging used	Follow-up	Retear rate	Outcome measure	Results	Other complications	Conclusion
D'Ambrosi et al	US	6 months	No retears	3-point rating scale (not validated)	8.5 +/- 1.2 (PRP) 7.9 +/- 1.5 (NA) p = 0,05	No complications	No significant difference in repair quality or retear rates
Malavolta et al	MRI	60 months	PRP: 7 partial thickness NA: 1 full-thickness 11 partial thickness	Sugaya PRP: 7 type III NA: 11 type III 1 type IV	p = 0,203	1 patient in each group with stiff shoulder p = 0,999	No significant difference in repair quality or retear rates
Pandey et al	US (doppler)	2 years	PRP: 2 (4%) NA: 10 (20%)	5-point rating scale (1-3 normal, 4-5 retear or failure to heal) Vascularity assessment (absent flow = 0 and 1, present flow = 2 and 3)	p = 0,035, only for large tears (1.6) Doppler vascularity better in PRP at 3 months (p < 0,05)	No complications	Significantly less retears for larger tears, better structural outcome and increased vascularity No effect in medium-sized tears
Ebert et al	MRI (2 blinded radiologists)	3,5 years	2 symptomatic, retears in NA (partial) and 2 in PRP (full-thickness)	Sugaya: PRP 66.7% as grade 1, NA 64.3% as grade 1	p > 0,05 retears in PRP beyond 16 weeks retears in NA under 16 weeks	not reported	Applications of PRP at 7 and 14 days after surgery provided no additional benefit to tendon integrity
Flury et al	US MRI	6 (US), 24 months	PRP: 5 NA: 9 retears	Sugaya	p = 0,285 for recurrent supraspinatus tendon defects	local complications: 40.7% in PRP (1,3x more likely) 30,5% in NA one infection with Cutibac. acnes in PRP	No significant difference in recurrent SSP tendon defect
Jo et al	MRI	3 months	PRP: 1 of 33 (3 %) NA: 6 of 30 (20%)	CSA of SSP	p = 0.032 for retear rate p = 0,014 for CSA	not reported	Decreased retear rates and increased CSA of SSP
Wang et al	MRI	16 weeks	PRP: 0% full-thickness retear NA: 7% full-thickness retear	Sugaya	p = 0,35	not reported	No significant differences in structural outcomes
Snow et al	MRI	3 and 12 months 39 PRP : 38 NA	PRP: 15,3% NA: 21%	Sugaya Goutallier	Retears: p = 0.77 Fatty infiltration in NA group higher (p = 0.32)	not reported	No difference in retear rates, higher rates of fatty infiltration in NA group
Walsh et al	MRI	6 months 86 patients	PRPFM: 7% NA: 10%	Sugaya	p > 0,05	not reported	No significant differences in retear rates
Zheng et al	MRI	12 months	PRP: 9 (30%) NA: 4 (14%)	Fuchs	p < 0,05	not reported	Lower recurrence rates

NA- non-augmented, SSP – supraspinatus, RC – rotator cuff, AP – anteroposterior, PROMs – patient-reported outcome measures, OSS – Oxford Shoulder Score, Constant – Constant-Murley Score, SST – Simple Shoulder Test, UCLA – University of California-Los Angeles score, ASES – The American Shoulder and Elbow Surgeons score, VAS – visual analogue scale, SPADI – Shoulder Pain and Disability Index, US – ultrasound, MRI – magnetic resonance imaging, WORC – Western Ontario, Rotator Cuff score, CSA – cross-sectional area

4. Functional results

Most of the reviewed studies have shown no significant difference in patient-reported outcome measures (PROMs) between groups [21,27–30,34]. Yet, there are some studies that showed better clinical outcomes in early follow-up. In a study by Pandey et al [20], results were better at 12 and 24 months in Constant scores (average 92.6 (standard deviation 5.07) PRP vs 88.9 (8.47) control, p = 0.008; and 93.2 (4.97) PRP vs 87.6 (8.12) control, p = 0.0001) and at 6, 12 and 24 months in UCLA scores (25.40 (1.58) PRP vs 23.50 (3.55) control, p = 0.002; and 34.73 (0.69) PRP vs 33.09 (3.67) control, p = 0.002; 34.75 (0.72) PRP vs 32.22 (3.55) control; p = 0.0001). Groups in the study were relatively heterogeneous regarding tear size, male predominance and they were without established consensus on treatment of concomitant lesions; but power analysis was strong and loss to attrition was small. D'Ambrosi et al [26] have published a double-blinded RCT study, where they compared two groups. One group had only single-row repair, the other had repair and PRP augmentation. Long head of biceps tenotomy was done without exception. Full-thickness

tears were included with classification of C2-C3 by Snyder on MRI [35]. Visual analogue scale (VAS), Constant-Murley score and the Disabilities of the Arm, Shoulder and Hand score (DASH), all showed significant improvement after operation in regard to preoperative scores, but displayed no significant differences between groups. There was however a significantly better VAS in the first week and during the first month (2.5 +/- 1.9 vs 5.3 +/- 2.1; $p < 0.05$). PRP thus led to a reduction in pain during a short-term follow-up (26). However, study had the smallest number of patients enrolled (20 in each group). Similar short-term pain reduction was demonstrated by Pandey et al (at 1, 3, and 6 months, but not latter). In a longer follow-up of 3.5 years by Ebert et al [31], there was a significant difference in Constant subscale of strength found, after adjusting for gender, in the PRP group (95% CI, 1.0-5.7; $p = 0.006$).

5. Radiological results

To evaluate quality and continuity of a repair, imaging control has to be employed, such as ultrasound (US) and/or magnetic resonance imaging (MRI). Jo et al have proved a decreased rate of re-tears in PRP group (3%) vs control group (20%); p=0.032 [34]. They also showed an increased cross-sectional area (CSA) of supraspinatus muscle on MRI, with significant difference between groups in benefit of PRP group (-36.76 ± 45.31 mm^2 in the PRP group and 267.47 ± 47.26 mm^2 in the conventional group ($p = 0.014$)). This parameter is however not reported in other research, so inter-study comparisons cannot be made. They also had a lower follow-up rate of MRI in the control group [34]. Pandey at al demonstrated a lower incidence of re-tears with large rotator cuff ruptures (3-5 cm), which was statistically significant in favour of PRP (1:6 re-tears, $p < 0.035$). Subjective assessment by US has showed significantly increased vascularity in augmented repairs (3 and 6 months; $p = 0.01$ to 0.0001) and in peri bursal tissue (3, 6 and 12 months; $p = 0.003$); results are influenced by subjective measurements and by an on-site designed score, that wasn't validated [20]. All results are based on a validated, morphological scoring system as a measurement tool, but still remain subjective and qualitative [31]. Other studies demonstrated no statistically significant differences between PRP and control groups in structural tendon quality or rate of re-tears.

6. Discussion

The aim of our review article was to recognise any relevant benefit, in augmenting arthroscopic rotator cuff repair with PRP, special focus being on patient-reported outcome measures and retear rates. Majority of studies haven't found differences, but there were a few reported statistically significant results. There doesn't seem to be any considerable advantage in compositional differences, production or carrier forms of PRP, neither is there a known the optimal timing of application.

Significant differences in level of pain in short-term outcomes, were published in a study by D'Ambrosi et al [26]. They compared groups with single-row arthroscopic repair, with and without PRP augmentation. Study had reportedly low risk of any bias [36], albeit with a relatively low number of patients. VAS, Constant-Murley score and DASH score in all groups

showed significant improvement in regard to preoperative scores but displayed no significant differences between groups. There was however a lower VAS in the first week and during the first month ($p < 0.05$) in PRP group. PRP thus led to a reduction in pain during a short-term follow-up [26], but it is however a study with the smallest number of patients enrolled. A possible explanation for this result, as explained by Asfaha, could be analgesic properties of platelets (analgesic mechanism related to protease-activated receptor-4 (or PAR4) peptides [37]. Pandey stated, that the analgesic effects of PRP are dose-dependent and that proper PRP can also exert a good analgesic effects [20]. There was a short-term comparison in pain levels by Flury et al, that resulted in the same pain-reducing effect of pure PRP injection, compared to anaesthetic (ropivacaine) injection [30]. In the same study, smoking at baseline was associated with decreased effect on Oxford Shoulder Score (OSS) in PRP group ($p=0.004$), and persisted at all time points. Strength of rotator cuff muscles was a parameter, that was not routinely independently observed and measured in studies. It is however a part of some patient-reported outcome measures, like Constant-Murley score [38]. Ebert et al have made a sub-analysis, adjusted to gender, and found out, that strength at a mean time of 3,5 years post-op was significantly better in PRP group ($p = 0.006$) [31]. Walsh et all have however not found any significant differences, in separately measured strength with dynamometer [29]. PRP augmentation gave better PROMs in two other studies. In a study by Pandey et al (2016)[20], results were significantly different at 12 and 24 months in Constant scores ($p = 0.008$, $p = 0.0001$, respectively) and at 6, 12 and 24 months in UCLA scores ($p = 0.002$; $p = 0.002$; $p = 0.0001$, respectively). Although differences were proven, there is a tendency towards bias in PROMs measurements, since patients were not blinded. Also, there was noted a ceiling effect in using measurement tools, like quickDASH and OSS, which are not sufficiently sensitive to detect differences in higher functioning shoulders [31].

Retear rate is one of the most studied outcomes in rotator cuff surgery in general and has a marked influence on functional outcome. Sonnabend et al [39], in a primate model of rotator cuff repair, showed that a significant proportion of Sharpey fibres begin to reconstitute at 3 months with maturation at 4 months after surgery. Thus, the early tendon healing stage is critical for long-term success of rotator cuff repair. There have been previous reports of improved structural tendon integrity, but only for small to medium-sized tears [40–42]. In a recent meta-analysis by Cavendish et al. (2020), they report a 25% reduction in the risk of repair failure with PRP augmentation, with low heterogeneity among 16 studies included. A significant protective effect was seen for studies, which included only small to medium tears (7 studies) ($p = 0.007$) and studies including large or massive tears (9 studies) ($p<0.001$) [36]. Although Malavolta et al. (2018) [28] haven't reported any statistically significant differences, they made a remark, that a better panorama was observed in PRP group (higher frequency of Sugaya types I and II and lower frequency of Sugaya types III, IV, and V), which may mean a positive effect of PRP in tendon healing. Most retears do occur in a period of the first 6 months [43], but only a few studies had a longer follow-up to asses retear rates [28,31]. Should a benefit exist in creating a more robust repair and therefore

creating a tendon, that is more resistant to future reinjuries, then RCTs with a longer follow-up are essential to evaluate the full potential benefit of PRP [31]. Research by Pandey et al (2016) had shown a decreased retear rate in PRP group for large tears (3-5 cm), but not for medium-sized tears. Doppler US control displayed increased vascularity, as subjectively assessed by an experienced radiologist in repair site at 3 months' follow-up. They theorize in discussion, that adding PRP produces an angiogenesis effect, especially in early phase up to 3 months, even in relatively avascular fields, and may stimulate healing of tendon [20]. Jo et al. (2015) have proved a decreased rate of retears in PRP group (3%) vs control group (20%) [34]. They included patients with medium- to large-sized tears, as this is the population where majority of patients are eligible for rotator cuff repair; also, smaller ruptures would not benefit largely from PRP, and massive ones would have to much collateral variables, that would make results meaningful [34].

Although not included for analysis in this review article, we have to acknowledge three very recent meta-analyses [36,44,45]. They also screened studies for PROMs and structural integrity and had some promising results. All patients underwent arthroscopic rotator cuff repair. Yang et al revealed a significant decrease in re-tear rate in PRP groups ($p = 0.0009$). They included 7 RCTs from 2013 to 2018 with 273 patients in the PRP groups and 268 patients in control groups [44]. Meta-analysis also revealed a difference in PROMs and pain levels in short-term outcomes Constant score ($p = 0.0004$), short-term UCLA score ($p = 0.0001$), and short-term VAS ($p = 0.002$). Wang et al have published a meta-analysis of randomised controlled studies, comprised of 566 patients altogether. They concluded, that although long-term re-tear rates and functional scores didn't show any statistical difference, the short-term outcomes in Constant and UCLA scores, together with re-tear rates and VAS scores, showed statistically significant differences, in favour of PRP groups [45]. Based on their meta-analysis they conservatively infer that PRP can only promote the recovery of short-term shoulder function, especially in single-row fixation. Cavendish reports in a 2020 meta-analysis, that among 16 studies investigating rotator cuff repairs, PRP augmentation resulted in a 25% reduction in the risk of repair failure (as defined by postoperative imaging studies including magnetic resonance imaging, ultrasound, and computed tomography) (pooled risk ratio [RR], 0.75; 95% confidence interval [CI], 0.67-0.85), with low heterogeneity among the included studies ($I^2 = 0\%$) (36). Intraoperative administration of PRP has thus led to a consistent reduction in the failure risk of rotator cuff repairs, regardless of tear size [36].

One important reason for controversies in interpreting outcomes, is the difference of PRP's used. These include: variation of preparation, variable cell concentration, viscosity level (liquid, gel or solid form), volume and number of applications, activation or no activation, and method of application [32]. Therefore, because all PRP products are not the same, the success or failure of specific PRP or PRP-related product cannot be universally applied to all [46]. It is not practical to standardize preparation and application of PRP in daily routine practice, but efforts should be sought in clinical research, to standardize the process and to provide adequate information that could characterize PRP [34]. Even so, important variations in the quantity and quality of platelets and growth factors can be detected in PRP

of different individuals [47]. Barberet al., (2011) concluded that the addition of two platelet-rich plasma fibrin matrix (PRPFM) constructs sutured into a primary rotator cuff tendon resulted in lower re-tear rates identified on magnetic resonance imaging (MRI) than repairs without the constructs [48]. Bergeson et al., (2012) however has not shown any improved retear rates or functional scores compared with control group [49]. Their study thus suggests a benefit with PRP for improving pain-free abduction strength.

The role of leukocytes in PRP is conflicting in the literature; leukocytes in fact increase catabolic signalling molecules. Furthermore, L-PRP has a proinflammatory effect when injected in rabbits and increases the levels of MMPs when assayed in tenocyte cultures [50,51]. Other studies, instead, report the positive role of leukocytes as regulating immune agents and as anti-infectious. The leukocyte content does not seem to induce negative effects or impair the potentially beneficial effects of PRP and no uncontrolled immune reactions of L-PRPs have been reported either; on the contrary, the use of L-PRP could diminish inflammation of the treated sites [52,53].

Another observed treatment difference is timing of PRP administration. Three studies have used a delayed technique, administering the substrate with the help of ultrasound-guided injection [21,30,31]. Interval from surgery to administration was 7 and 14 days (research by Ebert et al. (2017) [31] al and Wang et al. (2017) [21], and between 10 to 14 days in study by Snow et al. (2020) [27]. As explained by Wang et al. (2017), there are two reasons for this delayed technique. First being, sustained up-regulation. After activation, platelets release growth factors almost immediately with total elution within 1 hour [46], and the half-life of growth factors is a matter of minutes to hours [54]. However, it has been acknowledged that biological augmentation of tendon repairs too early in the tendon healing cascade may be ineffective [55]. Platelet-derived growth factors at day 7 have a more pronounced effect on tendon cellular maturation and biomechanical strength, than earlier application. Growth factors, including bone morphogenetic protein–13 (BMP- 13), platelet-derived growth factor–B, and transforming growth factor–B1, are expressed maximally at days 7 and 14, and the cytokine-mediated temporal expression of collagen types I and III increases from day 7 onward. The second reason being purely mechanical; delayed delivery of PRP can avoid the potential dilution and wash-out effect of arthroscopic administration [21]. Concentration of administered PRP at the site of repair is hence believed greater.

We still don't know which patients would benefit from augmented PRP treatment the most. There is no consensus on tear location, tear size and tendon quality. A recent study also reported a decrease of growth-factor receptor expression in ligament fibroblasts as a function of age [56]. Thus, it is not only the presence of growth factors that dictate the level of the healing response but also the presence and ability of target cells to use these factors in the appropriate manner. It is well established that fatty degeneration and muscle atrophy are independent predictors of poor functional outcomes. In study by Snow et al. (2020) [27], there was a significant reduction in fatty atrophy progression following repair in the PRP group. The mechanism of fatty atrophy is unclear. Suprascapular nerve entrapment has been implicated; however, there is evidence for a cellular mechanism regulated through the Wnt

pathway [57]. Takase et al. (2017) [58] have demonstrated, that PRP promoted proliferation of myoblast cells while inhibiting adipogenic differentiation of myoblast cells and suppressing fatty degeneration change in rat torn rotator cuff muscles.
Beyond PRP application treatment, there are also two other important factors, that surely have an effect on the final result: surgery and rehabilitation protocol. Some surgeons do a single-row fixation, others may trust in a double-row fixation; and there are also new techniques, like knotless bridge repair, incorporating biceps tendon, bursal tissue, and so on. With the exception of one study [26], there is only surgeon's preference in decision making about treatment of concomitant injuries, e.g. biceps tenotomy or tenodesis and acromioplasty. Even if we could standardise the surgical part, differences in surgical technique are in-avoidable, hence making comparison between studies even more difficult. Rehabilitation protocols after surgical treatment did differ but were still quite conservative for start of active motion. Active exercises were uniformly reserved until after 6th postoperative week, in which time only passive exercises were allowed. Rapid passive rehabilitation was omitted in only one study [34]. Rehabilitation protocol would continue with progressive active exercises and gentle strengthening program would usually commence after 10th week post-op.

7. Conclusion

Orthobiologic augmentation is a novel treatment in rotator cuff repairs, and PRP has been used often as substrate of choice. Augmentation in arthroscopic RC tendon repair has shown promising results. Although there still isn't enough evidence to provide clear advantage for routine use in clinical practice, there are some benefits. Short-term pain reduction could allow for more rapid mobilisation and also improvement in functionality, while lower retear rates optimistically suggest better healing and superior treatment outcomes.

References

1. Gomoll AH, Katz JN, Warner JJP, Millett PJ. Rotator cuff disorders: Recognition and management among patients with shoulder pain. Arthritis Rheum. 2004; 50(12):3751–3761. doi: 10.1002/art.20668
2. Rashid MS, Cooper C, Cook J, Cooper D, Dakin SG, Snelling S, et al. Increasing age and tear size reduce rotator cuff repair healing rate at 1 year. Acta Orthop. 2017; 88(6):606–611. doi:10.1080/17453674.2017.1370844
3. Ji X, Bi C, Wang F, Wang Q. Arthroscopic versus mini-open rotator cuff repair: an up-to-date meta-analysis of randomized controlled trials. Arthrosc J Arthrosc Relat Surg. 2015; 31(1):118–124. doi: 10.1016/j.arthro.2014.08.017
4. Boileau P. Arthroscopic repair of full-thickness tears of the supraspinatus: does the tendon really heal? J Bone Jt Surg Am. 2005; 87(6):1229. doi: 10.2106/JBJS.D.02035
5. Charousset C, Bellaïche L, Kalra K, Petrover D. Arthroscopic repair of full-thickness rotator cuff tears: is there tendon healing in patients aged 65 years or older? Arthroscopy. 2010; 26(3):302–309. doi: 10.1016/j.arthro.2009.08.027

6. Liem D, Bartl C, Lichtenberg S, Magosch P, Habermeyer P. Clinical outcome and tendon integrity of arthroscopic versus mini-open supraspinatus tendon repair: a magnetic resonance imaging–controlled matched-pair analysis. Arthroscopy. 2007; 23(5):514–521. doi: 10.1016/j.arthro.2006.12.028
7. Aurégan J-C, Klouche S, Levy B, Bauer T, Rousselin B, Ferrand M, et al. Autologous Conditioned Plasma for tendon healing following arthroscopic rotator cuff repair. Prospective comparative assessment with magnetic resonance arthrography at 6 months' follow-up. Orthop Traumatol Surg Res. 2019; 105(2):245–249. doi:10.1016/j.otsr.2019.01.00
8. McElvany MD, McGoldrick E, Gee AO, Neradilek MB, Matsen FA. Rotator Cuff Repair: Published evidence on factors associated with repair integrity and clinical outcome. Am J Sports Med. 2015; 43(2):491–500. doi: 10.1177/0363546514529644
9. Mall NA, Tanaka MJ, Choi LS, Paletta GA. Factors affecting rotator cuff healing. J Bone Joint Surg. 2014; 96(9):778–788. doi: 10.2106/JBJS.M.00583
10. Carpenter JE, Thomopoulos S, Flanagan CL, DeBano CM, Soslowsky J, Arbor A. Rotator cuff defect healing: A biomechanical and histologic analysis in an animal model. 1998; 7(6):599-605. doi: 10.1016/s1058-2746(98)90007-6
11. Park MC, ElAttrache NS, Ahmad CS, Tibone JE. "Transosseous-equivalent" rotator cuff repair technique. Arthroscopy. 2006; 22(12):1360.e1-1360.e5. doi:10.1016/j.arthro.2006.07.017
12. Virk MS, Bruce B, Hussey KE, Thomas JM, Luthringer TA, Shewman EF, et al. Biomechanical performance of medial row suture placement relative to the musculotendinous junction in transosseous equivalent suture bridge double-row rotator cuff repair. Arthroscopy. 2017; 33(2):242–250. doi:10.1016/j.arthro.2016.06.020
13. Dhillon M, Patel S, Shetty V, Behera P. Orthobiologics and platelet rich plasma. Indian J Orthop. 2014; 48(1):1. doi: 10.4103/0019-5413.125477
14. Martinelli D, Fornara P, Stecco A, Grassi F. Does intraoperative platelet-rich plasma improve clinical and structural outcomes after arthroscopic repair of isolated tears of the supraspinatus tendon? Indian J Orthop. 2019; 53(1):77. doi:10.4103/ortho.IJOrtho_35_17
15. Randelli P, Randelli F, Ragone V, Menon A, D'Ambrosi R, Cucchi D, et al. Regenerative Medicine in Rotator Cuff Injuries. BioMed Res Int. 2014; 2014:1–9. doi: 10.1155/2014/12951
16. Alves R, Grimalt R. A Review of platelet-rich plasma: History, biology, mechanism of action, and classification. Skin Appendage Disord. 2018; 4(1):18–24. doi: 10.1159/000477353
17. Foster TE, Puskas BL, Mandelbaum BR, Gerhardt MB, Rodeo SA. Platelet-rich plasma: From basic science to clinical applications. Am J Sports Med. 2009; 37(11):2259–2272. doi:10.1177/036354650934992

18. Blair P, Flaumenhaft R. Platelet α-granules: basic biology and clinical correlates. Blood Rev. 2009; 23(4):177–189. doi: 10.1016/j.blre.2009.04.00
19. Leslie M. Beyond Clotting: The powers of platelets. Science. 2010; 328(5978):562–564. doi:10.1126/science.328.5978.562
20. Pandey V, Bandi A, Madi S, Agarwal L, Acharya KKV, Maddukuri S, et al. Does application of moderately concentrated platelet-rich plasma improve clinical and structural outcome after arthroscopic repair of medium-sized to large rotator cuff tear? A randomized controlled trial. J Shoulder Elbow Surg. 2016; 25(8):1312–1322. doi:10.1016/j.jse.2016.01.036
21. Wang A, McCann P, Colliver J, Koh E, Ackland T, Joss B, Zheng M, Breidahl B. Do postoperative platelet-rich plasma injections accelerate early tendon healing and functional recovery after arthroscopic supraspinatus repair? A randomized controlled trial. Am J Sports Med. 2015; 43: 1430-1437. doi: 10.1177/0363546515572602
22. Holtby R, Christakis M, Maman E, MacDermid JC, Dwyer T, Athwal GS, et al. Impact of platelet-rich plasma on arthroscopic repair of small- to sedium-sized rotator cuff tears: A randomized controlled trial. Orthop J Sports Med. 2016; 4(9):232596711666559. doi: 10.1177/2325967116665595
23. Jo CH, Kim JE, Yoon KS, Shin S. Platelet-rich plasma stimulates cell proliferation and enhances matrix gene expression and synthesis in tenocytes from human rotator cuff tendons with degenerative tears. Am J Sports Med. 2012; 40(5):1035–1045. doi: 10.1177/0363546512437525
24. Dohan Ehrenfest DM, Rasmusson L, Albrektsson T. Classification of platelet concentrates: from pure platelet-rich plasma (P-PRP) to leucocyte- and platelet-rich fibrin (L-PRF). Trends Biotechnol. 2009; 27(3):158–167. doi:10.1016/j.tibtech.2008.11.009
25. Anitua E, Andia I, Ardanza B, Nurden P, Nurden A. Autologous platelets as a source of proteins for healing and tissue regeneration. Thromb Haemost. 2004; 91(01):4–15. doi:10.1160/TH03-07-0440
26. D'Ambrosi R, Palumbo F, Paronzini A, Ragone V, Facchini RM. Platelet-rich plasma supplementation in arthroscopic repair of full-thickness rotator cuff tears: a randomized clinical trial. Musculoskelet Surg. 2016; 100(S1):25–32. doi:10.1007/s12306-016-0415-2
27. Snow M, Hussain F, Pagkalos J, Kowalski T, Green M, Massoud S, et al. The Effect of delayed injection of leukocyte-rich platelet-rich plasma following rotator cuff repair on patient function: A randomized double-blind controlled trial. Arthrosc J Arthrosc Relat Surg. 2020; 36(3):648–657. doi: 10.1016/j.arthro.2019.09.026
28. Malavolta EA, Gracitelli MEC, Assunção JH, Ferreira Neto AA, Bordalo-Rodrigues M, de Camargo OP. Clinical and structural evaluations of rotator cuff repair with and without added platelet-rich plasma at 5-year follow-up: A prospective randomized study. Am J Sports Med. 2018; 46(13):3134–3141. doi: 10.1177/0363546518795895

29. Walsh MR, Nelson BJ, Braman JP, Yonke B, Obermeier M, Raja A, et al. Platelet-rich plasma in fibrin matrix to augment rotator cuff repair: a prospective, single-blinded, randomized study with 2-year follow-up. J Shoulder Elbow Surg. 2018; 27(9):1553–1563. doi:10.1016/j.jse.2018.05.003
30. Flury M, Rickenbacher D, Schwyzer H-K, Jung C, Schneider MM, Stahnke K, et al. Does pure platelet-rich plasma affect postoperative clinical outcomes after arthroscopic rotator cuff repair?: A randomized controlled trial. Am J Sports Med. 2016; 44(8):2136–2146. doi: 10.1177/0363546516645518
31. Ebert JR, Wang A, Smith A, Nairn R, Breidahl W, Zheng MH, et al. A midterm evaluation of postoperative platelet-rich plasma injections on arthroscopic supraspinatus repair: A randomized controlled trial. Am J Sports Med. 2017; 45(13):2965–2974. doi:10.1177/0363546517719048
32. Jo CH, Shin JS, Lee YG, Shin WH, Kim H, Lee SY, et al. Platelet-rich plasma for arthroscopic repair of large to massive rotator cuff tears: A randomized, single-blind, parallel-group trial. Am J Sports Med. 2013; 41(10):2240–2248. doi:10.1177/0363546513497925
33. Zhang Z, Wang Y, Sun J. The effect of platelet-rich plasma on arthroscopic double-row rotator cuff repair: a clinical study with 12-month follow-up. ACTA Orthop Traumatol Turc. 2016; 50(2):191-197 doi: 10.3944/AOTT.2015.15.0113
34. Jo CH, Shin JS, Shin WH, Lee SY, Yoon KS, Shin S. Platelet-rich plasma for arthroscopic repair of medium to large rotator cuff tears: a randomized controlled trial. Am J Sports Med. 2015; 43(9):2102–2110. doi: 10.1177/0363546515587081
35. Snyder SJ, Pachelli AF, Del Pizzo W, Friedman MJ, Ferkel RD, Pattee G. Partial thickness rotator cuff tears: results of arthroscopic treatment. Arthrosc J Arthrosc Relat Surg. 1991; 7(1):1–7. doi: 10.1016/0749-8063(91)90070-e
36. Cavendish PA, Everhart JS, DiBartola AC, Eikenberry AD, Cvetanovich GL, Flanigan DC. The effect of perioperative platelet-rich plasma injections on postoperative failure rates following rotator cuff repair: a systematic review with meta-analysis. J Shoulder Elbow Surg. 2020; 29(5):1059–1070. doi: 10.1016/j.jse.2020.01.084
37. Asfaha S, Cenac N, Houle S, Altier C, Papez MD, Nguyen C, et al. Protease-activated receptor-4: a novel mechanism of inflammatory pain modulation: PAR $_4$ is anti-nociceptive. Br J Pharmacol. 2007; 150(2):176–185. doi: 10.1038/sj.bjp.070697
38. Kukkonen J, Kauko T, Vahlberg T, Joukainen A, Äärimaa V. Investigating minimal clinically important difference for Constant score in patients undergoing rotator cuff surgery. J Shoulder Elbow Surg. 2013; 22(12):1650–1655. doi: 10.1016/j.jse.2013.05.002
39. Sonnabend DH, Howlett CR, Young AA. Histological evaluation of repair of the rotator cuff in a primate model. J Bone Joint Surg Br. 2010; 92-B(4):586–594. doi:10.1302/0301-620X.92B4.22371

40. Saltzman BM, Jain A, Campbell KA, Mascarenhas R, Romeo AA, Verma NN, et al. Does the use of platelet-rich plasma at the time of surgery improve clinical outcomes in arthroscopic rotator cuff repair when compared with control cohorts? A systematic review of meta-analyses. Arthrosc J Arthrosc Relat Surg. 2016; 32(5):906–918. doi:10.1016/j.arthro.2015.10.007
41. Vavken P, Sadoghi P, Palmer M, Rosso C, Mueller AM, Szoelloesy G, et al. Platelet-rich plasma reduces retear rates after arthroscopic repair of small- and medium-sized rotator cuff tears but is not cost-effective. Am J Sports Med. 2015; 43(12):3071–3076. doi:10.1177/0363546515572777
42. Cai Y, Zhang C, Lin XJ. Efficacy of platelet-rich plasma in arthroscopic repair of full-thickness rotator cuff tears: a meta-analysis. J Shoulder Elbow Surg. 2015; 24(12):1852-1898. doi: 10.1016/j.jse.2015.07.035
43. Iannotti JP, Deutsch A, Green A, Rudicel S, Christensen J, Marraffino S, et al. Time to failure after rotator cuff repair: a prospective imaging study. J Bone Joint Surg. 2013; 95(11):965–971. doi: 10.2106/JBJS.L.00708
44. Yang F-A, Liao C-D, Wu C-W, Shih Y-C, Wu L-C, Chen H-C. Effects of applying platelet-rich plasma during arthroscopic rotator cuff repair: a systematic review and meta-analysis of randomised controlled trials. Sci Rep. 2020; 10(1):17171. doi:10.1038/s41598-020-74341-0
45. Wang C, Xu M, Guo W, Wang Y, Zhao S, Zhong L. Clinical efficacy and safety of platelet-rich plasma in arthroscopic full-thickness rotator cuff repair: A meta-analysis. Fragkos KC, editor. PLOS ONE. 2019; 14(7):e0220392. doi: 10.1371/journal.pone.0220392
46. Arnoczky SP, Delos D, Rodeo SA. What is platelet-rich plasma? Oper Tech Sports Med. 2011; 19(3):142–148. doi:10.1053/j.otsm.2010.12.001
47. A. Zumstein M, Berger S, Schober M, Boileau P, W. Nyffeler R, Horn M, et al. Leukocyte- and platelet-rich fibrin (L-PRF) for long-term delivery of growth factor in rotator cuff repair: Review, preliminary results and future directions. Curr Pharm Biotechnol. 2012; 13(7):1196–1206. doi: 10.2174/138920112800624337
48. Barber FA, Hrnack SA, Snyder SJ, Hapa O. Rotator cuff repair healing influenced by platelet-rich plasma construct augmentation. Arthrosc J Arthrosc Relat Surg. 2011; 27(8):1029–1035. doi: 10.1016/j.arthro.2011.06.010
49. Bergeson AG, Tashjian RZ, Greis PE, Crim J, Stoddard GJ, Burks RT. Effects of platelet-rich fibrin matrix on repair integrity of at-risk rotator cuff tears. Am J Sports Med. 2012; 40(2):286–293. doi: 10.1177/0363546511424402
50. Everts PAM, Knape JTA, Weibrich G, Hoffmann J, Overdevest EP, Box HAM, et al. Platelet-rich plasma and platelet gel: A review. J Extra Corpor Technol. 2006; 8:174-187. A file:///C:/Users/Predavalnica/Downloads/c2.pdf
51. Zumstein MA, Rumian A, Thélu CÉ, Lesbats V, O'Shea K, Schaer M, et al. SECEC Research Grant 2008 II: Use of platelet- and leucocyte-rich fibrin (L-PRF) does not affect late rotator cuff tendon healing: a prospective randomized controlled study. J Shoulder Elbow Surg. 2016; 25(1):2–11. doi: 10.1016/j.jse.2015.09.018

52. Everts PA, Devilee RJJ, Brown Mahoney C, van Erp A, Oosterbos CJM, Stellenboom M, et al. Exogenous application of platelet-leukocyte gel during open subacromial decompression contributes to improved patient outcome. A prospective randomized double-blind study. Eur Surg Res. 2008; 40(2):203–210. doi: 10.1159/000110862
53. Mishra A, Pavelko T. Treatment of chronic elbow tendinosis with buffered platelet-rich plasma. Am J Sports Med. 2006; 34(11):1774–1778. doi: 10.1177/0363546506288850
54. Mooren RECM, Hendriks EJ, van den Beucken JJJP, Merkx MAW, Meijer GJ, Jansen JA, et al. The effect of platelet-rich plasma *in vitro* on primary cells: Rat osteoblast-like cells and human endothelial cells. Tissue Eng Part A. 2010; 16(10):3159–3172. doi:10.1089/ten.tea.2009.0832
55. Gulotta LV, Rodeo SA. Growth factors for rotator cuff repair. Clin Sports Med. 2009; 28(1):13–23. doi: 10.1016/j.csm.2008.09.002
56. Vavken P, Saad FA, Murray MM. Age dependence of expression of growth factor receptors in porcine ACL fibroblasts. J Orthop Res. 2010; 28(8):1107–1112. doi: 10.1002/jor.21111
57. Itoigawa Y, Kishimoto KN, Sano H, Kaneko K, Itoi E. Molecular mechanism of fatty degeneration in rotator cuff muscle with tendon rupture. J Orthop Res. 2011; 29(6):861–866. doi: 10.1002/jor.21317
58. Takase F, Inui A, Mifune Y, Sakata R, Muto T, Harada Y, et al. Effect of platelet-rich plasma on degeneration change of rotator cuff muscles: In vitro and in vivo evaluations. J Orthop Res. 2017; 35(8):1806–1815. doi: 10.1002/jor.23451

Review

Anatomic and kinematic planning of arthroscopic femoroacetabular osteoplasty

Šarler Taras[1,*], Stražar Klemen[1,2]
[1]University Medical Centre Ljubljana, Department for Orthopaedic Surgery, Ljubljana, Slovenia
[2]University of Ljubljana, Faculty of Medicine, Chair of Orthopaedics, Ljubljana, Slovenia
*taras.sarler@kclj.si

Abstract
Femoroacetabular impingement (FAI) is a common hip pathology entity. It is diagnosed with clinical examination and typical appearance on radiologic modalities.
In preoperative evaluation, the most important radiologic modality is radial MRI. The most frequent and the most important femoral radiologic parameter is the angle between the orientation of the femoral neck and the margin of the femoral head on axial radiogram (α angle). The treatment of FAI usually consists of hip arthroscopy with osteoplasty of femur, acetabulum or both. Osteoplasty can be planned anatomically or kinematically. In this contribution, both planning approaches are assessed in terms of their advantages and disadvantages. Additionally, our experience with different types of planning is presented based on a representative case.

1. Introduction

Femoroacetabular impingement (FAI), first mentioned in English literature in 1999 [1], is a pathologic condition in which the femoral head-neck junction abuts to the acetabular rim. It is classified as cam, pincer or mixed type [2]. FAI soon became an important clinical entity. The numbers of FAI treatment procedures are rising. Most FAI pathology can be treated arthroscopically. The results of FAI surgery are encouraging [3]. However, there is a lack of long-term clinical results comparing different plan approaches. There is also still no golden standard on how to plan and execute FAI patient treatment [4,5].

The focus of our research is on the computational planning of FAI treatment. In this contribution, we present both types of planning and demonstrate their use on a practical example.

2. Radiologic diagnostics

FAI is diagnosed when typical clinical signs are present and radiologic parameters are pathologic [2]. The radiologic parameters describe the pathoanatomy of the femoral head-neck junction and the inclination and the orientation of the acetabulum and its rim. Typical x-ray projections are pelvis AP, Dunn projection and false profile view projection. The pathologic values are most commonly defined as femoral head-neck offset < than 8mm, α angle > 50 and offset ratio < 0.18. Acetabular over coverage is defined as LCEA>35° and severe over coverage as LCEA>39 [6-8].

The most frequently used parameter for radiologic evaluation of cam deformity is α angle. It was first described on axial oblique MRI (magnetic resonance imaging) in 2002 [9]. It is defined as the angle formed by the line that goes through the center of the femoral head and the middle of the femoral neck and the line that goes through the center of the femoral head and through the point where the head loses sphericity (9). Later, more advanced imaging modalities were developed, the most advanced being radial MRI. In this imaging modality cuts are made radially through the femoral neck axis. Each MRI slice can be labeled with corresponding number using clock-face. 12h is superior and 3h is anterior. The related labeling convention is given in **Figures 1** and **2** [10]. In that way the extent and position of the most extensive cam deformity can be determined. α angle can be applied on every imaging modality, and its pathologic value is most commonly defined >50°[11].

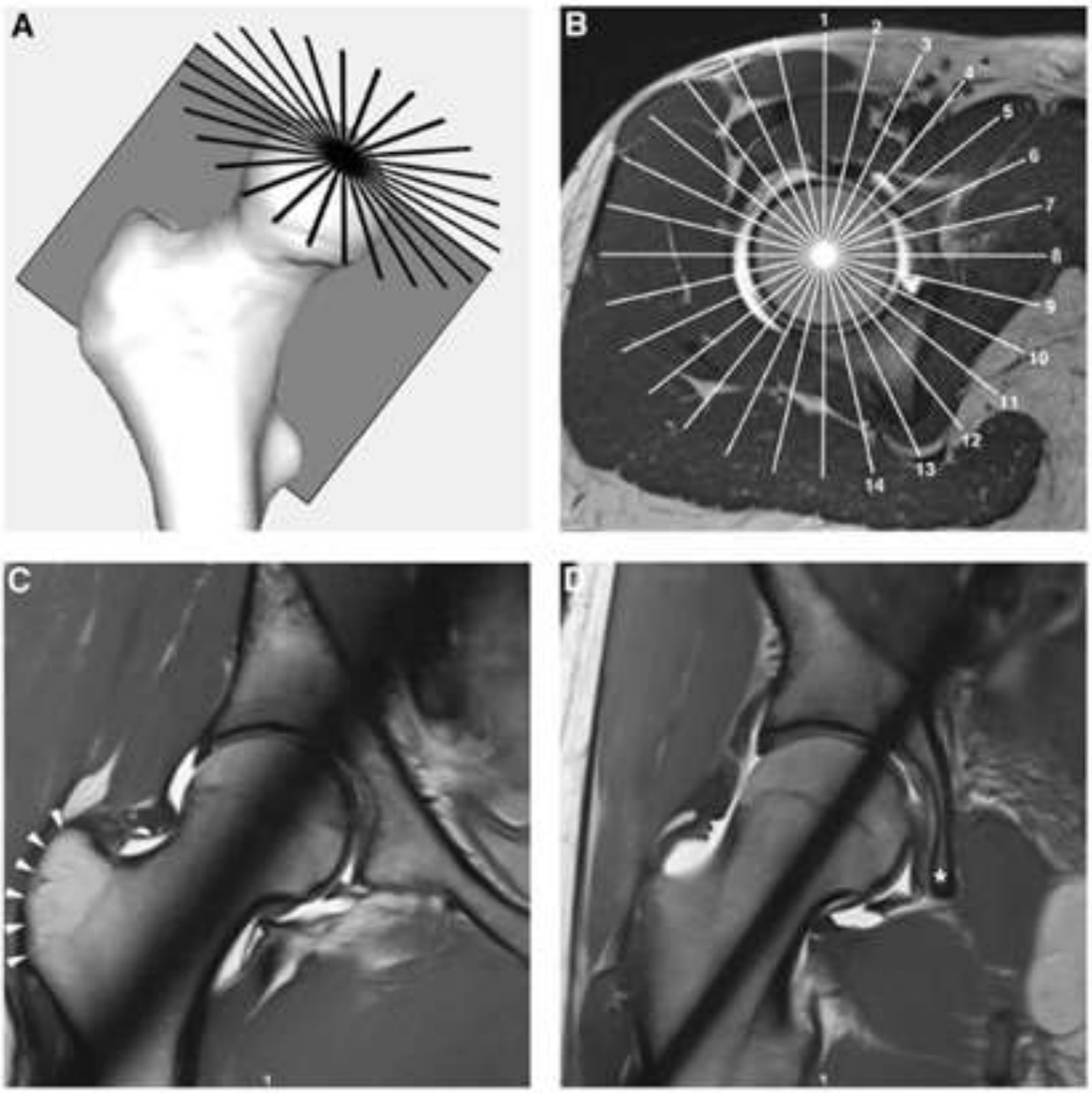

Figure 1. Radial MRI. From [10].

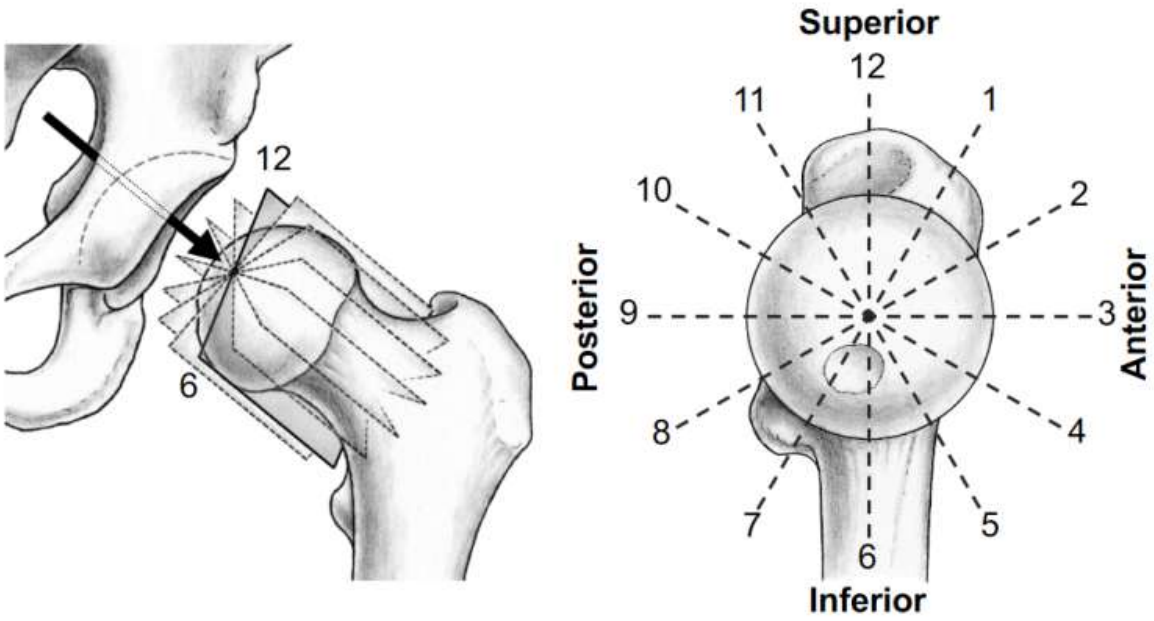

Figure 2. Clock-face positions. From [10].

3. Anatomic planning

The goal of anatomic planning is to restore the femoral head-neck offset and to reduce the α angle in all MRI planes to <50°. There is, however, no agreement regarding the optimal length and inclination of the corrective osteoplasty [12]. Too vigorous cam osteoplasty can cause the loss of labral "suction seal" effect, it can cause uneven edges cortical noticing and the most devastating complication, iatrogenic femoral neck fracture [13]. To delineate the boundaries of safe resection, finite element method stress analysis was performed by Rothenfluh in 2012. The study showed that the resection length should not exceed 35% and the depth of resection should not exceed 20% of the femoral neck [14].

Acetabular rim trimming is performed to decrease acetabular overcoverage. The LCEA angle is reduced to <35° and local acetabular over coverage is reduced to normal acetabular anteversion: 5° at 1h, 10° at 2h and 15° at 3h [15]. Excessive rim trimming can cause an increase of joint reactive forces with subsequent chondrolabral overload and iatrogenic instability [16].

4. Kinematic planning

Kinematic planning is composed of several steps. Firstly, 3D reconstruction by segmentation of pelvis and proximal femur is made from CT or, most recently, MRI scans [17].

Then the movement of the virtual proximal femur model is simulated. There are various possible simulation methods regarding the hip joint centre. The centre can be dynamic or static, as described by Puls et al. [18]. The femur is moved into desired ROM (range of motion) positions, and the overlap between the pelvis and the femur in various positions is marked. The overlaps from different positions are summed and removed from either pelvis, femur or proportionally from both as seen in **Figure 3** [19].

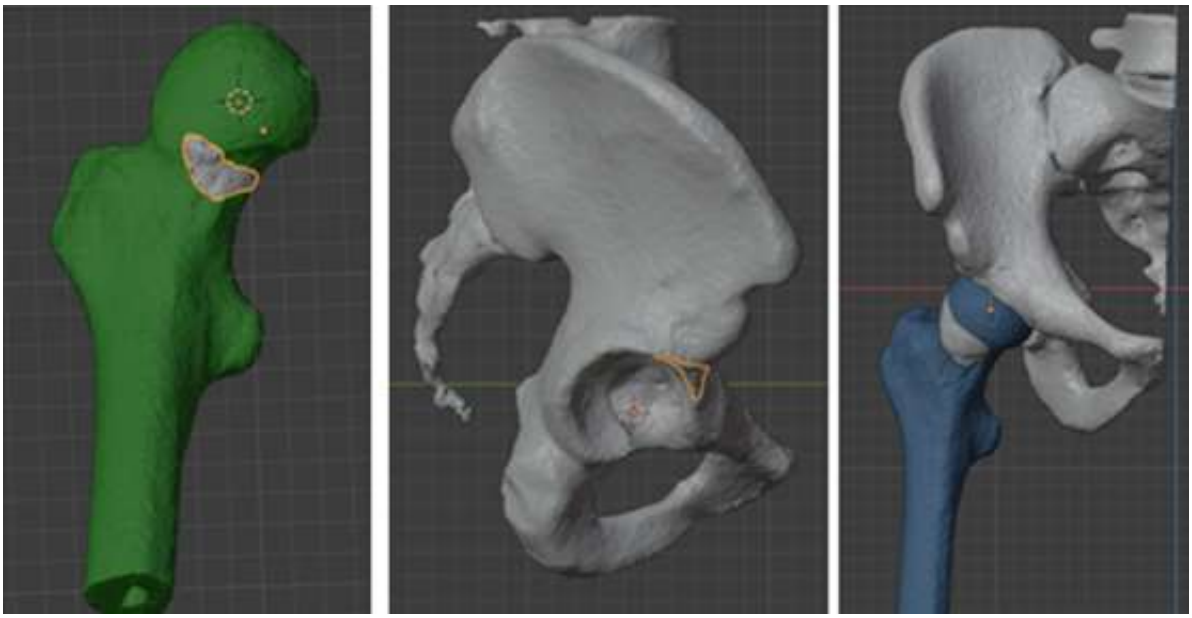

Figure 3. Kinematically planned model.

5. The model

CT scan of a patient with FAI was made. 3D reconstruction and segmentation were performed with EBS software (Ekliptik, Slovenia). STL files of the femur and pelvis were imported into the open-access Blender software. There, the centre of the femoral head and the centre of the femoral neck were determined. Radial cuts of femoral head and neck were made, equivalent to radial MRI. The position and extent of cam deformity (femoral head-neck offset, 3D α angle) were measured (**Figure 4**), and dynamic ROM measurements were made.

The femoral head-neck junction was remodelled so that the 3D α angle was 45°. We made four different virtual osteoplasties by changing the inclination, length and depth of the osteoplasty (**Figure 5**). In all cases, the depth and length of osteoplasties were in the boundaries of the safe zone [14].

Then the virtual ROM analysis with each virtual model was performed. Despite the same 3D α angle of 45°, we could observe differences in ROM. Femoral flexion and internal rotation increased with progressive resection depth and length. After acetabular rim trimming (LCEA corrected to 34° and AV corrected), ROM was further improved and achieved physiologic values, flexion >120° and internal rotation >30°at 90° flexion. The femur was also virtually reshaped using kinematic planning (Figure 3). Femur was set in 120° flexion position and 30°of IR at 90° flexion. The overlap from both positions was removed from the femoral side. Substantially less bone had to be removed to achieve the same virtual ROM by using kinematic planning.

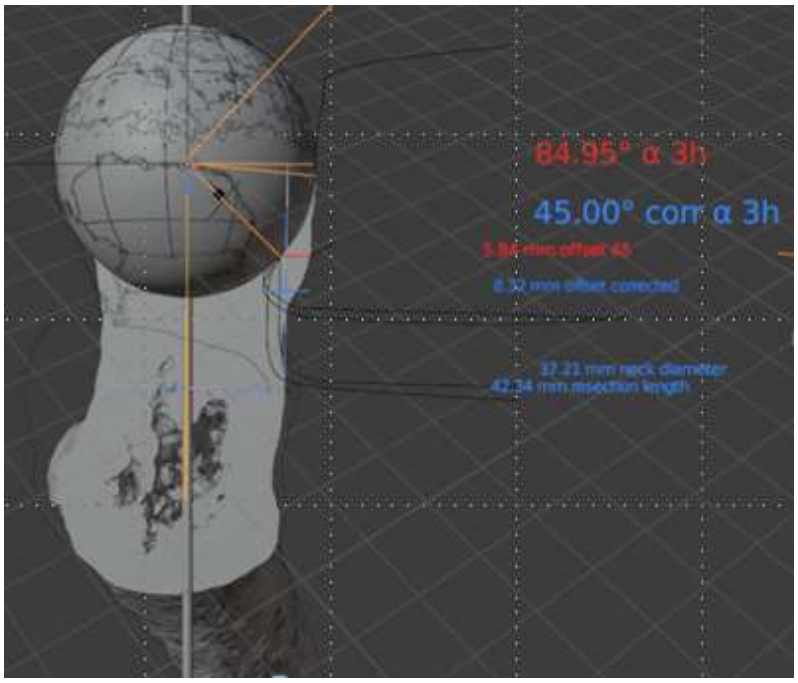

Figure 3. Different osteotomy lines on radial view (labeled black).

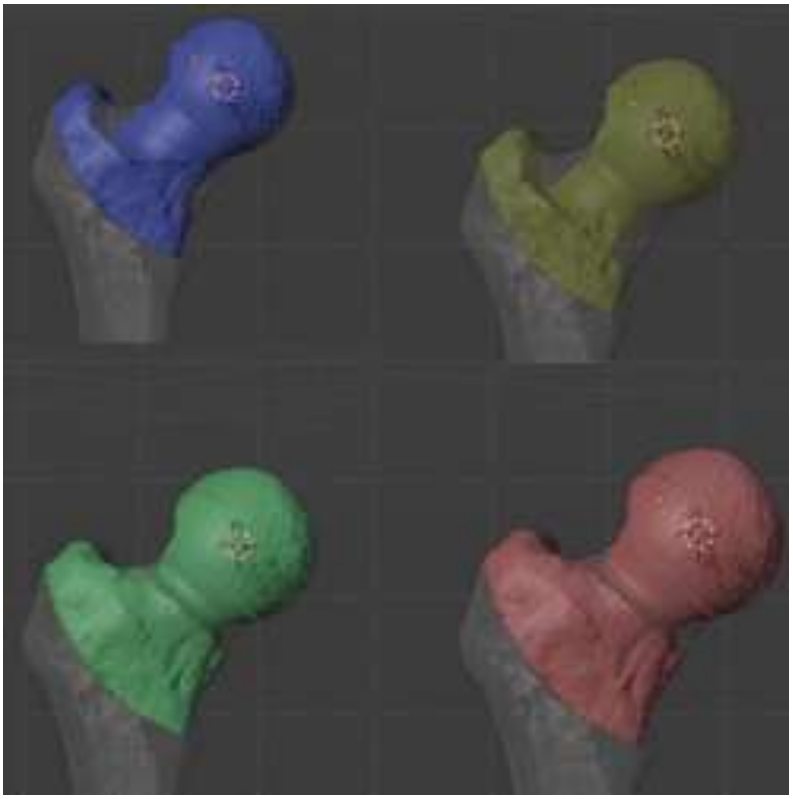

Figure 5. Different versions of anatomic osteoplasties with the 45° α angle.

6. Conclusions

The advantages of anatomic planning over kinematic planning are low cost and good availability. The execution of the plan is relatively simple, and it can be checked with intraoperative fluoroscopy. The disadvantages originate from the fact that FAI is a dynamic 3D problem, however, anatomic planning relies on static 2D measurements. Moreover, the values of radiologic parameters are frequently revised and modified [20].

The advantage of kinematic planning over anatomic planning is that it allows patient-specific detection of too prominent osseous margins. Based on our example, much less bone had to be removed to achieve the same virtual ROM. The drawbacks of this planning are high price and substantial time-consumption. When simulating ROM soft tissues are not taken into account. It requires advanced computer software and technical support. In order to be efficient, it later has to be coupled with navigation to achieve the desired surgical precision [21].

The upgrades of the presented research are focused on optimization of the anatomic planning by analyzing different virtual resection variants. The essential future goal is also to automate specific planning steps of anatomic and kinematic planning to make it more user friendly, reliable and less time-consuming.

Acknowledgements

The authors would like to thank Uroš Volk, PhD, for the technical support with EBS software and Leon Lazič for the technical support with Blender software.

References

1. Myers SR, Eijer H, Ganz R. Anterior femoroacetabular impingement after periacetabular osteotomy. Clin Orthop. 1999; (363):93–99.
2. Clohisy JC, Knaus ER, Hunt DM, Lesher JM, Harris-Hayes M, Prather H. Clinical presentation of patients with symptomatic anterior hip impingement. Clin Orthop. 2009; 467(3):638–644. doi: 10.1007/s11999-008-0680-y
3. Casp A, Gwathmey FW. Hip arthroscopy. Common Problems and Solutions. Clin Sports Med. 2018; 37(2):245–263. doi: 10.1016/j.csm.2017.12.005
4. Philippon MJ, Bolia I, Locks R, Utsunomiya H. Treatment of femoroacetabular impingement: labrum, cartilage, osseous deformity, and capsule. Am J Orthop. 2017; 46(1):23-27
5. Tibor LM, Leunig M. The pathoanatomy and arthroscopic management of femoroacetabular impingement. Bone Jt Res. 2012; 1(10):245–257. doi: 10.1302/2046-3758.110.2000105
6. Eijer H, Leunig M, Mahomed MN, Ganz R. Cross-table lateral radiographs for screening of anterior femoral head-neck offset in patients with femoro-acetabular impingement. HIP Int. 2001; 11(1):37–41. doi:10.1177/112070000101100104

7. Tannast M, Fritsch S, Zheng G, Siebenrock KA, Steppacher SD. Which radiographic hip parameters do not have to be corrected for pelvic rotation and tilt? Clin Orthop Relat Res. 2015; 473(4):1255–1266. doi: 10.1007/s11999-014-3936-8
8. Tannast M, Siebenrock KA, Anderson SE. Femoroacetabular impingement: radiographic diagnosis—What the radiologist should know. Am J Roentgenol. 2007; 188(6):1540–1552. doi: 10.2214/AJR.06.0921
9. Nötzli HP, Wyss TF, Stoecklin CH, Schmid MR, Treiber K, Hodler J. The contour of the femoral head-neck junction as a predictor for the risk of anterior impingement. J BONE Jt Surg. 2002; 84(4):5. https://doi.org/10.1302/0301-620X.84B4.0840556
10. Klenke FM, Hoffmann DB, Cross BJ, Siebenrock KA. Validation of a standardized mapping system of the hip joint for radial MRA sequencing. Skeletal Radiol. 2015; 44(3):339–343. doi: 10.1007/s00256-014-2026-z
11. Smith KM, Gerrie BJ, McCulloch PC, Lintner DM, Harris JD. Comparison of MRI, CT, Dunn 45° and Dunn 90° alpha angle measurements in femoroacetabular impingement. HIP Int. 2018; 28(4):450–455. doi: 10.5301/hipint.5000602
12. Kobayashi N, Inaba Y, Kubota S, Higashihira S, Choe H, Ike H, et al. Computer-assisted hip arthroscopic surgery for femoroacetabular impingement. Arthrosc Tech. 2018; 7(4):e397–403. doi: 10.1016/j.eats.2017.10.013
13. Mardones RM, Gonzalez C, Chen Q, Zobitz M, Kaufman KR, Trousdale RT. Surgical treatment of femoroacetabular impingement: Evaluation of the effect of the size of the resection. J Bone Jt Surg Essent Surg Tech. 2006; 88(1_suppl_1):84-91. doi: 10.2106/JBJS.E.01024
14. Rothenfluh E, Zingg P, Dora C, Snedeker JG, Favre P. Influence of resection geometry on fracture risk in the treatment of femoroacetabular impingement: A finite element study. Am J Sports Med. 2012; 40(9):2002–2008. doi: 10.1177/0363546512456011
15. Tannast M, Hanke MS, Zheng G, Steppacher SD, Siebenrock KA. What are the radiographic reference values for acetabular under- and overcoverage? Clin Orthop Relat Res. 2015; 473(4):1234–1246. doi: 10.1007/s11999-014-4038-3
16. Bhatia S, Lee S, Shewman E, Mather RC, Salata MJ, Bush-Joseph CA, et al. Effects of acetabular rim trimming on hip joint contact pressures: How much is too much? Am J Sports Med. 2015; 43(9):2138–2145. https://doi.org/10.1177/0363546515590400
17. Lerch TD, Degonda C, Schmaranzer F, Todorski I, Cullmann-Bastian J, Zheng G, et al. Patient-specific 3-D magnetic resonance imaging–Based dynamic simulation of hip impingement and range of motion can replace 3-D computed tomography–based simulation for patients with femoroacetabular impingement: Implications for planning open hip preservation surgery and hip arthroscopy. Am J Sports Med. 2019; 47(12):2966–2977. doi: 10.1177/0363546519869681
18. Puls M, Ecker TM, Tannast M, Steppacher SD, Siebenrock KA, Kowal JH. The equidistant method – a novel hip joint simulation algorithm for detection of femoroacetabular impingement. Comput Aided Surg. 2010; 15(4–6):75–82. doi: 10.3109/10929088.2010.530076

19. Kubiak-Langer M, Tannast M, Murphy SB, Siebenrock KA, Langlotz F. Range of motion in anterior femoroacetabular impingement. Clin Orthop Relat Res. 2007; 458:117-124. doi: 10.1097/BLO.0b013e318031c595
20. Kalia V, Fader RF, Mintz DN, Bogner EA, Buly RL, Carrino JA, et al. Quantitative evaluation of hip impingement utilizing computed tomography measurements. J Bone Jt Surg. 2018; 100(17):1526–1535. doi: 10.2106/JBJS.17.01257
21. Stražar K. Computer assistance in hip preservation surgery—current status and introduction of our system. Int Orthop. 2021; 45(4):897-905. doi: 10.1007/s00264-020-04788-3

Research

Computer assistance in periacetabular osteotomy

Zore Lenart Andrej[1], Stražar Klemen[1,2]

[1] Department for Orthopaedic Surgery, University Medical Centre Ljubljana, Zaloška 9, SI-1000 Ljubljana, Slovenia
[2] Chair of Orthopaedics, Faculty of Medicine, University of Ljubljana, Vrazov trg 2, SI-1000 Ljubljana, Slovenia
lenartzore@gmail.com

Abstract

Hip dysplasia has been recognized as one of main risk factors for pain in younger population. Dysplastic changes represent higher risk for early degenerative changes to the hip joint. Therefore, we recognize the importance of early diagnosis of this disease and precise surgical treatment with Bernese periacetabular osteotomy (PAO). PAO is a complex procedure where we need to resect dysplastic acetabulum from the pelvis, do the reposition of the free acetabular fragment and fix it in the new, biomechanically optimal position. By that we gain satisfactory acetabular coverage of the femoral head and get more symmetrical distribution of forces through the hip joint. Right position of the osteotomized acetabulum is chosen by direct visualization and by the AP radiograph of pelvis during the operation. These method is relatively subjective and do not provide optimal checkup. In our article we present our computer assisted planning and execution of PAO by EBS medical software and navigation with electromagnetic navigation system Guiding Star, which, we think, is much more precise.

1. Introduction

Hip dysplasia is a developmental disorder of variable pattern of shallow pelvic acetabulum and reduced femoral coverage which symptoms can present at various time points in the developing human skeleton. It can be congenital or can develop later during skeletal growth [1,2]. This pathoanatomy can result in instability and uneven distribution of stress in the hip joint, which can produce mechanical overloading of specific areas of acetabular surfaces and can trigger premature osteoarthritis of hip joint [1]. It is essential to recognize the pathology early and treat patients with symptomatic dysplastic deformities before the osteoarthritis develop [2,3]. The golden standard for hip dysplasia treatment is surgical procedure called periacetabular osteotomy (PAO) first described by Ganz et al. [4]. Bernese periacetabular osteotomy which maintains the integrity of posterior pillar and does not break the acetabular articular surface covered with cartilage [4,5] is used widely around the world as well as in our institution. PAO consists of pelvic osteotomies to release acetabulum as a free fragment, which enables its reorientation to achieve better acetabular coverage of femoral head and more balanced distribution of the loads on the articular surface of the hip joint. Free acetabular fragment is reoriented in order to correct lateral coverage of the femoral head, to medialize center of rotation of the femoral head and to correct the anterior-posterior femoral head coverage [4]. Reorientation is navigated under direct vision and under fluoroscopy, which is not as optimal as we would like, especially not with unexperienced or low volume surgeons. For many years surgeons try to objectivize the correct position of the osteotomized acetabular fragment [6,7,8].

2. The case

We present our patient, 27 years old female, with right groin pain. AP X-ray of pelvis with hips showed pronounced right hip dysplasia with Lateral central edge angle (CE) measured 14 degrees and Acetabular index (AI) 21 degrees.

The patient was operated with PAO procedure and the intraoperative fluoroscopy of pelvis was done to confirm the right position of acetabular fragment. The new position on intraoperative fluoroscopy showed improved lateral coverage, medialization of the femoral head and better anterior-posterior femoral coverage. We could also see the elevation of osteotomized pubic fragment.

After the surgery we did control x-ray of pelvis with hips and measured CE 16 degrees and AI 13 degrees, which showed insufficient operative correction. We further did CT scan with 3D reconstruction of pelvis which confirmed insufficient position of osteotomized acetabular fragment. The patient had to undergo revision surgery where we had to re-do the osteotomies and correct the free acetabular fragment of the right hip. Control x-ray of pelvis showed satisfactory angles CE 30 degrees and AI 9 degrees. Patients reported significant symptomatic improvement after revision surgery.

3. Can we better control the reposition of acetabular fragment and can it be done more precisely?

In orthopedics surgery two navigation systems are used. One type of navigation is visional [9] and other is via electromagnetic field. In collaboration with Slovenian company Ekliptik, which has developed intraoperative electromagnetic navigation, we use it in PAO surgery. To plan the navigation assisted surgery, we need low dosage CT scan of pelvis with hips in order to make 3D reconstruction of pelvis and hips. We import the 3D reconstruction in the EBS medical software application from

Ekliptik (**Figure 1**) and plan the osteotomies, divide osteotomized fragments, make their repositions and compare initial and corrected positions (**Figure 2**). We also do the kinematic simulations to prevent under or over correction and to preserve good mobility. The final plan is then to send electromagnetic system Guiding Star, a computer controlled, image guided navigation system.

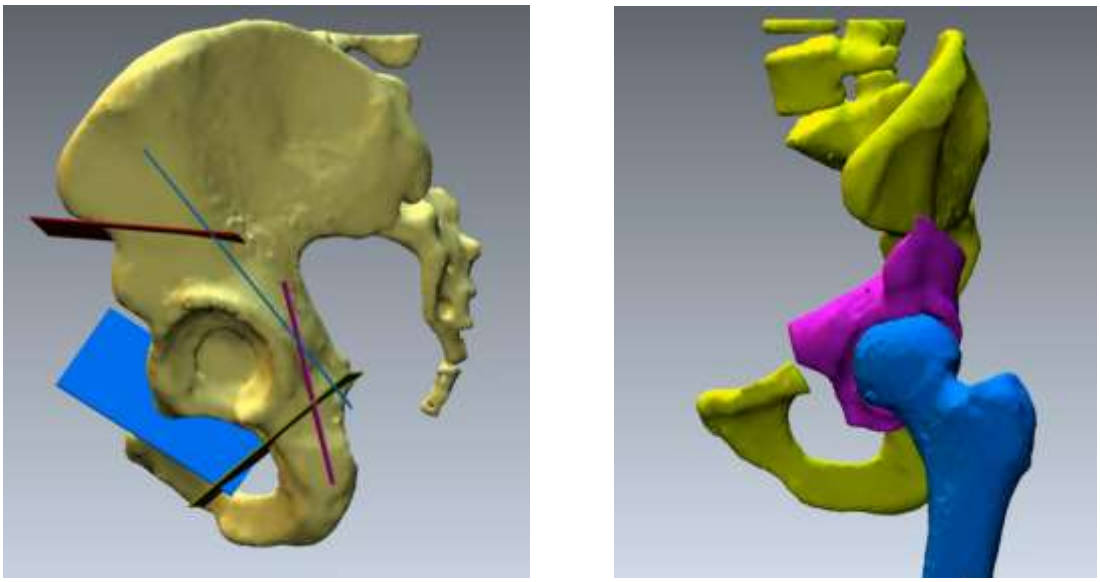

Figure 1. Planing the osteotomies in the 3D model (left) and testing for optimal position of free acetabular fragment (right).

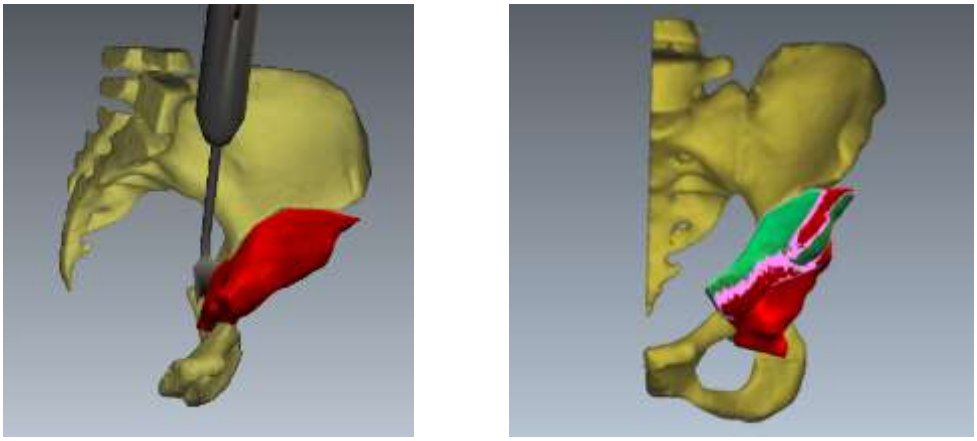

Figure 2. Live monitoring of osteotomies on the 3D model on the screen (left) and live monitoring of planed (red) with the actual position of free acetabular fragment (green) (right).

The surgical approach for PAO, using Guiding Star navigation, is the same as with classic surgery through minimally invasive approach. When we prepare the pelvis for osteotomies, we do calibration of Guiding Star to match points on pelvis with the points in the 3D plan on the screen. We than do the osteotomies with the specific osteotome recognized by electromagnetic navigation. As we move the osteotome we also see real time movements on the screen on our surgical plan so we can control progression of cuts and compare them with planned osteotomies. We place sensors in the free osteotomized acetabular fragment, do the reposition under the control of the plan on the screen and match it to the 3D planned reposition. After we get satisfactory result, we fix acetabular fragment in the standard manner with two or three screws. We make control x-ray to additionally confirm correct position of the acetabular fragment and to confirm right position of the screws.

Advances and drawbacks of using Guiding Star electromagnetic navigation

Firstly, any kind of navigation needs also a good initial screening with quality input data from where precise plan of surgery is made. Before navigation preoperative X-rays were sufficient to measure hip dysplasia, but with navigation we need low dosage CT scan of pelvis with hips with 3D reconstruction. This represents additional patient exposure to radiation but is needed for EBS software to plan the surgery. On other hand, we need less fluoroscopy during operation due to precise guidance of navigation which means less intraoperative radiation for patient and medical stuff during surgery. Making osteotomies under the navigation and checking position of the cuts live on screen on 3D model is done under better control as just with fluoroscopic 2D checkups. When osteotomies are done, moving the free fragment under 3D supervision is a lot easier and lead to optimal position for femoral head coverage as well as for optimal bone healing. On the other hand, we can also prevent overcorrection and impingement in hip joint.

Conclusion

After 30 years of standardized PAO procedure with only minor updates of technique, navigation is making this procedure a lot more controlable. PAO surgery is very demanding surgery done on young patients in order to relieve symptoms and preserve the hip joint. Some osteotomies and reposition of the free acetabular fragment are in standard procedure done only under indirect supervision of 2D fluoroscopy, which can lead in errors, especially with younger and low volume surgeons. Using navigation provide us with exact plan and control during the procedure.

References

1. Kamath AF. Bernese periacetabular osteotomy for hip dys- plasia: surgical technique and indications. World J Orthop. 2016; 7:280-286. doi: 10.5312/wjo.v7.i5.280
2. Klisic PJ. Congenital dislocation of the hip--a misleading term: brief report. J Bone Joint Surg Br. 1989; 71(1):136. doi: 10.1302/0301-620X.71B1.2914985

3. Henak CR, Abraham CL, Anderson AE, Maas SA, Ellis BJ, Peters CL, et al. Patient-specific analysis of cartilage and labrum mechanics in human hips with acetabular dysplasia. Osteoarthritis Cartilage. 2014; 22(2):210-217. doi: 10.1016/j.joca.2013.11.003
4. Ganz R, Klaue K, Vinh T, Mast J. A new periacetabular osteotomy for the treatment of hip dysplasias. Technique and preliminary results. Clin Orthop Relat Res. 1988; 232:26–36. PMID: 3383491
5. Troelsen A, Elmengaard B, Søballe K. A new minimally invasive transsartorial approach for periacetabular osteotomy. J Bone Joint Surg Am. 2008; 90:493-498. doi: 10.2106/JBJS.F.01399
6. Troelsen A. Surgical advances in periacetabular osteotomy for treatment of hip dysplasia in adults. Acta Orthop Suppl. 2009; 80(332): 1-33. doi: 10.1080/17453690610046585
7. Murphy RJ, Armiger RS, Lepistö J, Mears SC, Taylor RH, Armand M. Development of a biomechanical guidance system for periacetabular osteotomy. Int J CARS. 2015; 10(4):497-508. doi: 10.1007/s11548-014-1116-7.
8. Zaltz I. How to properly correct and to assess acetabular position: an evidence-based approach. J Pediatr Orthop. 2013; 33 Suppl 1:S21-8. doi: 10.1097/BPO.0b013e31828114a
9. Hooper JM, Mays RR, Poultsides LA, Castaneda PG, Muir JM, Kamath AF. Periacetabular osteotomy using an imageless computer-assisted navigation system: a new surgical technique. J Hip Preserv Surg. 2019; 6(4):426-431. doi: 10.1093/jhps/hnz058.

Research

Increasing hand dexterity through the use of various somatosensory stimuli: a pilot study

Vidovič Marko[1,2]*, Rugelj Darja[3]
[1]University Rehabilitation Institute – Soča, Republic of Slovenia, Ljubljana, Slovenia
[2]University of Ljubljana, Faculty of Medicine, Ljubljana, Slovenia
[3]University of Ljubljana, Faculty of Health Sciences, Biomechanical Laboratory, Ljubljana, Slovenia
*marko.vidovic@ir-rs.si

Abstract
Mechanoreceptors of the skin and muscle receptors influence motor behaviour if stimulated. Some methods, such as vibration, have been used for decades to alter cutaneous and proprioceptive input while, the effects of mechanical pressure stimulation have been studied less frequently, and its impact on the dexterity of the hand has not yet been widely researched. The purpose of the pilot study was to investigate which of the three different somatosensory stimulation has significant effect on hand dexterity. Methods: Forty healthy participants were assigned to four different groups: Group 1 (15 minutes mechanical stimulation; MS); group 2 (30 minutes focal muscle vibration; f-MV); group 3 (30 minutes somatosensory electrical stimulation; SES); control group (without stimulation; CON). Two outcome measurements were used: Purdue Pegboard test and Hand grip strength test. The results within the groups ANOVA showed a significant increase in all the Purdue Pegboard test tasks in all experimental groups (MS, f-MV, SES, including CON group) ($p < 0.001$). Post hoc testing showed significant increase in Purdue pegboard tasks for the f-MV and SES group for two and four measured tasks respectively. In the between-groups analysis ANOVA the right-hand task demonstrated a significant increase with Purdue Pegboard test ($p < 0.05$). Post hoc tests showed a significant increase after f-MV stimulation and SES stimulation as compared to CON group ($p < 0.05$). The Purdue Pegboard test with the left hand, both hands and both hand assembling the ANOVA analysis didn't show statistically significant changes ($p > 0.05$). Grip strength didn't show statistical different changes within and between groups. In conclusion, only the right hand, mostly dominant, resulted in a increased hand dexterity. But significant changes within F-MV and SES groups compared to the CON group suggests that these somatosensory stimuli have the potential to increase manual dexterity, however it is not clear the impact of motor learning.

1. Introduction

As we go about our daily activities, humans encounter external somatosensory stimuli that influence our motor control. Proprioception is important for effective motor control of voluntary as well as automatic movement, as it provides sensory information that the central nervous system uses to correct movement in real time [1]. The absence of proprioception input can suppress motor plasticity and learning [2,3]. To enhance process of motor recovery and motor learning is therapeutic option to increase somatosensory influx with sensory stimulation [4]. For this purpose, most frequently peripheral stimulation modalities include electrical nerve stimulation and vibration [5-7]. Natural modalities of peripheral stimulation, such as tactile and pressure through the use of textured materials have been studied less extensively [8,9]. These multiple effects of peripheral sensory stimulation is consistent with its impact on somatosensory networks involved in various sensory-motor functions. Enhanced peripheral stimulation may modulate somatosensory (S1) and motor (M1) cortex and may result in plastic reorganization at the spinal and supraspinal levels, perhaps changing the central nervous system's ability to elaborate available proprioceptive information [10].

Mechanical pressure stimulation of the skin whit rough textured material (MS) activates four types of afferents which are defined based on their receptive fields and discharge pattern: slow-adapting type I afferents (SA-I,) respond to static stimuli; slow-adapting type II for skin stretching; fast- adapting type I detecting flutter up to 40-50 Hz; and fast-adapting type II responding to high-frequency vibratory stimuli up to 400 Hz. Mechanical pressure of skin excites mainly SA-I afferents, which respond to static pressure, as well as mechanical stimulation with low frequency (usually below 5 Hz) and skin deformation [11,12]. Before reaching the cortex, information from cutaneous afferents is already combined with motor efferent signals at multiple levels of the central nervous system, including the spinal cord grey matter, brainstem nuclei and thalamus [6,13].

The use of focal muscle vibration (f-MV) in neuro-rehabilitation [14] has shown acute and long-lasting benefits, reducing spasticity and ameliorating motor function [15]. It is also known to influence motor performance in healthy participants [16]. Vibrations at low amplitude (1 mm) and a frequency of 80Hz are a strong and safe stimulus for activation of muscle spindle primary endings. Vibrations at this frequency increase kinesthetics inflows and thus modulate proprioceptive perception. In addition, Golgi tendon organs (Ib fibers), along with other somatosensory mechanoreceptors, can respond to mechanical vibrations [10].

Threshold somatosensory electrical stimulation (SES) is a promising therapeutic method for targeted recovery of hand motor skills [17]. It is known to be a powerful tool to focally modulate sensorimotor cortices in healthy and stroke participants [17-20]. Different studies have shown short-term and long-term improvements in hand function after SES [17-20]. Additionally, sensory amplitude electrical stimulation has been reported to induce changes in the corticospinal excitability of the hand area in healthy participants. Based on that report,

SES has been proposed as a possible supplemental therapy to facilitate motor functions, for example performing hand tasks in patients with stroke [21].
Peripheral afferent stimulation was therefore used to address plasticity of the human motor system with the aim of improving motor function [22], in our case increasing hand dexterity. However, the extent to which following various somatosensory stimulation might be related to substantial functional consequences in the hand dexterity has not been thoroughly investigated. In this pilot study we investigated which of three different somatosensory stimulation has the most pronounced influence on hand dexterity. We hypothesised those various somatosensory stimuli such as textured materials, vibration and electrical stimulation of the forearm will increase hand dexterity as measured with Purdue Pegboard test.

2. Methods

2.1 Participants

Forty healthy participants, (3 males and 37 females; mean age 27.3 years, range 20–33 years; mean height 167 cm, range 160- 185 cm; mean weight 59 kg, range 51–81 kg; 35 right and 5 left hands dominant) were included in this study. The participants were assigned to one of four different groups: group 1 (MS; n = 10;); group 2 (f-MV; n = 10;); group 3 (SES; n = 10;) group 4 (CON; n = 10) (without stimulation). All participants were free from any upper limb motor deficits. All participants were also free from cognitive, neurological, and visual impairment deficits. Prior to any measurements, all participants read the information about the testing protocol, received additional verbal explanations when required, and were provided with written informed consent.

2.2 Assessment protocol

2.2.1 Purdue Pegboard test

The Purdue Pegboard test (Lafayette Instrument Company, Lafayette, Indiana, USA) measures the ability to quickly and controllably manipulate small objects, which involves finger dexterity and goal-oriented hand-to-hand actions [23]. Participants are asked to retrieve a pin from a cup and place it into one of the holes on the board, beginning with the first hole that is closest to the cups. The objective is to fill as many holes with the pins as possible within a 30-second time limit. Participants are asked to begin with their dominant hand. Before the initial measurements begins participants had the opportunity to practice with 5 pins at the start of each session. The participants have only one attempt whit dominant hand and then continues these steps with their nondominant hand. Once this portion of the test is finished, the participants is asked to complete the task using both hands simultaneously to place as many pins as possible down both rows. The number of pins successfully inserted into the holes in 30 s represents the result for this task. The last task is to use both hands simultaneously while assembling pins, washers and collars. In this task, the participants have 60 second. The Validity coefficients of Purdue Pegboard among industrial jobs is ranged from .07 to .76, depending on the score used, the job, and the criterion [24].

2.2.2 Hand grip strength

The purpose of this test is to measure the maximum isometric strength of the hand and forearm muscles. We used a Jamar smart digital hand dynamometer (Patterson Medical Ltd., Nottinghamshire, United Kingdom). The participants hold the dynamometer in the tested hand, with the elbow by the side of the body and flexed 90 degrees. When ready the participants squeeze the dynamometer with maximum isometric effort, which is maintained for about 5 seconds [25]. No other body movement is allowed. Three trials were allowed and the average value was used for further analysis. The Hand grip test has excellent concurrent validity for 0.98 to 0.99 by healthy adults [26].

2.3 Experimental protocol

The participants were asked to attend the laboratory for one single experimental session. The measurements used in the experiment were the Purdue Pegboard test board test and hand grip strength. Purdue Pegboard test was performed four times (before, immediately after, then follow up after 10 minutes, and after 20 minutes). The hand grip was measured three times (before, immediately after and 20 minutes after sensory stimulation). The detailed sequence is illustrated in **Figure 1**. During sensory stimulation, participants sat comfortably in a chair with both hands resting on armrest.

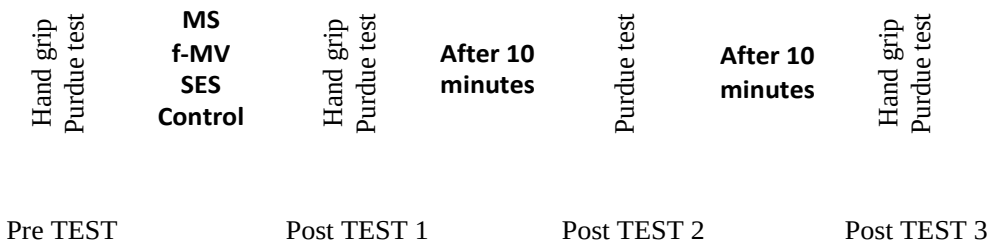

Figure 1. Experiment flow chart.

2.3.1. Protocol 1 – Mechanical stimulation

For the MS rough sand was used and applied on the dorsal and volar side of the forearm. The coarse sand massage lasted 15 minutes. We aimed at stimulation of skin mechanoreceptors [21].

2.3.2. Protocol 2 - Focal muscle vibration

f-MV stimulation was performed with the device EAI Tactor control unit (Engineering acoustics, INC, USA). Four vibration tactors were placed on the forearm muscles (m. extensor carpi ulnaris and m. fleksor carpi radialis). Tactors were placed perpendicular to the skin and with light pressure. The vibration frequency was set at 80 Hz and the oscillation amplitude was limited between 0.8 - 1 mm. During the stimulation itself, the muscles of the upper

extremity are relaxed and the forearm is in a neutral position (supination - pronation). The stimulation lasted 30 minutes.

2.3.3 Protocol 3 - Somatosensory electrical stimulation

For SES stimulation we used Tensmed S84 (Enraf Nonius Rotterdam. Netherlands) device. 2 x 3.5 cm electrodes were chosen (Axelgaard PALS, Axelgaard Manufecturing Co. Ltd., CA, USA). The Asymmetrical biphasic waveform was used with a frequency of 10 Hz. The intensity of the stimulus was increased until the participants reported strong still comfortable sensations of paraesthesia (tingling), but to a level where no muscle contraction was present and stimulation was painless. To prevent adaptation, we increased intensity of the stimulus to point they report again paraesthesia (tingling). Electrodes were placed in the area of the skin supplied by ulnar and median nerve. The second pair of electrodes was placed on the skin area supplied by radial nerve. We stimulated both hands simultaneously. The intensity of SES stimulation was adjusted for each participant and for each channel separately. And stimulation duration for 30 minutes.

2.3.4 Protocol 4 – Control without stimulation

During pre- and post-test period, participants remained sitting for 5 minutes in the absence of stimulation.

2.4. Statistical analysis

The Statistical Package for Social Sciences (SPSS 26, SPSS Inc., Chicago, IL USA) was used for the statistical analysis. Descriptive statistics were calculated for the considered variables. Normal distribution was checked by Shapiro-Wilks's test. For variables that are normally distributed ($p > 0.05$), the parametric ANOVA test for repeated measurements (RM ANOVA / Greenhouse - Geisser correction) was used. Where statistically significant differences were found, the Bonferroni correction and post-hoc test was used to determine the differences between the groups. A statistically significant difference was accepted at level $p < 0.05$.

3. Results

The intensity of SES stimulation was in the left arm: "Radial nerve / 7 ± 1.4 mA; ulnar and median nerve / 3.4 ± 1 mA". In the right arm: "Radial nerve / 3.9 ± 1.7 mA; ulnar and median nerve 3.4 ± 1.7mA".

Table 1. Results of Purdue Pegboard test and hand grip strength measures (Mean (SD)) for all three somatosensory stimuli groups and control group. The significant results are marked bold.

Group MS					P-value
	Pre	Post 1	Post 2	Post 3	ANOVA
Purdue Pegboard test					
Left hand (pins)	15.1 (1.2)	14.9 (1.2)	15.3 (1)	15.3 (0.6)	< 0.001
Right hand (pins)	15.9 (1.6)	15.8 (1.4)	15.9 (1.2)	16.2 (1.2)	< 0.001
Both hands (pins)	14.2 (1.6)	14.9 (0.8)	14.4 (1)	14.9 (0.8)	< 0.001
Both hand assembling (pins)	41.8 (5.9)	42.5 (6)	43 (5.5)	44 (2.4)	< 0.001
Grip strength					
Left hand (kg)	33.5 (7)	32.8 (7.1)	/	30.6 (11.8)	0,688
Right hand (kg)	36.8 (7.8)	35.6 (7.1)	/	36 (6.7)	0,884
Group f-MV					P-value
	Pre	Post 1	Post 2	Post 3	ANOVA
Purdue Pegboard test					
Left hand (pins)	14.2 (2.1)	**15.4 (1.4)***	**16.5 (1.1)***	**17.3 (1.8)***	< 0.001
Right hand (pins)	15.6 (2.3)	**17.3 (1.3)***	**18.3 (1.2)***	**18.5 (1.3)***	< 0.001
Both hands (pins)	13 (0.8)	14.1 (0.8)	15.1 (0.9)	15,4 (0.9)	< 0.001
Both hand assembling (pins)	40.5 (4.2)	43.5 (5.3)	47 (4.5)	48 (4)	< 0.001
Grip strength					
Left hand (kg)	29.3 (2)	29.6 (2.6)	/	30.2 (3)	0,688
Right hand (kg)	31.1 (3.2)	31.5 (3.2)	/	31.8 (3.2)	0,884
Group SES					P-value
	Pre	Post 1	Post 2	Post 3	ANOVA
Purdue Pegboard test					
Left hand (pins)	14.3 (1.1)	**16.6 (0.5)***	**17.2 (0.6)***	**17.3 (0.4)***	< 0.001
Right hand (pins)	15.5 (2.2)	**18.2 (0.7)***	**19.2 (1.3)***	**19 (1.5)***	< 0.001
Both hands (pins)	13.3 (1.6)	**14.7 (1)***	**14.7 (0.8)***	**15 (0.6)***	< 0.001
Both hand assembling (pins)	39.9 (4.9)	**42.7 (3.4)***	**47.4 (4.6)***	**47.2 (3.2)***	< 0.001
Grip strength					
Left hand (kg)	32.5 (3.7)	32.6 (2)	/	31.9 (5)	0,688
Right hand (kg)	35.6 (4.1)	37.8 (3.2)	/	35.5 (5.9)	0,884
Group control					P-value
	Pre	Post 1	Post 2	Post 3	ANOVA
Purdue Pegboard test					
Left hand (pins)	14.3 (1,6)	15.3 (1.7)	15.8 (1.5)	**16 (1.1)***	< 0.001
Right hand (pins)	15 (1.9)	15.7 (1.3)	16.4 (1.7)	16.8 (0.6)	< 0.001
Both hands (pins)	13.2 (1.8)	14 (1.6)	14.3 (1.1)	14.3 (1.5)	< 0.001
Both hand assembling (pins)	38.2 (7.2)	41.6 (6.6)	**43.7 (3.4)***	**45.6 (3.6)***	< 0.001
Grip strength					
Left hand (kg)	33.5 (6.3)	33.4 (5.6)	/	34.3 (5.3)	0,688
Right hand (kg)	36.7 (7.2)	36.2 (5.7)	/	37.3 (6)	0,884

MS Mechanical stimulation, *f-MV* focal muscle vibration, *SES* sensory electrical stimulation, *Pre* pre-intervention test, *Post 1* post-intervention performance, *Post 2* post-intervention performance after 10 minutes, *Post 3* post-intervention performance after 20 minutes, * represents a significant difference from pre-intervention - post hoc test (Bonferroni).

Overall, there was a significant increase in all the Purdue Pegboard test task within the groups (ANOVA $p < 0.001$; MS, f-MV, SES stimulations), also the control group ($p < 0.001$). Post hoc testing showed significant increase in the group within f-MV by left- and right-hand task. In SES stimulation group post hoc, testing showed significant increase in all 4 test conditions (left hand, right hand, both hands and both hand assembling). MS and control group post hoc testing did not show statistically significant changes ($p > 0.05$). Also, we found no differences in initial values across within the groups for grip strength ($p > 0.05$) in left and right hand. Detailed results are described in Table 1.
In the between-groups analysis ANOVA reviled a significant increase when performing Purdue Pegboard test with the right hand ($p < 0.05$). Post hoc testing showed significant increase in two different conditions; f-MV stimulation as compared to control group ($p < 0.05$); SES stimulation as compared to control group ($p < 0.05$). Performing Purdue Pegboard test with the left hand, both hands and both hand assembling ANOVA analysis didn't show statistically significant changes ($p > 0.05$). We also did not find statistically significant changes between-groups for grip strength ($p > 0.05$).

4. Discussion

This study was aimed at exploring the possibility of modulating the motor function via manipulation of somatosensory input by stimulation paradigm characterized by MS, f-MV and SES stimulation. The purpose of the present work was to compare various somato-sensory stimulation on hand dexterity and hand grip strength. Our results indicate, that various somatosensory stimulation has mild effect on hand dexterity. While there was no effect on hand grip strength. The difference after intervention was significant in two groups, (f-MV and SES group). We can relate these results to hand dominance since 35 participants were right-handed. Performing Purdue Pegboard test with the left hand, both hands and both hand assembling show significant changes. Our main finding is, that f-MV and SES stimulation may improve hand dexterity in the dominant hand of young healthy participants. The significant changes within the group also in CON group for Purdue Pegboard test. More precise and faster assembling of pegboard tasks is expected after several repetitions indicating motor learning. The increase in the control group after three repetition indicates motor learning. When comparing the results of CON group to results of other three groups with intervention it can be seen that dexterity increased immediately after intervention and not only during third post-test as it is the case in the CON group. These results indicate, that motor learning is not the only possible explanation for the obtained results.
Increase dexterity in dominant hand by Purdue Pegboard test indicate that f-MV effects on motor performance are probably due to the vibration impact on the proprioceptive networks involved in the motor control of movement. There is growing evidence that cortical connections between somatosensory and motor cortex during motor learning can change rapidly (27) and that motor practice rapidly establishes changes in motor cortex representations (10). In addition to affecting the somatosensory cortex, f-MV at high frequency can also cause plastic changes in the primary motor cortex, with the consequence that spindle endings might send to the brain a more accurate information ameliorating the

motor control. Therefore, it is reasonable to assume that these forms of vibration-induced neuronal reorganization may affect motor output to target muscles, thereby reducing unwanted activations and improving motor movement control [10]. It seems that the modulation of central proprioceptive networks due to vibration might allow a better representation of the desired movement and/ or a minimization of the execution error when the desired movement is provided, and this has an impact on increased dexterity in dominant hand.

Our results by SES stimulation showed that the same as with f-MV statistically significant improvements dexterity in dominant hand. The specific mechanism for increased fractionation ability after SES is unclear. Previous research suggests that SES affects complex motor skills through reorganization and altered sensorimotor cortex irritability. Neuroanatomical, electrophysiological, and imaging data have shown that unilateral electrical stimulation, including SES, can bilaterally activate contralateral S1 and S2 [28,29]. It's interesting that different studies have shown no effects on peripheral nerve M-wave and spinal cord excitability (H waves) with SES, further suggesting that the changes in excitability most likely occur at the level of the cortex [30]. Mechanical pressure stimulation has no effect on hand dexterity and hand grip strength. The rough textured material applied to forearm did not seem to activate enough skin mechanoreceptors to modulate somatosensory (S1) and motor (M1) cortex and may result in increasing hand dexterity or hand grip strength. Peripheral mechanical pressure stimulation with rough textured modalities muscle contraction overt involuntary tonic and phasic movements, postural sways, and modification of voluntary motor actions during and after the stimulation [6]. Similar modulation of motor behaviour, including involuntary motor responses and outlasting motor after effects, has also been demonstrated after mechanical pressure stimulation (MS) [11].

Limitation of our study is relatively small number of participants divided into four groups. Another limitation might be the recruitment of healthy participants as their hand dexterity is already at a high level and they cannot progress. A further limitation could be related to the participants' interpretation of the instruction to execute the task as rapidly as possible, which can cause panic and stress.

5. Conclusions

In conclusion, this study suggests that various somatosensory stimuli such as vibration, electrical stimulation, had facilitatory effect only for right (dominant) hand after f-MV and SES. While stimulation with textured materials was not effective. The increase after three repetitions in the control group indicates also motor learning as a confounding factor. In our experiment the improvement of hand dexterity after application of various somatosensory stimuli was mild. However, tendency to progress in the dominant hand with application of various somatosensory stimuli indicate that it would be interesting to use this stimulation in a group of stroke patients with decreased hand dexterity. These results will serve for the

sample size calculation in future studies where treatment will be applied to patients who suffered a stroke.

Acknowledgements
Authors acknowledge support of ARRS, grant P3-0388.

References

1. Desmurget M, Grafton S. Forward modeling allows feed- back control for fast reaching movements. Trends Cogn Sci. 2000; 4(11):423–431. doi: 10.1016/s1364-6613(00)01537-0
2. Pavlides C, Miyashita E, Asanuma H. Projection from the sensory to the motor cortex is important in learning motor skills in the monkey. J Neurophysiol. 1993; 70(2):733-741. doi: 10.1152/jn.1993.70.2.733
3. Rosenkranz K, Rothwell JC. Modulation of proprioceptive integration in the motor cortex shapes human motor learning. J Neurosci. 2012; 32(26):9000–9006. doi: 10.1523/JNEUROSCI.0120-12.2012
4. Wilson RD, Page SJ, Delahanty M*, et al*. Upper-limb recovery after stroke: a randomized controlled trial comparing EMG-triggered, cyclic, and sensory electrical stimulation. Neurorehabil Neural Repair. 2016; 30: 978–987. doi: 10.1177/1545968316650278
5. Chipchase LS, Schabrun SM, Hodges PW. Peripheral electrical stimulation to induce cortical plasticity: a systematic review of stimulus parameters. Clin Neurophysiol. 2011; 122(3):456-463. doi: 10.1016/j.clinph.2010.07.025
6. Proske U, Gandevia SC. Kinesthetic Senses. Compr Physiol. 2018; 8(3):1157-1183. doi: 10.1002/cphy.c170036
7. Souron R, Besson T, Millet GY, Lapole T. Acute and chronic neuromuscular adaptations to local vibration training. Eur J Appl Physiol. 2017; 117(10):1939-1964. doi: 10.1007/s00421-017-3688-8
8. Hok P, Opavský J, Kutín M, Tüdös Z, Kaňovský P, Hluštík P. Modulationof the sensorimotor system by sustained manual pressure stimulation. Neuroscience. 2017; 348:11-22. . doi: 10.1016/j.neuroscience.2017.02.005
9. Hok P, Opavský J, Labounek R, Kutín M, Šlachtová M, Tüdös Z, Kaňovský P, Hluštík P. Differential Effects of Sustained Manual Pressure Stimulation According to Site of Action. Front Neurosci. 2019; 13:722. doi: 10.3389/fnins.2019.00722
10. Contemori S, Dieni CV, Sullivan JA, et al. Sensory inflow manipulation induces learning-like phenomena in motor behavior. Eur J Appl Physiol. 2020; 120(4):811-828. doi: 10.1007/s00421-020-04320-w
11. Hok P, Hlustik P. Modulation of the human sensorimotor system by afferent somatosensory input: evidence from experimental pressure stimulation and physiotherapy. Biomed Pap Med Fac Univ Palacky Olomouc Czech Repub. 2020; 164(4):371-379. doi: 10.5507/bp.2020.052

12. Johansson RS, Flanagan JR. Coding and use of tactile signals from the fingertips in object manipulation tasks. Nat Rev Neurosci. 2009; 10(5):345-359. doi: 10.1038/nrn2621
13. Abraira VE, Ginty DD. The sensory neurons of touch. Neuron. 2013; 79(4):618-639. doi: 10.1016/j.neuron.2013.07.051
14. Murillo N, Valls-Sole J, Vidal J, Opisso E, Medina J, Kumru H. Focal vibration in neurorehabilitation. Eur J Phys Rehabil Med. 2014; 50(2):231–242.
15. Rosenkranz K, Butler K, Williamon A, Rothwell JC. Regain- ing motor control in musician's dystonia by restoring sensori- motor organization. J Neurosci 2009; 29(46):14627–14636. doi: 10.1523/JNEUROSCI.2094-09.2009
16. Pettorossi VE, Panichi R, Botti FM, Biscarini A, Filippi GM, Schiep- pati M. Long-lasting effects of neck muscle vibration and contraction on self-motion perception of vestibular origin. Clin Neurophysiol 2015; 126(10):1886–1900. doi: 10.1016/j.clinph.2015.02.057
17. Ikuno K, Kawaguchi S, Kitabeppu S, Kitaura M, Tokuhisa K, Morimoto S, Matsuo A, Shomoto K. Effects of peripheral sensory nerve stimulation plus task-oriented training on upper extremity function in patients with subacute stroke: a pilot randomized crossover trial. Clin Rehabil. 2012; 26(11):999–1009. doi: 10.1177/0269215512441476
18. Hamdy S, Rothwell JC, Aziz Q, Singh KD, Thompson DG. Long-term reorganization of human motor cortex driven by short-term sensory stimulation. Nat Neurosci. 1998; 1(1):64–68. doi: 10.1038/264
19. Kaelin-Lang A, Luft AR, Sawaki L, Burstein AH, Sohn YH, Cohen LG. Modulation of human corticomotor excitability by somatosensory input. J Physiol. 2002; 540(Pt 2):623–633. doi: 10.1113/jphysiol.2001.012801
20. CW W, van Gelderen P, Hanakawa T, Yaseen Z, Cohen LG. Enduring representational plasticity after somatosensory stimulation. NeuroImage. 2005; 27(4):872–884. doi: 10.1113/jphysiol.2001.012801
21. Ikuno K, Matsuo A, Shomoto K. Sensory Electrical Stimulation for Recovery of Hand and Arm Function in Stroke Patients: A Review of the Literature. J Nov Physiother. 2012; S1:007. doi:10.4172/2165-7025.S1-007
22. Ridding MC, McKay DR, Thompson PD, Miles TS. Changes in corticomotor representations induced by prolonged peripheral nerve stimulation in humans. Clin Neurophysiol. 2001; 112(8):1461-1469. doi: 10.1016/s1388-2457(01)00592-2
23. Desai, K., Kene, K., Doshi, M., More, S. H., & Desai, S. Normative data of Purdue pegboard on Indian population. IJOT. 2006; 37(3), 69–72.
24. Tiffin, J., & Asher, E. J. The Purdue Pegboard: norms and studies of reliability and validity. Journal of Applied Psychology. 1948; 32(3), 234–247. doi: 10.1037/h0061266
25. Schmidt RT, Toews JV. Grip force as measured by the Jamar dynamometer. Arch Phys Med Rehabil. 1970; 51:321–327.

26. Vahdat S, Darainy M, Milner TE, Ostry DJ. Functionally specific changes in resting-state sensorimotor networks after motor learning. J Neurosci. 2011; 31(47):16907–16915. doi: 10.1523/JNEUROSCI.2737-11.2011
27. Mathiowetz V. Comparison of Rolyan and Jamar dynamometers for measuring grip strength. Occup Ther Int. 2002; 9(3):201-209. doi: 10.1002/oti.165
28. Aman JE, Elangovan N, Yeh IL, Konczak J. The effectiveness of proprioceptive training for improving motor function: a system- atic review. Front Hum Neurosci. 2014; 8:1075. doi: 10.3389/fnhum.2014.01075
29. Sasaki R, Kotan S, Nakagawa M, Miyaguchi S, Kojima S, Saito K, Inukai Y, Onishi H. Presence and absence of muscle contraction elicited by peripheral nerve electrical stimulation differentially modulate primary motor cortex excitability. Front Hum Neurosci. 2017; 11:146. doi: 10.3389/fnhum.2017.00146
30. Ftime-Nielsen SD, Christensen MS, Vingborg RJ, Sinkjaer T, Roepstorff A, Grey MJ. Interaction of electrical stimulation and voluntary hand movement in SII and the cerebellum during simulated therapeutic functional electrical stimulation in healthy adults. Hum Brain Mapp. 2012; 33(1):40–49. doi: 10.1002/hbm.21191

Research

The effect of knee extensor and flexor strengthening, coupled with passive anterior tibial translation, on knee anterior laxity in the ACL injured knee. A case report

Rugelj Darja[1,2], Bedek Jure[1], Benko Žiga[1], Drobnič Matej[3], Vauhnik Renata[1,2,4,*]

[1]University of Ljubljana, Faculty of Health Sciences, Department of Physiotherapy, Ljubljana, Slovenia
[2]University of Ljubljana, Faculty of Health Sciences Biomechanics Laboratory, Ljubljana, Slovenia
[3]University Medical Centre Ljubljana, Department of Orthopaedic Surgery, Ljubljana, Slovenia
[4]Arthron, Institute for Joint and Sport Injuries, Slovenia

*renata.vauhnik@zf.uni-lj.si

Abstract

Increased knee anterior laxity results when the anterior cruciate ligament is injured. This increased laxity can cause knee dysfunction. Until recently, this laxity was believed to be only diminished through surgery. However, recent findings indicate that knee anterior laxity may be decreased with repeated loading of the knee. Subject was a 23-years old female. Her body height was 180 cm and her body mass was 72 kg. The ACL injury occurred 12 months before the first testing. A subtotal ACL injury was confirmed by MRI. Knee anterior laxity was measured with GNRB® knee arthrometer. The Lysholm Knee Scoring Scale was used to assess subjective knee function. Hop tests were used to evaluate lower limb function. Isokinetic muscle testing of knee extensors and flexors was performed at 60°/sec and 180°/sec on Cybex dynamometer to assess the muscle strength. The results showed that the 12-week knee-extensor and flexor-strengthening program, coupled with passive anterior translation did not change knee anterior laxity. In order to make a more comprehensive evaluation of the simultaneous effects of active and passive knee loading further research is required.

1. Introduction

Increased knee anterior laxity results when the anterior cruciate ligament is injured. It is believed that for the injured knee joint, the only way to decrease knee joint laxity is with a surgical reconstruction of the affected ligament. On contrary, certain animal experiments demonstrated an increased ligament strength after repeated mechanical loading [1-5]. Mechanical loading therefore plays a significant role in the maintenance and adaptation of the mechanical, ultrastructural, histological and functional properties of connective tissues [6] via mechanotransduction [7]. In vitro studies have demonstrated the ability of the knee medial collateral ligament complex to respond to mechanical loading (at loads that fall within the linear region of the load-deformation response curve for that tissue), via an increase in mechanical and ultrastructural properties such as ultimate load to failure, stiffness and cross sectional area [2-5]. In support of these animal studies, Morrissey et al. (2008) [8] have found that knee joint loading in ACL injured subjects can reduce knee anterior laxity. Similarly, study by Barcellona et al. (2015) [9] suggested that low load open kinetic chain knee extensor exercises decrease knee anterior laxity in ACL injured subjects. In these investigations, loading was applied with open chain resistance exercise of the knee extensor muscle group with knee anterior laxity reduced from this training. During this type of exercise, anterior directed load is placed on the knee joint structures such as the anterior cruciate ligament, which is the primary restraint of knee anterior laxity, indicating that the above mentioned training increase the strength not only of the muscles but it is coupled with changes in ligaments tensile properties. Ligaments are viscoelastic materials, designed especially to resist tensile forces, additional passive loading with anterior tibial translation might decrease knee anterior laxity. The purpose of this single case report was to evaluate the effect of knee extensor and flexor strengthening, coupled with passive anterior tibial translation on knee anterior laxity in the ACL injured knee.

2. Methods

Subject was a 23-years old female. Her body height was 180 cm and her body mass was 72 kg. The ACL injury occurred 12 months before the first testing. ACL injury was confirmed by MRI. The study was approved by Slovenia National Medical Ethics Committee (permit No. 164/07/13). Exercise programme took place 3 times per week over the course of 12 weeks. The exercise programme consisted of a 5-minute warm-up protocol using a stepper, an elementary training programme to strengthen knee flexor and extensor muscles and the final part of the exercise programme which included the use of the seated knee extensor training device, which allowed passive loading with added anterior tibial translation during knee extension exercise at the same time.

The elementary part of the exercise programme included three exercises: the first one was a squat with added resistance in the direction of adduction elicited by the Theraband® resistance tubing loop ending with a heel raise on the Airex® balance pad. The second exercise was the ball leg curl. The third one was a lunge with emphasis on the back leg. Each

exercise was performed in 3 sets of 10 repetitions. The number of repetitions was increased to 12 after 7 weeks of the exercise programme. Exercises were performed in a form of circuit training with 30 seconds of rest between exercises. Each circuit (set) was followed by 2 minutes of rest.

Figure 1. The machine with self-standing stand and the part fixed on the seated knee extensor training device for coupling active and passive loading of the knee.

The final part of the exercise programme was done on the seated knee extensor training device. The first exercise was done in 2 sets of 20 repetition maximum (RM) as suggested in study by Barcellona et al. (2015) [9]. The RM was adjusted according to the progress of the subject. The second exercise was done in 3 sets of 10 repetitions with a load of 10 kg and with added passive anterior tibial translation. Concentric knee extensor activity occurred during the extension of the knee joint. During the first 60° of knee flexion, eccentric contraction of knee extensors occurred. The last 30° of flexion was performed by concentric activation of knee flexors because of the anterior pull elicited by the device.
The device consisted of 2 components, the self-standing platform and the part fixed on the seated knee extensor training device (**Figure 1**). A dog collar was placed around the proximal part of the tibia of the patient. One end of a wire rope was attached to the collar, while two weights with a combined mass of 20 kg were attached to the other side. The rope ran from the dog collar, over the first sheave which was placed in a manner that ensured the force elicited on the tibia was perpendicular. From there, the rope ran upwards and sideways towards and over the second sheave, where it was redirected straight towards the ground by the force of the weights. The pulley caused the anterior translation of the tibia and ensured the force was perpendicular to the tibia throughout the full range of motion. One of the physiotherapists helped to stabilize the self-standing stand while the other lifted the weights between repetitions to relieve the pressure on the calf and prevent a reduction of

blood flow in the lower limb. Passive force in the direction of anterior tibial translation was measured by fixing a dynamometer attachment onto the dog collar. The force pulling on the calf was 150N with a fluctuation of 10N according to the measurement.

3. Results

Knee anterior laxity, the main outcome measure, was measured with the GNRB® knee arthrometer. Knee anterior laxity measurements were performed as described in Vauhnik et al. (2013)[10]. In addition to the knee anterior laxity measurements, the following outcome measures were used. The Lysholm Knee Scoring Scale [11] was used to assess subjective knee function before and after the training programme. Hop tests were used to evaluate lower limb function. A battery of tests was conducted that included the single leg hop for distance test, the triple hop for distance test, the one-legged timed hop test and the crossover triple hop for distance test. A modified version of hop tests, described by Barber et al., (1992) [12], was used. Isokinetic muscle testing of knee extensors and flexors was performed at 60°/sec and 180°/sec on Cybex dynamometer as described by the manufacturer. The first testing was performed before the start of the exercise programme, the second testing was performed after 6 weeks of the exercise programme and the third testing was performed after 12 weeks of the exercise programme. At the first and the third testing all 4 outcome measurements were performed, while during the second testing only the measurements of knee anterior laxity were performed. The results of the following outcome measurements, knee anterior laxity, hop tests and muscle strength are presented in **Table 1**. The Lysholm Knee Scoring Scale did not change between the first and the third testing. Subject had maximum score (100 points) in both occasions.

Table 1. Results of knee anterior laxity, hop tests and muscle strength

		1st testing			2nd testing		3rd testing		
Knee anterior laxity (mm)	FORCE	ULL	ILL		ULL	ILL	ULL	ILL	
	67 N	4,8	6,6		3,5	4,9	4,5	6,4	
	89 N	6,1	7,7		4,8	6,1	5,9	7,4	
	134 N	8,1	9,4		7,1	7,9	7,6	9,3	
	200 N	10,1	11,4		9,1	10	9,6	11,5	
	250 N	11,2	12,9		10,5	11,5	11,1	13	
Single leg hop for distance	Best result [cm]	180	179				168	173	
	Average [cm]	179	178				159,7	168,3	
	Symmetry index	99 %					105 %		
Triple hop for distance	Best result [cm]	466	480				462	437	
	Average [cm]	454,7	468,3				434,7	421,7	
	Simmetry index	103 %					97 %		
One-legged timed hop	Best result [s]	2,4	2,5				2,1	2,3	
	Average [s]	2,4	2,5				2,2	2,3	
	Simmetry index	96 %					96 %		
Crossover triple hop for distance	Best result [cm]	465	420				451	407	
	Average [cm]	441	405				412,3	385,3	
	Symmetry index	92 %					93 %		
		ULL	ILL	Deficit			ULL	ILL	Deficit
Isokinetic muscle performance at 60°/s	Extensors (Nm)	180	161	11 %			172	186	-7 %
	Flexors (Nm)	114	88	23 %			118	107	9 %
	Ratio F/E (%)	63	55	/			69	58	/
Isokinetic muscle performance at 180°/s	Extensors (Nm)	113	117	-3 %			121	125	-3 %
	Flexors (Nm)	87	91	-4 %			87	100	-14 %
	Ratio F/E (%)	77	78	/			72	80	/

Legend: ULL – uninjured lower limb; ILL – injured lower limb

4. Discussion

The purpose of this case report was to investigate the effect of knee extensor and flexor strengthening, coupled with passive anterior tibial translation on knee anterior laxity in the ACL injured knee. The results demonstrate that there is no training effect of knee extensor and flexor strengthening, coupled with passive anterior tibial translation on knee anterior laxity in the ACL injured knee after 12 weeks of training. There are several possible reasons for not finding a training effect of coupled active and passive knee loading on knee anterior laxity.

One possible reason for not finding a training effect might lie in case studied. Subject studied in this case report had a difference in knee anterior laxity between injured and injured knee less than 3 mm (1.9 mm at the force 250N) and this difference is within normal differences expected between right and left knee [13]. Furthermore, the subject also had 100 points in the Lysholm Knee Scoring Scale prior to the training programme, indicating no problems with instability or increased knee laxity.

Another possible reason why a lack of coupled active and passive loading training might have occurred is due to an insufficient training duration and load applied. Animal studies

investigating the response of connective tissues to load training, have used different durations of training, with training programs lasting from 6 to 40 weeks [14-16]. Since the duration of the training program in this case report was 12 weeks, it is possible that a training duration was not long enough, or the effect of a delayed nature did occur but was not found because of the lack of follow-up testing. Furthermore, we do not know accurately the amount of load transferred to the ligament. We performed the dynamometer measurement outside the knee joint and we can only speculate whether the measured load (150N) was transferred to the ligament inside the knee joint and this load might not be sufficient.

In addition, this case report was presented on a female patient. We are aware that female patients are not an appropriate model for pilot trial on ligaments due to the menstrual cycle significantly changing ligament strength. Future research is needed and should focus on male subjects with increased knee anterior laxity as a consequence of ACL injury.

Acknowledgements

The authors acknowledge the financial support from the Slovenian Research Agency (research core funding no. P3-0388).

References

1. Burroughs P, Dahners LE. The effect of enforced exercise on the healing of ligament injuries. Am J Sports Med. 1990; 18: 376-378. doi: 10.1177/036354659001800407
2. Laros GS, Tipton CM, & Cooper RR. Influence of physical activity on ligament insertions in knees of dogs. J Bone Joint Surg. 1971; 53A: 275-286.
3. Tipton CM, Vailas AC, Matthens RD. Experimental studies on the influences of physical activity on ligament, tendons and joints: A brief review. Acta Med Scand Suppl 1986; 711: 157-168. doi: 10.1111/j.0954-6820.1986.tb08945.x
4. Woo SLY, Amiel D, Akeson WH, Kuei SC, Tipton CM. Effect of long-term exercise on ligaments, tendons and bones of swine. Med Sci Sports Ex. 1979; 11: 105.
5. Woo SLY, Gomez MA, Woo YK, Akeson WH. Mechanical properties of tendons and ligaments: the relationships of immobilization and exercise on tissue remodelling. Biorheology. 1982; 19: 397-408. doi: 10.3233/bir-1982-19302
6. Woo SL, Abramowitch SD, Kilger R, Liang R. Biomechanics of knee ligaments: injury, healing, and repair. J Biomech. 2006; 39:1-20. doi: 10.1016/j.jbiomech.2004.10.025
7. Kjaer M. Role of extracellular matrix in adaptation of tendon and skeletal muscle to mechanical loading. Physiol Rev. 2004; 84: 649-698. doi: 10.1152/physrev.00031.2003
8. Morrissey MC, Perry MC, King JB. Is knee laxity change after anterior cruciate ligament injury and surgery related to knee extensor training load? Am J Phys Med Rehabil. 2009; 88: 369-375. doi: 10.1097/PHM.0b013e3181a0d7ed.

9. Barcellona MG, Morrissey MC, Milligan P, et al. The effect of knee extensor open kinetic chain resistance training in the ACL-injured knee. Knee Surg Sports Traumatol Arthrosc. 2015; 23:3168-3177. doi: 10.1007/s00167-014-3110-6.
10. Vauhnik R, Perme MP, Barcellona MG, et al. Robotic knee laxity testing: reliability and normative data. Knee. 2013; 20: 250-255. doi: 10.1016/j.knee.2012.10.010
11. Lysholm J, Tegner Y. Knee injury rating scales. Acta Orthop. 2007; 78:445-53. doi: 10.1080/17453670710014068
12. Barber SD, Noyes FR, Mangine R, DeMaio M. Rehabilitation after ACL reconstruction: function testing. Orthopedics. 1992; 15(8): 969-74.
13. Daniel DM, Stone ML, Dobson BE, Fithian DC, Rossman DJ, Kaufman KR. Fate of the ACL-injured patient. A prospective outcome study. Am J Sports Med. 1994; 22:632-644. doi: 10.1177/036354659402200511
14. Cabaud HE, Chatty A, Gildengorini V, Feltman RJ. Exercise effects on the strength of the rat anterior cruciate ligament. Am J Sports Med. 1980; 8: 79-86. doi: 10.1177/036354658000800204
15. Sakuma K, Mizuta H, Takagi K. Effects of enforced exercise on biomechanical properties of the anterior cruciate ligament in bipedal rats. J Japan Orthop Assoc 1992; 66: 1146-1155.
16. Vidik A. Elasticity and tensile strength of the anterior cruciate ligament in rabbits as influenced by training. Acta Physiol Scand 1968; 74: 372-380. doi: 10.1111/j.1748-1716.1968.tb04245.x

Research

Effect of repeated passive anterior loading on knee anterior laxity in injured knee: A case report

Rugelj Darja[1,2], Pilih Iztok[3], VauhnikRenata[1,2,3,*]
[1]University of Ljubljana, Faculty of Health Sciences, Department of Physiotherapy, Slovenia
[2]Biomechanics Laboratory, Faculty of Health Sciences, University of Ljubljana, Slovenia
[3]Arthron, Institute for Joint and Sport Injuries, Slovenia
*renata.vauhnik@zf.uni-lj.si

Abstract

It is believed that the only way to decrease knee joint laxity after anterior cruciate ligament (ACL) injury, is with the surgical tightening of the knee. However, recent studies are suggesting that low load open kinetic chain knee extensor exercises decrease knee anterior laxity in ACL injured subjects. During this type of exercise, anterior directed load is placed on the knee joint structures such as the ACL, which is the primary restraint of knee anterior laxity. If anterior directed load is placed to the knee joint passively by knee arthrometer, a decrease in knee anterior laxity might occur, since according to the mechanical properties, ligaments are viscoelastic materials, designed especially to resist tensile forces. The purpose was to evaluate the effect of repeated passive anterior loading on knee anterior laxity in the injured knee. The partial anterior cruciate ligament tear was confirmed with MRI. We performed repeated passive anterior loading with the GNRB® knee arthrometer. One loading unit contained of 40 repetitions of anterior tibial translation at the force of 250N. We performed passive anterior loading of the injured knee 3 to 5 times per week for a period of 20 weeks. Repeated passive anterior loading might decrease knee anterior laxity, however future research is needed to define the appropriate duration and the amount of loading.

1. Introduction

It is believed that the only way to decrease knee joint laxity after anterior cruciate ligament (ACL) injury, is with the surgical tightening of the knee. Morrissey et al. (2009) [1] have found that knee joint loading in ACL injured subjects can reduce knee anterior laxity. Similarly, recent study by Barcellona et al. (2015) [2] suggested that low load open kinetic chain knee extensor exercises decrease knee anterior laxity in ACL injured subjects. In these investigations, loading was applied with open chain resistance exercise of the knee extensor muscle group with knee anterior laxity reduced from this training. During this type of exercise, anterior directed load is placed on the knee joint structures such as the ACL, which is the primary restraint of knee anterior laxity. If anterior directed load is placed to the knee joint passively by knee arthrometer, a decrease in knee anterior laxity might occur, since according to the mechanical properties, ligaments are viscoelastic materials, designed especially to resist tensile forces. In vitro animal studies have demonstrated the ability of the knee medial collateral ligament complex to respond to mechanical loading (at loads that fall within the linear region of the load-deformation response curve for that tissue), via an increase in mechanical and ultrastructural properties such as ultimate load to failure, stiffness and cross sectional area [3-6]. The purpose of our case report was to evaluate the effect of repeated passive anterior loading on knee anterior laxity in the injured knee.

2. Methods

Female subject 39 years old, with body height 156 cm and body mass 51 kg participated in our case report. The partial ACL tear was confirmed with MRI and the ACL injury occurred a year prior to participation in the study. Slovenia National Medical Ethics Committee (permit No. 164/07/13) approved the study.

We performed passive anterior loading in the injured knee using GNRB® knee arthrometer. GNRB® allows automated anterior tibial translation at force of 250N. In one loading unit, we performed 40 repetitions of automated anterior tibial translation at force of 250N. We have chosen the force of 250N, since this force is used to assess the integrity of the ACL with GNRB® and since our previous work [7] of passive anterior loading done on uninjured knees indicated that the force of 170N might not be large enough for changes to occur in knee anterior laxity. We performed loading units from 3 to 5 times per week, for a period of 20 weeks. During the passive anterior loading of the knee, we have used EMG in order to detect any hamstring activity (V-AMP 16; Brain products). **Figure 1** presents the set up for the loading unit.

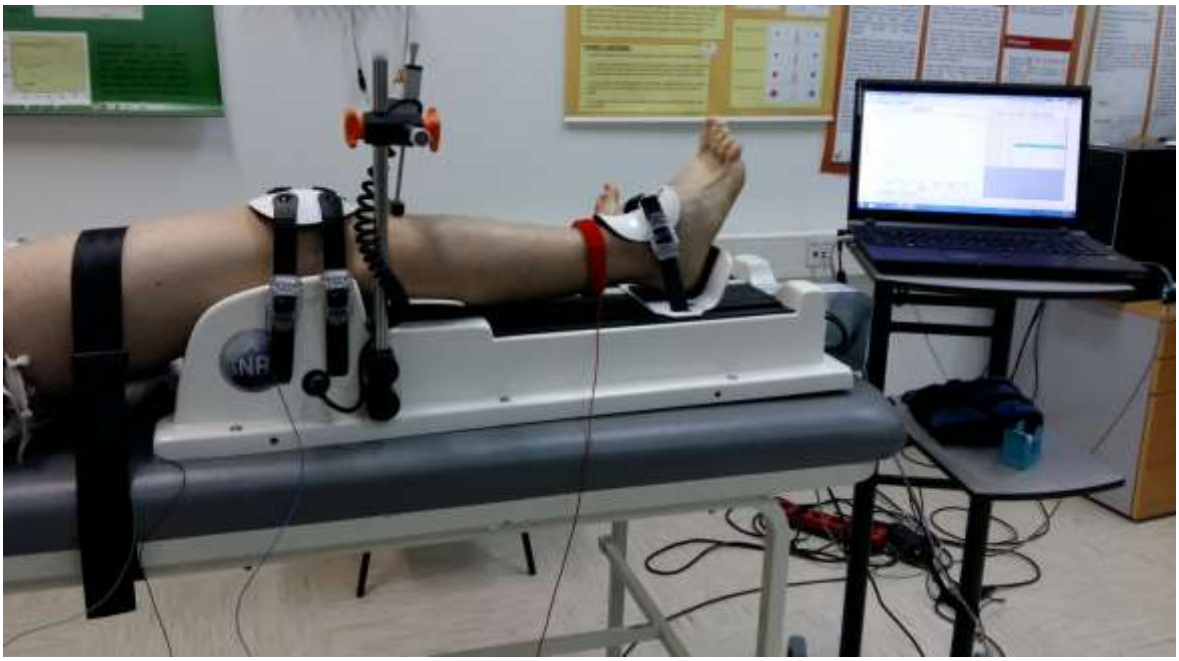

Figure 1. Set up for repeated passive loading of the knee.

We performed the measurements of knee anterior laxity before the first loading unit, at then at the 4th week, the 9th week and 22nd week (2 weeks after the last loading unit). Detailed description of knee anterior laxity measurements using the GNRB® is described in Vauhnik et al. (2013) [8]. One experienced examiner performed all the measurements of knee anterior laxity, in order to ensure optimal reliability.

3. Results

We performed 63 loading units during the period of 20 weeks. Changes in the slope of the curve (**Figure 2**) reflect changes in knee anterior laxity. Slope of the curve indicates the changes in knee anterior laxity at the forces from the 0N to 250N and the slope of the curve is advised to be used by GNRB® manufacturers (GENOUROB SAS, Montenay, France) when there is a partial rupture of the ACL. Slope of the curve indicates the changes in anterior tibial displacement occurring during the force from 0N to 250N, expressed in µm/N.

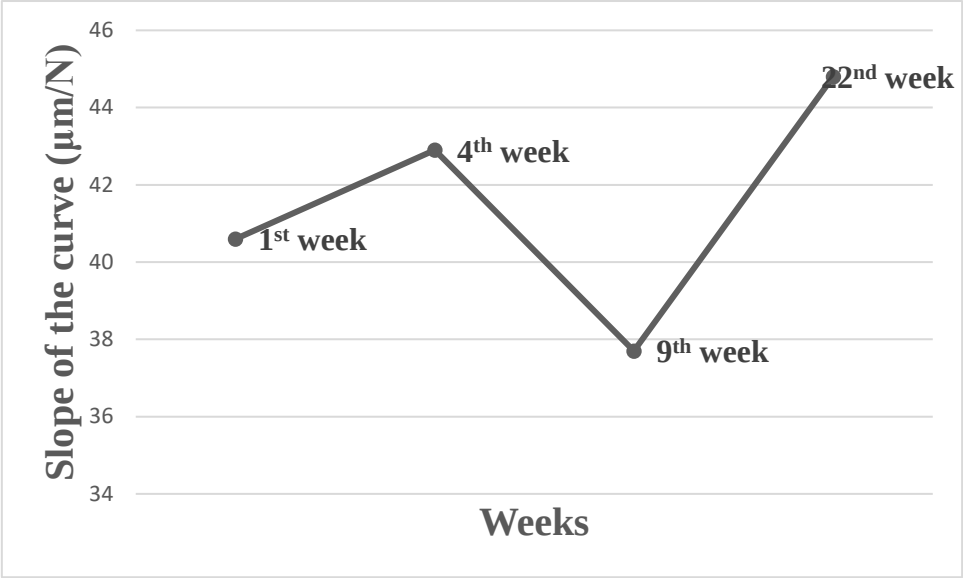

Figure 2. Changes in knee anterior laxity after repeated passive anterior loading

At the first measurement of knee anterior laxity (before the loading units), the slope of the curve was 40,6 µm/N. At the second measurement (4th week of loading) was 42.9 µm/N, at the third measurement (9th week of loading) was 37.7 µm/N and at the fourth measurement (22nd week (2 weeks after 20 weeks of loading)) was 44.8 µm/N, indicating the changes in knee anterior laxity.

4. Discussion

The hypothesis tested in our case report was that repeated passive knee loading over a number of weeks would decrease knee anterior laxity in the injured knee. The results demonstrated that there was a decrease in knee anterior laxity in the injured knee observed in the slope of the curve after the 8th weeks of repeated passive loading (42.9 µm/N vs 37.7 µm/N), however the knee anterior laxity increased then after 22 weeks, 2 weeks after 20 weeks of repeated passive loading. Since the slope of the curve after 22 weeks increased compared to the slope of the curve at the first measurement (44.8 µm/N vs 40.6 µm/N), this might indicate that passive anterior loading might increase knee anterior laxity.

For years, there is a debate in clinical and research areas, whether ACL injured subjects should performed open kinetic chain exercises or no and whether the anterior loading of the tibia is harmful or beneficial for ACL. Studies reports conflicting results. However, when considering mechanical and structural properties of the ligaments, it is normal to conclude that in order to make the ligament stronger, the proper loading must be applied and since ligaments are responding to the tensile force, passive loading where tensile forces are occurring in the ligament, would be a logical conclusion. Many animal studies have noted that the forces being transmitted to ligaments and tendons will generally increase the strength and functional capacity of these structures [3-6,9]. Mechanical loading therefore plays a significant role in the maintenance and adaptation of the mechanical, ultrastructural, histological and functional properties of connective tissues [10] via mechanotransduction [11]. In vitro studies, knee medial collateral ligament complex responded to mechanical

loading (at loads that fall within the linear region of the load-deformation response curve for that tissue), via an increase in mechanical and ultrastructural properties such as ultimate load to failure, stiffness and cross sectional area [3-6]. In support of these animal studies, Morrissey et al. (2009) [1] have proposed and Barcellona et al. (2015) [2] have found that joint loading can reduce joint laxity. In these studies, loading was applied with resistance open kinetic chain exercise of the knee extensor muscle group and knee anterior laxity decreased from this training. These studies indicate that ligament might become stiffer, which we suspect is due to soft tissue strengthening. Furthermore, recent study by Myrick et al. (2019) [12] indicated that the mean volume of the anterior cruciate ligament significantly increased from preseason to postseason among female collegiate athletes, indicating that physical demand of sport activities influence knee laxity. Loading can have contrasting, intensity-related effects. For example in bone, loading can be both beneficial and harmful, depending on intensity [13]. Therefore, the possibility exists that lesser amounts of passive joint loading may stimulate targeted tissues to increase their strength and this increased strength may result in enhancing the tissue's ability to resist loads thereby maintaining joint stability. In our case report, the laxity decreased after 8 weeks of passive anterior loading, but then the laxity increased and it might be that the duration of tensile loading more than 8 weeks is not beneficial for decreasing the knee anterior laxity in humans. Animal studies, investigating the response of ligaments to loading, have used different durations of training programs, with training programs lasting from 6 to 40 weeks [14-16]. Furthermore, maybe the next step is to combine active and passive knee (ligament) loading. Future research is warranted in order to confirm what kind of loading is beneficial for the ACL ligament in terms of the amount of force, number of repetitions and duration.

Acknowledgements

The authors acknowledge the financial support from the Slovenian Research Agency (research core funding no. P3-0388).

References

1. Morrissey MC, Perry MC, King JB. Is knee laxity change after anterior cruciate ligament injury and surgery related to knee extensor training load? Am J Phys Med Rehabil. 2009; 88: 369-375. doi: 10.1097/PHM.0b013e3181a0d7ed
2. Barcellona MG, Morrissey MC, Milligan P, et al. The effect of knee extensor open kinetic chain resistance training in the ACL-injured knee. Knee Surg Sports Traumatol Arthrosc. 2015; 23:3168-3177. doi: 10.1007/s00167-014-3110-6
3. Laros GS, Tipton CM, Cooper RR. Influence of physical activity on ligament insertions in knees of dogs. J Bone Joint Surg. 1971; 53A: 275-286.
4. Woo SLY, Amiel D, Akeson WH, et al. Effect of long-term exercise on ligaments, tendons and bones of swine. Med Sci Sports Ex. 1979; 11: 105.

5. Woo SLY, Gomez MA, Woo YK, Akeson WH. Mechanical properties of tendons and ligaments: the relationships of immobilization and exercise on tissue remodelling. Biorheology. 1982; 19: 397-408. doi: 10.3233/bir-1982-19302
6. Burroughs P and Dahners LE. The effect of enforced exercise on the healing of ligament injuries. Am J Sports Med. 1990; 18: 376-378. doi: 10.1177/036354659001800407
7. Vauhnik R, Perme MP, Barcellona MG, et al. Effect of repeated passive anterior loading on human knee anterior laxity. Man Ther. 2015; 20:709-714. doi: 10.1016/j.math.2015.02.007
8. Vauhnik R, Perme MP, Barcellona MG, et al. Robotic knee laxity testing: reliability and normative data. Knee. 2013; 20: 250-255. doi: 10.1016/j.knee.2012.10.010
9. Tipton CM, Vailas AC, Matthens RD. Experimental studies on the influences of physical activity on ligament, tendons and joints: A brief review. Acta Med Scand Suppl. 1986; 711: 157-168. doi: 10.1111/j.0954-6820.1986.tb08945.x
10. Woo SL, Abramowitch SD, Kilger R, Liang R. Biomechanics of knee ligaments: injury, healing, and repair. J Biomech. 2006; 39:1-20. doi: 10.1016/j.jbiomech.2004.10.025
11. Kjaer M. Role of extracellular matrix in adaptation of tendon and skeletal muscle to mechanical loading. Physiol Rev. 2004; 84: 649-698. doi: 10.1152/physrev.00031.2003
12. Myrick KM, Voss A, Feinn RS, Martin T, Mele BM, Garbalosa JC. Effects of season long participation on ACL volume in female intercollegiate soccer athletes. J Exp Orthop. 2019; 6-12. doi: 10.1186/s40634-019-0182-8
13. Guadalupe-Grau A, Fuentes T, Guerra B, Calbet JA. Exercise and bone mass in adults. Sports Med. 2009; 6: 439-468. doi: 10.2165/00007256-200939060-00002
14. Sakuma K, Mizuta H, Takagi K. Effects of enforced exercise on biomechanical properties of the anterior cruciate ligament in bipedal rats. J Japan Orthop Assoc. 1992; 66: 1146-1155.
15. Cabaud HE, Chatty A, Gildengorini V, Feltman RJ. Exercise effects on the strength of the rat anterior cruciate ligament. Am J Sports Med. 1980; 8: 79-86. doi: 10.1177/036354658000800204
17. Vidik A. Elasticity and tensile strength of the anterior cruciate ligament in rabbits as influenced by training. Acta Physiol Scand. 1968; 74: 372-380. doi: 10.1111/j.1748-1716.1968.tb04245.x

Research

Extraction of polyethylene terephthalate (PET) microplastics from alluvial soil: comparison of density separation and oil-based extraction

Leban Pia[1,*],Bavcon Kralj Mojca[1], Griessler Bulc Tjaša[1], Prosenc Franja[2,**]
[1]University of Ljubljana, Faculty of Health Sciences, Department for Sanitary Engineering, Ljubljana, Slovenia
[2]University of Ljubljana, Faculty of Health Sciences, Research Institute, Ljubljana, Slovenia

*cepic.p@gmail.com
**franja.prosenc@zf.uni-lj.si

Abstract
Microplastics (MPs) have become a global environmental problem, with high occurrence in marine and terrestrial environments. Research of MPs in soil and other organic-rich matrices has become important in recent years, but methods for extraction, analytical methods for quantification and identification of MPs have not yet been standardised. Two methods for extraction of MPs from alluvial soil were compared, oil-based extraction and density separation method. The recovery of the extracted MPs in both methods was higher than 90 %, with 97 ± 8 % (10 PET MPs per 10 g of soil) and 98 ± 3 % (20 PET MPs per 10 g of soil) obtained using oil-based extraction, and with 93 ± 5 % (10 PET MPs per 10 g of soil) and 99 ± 2 % (20 PET MPs per 10 g of soil) for density separation method. In further research, the two extraction methods will be tested on different MP polymers, as well as soils with varying organic content. The optimal protocol will then be used to extract MPs from environmental samples for further quantification and identification.

1. Introduction

Plastic is stable and widely applied material with intensive production worldwide, causing a large amount of plastic waste, where almost 90 % of it ends up directly or indirectly in terrestrial environment [1]. Plastics can enter terrestrial environment through littering and street runoff (containing tire wear). Other pathways are atmospheric deposition, wastewater irrigation, mulching film and application of biosolids, compost, and sewage sludge as fertiliser [2-5]. With different natural processes, such as weathering, mechanical wear, hydrolysis and others, plastic breaks down into countless small particles. Some of those particles are microplastics (MPs), which are smaller than 5 mm. MPs represent a great risk to the environment and also to the human health, because they can easily transport to different environmental media, they can be ingested by organisms and may enter the food chain [1]. They can also carry different hazardous substances, such as hydrophobic organic pollutants and pesticides [6]. With high occurrence and lack of analytical methods for quantification and identification, MPs have become and will remain a global environmental problem [1].

Polyethylene terephthalate (PET) is a commonly and widely used polymer, usually intended for packaging, often plastic bottles as well as clothing. It is produced by the polymerisation of ethylene glycol and terephthalic acid [7]. PET is classified as high and low-density polymer. The density of semi-crystalline high-density PET is between 1.37 and 1.40 g cm^{-3} and the melting point is in the 255–265 °C temperature range [8]. It can be found as MPs almost everywhere, in water, soil, compost and sewage sludge [4,5]. The method for extraction and quantification of MPs from soil has not yet been standardised and presents multiple challenges due to the complexity of the medium and the presence of organic matter [3].

In this study, two methods for MP extraction, made from the model polymer PET, from alluvial soil samples were compared. The oil-based extraction, which takes advantage of the lipophilic surface properties of most plastics, and a commonly used density separation method, which separates MPs from soil, based on the density difference of MPs and the saline solution were studied [9,10].

2. Methods

2.1 PET MP particle preparation

Two methods were tested on the alluvial soil and spiked with particles of the high-density PET polymer. Square pieces of PET plastics were cut manually in the dimension range from 0.1 to 2 mm, as shown in **Figure 1.**

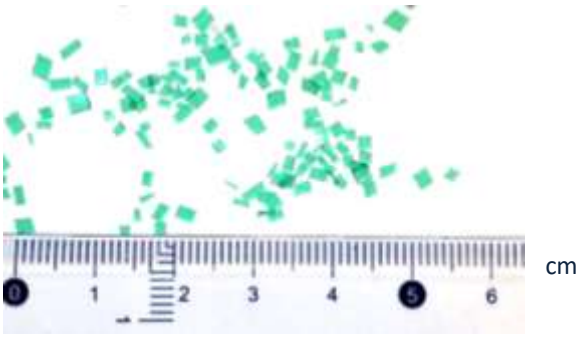

Figure 1. Manually prepared polyethylene terephthalate (PET) microplastic particles.

2.2 Oil-based extraction

The oil-based extraction method was tested on alluvial soil samples, spiked with PET MPs in different quantities. For this method, a custom-made polytetrafluoroethylene (PTFE) cylinder was made. In it, 10 g of alluvial soil was mixed with a defined number of PET MP particles (10 and 20), 10 mL of distilled water and 3 mL of olive oil. Firstly, the closed cylinder was shaken, then left settling for 2 h and finally put into the freezer overnight. Once frozen, the sample was pushed out of a cylinder with a piston and the oil layer was separated from the rest of the ice. The frozen oil layer, containing MPs was left to thaw on a glass fibre filter (Whatman GF/C 47 mm) and then filtered through and rinsed with water and subsequently with hexane to remove traces of oil. This protocol, shown in **Figure 2**, was adapted with changes from Scopetani et al. (2020) [10].

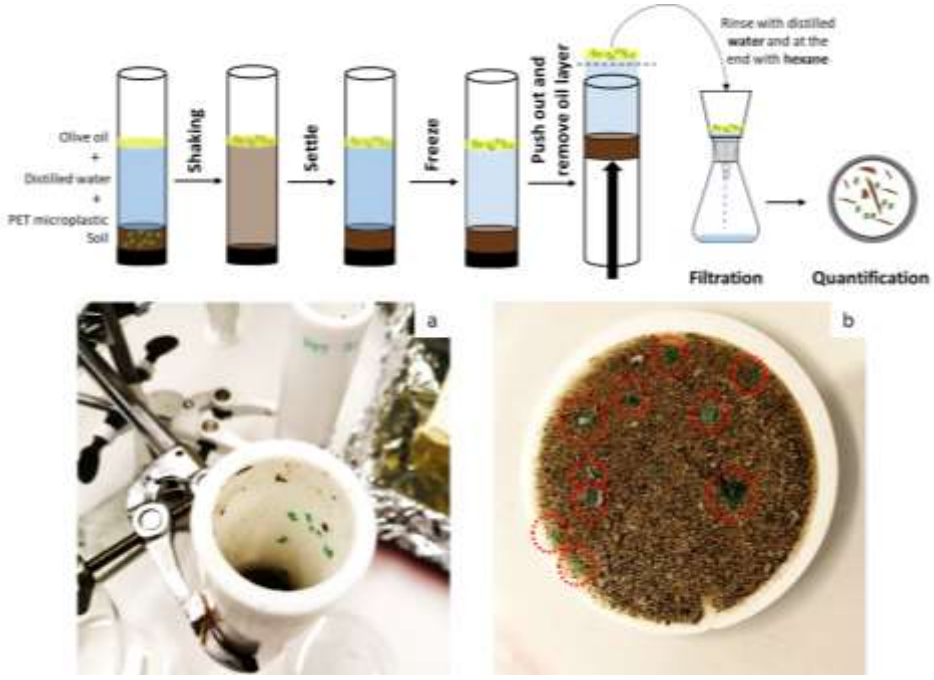

Figure 2. The oil-based extraction method procedure; a: sedimentation step, b: the sample of alluvial soil and 10 PET MP particles (marked with red circles) on a glass fibre filter.

2.3 Density separation

The density separation method was tested on alluvial soil sample, spiked with PET MPs in different quantities. The extraction was done in a centrifugation tube, as follows: 10 g of alluvial soil was mixed with a defined number of PET MP particles (10 and 20) and 50 mL of $ZnCl_2$ solution (ρ= 1.6 g cm^{-3}) were added to the tube. Firstly, the closed centrifugation tube was shaken, then put in a centrifuge (Hettich, UNIVERSAL 320) for 30 minutes at 5500 rpm. The supernatant was gently removed from the centrifugation tube, filtered through a glass fibre filter, and rinsed with distilled water. This protocol, shown in **Figure 3**, was adapted with changes from Konechnaya *et al.* (2020) [9], considering speeding up the settling with the use of a centrifuge [11].

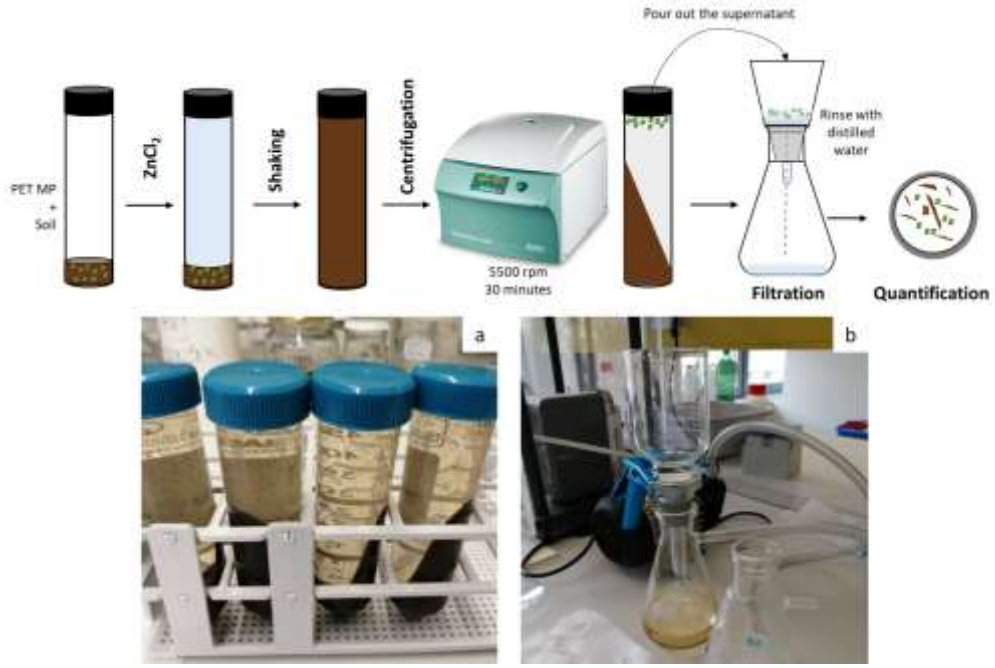

Figure 3. The density separation method procedure; a: centrifugate tubes with samples after centrifugation, b: filtration and recycling the $ZnCl_2$ solution.

2.4 Quantification of extracted MPs

After both extraction procedures, samples on the glass fibre filters were left to air dry and MPs were then manually quantified. Recovery was calculated as follows:

$$Recovery\ (\%) = \frac{N_{extracted}}{N_{spiked}} \times 100 \qquad (1)$$

3. Results

a. Oil-based extraction

Based on a literature review of various oil-based extraction protocols and on the empirical experiences gained in the presented research, several advantages and disadvantages of the method were identified [10,12-14] as reported in **Table 1.**

Table 1. Advantages and disadvantages of oil-based extraction method.

Advantages	Disadvantages
Safe and cheap method	Time consuming (at least 12 h) (Scopetani *et al*., 2020)[11]
	Custom made equipment needed (Scopetani *et al*., 2020) [11]
No hazardous saline solutions	Using foodstuffs (olive oil)
Highly applicative to different polymer types (Scopetani *et al*., 2020)[11]	Required removal of oil traces (with hexane) (Scopetani *et al*., 2020)[11]
	Require an additional step to remove organic substances from a sample
Highly applicative to various soil types and mixtures	Low repeatability in real samples (He *et al.,* 2020)[14]
	Co-adhesion of contaminants to MPs surface (He *et al.,* 2020)[14]

Table 2. Differences in experimental design between this and other studies.

Study	Polymer type	Size and shape	Number of MP in sample	Matrix used	Oil
Crichton *et al.*, 2017 [12]	Expanded polystyrene (EPS) Polyvinyl chloride (PVC) Acrylonitrile butadiene styrene (ABS) Vinyl Polyamide (PA) Polyester (PES) Nylon	Particles (minimum 0.43 mm width and maximum 6.17 mm length) Fibers (minimum 0.1 mm width and maximum 20.81 mm length)	Spiked in environmental samples 10 particles of each polymer type added (60 in total) per sample (50 g of sediment)	Medium-grained sediment	Canola oil
Mani *et al.,* 2019 [13]	Polystyrene (PS) Polypropylene (PP) Polymethyl methacrylate (PMMA) Glycol modified polyethylene terephthalate (PET)	Particles Mechanically fragmented and sieved into small (0.3–0.5 mm) and large (0.5–1.0 mm) fractions	100 MP particles (15 small and 10 large fragments of each polymer type) added per sample (1.0 g for FSS and MSS and 10.0 g for MBS and AS)	Marine suspended surface solids (MSS) Fluvial suspended surface solids (FSS) Marine beach sediments (MBS) Agricultural soil (AS)	Castor oil
Scopetani et al., 2020 [10]	Polyethylene (PE) Polyurethane (PU) Polystyrene (PS) Polycarbonate (PC) Polyvinyl chloride (PVC) Polyethylene terephthalate (PET)	Mechanically fragmented particles 0.2 – 2 mm	60 MP particles (10 particles of each polymer type) added per sample (25 g of soil and 10 g of compost)	Soil Compost	Olive oil
This study	Polyethylene terephthalate (PET)	Mechanically fragmented particles 0.1 – 2 mm	10 or 20 MP particles added per sample (10 g of soil)	Alluvial soil	Olive oil

The MPs recovery rate reported in the literature was on average 95 ± 4 % [10,12,13]. Our oil-based extraction method recovery rate was 97 % ± 8 % and 98 % ± 3 % for 10 and 20 PET MP particles, respectively. The recovery obtained in this study is higher than in the reported literature, however, some important differences in the experimental design between this and other studies exist and are shown in **Table 2.**

b. Density separation

With a literature review of various density separation protocols as well as the empirical experience gained in this study, several advantages and disadvantages of the method were identified [3,9,11,14,15] as shown in **Table 3** below.

Table 3. Advantages and disadvantages of density separation method.

Advantages	**Disadvantages**
Simply applicable method	Expensive saturated saline solutions
High density range	Hazardous solutions (NaI, $ZnCl_2$, $ZnBr_2$ toxic and corrosive salts) [12,14,16]
Saline solution can be recycled and reused	
Highly applicative to different polymer types [15]	Reactive extraction solution ($CaCl_2$, $ZnCl_2$) [3]
Highly applicative to various soil types and mixtures	Different for low-/high-density MPs [14]
	Require an additional step to remove organic substances from a sample
Time-efficient (cca. 4 samples per hour)	

On average, the recovery rates mostly ranged between 94 % and 97 % with standard deviation (SD) between 0.3 % and 3.3 % with decreasing particle size [9,11,15]. The recovery rate obtained in this study was 93 ± 5 % and 99 ± 2 % 10 and 20 PET MPs, respectively.. The recovery rate obtained in this study is in agreement with the reported literature, however, some important differences in experimental design between this and other studies exist and are shown in **Table 4.**

Table 4. Differences in experimental design between this and other studies.

Study	Polymer type	Size and shape	Number of MP in sample	Matrix used	Density separation
Konechnaya *et al.,* 2020 [9]	Polyethylene (PE) Polypropylene (PP) Polyvinyl chloride (PVC) Polystyrene (PS) Polyethylene terephthalate (PET) Polymethyl methacrylate (PMMA) Polyurethan (PU) Polyamide (PA)	Particles Grain size fractions of 1-5 mm, 400-1,000 μm, 200-400 μm and 100-200 μm	0.5 g of each grain size fraction of each polymer particles per sample (10 g of sea sand)	Precleaned calcinated sea sand	Stirring (3x for 2 min) Sedimentation (10 minutes) Floatation $ZnCl_2$ solution
Vermeiren *et al.,* 2020 [11]	Polyethylene (PE) Polypropylene (PP) Polystyrene (PS) Expanded polystyrene (EPS) Polyethylene terephthalate (PET) Nylon (PA) Polyvinyl chloride (PVC)	Mechanically fragmented particles 0.16 – 12.13 mm	60 mL of sediment was then spiked with different sized MP of different polymers	Sediment: Low intertidal mudflat High intertidal mudflat Saltmarsh (Phragmites australis)	Overflow column with top inflow Stirring (5 min followed by 5 min rest and three short stirring bursts) Sedimentation (24 h) Floatation $ZnCl_2$ solution
This study	Polyethylene terephthalate (PET)	Mechanically fragmented particles 0.1 – 2 mm	10 or 20 MP particles added per sample (10 g of soil)	Alluvial soil	Centrifugation 30 minutes at 5500 rpm Floatation $ZnCl_2$ solution

3.3 Comparison of the two extraction methods

In terms of recovery, the two extraction methods were comparable, however, the density separation method yielded better recovery rate for 20 PET MPs than the oil-based extraction. For extraction of 10 PET MPs, the oil-based extraction was slightly better than density separation method, as shown in **Figure 4.** The variability of measurements (shown as SD values on the graph) were lower for density separation method for both, 10 and 20 PET MPs, making density separation a more replicable method.

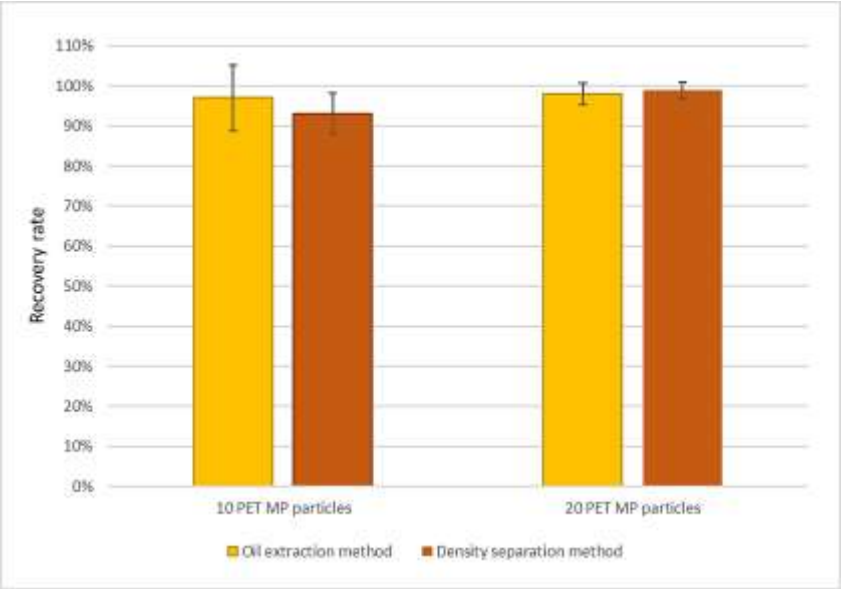

Figure 4. Oil extraction and density separation from alluvial soil recovery rates (%) of 10 and 20 PET MPs (N=6).

4. Discussion

Both extraction methods have proven advantages and disadvantages in terms of cost, time effectiveness and material safety.

Oil-based extraction is a safe and cheap method, which does not use any hazardous saline solution. It is highly applicative to different polymer, such as PE, PU, PS, etc. and soil types, such as compost and agricultural soil [10]. On the other hand, it is time consuming due to the overnight freezing process and subsequent thawing. It also requires a custom-made equipment (PTFE cylinder and a piston). An oil layer frequently formed on the cylinder's wall, where the MP particles got trapped and had to be washed off the inner walls. Moreover, the PET MP particles also tended to stick to the outside of the frozen sample cylinder and had to be, therefore, scraped from the surface of the frozen sample. Furthermore, this method, albeit in small quantities, uses foodstuff. Before further analysis, removal of oil traces with hexane is required [10]. Oil-based extraction method efficiency and accuracy vary due to different properties of environmental samples. Lipophilic properties of plastic polymers may also be modified, due to contaminants adhered to the surface of MPs [14].

Density separation method is a simple method and easily applicable in the laboratory. Saline solutions with sufficiently high density can cover a wide range of different MP polymers, from low to high-density polymers, and is, therefore, highly applicable to different polymer and soil types [14,15]. The density of $ZnCl_2$ solution has not changed after the first filtration, therefore, $ZnCl_2$ solution can be recycled to be used in further filtration processes. However, the preparation of saturated saline solutionrequires large quantities of a chosen salt, which makes density separation method expensive. In our study, 1 kg of $ZnCl_2$ salt was used to prepare 1.2 L of saturated solution with density of1.6 g cm^{-3}. Saline solutions for density separation method (NaI, $ZnCl_2$, $ZnBr_2$) are toxic and corrosive salts, hazardous to the environment, and what is more, highly reactive. Möller *et al.* (2020)[3] reported that $ZnCl_2$

solution can react with natural components of the sediment, especially with carbonates (resulting in bubbling and foam), which can hamper the procedure, however, no such thing had occurred in our samples when $ZnCl_2$ was used. Literature reports that low-density MPs can be more easily extracted than high-density MPs [14], however, PET is at the high-end of density of plastic polymers (1.38 g cm^{-3}), and the recoveries obtained in this study show otherwise.

Both methods require an additional step to remove or decrease organic content from a sample, especially for soil samples rich in organic matter (agricultural soil, compost and soil-compost mixtures). This step was not required in our study since alluvial soil is poor in organic matter content (2.30 ± 0.13 %).

Recovery obtained with both extraction methods in this study was better or in the similar range as the one reported in the literature. It should be noted, however, that experimental designs (e.g., number and size of MPs used, environmental matrices used) was different in different studies, therefore, comparison of recovery rates is not straightforward.

Currently, oil extraction method appears to be safer for the environment, however, density separation method is more time efficient, is easier to handle and $ZnCl_2$ solution can be recycled and reused again. Density separation method is able to achieve slightly higher recovery rates and lower variability. By optimising and testing both methods on a wide range of different polymer types, concentrations and sizes of MPs and different matrices with varying organic matter content in comparable experimental designs, we will be able to determine which method is more suitable and yields better recoveries.

Further work will focus on quantification and identification of microplastics in real environmental samples, such as agricultural soil, bio-waste compost, sludge from wastewater treatment plants and others.

Acknowledgements

This work was supported by the Slovenian Research Agency, research core funding No. P3-0388 (Mechanisms of Health Maintenance), and research project No. Z2-2643 (Agri-iMPact: Microplastic Prevalence and Impact in Agricultural Fields).

References

1. Zhou Y, Wang J, Zou M, Jia Z, Zhou S, Microplastics in soils: A review of methods, occurrence, fate, transport, ecological and environmental risks. Sci Total Environ. 2020; 748: 141368. doi: 10.1016/j.scitotenv.2020.141368
2. Kumar M, Xiong X, He M, et al. Microplastics as pollutants in agricultural soils. Environ Pollut. 2020; 265: 114980. doi: 10.1016/j.envpol.2020.114980
3. Möller J N, Löder M G, Laforsch C, Finding microplastics in soils: A review of analytical methods. Environ Sci Technol. 2020; 54(4): 2078-2090. doi: 10.1021/acs.est.9b04618
4. Müller A, Goedecke C, Eisentraut P, Piechotta C, Braun U, Microplastic analysis using chemical extraction followed by LC-UV analysis: a straightforward approach to determine PET content in environmental samples. Environ Sci Eur. 2020; 32(85): 1-10. doi: 10.1186/s12302-020-00358-x

5. Wang C, Zhao J, Xing B, Environmental Source, Fate, and Toxicity of Microplastics. J Hazard Mater. 2021; 407: 124357. doi: 10.1016/j.jhazmat.2020.124357
6. Šunta U, Prosenc F, Trebše Polonca, Griessler Bulc Tjaša, Bavcon Kralj M. Adsorption of acetamiprid, chlorantraniliprole and flubendiamide on different type of microplastics present in alluvial soil. Chemosphere. 2020; 261: 1-9, doi:10.1016/j.chemosphere.2020.127762
7. Britannica, T. Editors of Encyclopaedia (2020), Polyethylene terephthalate [Encyclopedia Britannica], Accessed 29. 1. 2021. Available from https://www.britannica.com/science/polyethylene-terephthalate
8. Nisticò R, Polyethylene terephthalate (PET) in the packaging industry. Polym Test. 2020; 90: 106707. doi: 10.1016/j.polymertesting.2020.106707
9. Konechnaya O, Lüchtrath S, Dsikowitzky L, Schwarzbauer J, Optimized microplastic analysis based on size fractionation, density separation and µ-FTIR. Water Sci Technol. 2020; 81(4): 834-844. doi: 10.2166/wst.2020.173
10. Scopetani C, Chelazzi D, Mikola J, et al. Olive oil-based method for the extraction, quantification and identification of microplastics in soil and compost samples. Sci Total Environ. 2020; 733: 139338. doi: 10.1016/j.scitotenv.2020.139338
11. Vermeiren P, Muñoz C, Ikejima K, Microplastic identification and quantification from organic rich sediments: A validated laboratory protocol. Environ Pollut. 2020; 262: 114298. doi: 10.1016/j.envpol.2020.114298
12. Crichton E M, Noël M, Gies E A, Ross P S, A novel, density-independent and FTIR-compatible approach for the rapid extraction of microplastics from aquatic sediments. Anal Methods. 2017; 9(9): 1419-1428. doi: 10.1039/C6AY02733D
13. Mani T, Frehland S, Kalberer A, Burkhardt-Holm P, Using castor oil to separate microplastics from four different environmental matrices. Anal Methods. 2019; 11(13): 1788-1794. doi: 10.1039/C8AY02559B
14. He D, Zhang X, Hu J, Methods for separating microplastics from complex solid matrices: Comparative analysis. J Hazard Mater. 2021; 409:124640. doi: 10.1016/j.jhazmat.2020.124640
15. Li J, Song Y, Cai Y, Focus topics on microplastics in soil: analytical methods, occurrence, transport, and ecological risks. Environ Pollut. 2020; 257: 113570. doi: 10.1016/j.envpol.2019.113570
16. Scheurer M, Bigalke M, Microplastics in Swiss Floodplain Soils. Environ Sci Technol. 2018; 52(6): 3591−3598. doi: 10.1021/acs.est.7b0600

Research

European spruce (*Picea abies*) as a possible sustainable source of cellular vesicles and biologically active compounds

Jeran Marko[1,2,*], Božič Darja[1,2], Novak Urban[3], Hočevar Matej[4], Romolo Anna[1], Iglič Aleš[2], Kralj-Iglič Veronika[1]

[1]University of Ljubljana, Faculty of Health Sciences, Laboratory of Clinical Biophysics, Ljubljana, Slovenia
[2]University of Ljubljana, Faculty of Electrical Engineering, Laboratory of Physics, Ljubljana, Slovenia
[3]National Institute of Chemistry, Laboratory for Biomolecular Structure, Ljubljana, Slovenia
[4]Institute of Metals and Technology, Physics and Chemistry of Materials, Ljubljana, Slovenia

*Marko.Jeran@fe.uni-lj.si

Abstract

Cells secrete different types of particles into the extracellular space. Cellular vesicles (CVs) are such particles that span in size downto 30 nm. CVs have been found to be involved in various applications. Research of the formation of naturally formed CVs dates back to 1960. The main motivation of this work is study of processes to develop large-scale production of vesicles, which requires simple, robust, and inexpensive methods. We focused on processing European spruce needles, which represent a "green" source of various natural organic compounds and cellular particles. CVs were isolated from spruce needle macerates of raw, ultrasound-treated and lecithin –treated samples by centrifugation and characterized by microscopy (light and scanning electron (SEM) technique), flow cytometry and Fourier Transform IR spectroscopy (FTIR). We found that macerates contained CVs of different sizes, that CVs were formed also during processing of samples and that the concentration and the size of CVs in isolates depended on the centripetal acceleration of the centrifuge rotor.

1. Introduction

Cells secrete different kinds of small particles into the extracellular space. Cellular vesicles (CVs) are such particles that are enclosed by biomembranes. Their size extends downto about 30 nm. It was found that CVs are involved in the horizontal transfer of cargoes, especially nucleic acids (DNA, *m*RNA and *micro*RNA) and other molecules such as carbohydrates, lipids and secondary metabolites [1,2]. Due to these properties, CVs are considered as mediators of cell-to-cell communication and exhibit important functions in different physiological and pato-physiological processes; for example they are enroled in signal transduction, cell cycle, immune response, neurological diseases, inflammation and tumorigenesis [2]. Recently, the demands for large-scale production of vesicles has been recognized and simple, robust, and inexpensive methods are required.

CVs are being studied in different systems, including plants [3]. Already in the sixties, Halperin and Jensen (1967) studied embryogenesis in cell cultures derived from the wild carrot (*Daucus carota*) [3,4]. By using transmission electron microscopy they observed CVs within multivesicular bodies which seemed to fuse with the cell membrane and release the cargo of secondary vesicles into the wall space [4]. Also they reported of smooth endoplasmatic reticulum containing small vesicles similar to the vesicles seen in multivesicular bodies [4].

Ultracentrifugation-based isolation methods for CVs were developed [3,6]. Low centrifugal accelerations (*cca* 500 × g) were used to pellet cellular debris from macerates, followed by higher centrifugal accelerations (*cca* 10 000 × g) to pellet CVs from supernatant of the first centrifugation step [3,6]. Gradient centrifugation methods were also applied to fractionate the samples according to the density of CVs [3]. Ju et al., (2013) isolated grape exosome-like nanoparticles (GELNs) from grape juice using differential centrifugation and sucrose gradient method [7]. Cryogenic electronic microscope images of a particular CV fraction of the isolate revealed numerous vesicles with diameters between 50 and 300 nm [3,7]. Later, several studies reported the presence of CVs in many different plant sources; e.g. in the germination medium of olive pollen grains, in the extracellular fluid of sunflower seedlings, in coconut milk and others [3].

Plants have the incredible ability to synthesize many of the active compounds on which today's drugs and therapies are based. They are able to defend themselves against external influences (enemies) by releasing the appropriate molecules in different body parts [8]. One of them is the European spruce (*Picea abies*), which is a widespread and common tree [9]. Different parts of spruce tree contain different mixtures of complex biologically active substances. The presence and concentration of these substances in a given plant depends on several factors (e.g. climate, time of collection in the year, accessibility to nutrients, etc.) [8]. Large-scale production of vesicles requires simple, robust, and inexpensive methods.

As phospholipid molecules form vesicles in aqueous media, we expected that their addition to the macerate would involve them in formation of mixed vesicles. We expected that vesicles will be forming during maceration of spruce needles.

Sonication can induce disruption of cell walls and membranes and is often used to improve efficiency of isolation of active ingredients (compounds) from natural sources. Combined with sequential extraction steps using different solvents, ultrasonic disintegration has been shown to be effective in separating and/or resolving various natural compounds [10]. To increase the production of CVs from plant tissues, ultrasonication (US) was used as a pretreatment for the isolation of CVs in this study.
We report preliminary results on CVs isolated from a macerate of needles of European spruce. We have isolated CVs by centrifugation and analyzed them by flow cytometry, FTIR spectroscopy and scanning electron microscopy (SEM).

2. Materials and Methods

2.1. Plant material and its preparation

Branches of spruce were cut from the tree and used immediately. Branches were immersed into 1.5 L of water at 30 °C with dissolved sodium hypochlorite (NaClO, 0.1 %) for 1 hour. The branches were rinsed with water. The needles were cut off from the branches. Macerate was prepared from 50 g of needles and 300 mL of 0.9 % saline solution by stirring for about 20 seconds with the stick hand mixer, (HBC804QW, Gorenje, Velenje, Slovenia). To prepare the CVs with addition of lecithin, 5 g of lecithin granules were added to the sample during the stirring. After maceration, larger parts were removed from the sample by filtering through a sterile gauze. The filtered sample was left in closed sterile plastic 50 mL containers to sediment for 2 hours while the supernatant (of almost equal volume) was used for further processing.

2.2. Sonication of macerate

In 50 mL or 15 mL conical plastic centrifuge tubes (Isolab, Germany), the sap sample (plant material in saline) was added and sonicated in “sweep” mode for 5 min at 37 kHz at room temperature (ultrasonic bath Elma S 100 H, Germany).

2.3. Isolation of CVs

CVs were isolated by centrifugation as schematically depicted in **Figure 1**. The sample was aliquoted in 50 mL or 15 mL conical plastic centrifuge tubes (Isolab, Germany). The aliquots were centrifuged for 10 minutes at 300 × g and 5 °C in the Centric 400R centrifuge (Domel, Železniki, Slovenia) equipped with the swinging rotor. After pelleting larger particles, the supernatant was centrifuged for 30 minutes at 2000 × g and 5 °C to sediment possibly present bacteria. The supernatant was further centrifuged for 60 minutes at 10000 × g or 17500 × g in the Centric 200R centrifuge (Domel, Železniki, Slovenia) with the Lilliput swinging rotor or for 60 minutes at 50 000 × g at 5 °C with the L8-70M ultracentrifuge (Beckman Coulter, USA, rotor type SW55Ti).

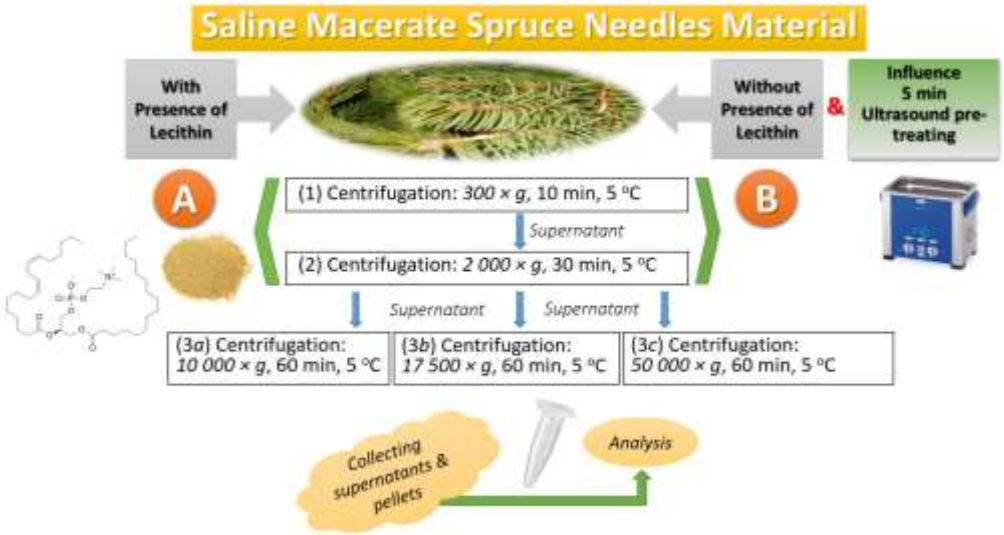

Figure 1: Flowchart of the experimental design for isolation of CVs by centrifugation.

2.4. Flow cytometry (FCM)

FCM measurements were performed using MACS QUANT flow cytometer (Miltenyi, Bergisch-Gladbach, Germany), with lasers set at 458 V (FSC), 467 V (SSC), and the trigger set at SSC: 1.8. Particles in fresh isolates were analyzed by flow cytometry immediately after isolation. Gates were set based on analysis of standard beads of size 2 and 3 µm (MACSQuant Calibration Beads, Ref: 130-093-607) (**Figure 2A**). A representative scatterplot pertaining to the isolate is presented in **Figure 2B.**

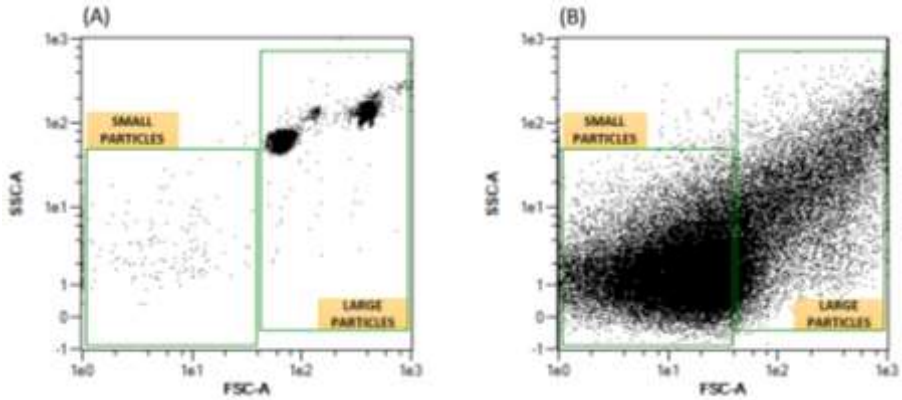

Figure 2. Flow cytometer scatter plots of: (A) standard beads of size 2 and 3 µm – MACSQuant Calibration Beads and (B) a representative sample of the supernatant after centrifugation for 30 minutes at 2000 × g.

2.5. Fourier Transform IR spectroscopy (FTIR)

The FTIR spectra were measured using the Bruker Vertex 80 FTIR spectrometer. We employed Specac's Golden gate ATR cell with diamond crystal and heated top plate. Spectra were recorded in the range between 4000 and 600 cm^{-1}. The final spectrum was averaged from 128 interferograms. Before any spectral analysis, the spectrum of pure buffer was subtracted. ATR absorbance spectra were used as recorded without post-processing due to reflection contributions to the overall absorbance spectra. Subtracted spectra were

integrated in two separate regions. The first region (3000–2850 cm^{-1}) corresponds to CH_2 and CH_3 stretching vibrations of fatty acids. Meanwhile, the second region (1180–960 cm^{-1}) corresponds to C-O and C-C stretching vibrations in combination with C-O-H, C-O-C deformation vibrations of carbohydrates [11]. Finally, the ratio between integrated areas of the first and the second spectra region was calculated.

2.6. Scanning electron microscopy (SEM)

The samples were fixed with OsO_4, following a modified protocol adopted from Božič, et al [12]. The pellets and the starting material (saline macerate of the plant material) were fixed on 0.05-micron mixed-cellulose-esters' filters (Sterlitech, USA).
Samples were incubated in 1% OsO_4 for 2 h, washed 3 times with distilled water (incubation time 10 min each), then dehydrated in graded series of ethanol (30%, 50%, 70%, 80%, 90% and "absolute", 10 min each; absolute ethanol was replaced 2 times) and hexamethyldisilazane (mixed with absolute ethanol; 30%, 50% and "absolute", 10 min each) and finally air dried. Samples were coated with Au/Pd (PECS Gatan 682) and analyzed using a JSM-6500F Field Emission Scanning Electron Microscope (JEOL Ltd., Tokyo, Japan).

3. Results and Discussion

3.1. Visualization of samples

During the maceration, samples produced foam (**Figure 3**) indicating presence of membranous structures in the samples.

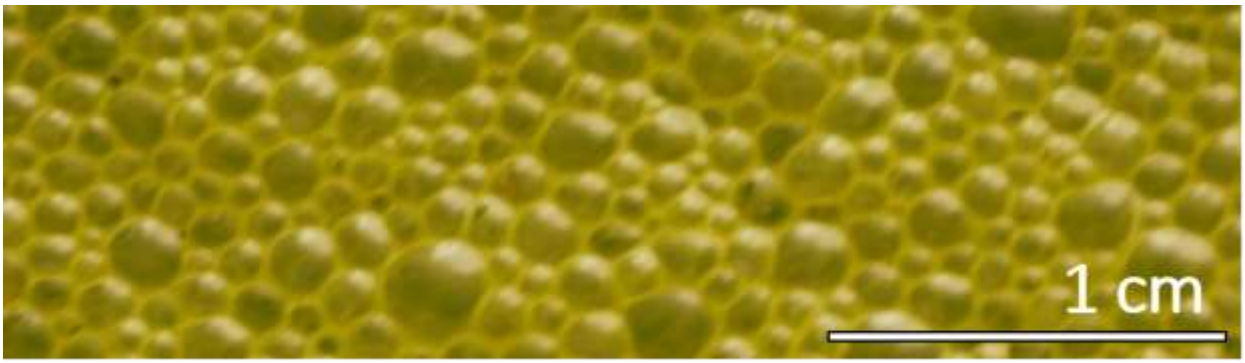

Figure 3. Foam formed during maceration.

Light microscopy of the foam collected from the top of the macerate revealed giant colloid vesicles in raw samples and in lecithin-treated sample (**Figure 4A** and **B**, respectively). Pellet after centrifugation at 300g of the raw sample and supernatant after sedimentation of the macerate in gravity field of the lecithin-treated sample exhibited numerous particles with smooth contours (**Figure 4C,D)**, heterogeneous in size. As internal structures are not recognized, and due to the size of these particles (of the order of several μm) these particles could be cell remnants (empty cell walls, or smaller colloid vesicles). There were also numerous smaller particles, heterogeneous in size and shape that tended to form clusters (**Figure 4C,D**). Figure 4E shows supernatant of raw sample after centrifugation at 2000g with

numerous particles of which some have shapes of minimal membrane free energy characteristic for membrane – enclosed particles without internal structure [13] – *i.e.* CVs (**Figure 4E**). Giant vesicles of lecithin in saline are shown for comparison (**Figure 4F**). Visualization of macerates by SEM revealed remnants of cells (white arrows), amorphous material and sub-micrometer-sized particles (yellow arrows) which were more abundant in the samples prepared by addition of lecithin (**Figures 5A** and **5C**, respectively). Also isolates (**Figures 5B** and **5D**) contained sub-micron-sized particles with smooth contours. The morphology of particles in samples seemed similar in supernatants and pellets, however, with varying sizes and concentrations.

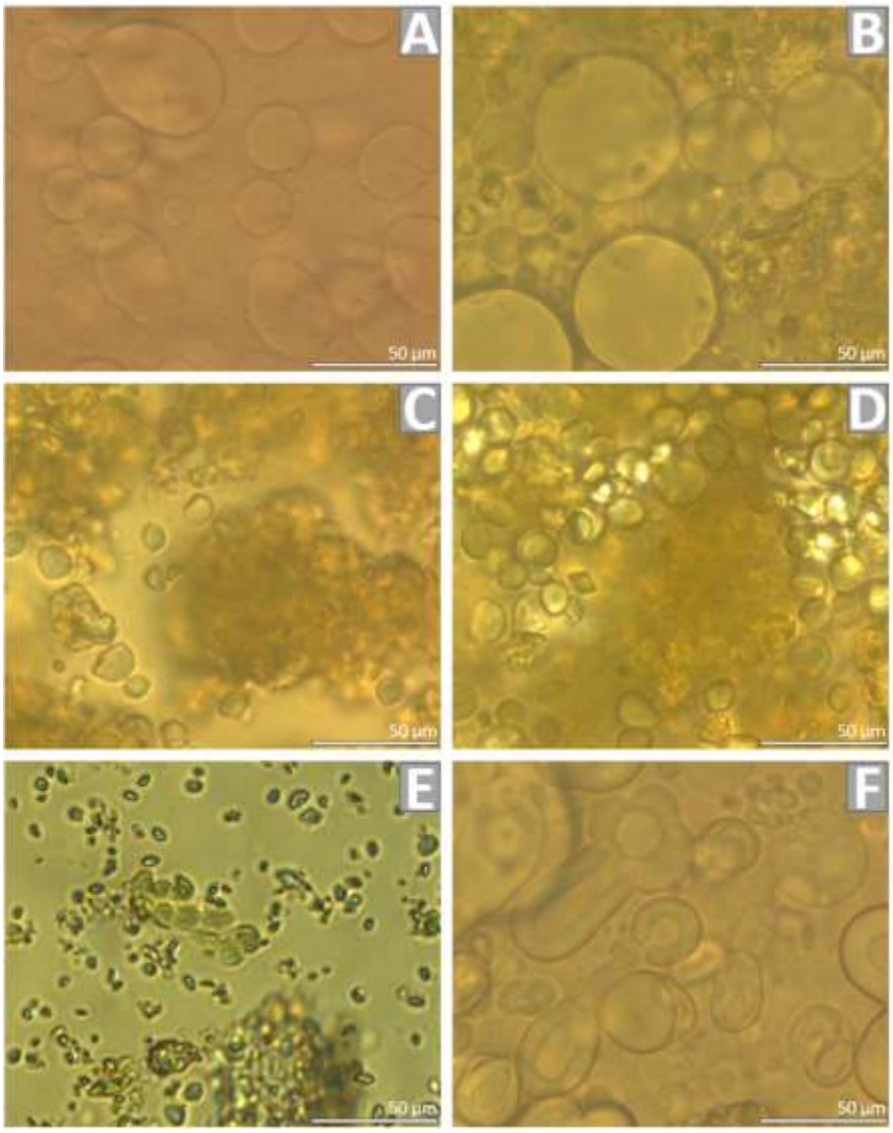

Figure 4: Visualization of European spruce macerate and isolate of CVs by light microscopy. A: Lecithin in 0.9% saline solution, B: spruce needle macerate with addition of lecithin, foam phase, C: supernatant of sedimentation of the filtered macerate in gravitational field, D: pellet of the sample C after centrifugation for 30 minutes at 200 × g. E - pellet of raw sample after centrifugation at 2000g, F - Giant vesicles of lecithin in saline.

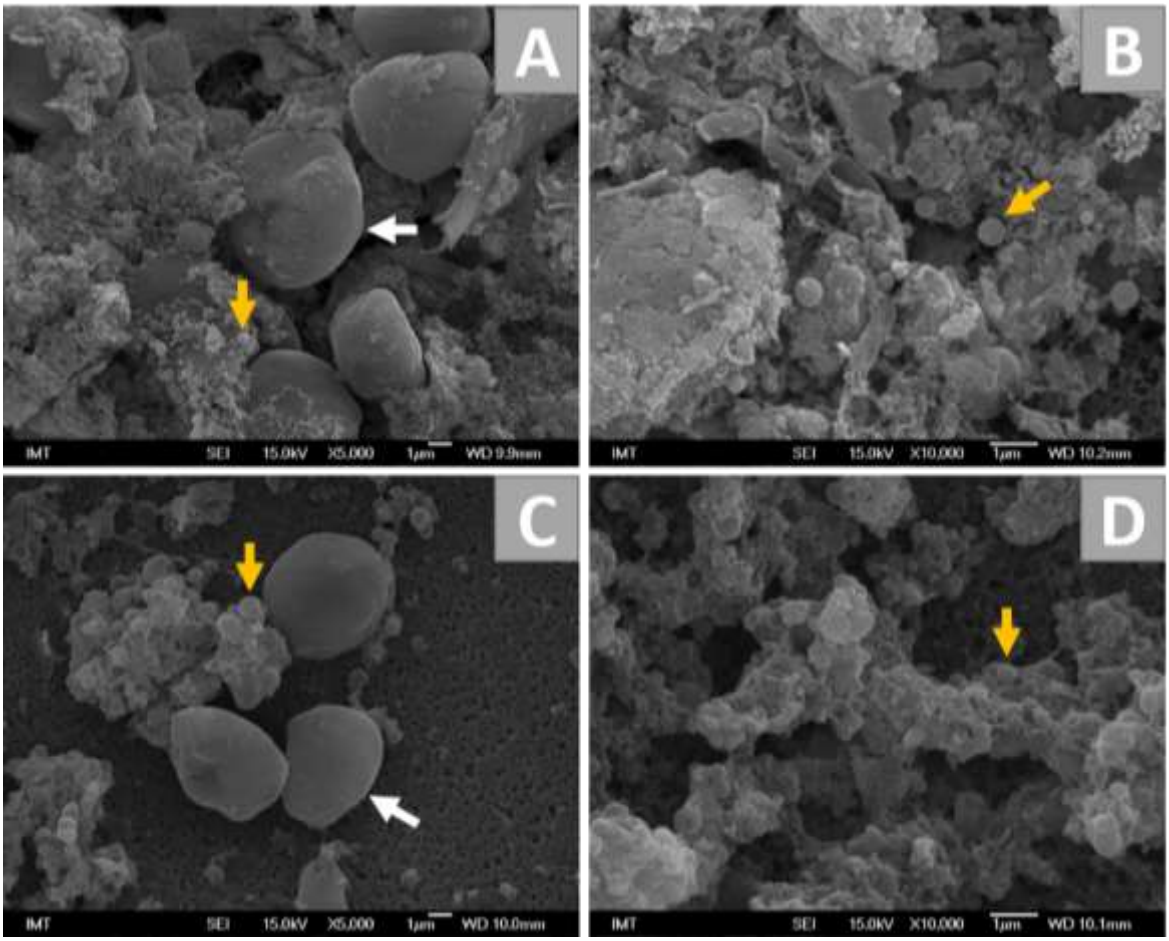

Figure 5: Visualization of European spruce macerate and isolate of CVs by SEM. A: macerate prepared without addition of lecithin, B: isolate from the macerate prepared without addition of lecithin, C: macerate prepared with addition of lecithin, D: isolate from the macerate prepared with addition of lecithin. White arrows point to large cell remnants and yellow arrows point to CVs.

3.2. Flow cytometry

Figure 6 shows the FCM results of the prepared samples. Three groups of samples are shown (raw, treated with ultrasound and treated by addition of lecithin). The respective supernatants after the centrifugation at 300g showed increased concentration of small particles due to treatment with ultrasound and increased concentration of large particles due to addition of lecithin.

Centrifugation of samples at 2000g caused a considerable increase of the concentration of small particles in the supernatant of raw sample with respect to the supernatant of the 300g centrifugation while the concentration of small particles remained almost the same in the respective ultrasound-treated sample and decreased in the lecithin-treated sample. There were no considerable changes in concentration of larger particles in raw sample and ultrasound-treated sample while the concentration of larger particles decreased in the lecithin-treated sample. The effect of centripetal acceleration of the centrifuge rotor showed

increased concentration of both small and large particles in the pellets of all three samples (comparing 17500g and 50 000g pellets), although the effect was considerably stronger for small particles in raw samples and in lecithin-treated samples. There was a saturation effect for large particles at high centripetal accelerations in all three samples. Increasing number of small particles with centripetal acceleration indicates formation of a significant part of small particles in these samples during the centrifugation.

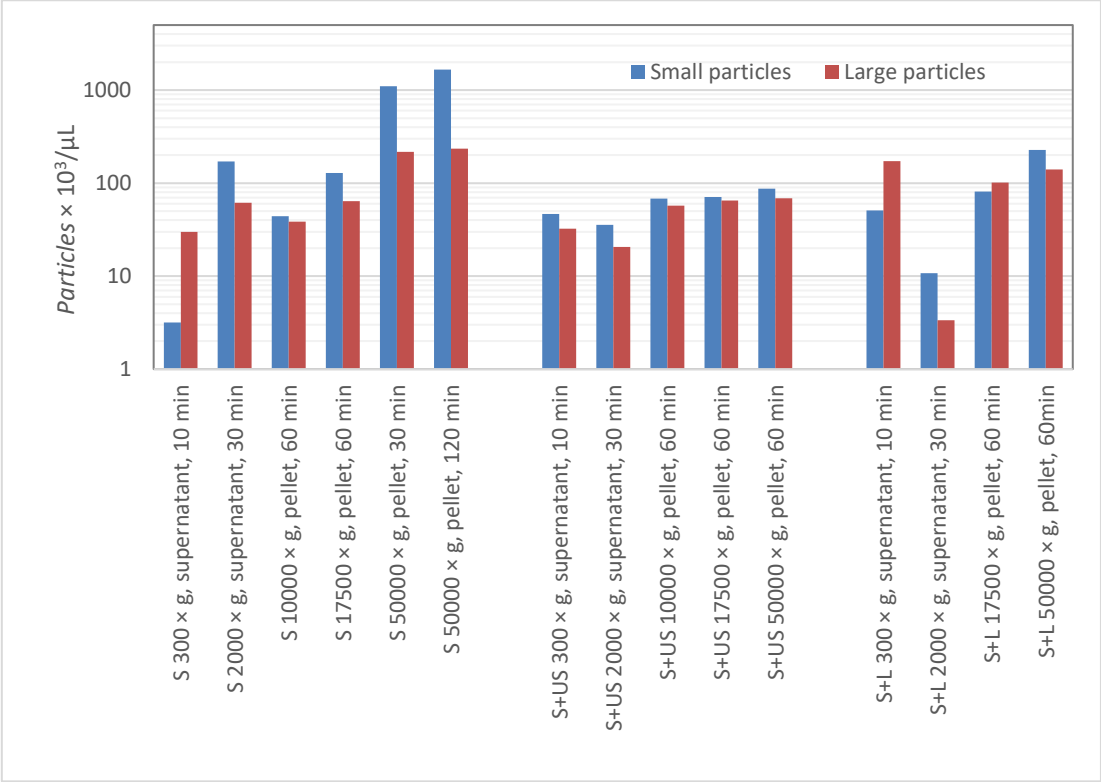

Figure 6: Flow cytometry measurements of: *S* – raw samples of spruce needle macerate; *S+US* – samples treated with ultrasound; *S+L* – samples with addition of lecithin.

3.3. FTIR spectroscopy

The spectrum of the FTIR exhibiting the quantity of characteristic bonds in the constituents for the ultrasound-treated samples and the lecithin-treated sample is shown in Figure 7. Two main peaks are notable in the spectrum. Roughly, the one corresponding to smaller $1/\lambda$ pertains to carbohydrates and the other to the lipids. The peak corresponding to carbohydrates is more pronounced (**Figure 7**) in both samples, however, the proportion of lipids versus carbohydrates is different in the supernatants and pellets (**Table 1**) and in the spectra in **Figure 7**.

It can be seen from **Figure 7** and **Table 1** that centrifugation at 50 000 × g for 60 min had been more efficient to sediment particles containing higher lipid/carbohydrate ratio than processing at 17500 × g for 60 min. It can also be seen that lipid/carbohydrate ratio was different in the pellets, suggesting that particles with higher contents of lipids pelleted at

higher forces. It should be noted however that different centrifuges were used in the two protocols at different centripetal accelerations.

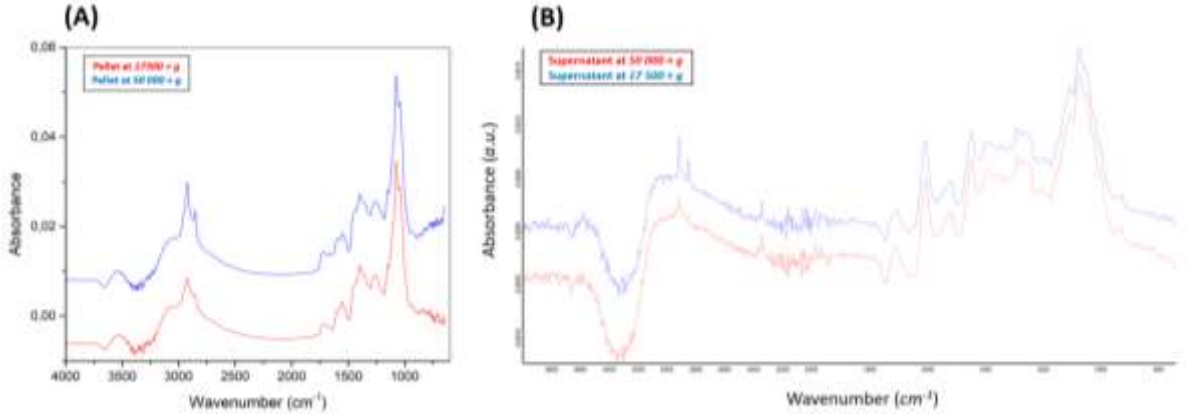

Figure 7. FTIR spectra of the pellet and of the supernatant of the isolates from the ultrasound-treated samples.

Table 1: Proportion of absorbance pertaining to lipids versus absorbance pertaining to carbohydrates in isolates and supernatants in isolates obtained by different centripetal accelerations of the centrifuge rotor. Samples were treated by ultrasound.

Sample	**Proportion of lipids vs. carbohydrates**
Pellet at 17 500 × g	0.175
Pellet at 50 000 × g	0.283
Supernatant at 17 500 × g, 60 min	0.11
Supernatant at 50 000 × g, 60 min	0.08

4. Conclusions

European spruce represents a "green" source of various natural organic compounds and cellular particles. The innovative approach to characterize the prepared isolates in this work was FTIR spectroscopy, which proved to be fast, simple and efficient. Moreover, this non-destructive technique can be used to study samples in all states of aggregation. In addition, only a small amount of sample is required when measuring solids or liquids (approximately 20 µL liquid sample). Preliminary results on the effects of different sample preparations are presented. The study showed the importance of processing parameters on the amount and size of final particles in the processed samples. The more detailed studies will be following.

Acknowledgements

Authors acknowledge support from the European Union's Horizon 2020 research and innovation program under grant agreement No. 801338 (VES4US project) and Slovenian Research Agency (ARRS. Research core findings No. P3-0388 and projects No. J3-9262, L3-2621).

References

1. Yáñez-Mó M, Siljander PR-M, Andreu Z, Bedina Zavec A, Borràs FE, et al. Biological properties of extracellular vesicles and their physiological functions. J Extracell Vesicles. 2015; 4: 1–60. doi: 10.3402/jev.v4.27066

2. de Palma M, Ambrosone A, Leone A, del Gaudio P, Ruocco M, et al. Plant roots release small extracellular vesicles with antifungal activity. Plants. 2020; 9: 1–14. doi: 10.3390/plants9121777
3. Cui Y, Gao J, He Y, Jiang L, Plant extracellular vesicles. Protoplasma. 2020; 257: 3–12. doi: 10.1007/s00709-019-01435-6
4. Halperin W, Jensen WA, Ultrastructural changes during growth and embryogenesis in carrot cell cultures. J. Ultrasructure Res. 1967; 18: 428–443. doi: 10.1016/S0022-5320(67)80128-X
5. Halperin W, Alternative morphogenetic events in cell suspensions. Am J Bot. 1966; 53(5): 443–453. doi: https://doi.org/10.2307/2440343
6. Zhuang X, Xiang X, Grizzle W, Sun D, Zhang S, et al. Treatment of brain inflammatory diseases by delivering exosome encapsulated anti-inflammatory drugs from the nasal region to the brain. Mol Ter. 2011; 19(10): 1769–1779. doi: 10.1038/mt.2011.164
7. Ju S, Mu J, Dokland T, Zhuang X, Wang Q, et al. Grape exosome-like nanoparticles induce intestinal stem cells and protect mice from DSS-induced colitis. Mol Ther. 2013; 21(7): 1345–1357. doi: 10.1038/mt.2013.64
8. Jeran M, Barrios-Francisco R, Sedušak Kljakič A, Remškar H, Novak U, Non-destructive characterisation of natural materials: quantitative determination of borneol and limonene in European spruce needles (*Picea abies*) by FTIR spectroscopy. In Kralj-Iglic V, editor. Socratic lectures: 4th International Minisymposium, Ljubljana, Faculty of Health Sciences, University of Ljubljana (Slovenia). 2021; pp. 79–86. ISBN: 978-961-7112-02-3
9. Jeran M, Navadna smreka (*Picea abies*) kot vir aktivnih učinkovin/ *Engl*. European spruce (*Picea abies*) as a source of biologically active compounds. Trdoživ. 2020; 9(2): 22–24. ISSN: 2232-5999. Available from: https://issuu.com/trdoziv/docs/trdoziv18_web_v01
10. Ebringerová A, Hromádková Z, An overview on the application of ultrasound in extraction, separation and purification of plant polysaccharides. Cent Eur J Chem. 2010; 8(2): 243–257. doi: 10.2478/s11532-010-0006-2
11. Naumann D, Infrared Spectroscopy of cells, tissues and body fluids. In Roberts GCK, editor. Encyclopedia of biophysics, Berlin, Heidelberg: Springer. 2013; pp. 1057–1065. doi: https://doi.org/10.1007/978-3-642-16712-6_120
12. Božič D, Hočevar M, Kononenko V, Jeran M, Štibler U, et al. Pursuing mechanisms of extracellular vesicle formation. Effects of sample processing. In Bongiovanni A, Pocsfalvi G, Manno M, Kralj-Iglič V, editors. Adv. Biomembr. Lipid Self-Assembly. 2020; 32: 113–155. doi: 10.1016/bs.abl.2020.09.003
13. Kralj-Iglič V, Pocsfalvi G, Mesarec L, Šuštar V, Hägerstrand H, Iglič A, Minimizing isotropic and deviatoric membrane energy – An unifying formation mechanism of different cellular membrane nanovesicle types. PLoS One. 2020; 15(12): 1–25, doi: 10.1371/journal.pone.0244796

Research

Renin-angiotensin system inhibitors and their implications for COVID-19 treatment

Koren Jerneja[1], Scott Derek[1], Jeran Marko[2,3,*]
[1]School of Medicine, Medical Sciences and Nutrition, University of Aberdeen, Aberdeen, UK
[2]Laboratory of Clinical Biophysics, Faculty of Health Sciences, University of Ljubljana, Slovenia
[3]Laboratory of Physics, Faculty of Electrical Engineering, University of Ljubljana, Slovenia
*marko.jeran@fe.uni-lj.si

Abstract
The novel coronavirus, SARS-CoV-2, is responsible for the recent epidemic outbreak and has raised a lot of concern over the past year. It has so far been identified that the virus enters the human body via a membrane-bound enzyme called Angiotensin-converting enzyme II (ACE2), an important part of the Renin-Angiotensin System (RAS). RAS is responsible for regulating blood pressure and volume and therefore often used as a drug target to treat hypertension, heart conditions and diabetes. These drugs that can affect the blood pressure by working on RAS are known as RAS inhibitors. These facts made scientists and clinicians question, whether taking RAS inhibitors might positively or negatively impact the onset and progression of COVID-19. This review aims to briefly explain the RAS pathway, its major elements and roles in human physiology as well as how that is affected by RAS inhibitors. It also aims to relate that to COVID-19 and outline the possible correlations.

1. Introduction

Severe acute respiratory syndrome coronavirus (SARS-CoV-2) is the novel coronavirus that has rapidly spread around the globe since its first detection in December 2019, causing a global pandemic [1, 2]. It is the cause of COVID-19, which is associated with respiratory problems, fever and, in some cases, inappropriate inflammatory response resulting in mild to severe lung damage [2, 3]. It enters the body by interacting with the Angiotensin-Converting Enzyme 2 (ACE2) expressed on the cell surface of different tissues, including the lungs and kidneys [3-10]. ACE2 is a part of a very important system in our body called the Renin-Angiotensin system (RAS), which is involved in controlling blood volume and pressure as well as, to a certain extent, inflammation [1, 9, 11]. Therefore, drugs that inhibit certain parts of the RAS pathways, collectively known as RAS inhibitors, are often utilised to treat hypertension in patients with cardiovascular diseases, diabetes and other pathologies, many of which have recently been associated with potentially higher risk of severe COVID-19 [2, 3, 7, 8, 12]. Since the SARS-CoV-2 and RAS inhibitors share a target pathway, there has been a concern that the two may interfere, resulting in increased risk of severe infection in patients taking RAS inhibitors [3, 14]. This review systematically covers the concerning pathways and the recent implications for RAS inhibitors in COVID-19 treatment.

2. RAS Pathway

The renin-angiotensin system (RAS) involves a cascade of enzymes, particularly proteases, which ultimately work to regulate the blood pressure and volume as well as, to a certain extent, inflammation [3, 9, 11, 15]. The whole process (schematically depicted in **Figure 1**) starts with production of angiotensinogen in the liver, which then travels to the kidneys, where it is cleaved by a protease called renin to produce angiotensin I (Ang I) [11]. The next step in the pathway is cleavage of Ang I to its active form, angiotensin II (Ang II), which is done by angiotensin-converting enzyme I (ACE), expressed on the surface of cells in the lungs, kidneys, intestine and other organs [3, 9, 11]. Ang II can then exhibit its effects by binding to either one of its two receptors – angiotensin II receptor type 1 (AT1R) or type 2 (AT2R). Both are G-protein coupled receptors, but they exhibit opposite effects [10, 11]. AT1R is associated with increased inflammation, mainly through the release of cytokines including TNF-α and IL-1, water retention as well as constriction of the blood vessels [2, 3, 7, 9, 11]. AT2R, on the other hand, has primarily anti-inflammatory effects coupled with vasodilation [3, 7, 9, 11]. AT1R and AT2R therefore exhibit antagonistic actions and work to oppose one another [7]. An alternative Ang II pathway involves a carboxypeptidase called Angiotensin-converting enzyme II (ACE2), which is the known entry point for SARS-CoV-2 expressed on the surface of certain cells in the lungs, blood vessels and some other specific tissues [3, 9, 11]. ACE2 cleaves Ang II into Angiotensin-(1-7) (Ang-(1-7)) or Ang I into Angiotensin-(1-9) (Ang-(1-9)), which is then transformed into Ang-(1-7) by ACE [4, 9, 11, 12]. Ang-(1-7) can then bind to G-protein coupled receptors called Mas receptors to achieve similar effects than Ang II binding to AT2R – vasodilation, decreased inflammation, primarily by lowering levels of cytokines like IL-6, and increased renal water secretion [2-4, 9, 10, 11, 16]. ACE2, Ang-(1-7) and Ang-(1-9) show opposing functions to the ACE-Ang II pathway and

due to this fact, ACE2 and its pathway are thought to play a protective role against respiratory infection, lung injury, cardiovascular diseases and diabetes and reduced ACE2 presence can lead to several health issues [2-4, 7, 12, 16, 17].

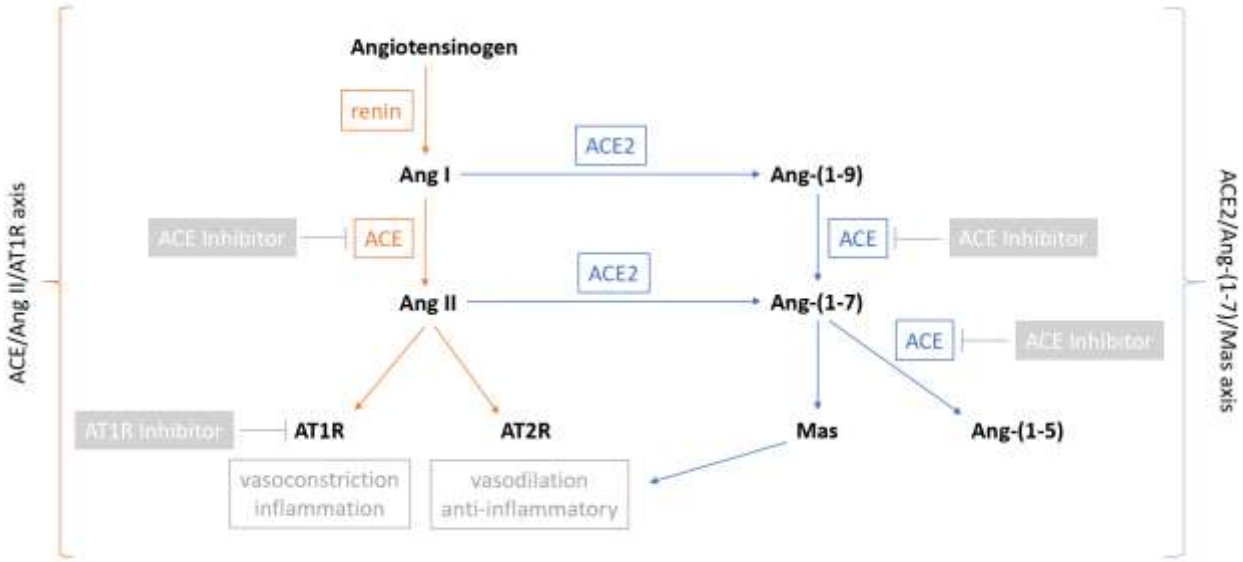

Figure 4. The two opposing axis of the RAS pathway and the effects of ACE inhibitors and AT1R inhibitors on different intermediates and enzymes in the pathway. Adapted from [11].

As outlined in this section, ACE and ACE2 have opposing effects, similar to the ones described in AT1R and AT2R, and can therefore regulate the RAS pathway and its physiological effects on the body [2, 3, 9, 11]. They form two important opposing axis of the RAS pathway – the ACE/Ang II/AT1R axis and the ACE2/Ang(1-7)/Mas axis [3, 4, 9, 11]. They have to be kept in strict balance as interruptions in regulation of these two pathways are critical in cardiovascular diseases and hypertension [3, 9, 15, 18].

3. RAS inhibitors

There are different pharmacological substances, collectively known as RAS inhibitors, that can interfere with specific steps in the RAS pathway to prevent increased blood pressure and vasoconstriction [5]. These include, but are not limited to, angiotensin-converting enzyme I (ACE) inhibitors and angiotensin II receptor type 1 blockers (ARB), which block AT1R [2, 5, 11]. They are administered to patients with increased blood pressure and different cardiovascular problems [2]. ACE inhibitors are mainly involved in preventing ACE from cleaving Ang I into Ang II and include clinically approved drugs like captopril and enalapril [4, 12]. Although they act via a different pathway than ACE2, it has been indicated that they can cause upregulation of ACE2 expression as well, but only very moderate evidence is available up to date [4, 9]. That indicates they could potentially be effective in different lung conditions by maintaining the ACE/ACE2 ratio and therefore preserving the protective functions of ACE2 [4]. ARBs, on the other hand, mainly inhibit AT1R and include drugs like

losartan and olmesartan [4, 11]. They have known anti-inflammatory abilities and experiments on animal models showed that they can act to upregulate ACE2 expression as well and this association seems to be more supported by evidence than the one regarding ACE [4]. However, neither of the two mentioned RAS inhibitors interacts with ACE2 directly [1].

4. RAS inhibitors and COVID-19

As outlined in section 2, angiotensin converting enzyme 2 (ACE2) has a role diagonally opposite to ACE, the enzyme that ACE inhibitors act on. Through the downstream signalling pathways, it can cause dilation of the blood vessels and consequently, a decrease in blood pressure [16, 19]. ACE2 serves as the entry point for SARS-CoV-2 through the binding of the viral spike proteins (S proteins), particularly the S1 subunit, with the enzyme on the cell surface [2, 3, 4, 6, 9, 17, 19]. For the virus to successfully enter the cell, another membrane enzyme called transmembrane protease, serin 2 (TMPRSS2) has to be present alongside ACE2 as well [2, 12].

Studies done indicate that binding and entry of the SARS-CoV-2 lowers the presence of ACE2 on the cell surface through endocytosis of the bound virus as well as potentially targeted downregulation of the enzyme expression, primarily by increasing metallopeptidase domain-containing protein 17 (ADAM-17) expression [1, 2, 7, 9, 17]. ADAM-17 can then cleave of the membrane-bound ACE2 and cause further repression of ACE2 expression, which was shown in murine animal models [1, 2, 7, 15]. That means that the ACE1/ACE2 balance and therefore the protective effects of the ACE2/Ang(1-7)/Mas pathway in respiratory conditions are lost and Ang II starts accumulating leading to its increased action [2, 4, 10, 11]. It has been proposed that administering synthetic Ang-(1-7) and Mas and AT2R agonists could counterbalance that and therefore help in lung injury, which often presents in COVID-19 patients [10, 11]. However, the details of the signalling pathways associated with Mas receptors are still not well understood so further preclinical and research data is required to support the implications [10]. Another proposed novel therapeutic approach currently still being researched is synthetic ACE2 that could be administered to COVID-19 infected patients to reinforce the appropriate ACE/ACE2 balance [10].

Another concerning consequence of the ACE2 downregulation that offers another possible treatment target, are high levels of Ang II, which play an important role in lung damage and have been detected in patients with COVID-19 [2, 8, 9, 10, 17]. Ang II induces vasoconstriction, which can lead to lower blood flow in the lungs, interrupting the gas exchange. Additionally Ang II can also increase infiltration of immune cells and damage to the blood vessels [2]. It has also been implicated that Ang II can act to stimulate ADAM-17 activity when it binds to AT1R [17]. In fact, higher levels of Ang II have been associated with the onset of acute respiratory distress syndrome (ARDS), a frequent and very serious manifestation of COVID-19 [2, 16, 18]. Based on those facts, it was suggested that using ACE inhibitors and ARBs could potentially be beneficial as they could reduce lung damage in COVID-19 patients by preventing the increased Ang II levels from having an effect [2, 10, 11, 18]. Although both ACE inhibitors and ARBs are well established and safe drugs, the different

pathways they use to achieve the results offer different possibilities as well possible disadvantages [10].

ARBs, specifically AT1R inhibitors would prevent the Ang II from binding to AT1R and therefore facilitate its binding to AT2R [11]. As outlined, that would result in a downstream anti-inflammatory response and therefore exhibit protective functions – however, these signalling pathways are still not well understood so further data must be provided to confirm these effects [11, 18]. In addition, Ang II, not able to bind its receptor, would start to accumulate and therefore form a pool of substrate for ACE2 [18]. ACE inhibitors, on the other hand, inhibit Ang II formation and prevent the body from using Ang-(1-7) to form Ang-(1-5), meaning that more of it would be preserved to bind to Mas receptors. ACE inhibitors therefore lead to higher levels of Ang-(1-7) and decreased Ang II, which indicates that they could have beneficial effects for COVID-19 patients [1, 11]. However, one problem associated with this proposal is that ACE inhibitors can cause potential side effects that include coughing, which could affect the progression of COVID-19 as a respiratory disease [10]. However, whether these implications are clinically significant in terms of COVID-19 treatment is yet to be proven with consistent scientific clinical research [10, 11]. It is known that there are many other factors that affect the progression of COVID-19 and even if RAS inhibitors did prove to be efficient, detailed clinical data would have to be collected to determine any unwanted side effects as well as the correct dose and timing of administration [10, 11].

The points discussed mostly mention using RAS inhibitors as a treatment options in diagnosed COVID-19 patients. However, the major concern associated with RAS inhibitors is that they could potentially lead to higher risk of infection with SARS-CoV-2 for those taking them [18]. That was postulated based on the implication that AT1R and ACE inhibitors might cause an increase in ACE2 expression, which could facilitate SARS-CoV-2 entry into the cells [3, 5, 9, 10, 20]. That is, of course, not beneficial for patients with pre-existing health conditions such as hypertension and cardiovascular diseases [9, 20]. These effects have been implicated mostly in ARBs, while limited data is available for ACE inhibitors [12, 18]. However, even in ARBs most evidence for these implications comes from animal studies, where higher doses of ACE and AT1R inhibitors are often utilised [20]. In fact, most human studies found no correlation between RAS inhibitors and increased ACE2 expression and clinical data does not show any strong support for a higher risk of SARS-CoV infection associated with ARBs or ACE inhibitors [10, 18, 20, 21].

Despite this contradicting evidence, much of which still needs further evaluation, it is still hard to say, whether RAS inhibitors significantly affect the progression of COVID-19 or increase the chances of infection for the patients taking them [3, 9]. However, it is important to note that RAS inhibitors provide other major health benefits for the patients taking them and strong scientific evidence proving the correlation between these drugs and an increased risk of severe COVID-19 infection would have to be provided to outweigh the benefit [5, 9, 19]. Therefore, most scientific data advises continuing administration of RAS inhibitors until or unless further clinical data supporting the negative correlation is provided [3, 20].

5. Clinical results

Consistent clinical research in this area is difficult to carry out in larger groups that would allow statistically significant results and conclusions to be made. As outlined in the report, there are implications for both negative and positive effects of RAS inhibitors on COVID-19 progression and infection [2]. Since the onset of the COVID-19 pandemic, several clinical studies have been carried out to establish the link between RAS inhibitors and COVID-19 [2]. One of them was a retrospective study that included 126 patients with diagnosed hypertension done in 2020 in Wuhan, China by Yang et al [22]. It included 126 patients, 43 of them received either ARBs or ACE inhibitors and 83 of them received other medication [22]. Scientists found no correlation between ACE inhibitors and ARBs an increased risk of COVID-19 infection [22]. It was observed that patients taking ACE inhibitors or ARBs actually had a lower risk of severe infection as well as mortality rate, but these results were not statistically significant (p = 0.061 and p = 0.216 respectively) [22]. A similar, but larger-scale study was done on a national level in South Korea in 2020 by Jung et al. [23]. In this case, 5179 patients were studied, of which 762 used RAS inhibitors, while the remaining 4417 did not [23]. The results showed that RAS inhibitors did not independently statistically significantly affect the mortality (p = 0.60) or the severity of the diseases [23]. Similar results were obtained by Lam et al., who studied 614 patients with diagnosed hypertension that were hospitalised due to COVID-19 [24]. The main aim of this study was to assess, whether it is more beneficial to stop ACE inhibitor/ARBs therapy or continue with normal administration of these drugs [24]. 279 of these patients did not take ACE inhibitors or ARBs (control), 171 patients stopped using ACE inhibitors or ARBs upon hospitalisation and 164 patients followed their normal ACE inhibitor/ARB therapy [24]. The results showed that continuous usage of ACE inhibitors or ARBs statistically significantly lowered the mortality rate compared to terminated usage of these drugs (p = 0.001) [24]. However, some other reported studies found no correlation between RAS inhibitors and COVID-19 [8, 25]. This shows that the results are still lacking consistency and more large-scale trials are needed to provide more accurate results – until then, such data should be treated carefully [2, 18]. Several trials are currently in progress or recruiting and more data is expected soon.

6. Conclusion

COVID-19 occurs as a consequence of an infection with the novel coronavirus, SARS-CoV-2 [26]. As outlined in the report, there are implications for both advantageous and harmful effects of ARBs and ACE inhibitors on the infection or progression of COVID-19 [10]. It is indicated that RAS inhibitors could stimulate expression of ACE2, which could facilitate SARS-CoV-2 infection, but their role in limiting the damaging effects of elevated Ang II could prevent some very serious conditions associated with COVID-19 [2, 17]. Clinical data suggests that there is currently no strong scientific proof that ACE inhibitors or ARBs carry a higher risk for severe COVID-19 and should therefore continue to be administered to the

appropriate patients [21]. Further research in preclinical and clinical trials are required to assess those implications and form any conclusions that could affect the patients.

Acknowledgements

Authors acknowledge support from the European Union's Horizon 2020 research and innovation program under grant agreement No. 801338 (VES4US project) and Slovenian Research Agency (ARRS. Research core fundings No. P3-0388 and projects No. J3-9262, L3-2621).

References

1. Brojakowska A, Narula J, Shimony R, Bander J. Clinical Implications of SARS-CoV-2 Interaction With Renin Angiotensin System. J Am Coll Cardiol. 2020; 75: 3085-3095. doi: 10.1016/j.jacc.2020.04.028
2. Wang J, Edin M, Zeldin D, Li C, Wang D, Chen C. Good or bad: Application of RAAS inhibitors in COVID-19 patients with cardiovascular comorbidities. Pharmacol Ther. 2020; 215: 107628. doi: 10.1016/j.pharmthera.2020.107628
3. Parit R, Jayavel S. Association of ACE inhibitors and angiotensin type II blockers with ACE2 overexpression in COVID-19 comorbidities: A pathway-based analytical study. Eur J Pharmacol. 2021; 896: 173899. doi: 10.1016/j.ejphar.2021.173899
4. Chatterjee B, Thakur S. ACE2 as a potential therapeutic target for pandemic COVID-19. RSC Adv. 2020; 10: 39808-39813. doi: 10.1039/D0RA08228G
5. Haroon S, Subramanian A, Cooper J, et al. Renin–angiotensin system inhibitors and susceptibility to COVID-19 in patients with hypertension: a propensity score-matched cohort study in primary care. BMC Infect Dis. 2021; 21. doi: 10.1186/s12879-021-05951-w
6. Kralj Iglič V, Dahmane R, Griessler Bulc T, et al. From Extracellular Vesicles to Global Environment: A Cosmopolite Sars-Cov-2 Virus. 2020; IJCMCR, 4. doi: 0.46998/IJCMCR.2020.04.000079
7. Santos RAS, Oudit GY, Verano-Braga T, Canta G, Steckelings UM, Bader M. The renin-angiotensin system: going beyond the classical paradigms. Am J Physiol Heart Circ Physiol. 2019; 316: H958-H970. doi: 10.1152/ajpheart.00723.2018
8. Shukla A, Banerjee M. Angiotensin-Converting-Enzyme 2 and Renin-Angiotensin System Inhibitors in COVID-19: An Update. High Blood Press Cardiovasc Prev. 2021; 28: 129-139. doi: 10.1007/s40292-021-00439-9
9. South AM, Brady TM, Flynn JT. ACE2 (Angiotensin-Converting Enzyme 2), COVID-19, and ACE inhibitor and Ang II (Angiotensin II) receptor blocker use during the pandemic. Hypertension. 2020; 76: 16-22. doi: 10.1161/HYPERTENSIONAHA.120.15291
10. Sriram K, Loomba R, Insel P. Targeting the renin–angiotensin signaling pathway in COVID-19: Unanswered questions, opportunities, and challenges. Proc Natl Acad Sci USA. 2020; 117: 29274-29282. doi: 10.1073/pnas.2009875117

11. D'Ardes D, Boccatonda A, Rossi I, et al. COVID-19 and RAS: Unravelling an Unclear Relationship. Int J Mol Sci. 2020; 21: 3003. doi: 10.3390/ijms21083003
12. Danser A, Epstein M, Batlle D. Renin-Angiotensin System Blockers and the COVID-19 Pandemic. Hypertension. 2020; 75: 1382-1385. doi: 10.1161/HYPERTENSIONAHA.120.15082
13. Sharma S. COVID-19: A Concern for Cardiovascular Disease Patients. Cardiovasc Toxicol. 2020, 20: 443-447. doi: 10.1007/s12012-020-09596-0
14. Wysocki J, Lores E, Ye M, Soler M, Batlle D. Kidney and Lung ACE2 Expression after an ACE Inhibitor or an Ang II Receptor Blocker: Implications for COVID-19. J Am Soc Nephrol. 2020; 31: 1941-1943. doi: 10.1681/ASN.2020050667
13. Patel VB, Zhong JC, Grant MB, Oudit GY. Role of the ACE2/Angiotensin 1–7 Axis of the Renin–Angiotensin System in Heart Failure. Circ Res. 2016; 118: 1313-1326. doi: 10.1161/CIRCRESAHA.116.307708
14. Santos RAS, Sampaio WO, Alzamora AC, Snatos DM, Alenina N, et al. The ACE2/Angiotensin-(1–7)/MAS Axis of the Renin-Angiotensin System: Focus on Angiotensin-(1–7). Physiol Rev. 2018; 98: 505-553. doi: 10.1152/physrev.00023.2016
15. Gheblawi M, Wang K, Viveiros A, et al. Angiotensin-Converting Enzyme 2: SARS-CoV-2 Receptor and Regulator of the Renin-Angiotensin System. Circ Res. 2020; 2020: 1456–1474. doi: 10.1161/CIRCRESAHA.120.317015
16. Sarzani R, Giulietti F, Di Pentima C, Giordano P, Spannella F. Disequilibrium between the classic renin-angiotensin system and its opposing arm in SARS-CoV-2-related lung injury. Am J Physiol Lung Cell Mol Physiol. 2020; 319: L325-L336. doi: 10.1152/ajplung.00189.2020
17. Patoulias D, Katsimardou A, Stavropoulos K, Imprialos K, Kalogirou M, Doumas M. Renin-Angiotensin System Inhibitors and COVID-19: a Systematic Review and Meta Analysis. Evidence for Significant Geographical Disparities. Curr Hypertens Rep. 2020; 22(11):90. doi: 10.1007/s11906-020-01101-w
18. Sriram K, Insel P. Risks of ACE Inhibitor and ARB Usage in COVID-19: Evaluating the Evidence. Clin Pharmacol Ther. 2020; 108: 236-241. doi: 10.1002/cpt.1863
19. Mackey K, Kansagara D, Vela K. Update Alert 7: Risks and Impact of Angiotensin-Converting Enzyme Inhibitors or Angiotensin-Receptor Blockers on SARS-CoV-2 Infection in Adults. Ann Intern Med. 2021; 174: W25-W29. doi: 10.7326/L20-1446
20. Yang G, Tan Z, Zhou L, et al. Effects of Angiotensin II Receptor Blockers and ACE (Angiotensin-Converting Enzyme) Inhibitors on Virus Infection, Inflammatory Status, and Clinical Outcomes in Patients With COVID-19 and Hypertension. Hypertension. 2020; 76: 51-58. doi: 10.1161/HYPERTENSIONAHA.120.15143
21. Jung SY, Choi JC, You SH, Kim WY. Association of Renin-angiotensin-aldosterone System Inhibitors With Coronavirus Disease 2019 (COVID-19)- Related Outcomes in Korea: A Nationwide Population-based Cohort Study. Clin Infect Dis. 2020; 71: 2121-2128. doi: 10.1093/cid/ciaa624

22. Lam KW, Chow KW, Vo J,Hou W, Li H, et al. Continued In-Hospital Angiotensin-Converting Enzyme Inhibitor and Angiotensin II Receptor Blocker Use in Hypertensive COVID-19 Patients Is Associated With Positive Clinical Outcome. J Infect Dis. 2020; 222: 1256-1264. doi: 10.1093/infdis/jiaa447
23. Mancia G, Rea F, Ludergnani M, Apolone G, Corrao G. Renin–Angiotensin–Aldosterone System Blockers and the Risk of Covid-19. N Engl J Med. 2020; 382: 2431-2440. doi: 10.1056/NEJMoa2006923
24. Choate J, Aguilar-Roca N, Beckett E, et al. International Educators' Attitudes, Experiences, and Recommendations After an Aabrupt Transition to Remote Physiology Laboratories. Adv Physiol Educ. 2021; 45: 310-321. doi: 10.1152/advan.00241.2020

Research

Study of the cannabinoid profile and microbiological activity of industrial hemp (*Cannabis Sativa* subsp. *Sativa L.*)

Pečan Luka Irenej[1], Štukelj Roman[2,*], Torkar Godič Karmen[3], Jeran Marko[2,4,*]
[1]University of Ljubljana, Biotechnical faculty, Department of Biotechnology, Ljubljana, Slovenia
[2]University of Ljubljana, Faculty of Health Sciences, Laboratory of Clinical Biophysics, Ljubljana, Slovenia
[3]University of Ljubljana, Faculty of Health Sciences, [3]Department of Sanitary Engineering, Ljubljana, Slovenia
[4]University of Ljubljana, Faculty of Electrical Engineering, Laboratoy of Physics, Ljubljana, Slovenia
roman.stukelj@zf.uni-lj.si
marko.jeran@fe.uni-lj.si

Abstract
The main motive of this research is to study cannabis for therapeutic and clinical usage. For this purpose, chemical and microbiological analysis of ten cannabis samples for industrial usage were studied. In the chemical part, the content of cannabinoids in the dried buds of hemp from two different growing seasons were characterized by high performance liquid chromatography (HPLC). We found that only the variety Futura-75 had a total concentration of cannabidiol within the variety specification (1.50–2.00%), while the concentrations of cannabidiol in the remaining nine varieties from both seasons were below the lower limit of the specification for each variety. The measured Δ-9-tetrahydrocannabinol contents ranged from 0.01% in the Uso-31 variety to 0.63% in the Antal variety. All samples had a total % Δ-9-tetrahydrocannabinol below the permissible limit of 0.20%, except for the Tizsa and Antal varieties. We also examined the microbiological quality of these samples after storage, following the guidelines for the microbiological safety of food. The analysis determined the presence of microorganisms in the samples that could be pathogenic at higher concentrations for the end consumer when used for the preparation of herbal infusions. The microbiological quality of all tested samples corresponded to the normatives according to national legislation. We found differences in microbiological quality between individual varieties, which were otherwise grown in identical growing conditions and later treated equally in all phases of storage. The analysed material was both microbiologically and chemically safe for use for human consumption.

1. Objective and purpose

The main goal of the research was to determine the chemical and microbiological profile of ten varieties of cannabis, to find out the concentration of phytocannabinoids in each variety and to check how the concentration of the same variety changes in two different growing seasons.

The purpose of the research was to check the microbiological quality of dried cannabis samples after the storage phase and determine how the quality itself is affected by growth and storage factors. In order to determine the safety of every single sample that could be used as food, we also determined the presence of mycotoxins (or more precisely aflatoxins) in individual samples of dried cannabis.

2. Introduction

Cannabis (*Cannabis sativa*), commonly known as marijuana, has been used by mankind since ancient times. From more than a millennium BC to the end of the 19th century, it was among the most important agricultural crops and industrial raw material. The vast majority of fibres and fabrics, light oil, paper, incense and medicines were made from hemp. Cannabis acts as a stimulant, depressant (antipsychotic) and a hallucinogen. Its main psychoactive ingredient is tetrahydrocannabinol (THC); it also contains more than 80 cannabinoids. Today it is used for recreational, medical, nutritional and industrial purposes.

In 2019, important legal steps were taken for the "rehabilitation" of cannabis and its decriminalization at the level of the European Union since the European Parliament approved a Resolution on the use of cannabis for medical purposes with the aim of encouraging governments' support for research and the availability of medical cannabis in EU countries. In the same year on December, a meeting of the Commission on Narcotic Drugs was held in Vienna, attended by all EU Member States and signatories of the 1961 Convention on Narcotic Drugs and placed Cannabis in a group of predominantly harmless substances. Tetrahydrocannabinol (THC) was also included in this group, and cannabidiol (CBD) was excluded from the system of international surveillance, as no harm to health can be demonstrated [1].

3. Hemp

a. Cannabis

Cannabis is a genus of flowering plants from the family *Cannabaceae*. It is found in all latitudes, as it is phenotypically very adaptable to environmental factors. Cannabis is an annual, dioecious, flowering herb. The leaves are palmately compound or digitate with serrate leaflets. The first pair of leaves usually have a single leaflet, the number gradually increases up to a maximum of about thirteen leaflets per leaf (usually seven or nine), depending on the variety and growing conditions. Cannabis has been described as having one of the most complicated mechanisms of sex determination among the dioecious plants [2].

b. Biologically active compounds in hemp

Nowadays hemp is one of the most chemically researched plants along with more than 420 known compounds. The most interesting ingredients are found in the secretion glands called trichomes, which are distributed over the surface of hemp plant. Although trichomes are found distributed over the entire surface of both male and female plants, they are especially concentrated in some parts of the female inflorescence. The resin secreted by trichomes contains various ingredients, among which cannabinoids, terpenes and flavonoids are the important ones which are secondary metabolism products [1].

Cannabinoids are the main biologically active components of cannabis. Literature reports over 90 different cannabinoids that have been detected until today, although some of them are degradation products. Cannabinoids are, in a broader sense, substances that bind to cannabinoid receptors and cause certain effect through this binding [3].

c. Δ-9-Tetrahydrocannabinol (THC)

THC is a glassy solid, soluble in alcohols, hydrocarbons and oils but insoluble in water. The boiling point of THC is 165 °C, which is the lowest required heating temperature when administered by inhalation. As a narcotic, it is classified in the second group of illicit drugs, so it is allowed for medical and research purposes. THC is an active substance authorized by the US Food and Drug Administration and the European Medicines Agency, as it is used in authorized medicines such as Marinol®, Cesamet™ and Sativex® [4].

The actions of THC result from its partial agonist activity at the cannabinoid receptor CB_1 (K_i = 10 *n*M), located mainly in the central nervous system, and the CB_2 receptor (K_i = 24 *n*M), mainly expressed in cells of the immune system. The psychoactive effects of THC are primarily mediated by the activation of cannabinoid receptors which result in a decrease in the concentration of the second messenger molecule cAMP through inhibition of adenylate cyclase. The presence of these specialized cannabinoid receptors in the brain led researchers to the discovery of endocannabinoids, such as anandamide and 2-arachidonoyl glyceride (2-AG) [5].

THC is a lipophilic molecule which may bind non-specifically to a variety of entities in the brain and body, such as adipose tissue (fat). THC, as well as other cannabinoids that contain a phenol group, possess mild antioxidant activity sufficient to protect neurons against oxidative stress, such as that produced by glutamate-induced excitotoxicity [6].

d. Cannabidiol (CBD)

Cannabidiol (CBD) was first isolated from cannabis in 1940, and its structure was discovered in 1963. Numerous synthetic extraction processes are known, and it is semi-synthetically derived from limonene. At room temperature it is a colourless, white to yellow crystalline solid boiling at 175 °C. In the presence of certain acids or high temperature during pyrolysis, smoking can cyclize it to THC, but in very small amounts. CBD is a very popular raw material in dietary supplements and cosmetics. Cannabidiol is a phytocannabinoid derived from the cannabis type and has analgesic, anti-inflammatory, antineoplastic and chemo preventive effects but no psychoactive action. CBD stimulates endoplasmic reticulum (ER) stress and

inhibits AKT/*m*TOR signalling, thereby activating autophagy and promoting apoptosis. CBD also increases the production of reactive oxygen species (ROS), which further increases apoptosis. This agent also regulates the expression of intercellular adhesion molecule 1 (ICAM-1) and tissue matrix metalloproteinase-1 (TIMP1) inhibitors and reduces the expression of DNA 1 binding inhibitor (ID-1). This inhibits the invasiveness and metastasis of cancer cells. CBD can also activate the transient receptor potential of vanilloid type 2 (TRPV2) which may increase the uptake of various cytotoxic agents into cancer cells. The analgesic effect of CBD is mediated through its binding to CB1 receptors [7].

4. Hypotheses

a. Quantitative determination of cannabinoid concentration

Hypothesis 1: In cannabis varieties for the purpose of cultivation for stems, the content of cannabidiol (CBD) and other cannabinoids (THC, CBG, CBD, THC) will be detected by HPLC analysis and cannabis buds at full maturity will be useful for further processing in terms of cannabinoid content and concentration.

Hypothesis 2: Weather conditions in two seasons (2017 and 2018), harvesting time and the entire growing season will significantly affect the presence and concentration of cannabinoids in the same varieties. In plants with a shorter growth time, the concentration of cannabinoids will be lower.

b. Microbiological quality of samples

Hypothesis 3: In samples representing different varieties of cannabis, the number and the presence of individual species of microorganisms will be different. These differences will be due to weather and the specificity of each cannabis variety.

Hypothesis 4: The presence of microorganisms in cannabis samples will be under the limits of the normative specified in the Guidelines for microbiological safety of food intended for the final consumer.

c. Mycotoxins

Hypothesis 5: In the samples in which microbiological analyses will show a higher presence of mould and yeast, higher presence of mycotoxins will also be detected.

5. Experimental

a. Method of drying hemp samples

After collecting the plant samples, they were dried in the same way under the same conditions. The samples were dried in an oven as drying under direct sunlight affects oxidative processes and cannabinoid degradation. In both years, the harvested plant parts were tied into a bundle of 15 together; drying in the kiln began immediately. The bundles were dried for 50 hours at 40 °C.

b. Samples

Ten different cannabis varieties were used for the samples, namely four monoecious (Fedora 17, Santhica 27, Futura 75 and Uso 31) and six dioecious varieties (KC Dora, Kompolti hybrid TC, Monoica, Tisza, Tiborszallasi, and Antal). All samples were obtained in 2017 in the

laboratory field of the Biotechnical Faculty at University of Ljubljana, where a varietal experiment of hemp production for stem purposes was performed.

c. Preparation of the general suspension for microbiological analysis

The bags in which the samples were stored were first shaken to ensure that cannabis leaves are well mixed. They were then disinfected with 70% ethanol and aseptically opened near the burner. Using a sterile spoon, 10.0 g of the sample was transferred to sterile bags, which were placed in a larger beaker for easier work. 90.0 mL of sterile 2% potassium dihydrogenphosphate was added to the bags, sealed tightly and kneaded in a kneader.

d. Determination of the number of microorganisms in the samples

We used the method of colony counting on solid media after decimal dilution of the sample to determine the number of selected groups of microorganisms using selective media according the international standards. The number of aerobic mesophilic microorganisms (aerobic colony count) [8], the number of *Enterobacteriaceae* including *E. coli* [9], yeasts and moulds [10] and endospores of the genus *Bacillus* were determined in samples, using standard colony count method [11]. The presence of *Salmonella* was also detected in 25 g of each sample [12].

Results were expressed in number of colony forming units (CFU) per gram of sample.

e. Chromatographic analysis for the determination of cannabinoids

Cannabinoids were determined using an 1100 Series Agilent Technologies liquid chromatograph, under the conditions shown in table below. Prior to analysis, the entire system was rinsed with the mobile phase for half an hour. The labelled vials were stacked in order on an HPLC apparatus. First, vials with prepared standard solutions were inserted, the results of which were used to construct a calibration curve. Other sample vials followed. Using the program, we then determined the areas under the chromatographic peaks from the obtained chromatograms, and using the calibration curve, we determined the concentration of cannabinoids in the dried cannabis tops.

Table 1: Conditions for chromatography separation.

Column	Supelco Ascentis® Express 5 µm, C18 (5 µm, 150 mm × 4.6 mm)
Mobile phase	Methanol : 1% acetic acid (65:35)
Mobile phase flow	1 mL/min
Injection volume	20 µL
Column temperature	30 °C
Pressure	105 bar
Analysis time	26 minutes

f. Preparation of samples for the determination of cannabinoid concentrations

Sheaves of individual varieties were shredded and homogenized in a coffee grinder. Weighing approximately between 500–510 mg of the homogenized sample (in 2 batches) into a 50 mL Falcon tube and added 10.0 mL of solvent (MeOH/$CHCl_3$, 9:1).

The sample was placed in an ultrasonic bath for 15 min. 1.0 mL of the thus prepared sample was diluted twice in the same volume of mobile phase and it was filtered via syringe into vials.

g. Preparation of samples for the determination of mycotoxins

We put 10.0 g of the dried plant sample into a conical flask and added 150.0 mL of 10% NaCl solution. The sample was homogenized in an ultrasonic bath for 15 minutes at 25 °C. The contents were filtered into a beaker and from there 20.0 mL of the filtrate was pipetted into a flask. 20.0 mL of the filtrate was transferred to 50.0 mL of a mixture of distilled water and methanol in a ratio (85:15, v/v) and stirred in an ultrasonic bath for 15 minutes. After that, 50.0 mL of dichloromethane was added and shaken for 30 min. The phases were separated in a separatory funnel by collecting dichloromethane at the bottom of the separating funnel in a 200 mL conical flask. The contents were dried over water-binding sodium sulphate, which was filtered after 45 minutes. The dichloromethane phase was evaporated on a miVac Quattro rotary evaporator and the residue dried to dryness. The dry extract was dissolved in 1.0 mL of methanol and filtered into vials by syringe through a cellulose-acetate filter.

6. Results and Discussion

a. Microbiological quality of samples

The purpose of microbiological examinations was to determine the microbiological safety of individual leaf samples of different varieties of hemp grown in the 2017 season, after two years of storage in a closed dark place with an average temperature of 20.5 °C and relative humidity (39%). Microbiological quality was checked according to the Guidelines for microbiological food safety, which are intended for the final consumer [13]. The results showed that all samples contained different amounts of microorganisms (**Table 2**), which is most likely due to the design and characteristics of each of the variety and its resistance to pathogens. Samples were stored in food storage bags with a closure system and appropriately labelled. Samples of dried cannabis leaves could be used as herbal infusions, so we used guidelines to determine the permitted limit values of individual microorganisms for tea, coffee and similar products to determine microbiological quality. As can be seen from the standards in **Table 3**, none of the samples exceeds the permitted limit values, which indicates good manufacturing practice, appropriate hygiene standards and appropriate storage. All tested samples corresponded to the normative according national legislation. In addition to the groups of microorganisms defined in our legislation, we also determined the presence of *Bacillus* species, because they represent a part of cannabis bacterial microbiome, but can also be pathogen to humans [14].The results showed (**Table 2**) that all samples contained different amounts of microorganisms, which is most likely due to the design and characteristics of each of the variety and its resistance to pathogens. Some studies used the bioprospecting rationale that hemp and marijuana contain medicinal compounds that might also harbour competent microbial endophytes capable of providing health benefits to the host plant and inhibit the growth of pathogen fungi and bacteria [14].

The most common endophytes harboured in buds and leaves of *Cannabis sativa* belong to the genuses *Bacillus*, *Pseudomonas* and *Pantoea* [15].
It can be concluded that the microbiological quality depends mainly on the individual variety and its resistance and adaptability to growing conditions, but in any case, there could be contamination of the sample during treatment. This factor cannot be ruled out as a possible source of plant contaminants, as soil quality, soil moisture, soil microbial flora, humidity, air temperature and the number of sunny and rainy days significantly affect plant health and consequently the presence of microorganisms.

Table 2: Number of individual microorganisms (MO) in CFU/g.

Variety	Total number of microorganisms (log_{10}CFU)	Yeasts and moulds (log_{10}CFU)	Enterobacteria (log_{10}CFU)	*Bacillus* vegetative forms (log_{10}CFU)	*Bacillus* endospores (log_{10}CFU)
Santhica 27	4.518514	3.30103	2.633468	1.60206	2.041393
Fedora 17	3	3.30103	2.653213	1.477121	1.30103
Antal	3.908485	3	3.267172	1.477121	1.30103
Uso 31	5.322219	3.69897	3.478566	2,146128	0.69897
Tibor	4	3	3.176091	1.69897	1.477121
KC Dora	4.176091	3	2.579784	1.30103	1.60206
Tisza	4.544068	3	3.294466	1.954243	1.60206
Kompolti Hybrid TC	4.544068	3	2.662758	1.812913	1
Monoica	4.886491	3.30103	3.482874	1.477121	1.60206
Futura 75	3	3	2.518514	1.30103	0.69897

Table 3: Type of microorganism and quality criterion [13].

Type of microorganism	Quality criterion
Salmonella spp.	*n. n.* in 25 g (c = 0)
Escherichia coli	m = 10^3 cfu/gM = 10^4 cfu/g (c = 2)
Molds and Yeasts	m = 10^5 cfu/g, M = 10^6 cfu/g (c = 1)
Aerobic mesophilic bacteria	m = 10^7 cfu/gM = 10^8 cfu/g (c = 2)
Enterobacteriaceae	m = 10 cfu/gM = 10^2 cfu/g (c = 1)

b. Quantitative determination of cannabinoid concentration

When determining the concentrations of total cannabinoids for 2017, the highest value for total CBD was 15.9 mg/g for the variety Futura 75, and the lowest 2.1 mg/g for the variety Santhica 27. Only the Futura 75 variety had a total cannabidiol (CBD) value within the specification limits, while the other nine varieties were below the expected lower limit (specification in **Table 6**). The measured THC values ranged for the highest measured in the Antal variety, namely 3.6 mg/g and the lowest 0.3 mg/g in the Fututra 75 variety. It can be concluded that all varieties have a total THC below the permissible limit, which is 0.2%, except for the Tisza and Antal varieties (**Table 4**).

When determining the concentrations of total cannabinoids for 2018, the highest value for total CBD was 1.18 mg/g in the variety KC Dora, and the lowest 0.28 mg/g in the variety Uso 31. In the latter, the cannabinoid cannabidiol is the most pronounced, so it is the result is also expected and in line with the references. All ten varieties were below the expected lower limit (**Table 5**). The measured THC values ranged for the highest measured in the variety Antal, namely 0.6 mg/g and the lowest 0.01 mg/g in the variety Uso 31. It can be established that all varieties have a total THC below the permissible limit, which is 0.2%, except for the Antal variety (**Table 5** and **6**). As can be seen from the graphs and tables, the concentration of cannabinoids in the same varieties is different in two years, namely in most varieties lower in 2018 than in 2017, except for the varieties Antal and KC Dora. The main reason is most likely the earlier collection of cannabis samples (26 days in 2018 compared to 2017), which also meant a shorter vegetation cycle and cessation of growth during the period when the plant produces the most cannabinoids.

Cannabinoid content is more influenced by factors during plant growth, such as soil composition, fertilization, soil moisture and weather conditions, with precipitation, air temperatures and solar radiation, so the growing season also affects cannabinoid concentration. The current results suggest a possible negative relationship between cannabinoid concentration and the microorganisms studied.

Table 4: Shows the weight (m) and average values of two measurements of cannabinoids (wt%) with the corresponding standard deviations (SD) for cannabis varieties for industrial use from 2017. The average total values of Δ-9-THC and CBD calculated by the equation (THC *total* = Δ-9-THC-a × 0.877) + Δ-9-THC are also shown; (CBD *total* = CBD × 0.877) + CBD. PMD = below the detection limit. wt% 0.1 = 10 mg.

Variety	Weight (mg ± SD)	CBD-a (wt% ± SD)	CBG (wt% ± SD)	CBD (wt% ± SD)	Δ-9-THC (wt% ± SD)	Δ-9-THC-a (wt% ± SD)	Sum CBD (wt% ± SD)	Sum THC (wt% ± SD)
Monoica	500.4 ± 0.28	1.00 ± 0.02	0.01	0.14 ± 0.01	0.04	0.14	1.02 ± 0.02	0.16
Tibor Szallasi	500.6 ± 0.42	1.18 ± 0.10	0.01	0.21 ± 0.02	0.05	0.13 ± 0.01	1.24 ± 0.11	0.17 ± 0.02
Tisza	500.8 ± 0.07	1.16 ± 0.05	0.01	0.23 ± 0.02	0.10 ± 0.01	0.20 ± 0.01	1.25 ± 0.07	0.27 ± 0.02
Fedora 17	500.3 ± 0.35	1.26 ± 0.03	0.01	0.19	0.04	0.12	1.30 ± 0.03	0.15 ± 0.01
Kompolti Hybrid TC	500.4 ± 0.28	0.96 ± 0.11	0.01	0.18	0.01	0.04 ± 0.01	1.02 ± 0.09	0.05
Santhica 27	500.5 ± 0.42	0.21 ± 0.04	0.09 ± 0.01	0.02	0.01	0.03 ± 0.01	0.21 ± 0.04	0.04
Futura 75	500.5 ± 0.21	1.47	0.01	0.30 ± 0.01	0.02	0.06	1.59 ± 0.01	0.08
Antal	500.3 ± 0.42	1.09 ± 0.03	0.01	0.15 ± 0.01	0.10 ± 0.01	0.29 ± 0.01	1.11 ± 0.04	0.35 ± 0.01
Uso 31	500.8	0.42 ± 0,07	*n.d.*	0.05 ± 0.01	0.01	0.03 ± 0.01	0.42 ± 0.07	0.03 ± 0.01
KC Dora	500.1 ± 0.07	1.13 ± 0.05	0.01	0.16 ± 0.07	0.03 ± 0.02	0.10 ± 0.04	1.15 ± 0.12	0.11 ± 0,07

Table 5: Mass (m) and average values of two measurements of cannabinoids (wt%) with the corresponding standard deviations (SD) on cannabis varieties for industrial use from 2018. The average total values of Δ-9-THC and CBD calculated according to (THC_{total} = Δ-9-THC-a × 0.877) + Δ-9-THC;
(CBD *total* = CBD-a × 0,877) + CBD.

Variety	Mass (mg ± SD)	CBD-a (wt% ± SD)	CBG (wt% ± SD)	CBD (wt% ± SD)	Δ-9-THC (wt% ±SD)	Δ-9-THC-a (wt% ± SD)	Sum CBD (wt% ± SD)	Sum THC (wt% ± SD)
Monoica	500.8 ± 0.07	1.00 ± 0.06	0	0.10 ± 0.01	0.02	0.05 ± 0.01	0.98 ± 0.06	0.06 ± 0.01
Tibor Szallasi	500.1	1.20 ± 0.06	0.01 ± 0.02	0.11 ± 0.01	0.02 ± 0.01	0.11 ± 0.01	1.07 ± 0.06	0.12 ± 0.01
Tisza	500.5 ± 0.21	1.16 ± 0.09	0.01	0.13 ± 0.01	0.02	0.09 ± 0.01	1.15 ± 0.08	0.10 ± 0.01
Fedora 17	500.8 ± 0.14	1.04 ± 0.10	0	0.14 ± 0.02	0.01	0.06 ± 0.01	1.05 ± 0.11	0.06 ± 0.01
Kompolti Hybrid TC	500.4 ± 0.64	1.12 ± 0.04	0.01	0.11 ± 0.01	0.01	0.04	1.09 ± 0.04	0.05
Santhica 27	500.6± 0.35	0.32 ± 0.03	0.10 ± 0.02	0.03	0	0.02	0.31 ± 0.03	0.02
Futura 75	500.7 ± 0.28	1.14 ± 0.06	0.01	0.23 ± 0.01	0.02	0.07 ± 0.01	1.47 ± 0.01	0.08
Antal	500.4 ± 0.63	1.29 ± 0.02	0.01	0.25 ± 0.01	0.11	0.59 ± 0.03	1.38 ± 0.01	0.63 ± 0.03
Uso 31	500.2 ± 0.28	0.28 ± 0.03	*n.d.*	0.03	0	0.01 ± 0.01	0.28 ± 0.03	0.01
KC Dora	500.4 ± 0.64	1.14 ± 0.01	0.01	0.18	0.03	0.11	1.18 ± 0.01	0.13

Table 6: Specifications of growth.

Variety	*2017 (days of growth)	**2018 (days of growth)	Vegetation cycle	THC (wt%)	CBD (*CBG) (wt%)
Monica	142	116	135	< 0,12	1.50 – 2.00
Tibor-Szallasi	142	116	145	< 0,20	2.00 – 3.00
Tisza	142	116	145	< 0,12	2.00 – 3.00
Fedora	142	116	125	< 0,06	1.5 – 2.0
Kompolti hybrid TC	142	116	160	< 0,12	2.00 – 3.00
Santhica 27	142	116	135	< 0,12	1.50 – 2.00*
Futura	142	116	145	< 0,12	1.50 – 2.00
Antal	142	116	140	< 0,12	2.00 – 3.00
Uso 31	142	116	125	< 0,06	0.50 – 1.00
KC Dora	142	116	145	< 0,12	2.00 – 3.00

c. Quantitative determination of mycotoxin concentration

As can be seen from **Table 7**, we determined a certain quantity of mycotoxins in most samples, but this amount is generally below the statutory limit. In addition to previously performed microbiological analyses, we also performed morphological identification of moulds that had grown on the media using imaging keys. We found the presence of moulds: *Fusarium*, *Cladosporium*, *Alternaria* and *Rothotorula*, none of these moulds excrete large amounts or do not excrete aflatoxins at all which is also evident from the results of measurements of the presence of aflatoxins. The highest concentration of aflatoxin G2 was detected in the variety Fedora 17, 0.6064 µg/kg, and the lowest in the variety Uso 31, 0.0098 µg/kg. The presence of G2 toxin was not detected in the Kompolti Hybrid TC variety. The highest presence of aflatoxin G1 was detected in the variety Fedora 17, namely 0.9438 µg/kg, the lowest in the variety Uso 31. Aflatoxin G1 was not detected in the variety Santica 27. The Uso 31 variety showed the highest presence of mould in microbiological analysis, but the analysis of aflatoxins G1 and G2, unexpectedly compared to other samples, contained the lowest concentration of them.

The highest presence of aflatoxin B2 was detected in the variety Kompolti hybrid TC, 1.1910 µg/kg, and the lowest in the variety Uso 31, otherwise 0.024 µg/kg. The presence of aflatoxins B2 was not detected in the variety KC Dora and Santica 27. The highest concentration of aflatoxins B1 was measured in the variety Tisza, namely 0.3373 µg/kg, and the lowest in the variety Fedora 17, otherwise 0.1778 µg/kg. The concentration of aflatoxins was not determined in the varieties Kmpolti hybrid TC, KC Dora, Tiborszallasi, on Santica 17. Unfavourable growing conditions, improper handling of plant material and storage cause the growth of moulds that release aflatoxin. During storage, moisture is one of the key factors influencing the quality of the sample, as it creates a favourable environment for mould growth, so it has to be monitored at regular intervals.

Table 7: Concentrations of aflatoxins (in µg/kg and ppb) G2, G1, B2 and B1 which were determined by HPLC.

	Aflatoksin G2		Aflatoksin G1		Aflatoksin B2		Aflatoksin B1	
Variety	Conc. µg/kg	Conc. ppb	Conc. µg/kg	Conc. ppb	Conc. µg/kg	Conc. ppb	Conc. µg/kg	Conc. ppb
Santica 27	0.253	0.025	0	0	/	/	0	0
Fedora 17	0.605	0.061	0.944	0.094	0.944	0.094	0.178	0.018
Antal	0.147	0.015	0.133	0.013	0.133	0.013	0.059	0.006
Uso 31	0.010	0.001	0.025	0.003	0.025	0.003	0.036	0.004
Tibor-Szallasi	0.053	0.005	0.126	0.013	0.126	0.013	0	0
KC Dora	0.041	0.004	0.135	0.014	/	/	0	0
Tisza	0.019	0.002	0.067	0.007	0.067	0.007	0.373	0.037
Kompolti hybrid TC	0	0	1.191	0.120	1.191	0.119	0	0
Monoica	0.139	0.014	0.146	0.015	0.146	0.015	0.231	0.023
Futura	0.049	0.005	0.270	0.027	0.270	0.027	0.249	0.025
Tisza	0.245	0.025	0.247	0.025	0.247	0.025	0.231	0.023

7. Conclusions

We found that in the same varieties growing in two different growing seasons, a difference in cannabinoid concentration occurred. One of the key factors influencing this difference was the shorter vegetation cycle, which meant that the phytocannabinoid formation and excretion phase was not completed. Based on the treatment of samples, quality of growing conditions and appropriate drying and storage, we anticipated that the amount of microorganisms present will be less than specified by the standards listed in the Guidelines for microbiological safety of food intended for the final consumer. The samples were dried and stored for a long time which creates quite unfavourable conditions for the growth and reproduction of microorganisms. We can concluded that we handled the samples appropriately throughout the process and that they would be appropriate and safe for the end consumer. We anticipated that a higher presence of mycotoxins would also be detected in those samples in which microbiological analyses would show a higher presence of mould and yeast. A higher amount of mould was detected mainly in the variety USO 31. When the analysis of the concentration of aflatoxins in the plant material was deducted we did not detect them. Therefore, the last hypothesis is the only one that we did not confirm. Mycotoxins are usually released into the environment by moulds of the genus *Aspergillus*, but these have not been identified in any of the samples, and consequently the concentration of aflatoxins is very low. The plant analysed material is both microbiologically and chemically safe for use in human nutrition.

Acknowledgements

Luka Irenej Pečan, *B. Sc. student* was awarded 3th prize for this research work entitled "Quantitative determination of biologically active compounds in industrial hemp (*Cannabis Sativa* subsp. *Sativa* L.) and its Microbiological Quality" in 30th International competition of young scientists "Step into the Future". The competition was organized by the Bauman Moscow State Technical University and the Russian Youth Engineering Society. The mentor of the work was Marko Jeran and co-mentors Roman Štukelj and Karmen Godič Torkar. The authors would like to thank the Slovenian Research Agency (ARRS) and the Ministry of Agriculture, Forestry and Food Republic Slovenia for supporting the applicant CRP Project No. V4-1611 and the Slovenian Research Agency for core funding No. P3-0388 and Projects No. J1-9162, L3-2621. The authors thank the RN Institute, Ljubljana, for analytical support.

References

1. Štukelj R, Benčina M, Fanetti M, et al. Synthesis of stable cannabidiol (CBD) nanoparticles in suspension. Mater Tehnol 2019; 53 (4): 543–549. doi: 10.17222/mit.2018.253
2. Amaducci S, Colauzzi M, Zatta A, Venturi G, Flowering dynamics in monoecious and dioecious hemp genotypes. J Ind Hemp 2008; 13 (1): 5–19. doi: 10.1080/15377880801898691
3. Andre CM, Hausman J-F, Guerriero G, *Cannabis sativa*: the plant of the thousand and one molecules. Front Plant Sci 2016; 7: 1–17. doi: 10.3389/fpls.2016.00019
4. Ashton CH, Pharmacology and effects of cannabis: a brief review. Br J Psychiatry 2001, 178: 101–106. DOI: 10.1192/bjp.178.2.101
5. Elphick MR, Egertová M, The neurobiology and evolution of cannabinoid signalling. Philos Trans R Soc Lond B Biol Sci 2001; 356 (1407): 381–408. doi: 10.1098/rstb.2000.0787
6. Pertwee RG, The pharmacology of cannabinoid receptors and their ligands: an overview. Int J Obes (Lond) 2006; 30 (1): S13–S18, doi: 10.1038/sj.ijo.0803272
7. Germano C, Baker S, Carl Germano, CNS, CDN: simple guide to the endocannabinoid system, hemp phytocannabinoids/CBD and your health. Altern Ther Health Med 2020; 26 (S1): 32–34.
8. ISO 4833 (2003), Microbiology of food and animal feeding stuffs – Horizontal method for the enumeration of microorganisms – Colony-count technique at 30 °C. International Standard Organization, Brussels, Belgium, 1–6. https://www.iso.org/standard/34524.html

9. ISO 16649-2 (2001), Microbiology of food and animal feeding stuffs — Horizontal method for the enumeration of beta-glucuronidase-positive *Escherichia coli* — Part 2: Colony-count technique at 44 degrees C using 5-bromo-4-chloro-3-indolyl beta-D-glucuronide. International Standard Organization, Brussels, Belgium, 1–8. https://www.iso.org/obp/ui/fr/#iso:std:iso:16649:-2:ed-1:v1:en
10. ISO 21527-1 (2008), Microbiology of food and animal feeding stuffs — Horizontal method for the enumeration of yeasts and moulds — Part 1: Colony count technique in products with water activity greater than 0.95. International Standard Organization, Brussels, Belgium, 1–8. https://www.iso.org/standard/38275.html
11. ISO 6887-4 (2017), Microbiology of the food chain — Preparation of test samples, initial suspension and decimal dilutions for microbiological examination — Part 4: Specific rules for the preparation of miscellaneous products. Standard Organization, Brussels, Belgium, 1–16. https://www.iso.org/standard/63338.html
12. ISO 6579-1 (2017), Microbiology of the food chain — Horizontal method for the detection, enumeration and serotyping of *Salmonella* — Part 1: Detection of *Salmonella* spp. International Standard Organization, Brussels, Belgium, 1–50. https://www.iso.org/standard/56712.html
13. NLZOH, NVI (2019), Guidelines for the microbiological quality of food intended for the final consumer (*Slo*. Smernice za mikrobiološko kakovost živil, ki so namenjena končnemu potrošniku). In Rupel T, Lušicky M, Pavlica T, et al., editors. National Laboratory for Health, Environment and Food, and Veterinary Faculty, University of Ljubljana, Slovenia, 1–41.
14. Taghinasab M, Jabaji S, Cannabis microbiome and the role of endophytes in modulating the production of secondary metabolites: an overview. Microorganisms 2020; 8 (3): 355. doi: 10.3390/microorganisms8030355
15. Kusari P, Kusari S, Lamshöft M, et al. Quorum quenching is an antivirulence strategy employed by endophytic bacteria. Appl Microbiol Biotechnol 2014; 98 (16): 7173–7183. doi: 10.1007/s00253-014-5807-3

Review

In vitro cell experiments as important approach in cellular vesicles research

Jan Zala[1,*]

[1]University of Ljubljana, Faculty of Health Sciences, Laboratory of Clinical Biophysics

*zala.jan@gmail.com

Abstract: In the last years cellular vesicles (CVs) gain more and more interest in the scientific community due to their specific characteristics. Research is focused on origin and function of CVs, among which intercellular communication is the most interesting and promising. Potential usage of CVs in diagnostic, therapy for different diseases and biotechnology is of interest. Main reason why CVs are not yet used outside the research borders is problematic analytics with poor robustness and low reliability of the results. To deepen knowledge about CVs, different research approaches are used. CVs are monitored in *in vitro* and *in vivo* processes. In this contribution, we will focus more on *in vitro* research with different cell lines. Among vesiculation of the cells, also oxidative stress and inflammatory processes are monitored to gain more information about cell development.

1. About cellular vesicles and *in vitro* cell experiments

It was suggested that cellular vesicles (CVs) are formed in the final stage of membrane budding [1] by pinching off of the buds from the cell membranes and that they present an intercellular communication system within the body [2,3]. CVs, discharged into the circulation could assist with disposal of cellular waste products generated under stress conditions and help the cells to preserve homeostasis [4]. CV formation by animal cells is considered a physiological process [5] that can be accelerated by oxidative stress [6] and by inflammation process [7]. CVs can be formed also by other organisms such as microalgae [8], which are also more and more commonly used in CVs research in the last years. One of the approaches for CVs research are *in vitro* cell experiments. *In vitro* studies are performed with cells outside their normal biological context. It is important to establish and maintain high standards of reproducibility and reliability when performing *in vitro* studies [9]. To improve the quality of in vitro research, the concept of *Good Cell Culture Practice* was developed and was widely adapted to ongoing scientific process [10]. Most commonly for *in vitro* studies with cells, cancer cells are used.

Changes in *in vitro* cells, after being treated with CVs preparation, can be monitored in more controlled conditions as when monitoring the *in vivo* changes. Among cell changes such as cytotoxicity, oxidative stress and inflammation process [11], also vesiculation of *in vitro* cells offers the information about cell response to different treatments. Also, *in vitro* experiments are performed to evaluate the safety of EVs that may be therapeutically used.

2. Experiments on *in vitro* cells treated with preparations rich with vesicles

2.1. Cytotoxicity

For testing cytotoxicity, it is best to use different tests simultaneously to ensure better reliability of the results. One of the most used cytotoxicity tests is uptake of the vital dye neutral red (NR) assay provides quantitative estimation of viable cells number in a cell culture. NR has properties of weak cationic dye, which can be retained in lysosomes only when cell has an ability to maintain acidic pH. Test is based on the ability of viable cells to absorb and bind the dye neutral red in the lysosomes. The absorbance of the dye is read using a spectrophotometer [12].

Resazurin, or alamarBlue® is used as a cell health indicator - the redox reaction in resazurin-based assays provides information about the intercellular processes and metabolic activity. Resazurin undergoes a redox reduction to resorufin, a pink, fluorescent chemical which can be detected via fluorescence or spectrophotometry [13]. Usually, NR and resazurin assays are implemented together, because they can both be done on the same sample – first resazurin and then NR assay is performed.

Trypan blue exclusion test is test for cell viability – it determines the number of viable cells present in a cell suspension. Live cells possess intact cell membranes that exclude certain dyes, such as trypan blue, eosin, or propidium, whereas dead cells do not. In Trypan blue test, a cell suspension is treated with dye and then visually examined to determine whether cells take up or exclude dye – examine and counting cells observed with microscope. It can

be seen that viable cells have a clear cytoplasm whereas a nonviable cells have a blue cytoplasm [14].
With MTT (3-(4,5-dimethylthiazol-2-yl)-2,5-diphenyl tetrazolium bromide) assay cellular metabolic activity is measured as an indicator of cell viability, proliferation and cytotoxicity. This colorimetric assay is based on the reduction of a yellow tetrazolium salt - MTT to purple formazan crystals by metabolically active cells. The quantity of the purple formazan crystals is proportional to the number of living cells and is measured spectrophotometrically [15].

2. Oxidative stress

Oxidative stress is a phenomenon caused by an imbalance between production and accumulation of oxygen reactive species (ROS): superoxide radicals ($O_2^{\bullet -}$), hydrogen peroxide (H_2O_2), hydroxyl radicals (•OH), and singlet oxygen ($^1O_2$), in cells and tissues and the ability of a biological system to detoxify these reactive products. Oxidative stress is mentioned mostly as harmful for human body, yet it is also exploited as a therapeutic approach to, with certain degree of success, treat clinical conditions such as cancer [16]. CVs formation is considered to be provoked by oxidative stress [6] and it is suggested that during oxidative stress, oxidized proteins are formed, and cells release CVs as a compensatory mechanism to remove them and to maintain homeostasis [17]. ROS are generated from both endogenous (mainly produced by mitochondria, during both physiological and pathological conditions) and exogenous sources - immune cell activation, inflammation, ischemia, infection, cancer, excessive exercise, mental stress, and aging [16]. As research show oxidative stress can be responsible for different diseases, i.e., cancer, diabetes, metabolic disorders, atherosclerosis, and cardiovascular diseases [18].
Assay for ROS detection uses cell-permeant H2DCFDA which passively diffuses into cells and is retained in the intracellular level after cleavage by intracellular esterases. Upon oxidation by ROS, the nonfluorescent H2DCFDA is converted to the highly fluorescent 2', 7'-dichlorofluorescein (DCF). Dead or dying cells produces ROS, therefore for detection of ROS in living cells, propidium iodide (PI) or 7-AAD is used to evaluate ROS production only in living cells which are PI/7-AAD negative. Fluorescence emission can be assessed by flow cytometry, a standard fluorometer or fluorescence microscopy using appropriate filter [19].
Glutathione S-transferase (GST) are a family of antioxidant enzymes that act in antioxidant defense, help in decreasing reactive oxygen species and in protecting cells from oxidative stress [20]. It is one of the parameters, measured in connection with oxidative stress occurrence - erythrocyte suspension GST activity has been proposed as a potential marker for oxidative stress [21]. GST assay is measured spectrophotometrically [22].
Cholinesterase (ChE) is an enzyme needed for proper function of the nervous system, since it is responsible for breaking down neurotransmitter acetylcholine that is believed to modulate immune and anti-inflammatory response via the cholinergic system; a key factor in the anti-inflammatory cholinergic pathway is supposed to be oxidative stress [23]. It was suggested that decrease in erythrocyte suspension ChE activity may reflect an increased response of the human body to oxidative stress [24]. For the detection of ChE activity, spectrophotometric method adopted by Ellman [25] is used.

3. Inflammatory markers

Inflammation is a biological response of the immune system that can be triggered by different factors, among which are pathogens, damaged cells and toxic compounds. These factors can induce acute and/or chronic inflammatory responses that can result in tissue damage or disease [26]. Systemic or acute-phase inflammation can be detected by monitoring CRP production, stimulated by cytokines IL-6 and TNF-α, indicators of local inflammatory response [27]. Inflammatory processes in connection with CVs are mostly described for platelet-derived CVs (PCVs). PCV cargo can interact with cells involved in inflammatory reactions. Also, increase in blood PCV levels has been reported in inflammatory-associated disorders. Proinflammatory action of PCVs modulates several processes, including activation of both immune cells and endothelium. Moreover, PCVs is considered to be a rich potential source of proinflammatory cytokines and complement components [28].

Interleukin-6 (IL-6) is a myokine which acts as an inflammatory mediator [29]. Tumor necrosis (TNF-∝) was originally described as a circulating factor that can cause necrosis of tumors but has since been identified as a key regulator of the inflammatory response [30]. Also, inflammatory cytokine interleukin 1- β (IL-1β) is of interest, since it is an important regulator of inflammation with controlling many innate immune processes. For measurement of cytokines in samples, commercial ELISA kits are used.

4. Isolation and characterization of cellular vesicles

Cell-derived vesicles from eukaryotic cells are considered to be important intercellular "multipurpose carriers" involved in communication, protection against external and internal cellular stress and in the exchange of genetic information [31].

There are many known strategies for isolation of the *in vitro* cell-derived vesicles. Different authors describe different approaches for CVs isolation: using precipitation kits (ExoQuick™ [32], Total Exosome Isolation™ [33]), differential centrifugation including ultracentrifugation (UC) [34], filtration [35], density gradient UC [35], sucrose cushion UC [36], custom charge-based precipitation method [37]. After CVs isolation, different approaches are used for characterization and analysis of CVs: transmission electron microscopy (TEM) [20] or immunogold TEM [38], flow cytometry [39], western blot [23], nanoparticle tracking analysis (NTA), atomic force microscopy (AFM) [34], fluorescence microscopy [40], dynamic light scattering (DLS) [38], bicinchoninic acid (BCA) assay [38], Bradford assay [35], RNA [39], proteomics [41], custom colorimetric nanoplasmonic assay (molar concentration)[34], zeta potential [42], quantitative real-time polymerase chain reaction (qRT-PCR) [43,44].

5. Conclusions

Every new approach and method are an important contribution in understanding formation and role of CVs in human body and a step closer to new era of diagnostics and therapy. Monitoring response of *in vitro* cells on treatment with preparations rich with CVs can offer

improvement of protocols for diagnostics and therapy *in vivo*. With appropriate isolation and analysis of isolates from *in vitro* cells, CVs formation mechanisms can be better understood.

References

1. Hurley JH, Boura E, Carlson LA, Różycki B. Membrane budding. Cell. 2010; 143(6):875-87. doi:10.1016/j.cell.2010.11.030
2. Sorkin R, Huisjes R, Bošković F, et al. Nanomechanics of Extracellular Vesicles Reveals Vesiculation Pathways. Small. 2018; 14(39):e1801650. doi:10.1002/smll.201801650
3. Oszvald Á, Szvicsek Z, Sándor GO, et al. Extracellular vesicles transmit epithelial growth factor activity in the intestinal stem cell niche. Stem Cells. 2020; 38(2):291-300. doi:10.1002/stem.3113
4. Frühbeis C, Helmig S, Tug S, Simon P, Krämer-Albers EM. Physical exercise induces rapid release of small extracellular vesicles into the circulation. J Extracell Vesicles. 2015; 4:28239. doi:10.3402/jev.v4.28239
5. Morshed A, Karawdeniya BI, Bandara YMND, Kim MJ, Dutta P. Mechanical characterization of vesicles and cells: A review. Electrophoresis. 2020; doi:10.1002/elps.201900362
6. Borras C, Mas-Bargues C, Sanz-Ros J, et al. Extracellular vesicles and redox modulation in aging. Free Radic Biol Med. 2020; 149:44-50. doi:10.1016/j.freeradbiomed.2019.11.032
7. Chaar V, Romana M, Tripette J, et al. Effect of strenuous physical exercise on circulating cell-derived microparticles. Clin Hemorheol Microcirc. 2011; 47(1):15-25. doi:10.3233/CH-2010-1361
8. Picciotto S, Barone ME, Fierli D, et al. Isolation of extracellular vesicles from microalgae: towards the production of sustainable and natural nanocarriers of bioactive compounds. Biomater Sci. 2021; doi:10.1039/d0bm01696a
9. Hirsch C, Schildknecht S. Research Reproducibility: Keeping Up High Standards. Front Pharmacol. 2019; 10:1484. doi:10.3389/fphar.2019.01484
10. Coecke S, Balls M, Bowe G, et al. Guidance on good cell culture practice. a report of the second ECVAM task force on good cell culture practice. Altern Lab Anim. 2005; 33(3):261-87. doi:10.1177/026119290503300313
11. Jan Z, Drab M, Drobne D, et al. Decrease in Cellular Nanovesicles Concentration in Blood of Athletes More Than 15 Hours After Marathon. Int J Nanomedicine. 2021; 16:443-456. doi:10.2147/IJN.S282200
12. Repetto G, del Peso A, Zurita JL. Neutral red uptake assay for the estimation of cell viability/cytotoxicity. Nat Protoc. 2008; 3(7):1125-31. doi:10.1038/nprot.2008.75
13. Pace RT, Burg KJ. Toxic effects of resazurin on cell cultures. Cytotechnology. 2015; 67(1):13-7. doi:10.1007/s10616-013-9664-1
14. Strober W. Trypan Blue Exclusion Test of Cell Viability. Curr Protoc Immunol. 2015; 111:A3.B.1-A3.B.3. doi:10.1002/0471142735.ima03bs111

15. Śliwka L, Wiktorska K, Suchocki P, et al. The Comparison of MTT and CVS Assays for the Assessment of Anticancer Agent Interactions. PLoS One. 2016; 11(5):e0155772. doi:10.1371/journal.pone.0155772
16. Pizzino G, Irrera N, Cucinotta M, et al. Oxidative Stress: Harms and Benefits for Human Health. Oxid Med Cell Longev. 2017; 2017:8416763. doi:10.1155/2017/8416763
17. Yarana C, St Clair DK. Chemotherapy-Induced Tissue Injury: An Insight into the Role of Extracellular Vesicles-Mediated Oxidative Stress Responses. Antioxidants (Basel). 2017; 6(4)doi:10.3390/antiox6040075
18. Ray PD, Huang BW, Tsuji Y. Reactive oxygen species (ROS) homeostasis and redox regulation in cellular signaling. Cell Signal. 2012; 24(5):981-90. doi:10.1016/j.cellsig.2012.01.008
19. Ameziane-El-Hassani R, Dupuy C. Detection of Reactive Oxygen Species in Cells Undergoing Oncogene-Induced Senescence. Methods Mol Biol. 2017; 1534:139-145. doi:10.1007/978-1-4939-6670-7_13
20. Mergani A, Mansour AA, Askar T, et al. Glutathione S-Transferase Pi-Ile 105 Val Polymorphism and Susceptibility to T2DM in Population from Turabah Region of Saudi Arabia. Biochem Genet. 2016; 54(4):544-551. doi:10.1007/s10528-016-9740-2
21. Neefjes VM, Evelo CT, Baars LG, Blanco CE. Erythrocyte glutathione S transferase as a marker of oxidative stress at birth. Arch Dis Child Fetal Neonatal Ed. 1999; 81(2): F130-133. doi:10.1136/fn.81.2.f130
22. Mannervik B. The isoenzymes of glutathione transferase. Adv Enzymol Relat Areas Mol Biol. 1985; 57:357-417. doi:10.1002/9780470123034.ch5
23. Villeda-González JD, Gómez-Olivares JL, Baiza-Gutman LA, et al. Nicotinamide reduces inflammation and oxidative stress via the cholinergic system in fructose-induced metabolic syndrome in rats. Life Sci. 2020;250:117585. doi:10.1016/j.lfs.2020.117585
24. Duchnowicz P, Ziobro A, Rapacka E, Koter-Michalak M, Bukowska B. Changes in Cholinesterase Activity in Blood of Adolescent with Metabolic Syndrome after Supplementation with Extract from. Biomed Res Int. 2018; 2018:5670145. doi:10.1155/2018/5670145
25. ELLMAN GL, COURTNEY KD, ANDRES V, FEATHER-STONE RM. A new and rapid colorimetric determination of acetylcholinesterase activity. Biochem Pharmacol. 1961; 7:88-95. doi:10.1016/0006-2952(61)90145-9
26. Chen L, Deng H, Cui H, et al. Inflammatory responses and inflammation-associated diseases in organs. Oncotarget. 2018; 9(6):7204-7218. doi:10.18632/oncotarget.23208
27. Petersen AM, Pedersen BK. The anti-inflammatory effect of exercise. J Appl Physiol (1985). 2005; 98(4):1154-62. doi:10.1152/japplphysiol.00164.2004
28. Słomka A, Urban SK, Lukacs-Kornek V, Żekanowska E, Kornek M. Large Extracellular Vesicles: Have We Found the Holy Grail of Inflammation? Front Immunol. 2018; 9:2723. doi:10.3389/fimmu.2018.02723

29. Mendham AE, Donges CE, Liberts EA, Duffield R. Effects of mode and intensity on the acute exercise-induced IL-6 and CRP responses in a sedentary, overweight population. Eur J Appl Physiol. 2011; 111(6):1035-45. doi:10.1007/s00421-010-1724-z
30. Bradley JR. TNF-mediated inflammatory disease. J Pathol. 2008; 214(2):149-60. doi:10.1002/path.2287
31. Nieuwland R, Sturk A. Why do cells release vesicles? Thromb Res. 2010; 125 Suppl 1:S49-51. doi:10.1016/j.thromres.2010.01.037
32. Brandon-Warner E, Feilen NA, Culberson CR, et al. Processing of miR17-92 Cluster in Hepatic Stellate Cells Promotes Hepatic Fibrogenesis During Alcohol-Induced Injury. Alcohol Clin Exp Res. 2016; 40(7):1430-1442. doi:10.1111/acer.13116
33. Raji GR, Sruthi TV, Edatt L, Haritha K, Sharath Shankar S, Sameer Kumar VB. Horizontal transfer of miR-106a/b from cisplatin resistant hepatocarcinoma cells can alter the sensitivity of cervical cancer cells to cisplatin. Cell Signal. 2017; 38:146-158. doi:10.1016/j.cellsig.2017.07.005
34. Berardocco M, Radeghieri A, Busatto S, et al. RNA-seq reveals distinctive RNA profiles of small extracellular vesicles from different human liver cancer cell lines. Oncotarget. 2017; 8(47):82920-82939. doi:10.18632/oncotarget.20503
35. He M, Qin H, Poon TC, et al. Hepatocellular carcinoma-derived exosomes promote motility of immortalized hepatocyte through transfer of oncogenic proteins and RNAs. Carcinogenesis. 2015; 36(9):1008-1018. doi:10.1093/carcin/bgv081
36. Kapoor NR, Chadha R, Kumar S, Choedon T, Reddy VS, Kumar V. The HBx gene of hepatitis B virus can influence hepatic microenvironment via exosomes by transferring its mRNA and protein. Virus Res. 2017; 240:166-174. doi:10.1016/j.virusres.2017.08.009
37. Deregibus MC, Figliolini F, D'Antico S, et al. Charge-based precipitation of extracellular vesicles. Int J Mol Med. 2016; 38(5):1359-1366. doi:10.3892/ijmm.2016.2759
38. Povero D, Eguchi A, Niesman IR, et al. Lipid-induced toxicity stimulates hepatocytes to release angiogenic microparticles that require Vanin-1 for uptake by endothelial cells. Sci Signal. 2013; 6(296):ra88. doi:10.1126/scisignal.2004512
39. Takahashi K, Yan IK, Kogure T, Haga H, Patel T. Extracellular vesicle-mediated transfer of long non-coding RNA ROR modulates chemosensitivity in human hepatocellular cancer. FEBS Open Bio. 2014; 4:458-467. doi:10.1016/j.fob.2014.04.007
40. Chen L, Brigstock DR. Integrins and heparan sulfate proteoglycans on hepatic stellate cells (HSC) are novel receptors for HSC-derived exosomes. FEBS Lett. 2016; 590(23):4263-4274. doi:10.1002/1873-3468.12448
41. Cho YE, Im EJ, Moon PG, Mezey E, Song BJ, Baek MC. Increased liver-specific proteins in circulating extracellular vesicles as potential biomarkers for drug- and alcohol-induced liver injury. PLoS One. 2017; 12(2):e0172463. doi:10.1371/journal.pone.0172463

42. Chen L, Charrier A, Zhou Y, et al. Epigenetic regulation of connective tissue growth factor by MicroRNA-214 delivery in exosomes from mouse or human hepatic stellate cells. Hepatology. 2014; 59(3):1118-1129. doi:10.1002/hep.26768
43. Lambrecht J, Jan Poortmans P, Verhulst S, Reynaert H, Mannaerts I, van Grunsven LA. Circulating ECV-Associated miRNAs as Potential Clinical Biomarkers in Early Stage HBV and HCV Induced Liver Fibrosis. Front Pharmacol. 2017; 8:56. doi:10.3389/fphar.2017.00056
44. Lv LH, Wan YL, Lin Y, et al. Anticancer drugs cause release of exosomes with heat shock proteins from human hepatocellular carcinoma cells that elicit effective natural killer cell antitumor responses in vitro. J Biol Chem. 2012; 287(19):15874-15885. doi:10.1074/jbc.M112.340588

Research

Music and protocol

Kušej Gala Nina *
*nina.kusej@gmail.com

Abstract

The article Music and Protocol examines the role of music in protocol and its effect on the listener. It systematically sums up standard protocol occasions as well as standard music pieces that are being used during ceremonies. In connection with that, the Police Orchestra as the official protocol orchestra of the Republic of Slovenia is briefly presented. Furthermore, the article stresses state celebrations as the freest performative platform in terms of protocol music and - last but not least - in connection with that emphasizes the importance of the performative context on the listener's qualitative perception of music and ceremonies in general.

1. Introduction

Protocol by definition means a set of formal and social rules of interaction between official state representatives. Consequently protocol music presents the means of achieving these rules [1].

Music as a protocol element represents a notable part of a ceremonial, as it helps to frame it and has the ability to structurally dictate the course of action through sound and its form. At the same time, it has the power to emotionally impact the individual and in such way underline the true meaning of an individual protocol occasion or event.

Music has always had an important role in protocol as well as in diplomacy. The contextual area of using music in this way is extensive and includes a wide range of various protocol events, from strictly prescribed ceremonials (such as a reception of a foreign statesman during an official visit), to freer ceremonial forms (such as a state celebration) [2]. No matter the form, required for an individual event, a necessary constant of such music is its message and its effect on the listener, be it to strengthen national consciousness, glorify authority or something else connected with »protocol«. So it is about music as a protocol element, which is actually music in a specific function that fulfills its role to the fullest extent only when placed within an institution or context. The signal function of the military horn would not fulfill its actual role outside a military battle, just as a composition at a state celebration would not fulfill its actual function without the set design or visual framing, the right opportunity for a performance and an audience it can address.

2. Music as a key structural element of protocol events

Despite the fact that contemporary protocol of Central Europe is mostly modernized, simplified and minimized, the traditional foundations are still visible in the primary goals of the ceremonial, which remain largely, above all the element of music, consistently aimed at glorifying the state, raising the national consciousness and paying homage to foreign statesmen, while at the same time performing a signaling function (performance of an elegy by a wind instrument ensemble during a ceremonial wreath laying is for example a sign for the president of the republic to start walking behind the wreath bearers towards the memorial). Protocol remains the organizational foundation for the functioning of the state apparatus and managing the relations between individuals within this framing.

While the strict ceremonial preserves the use of traditional music forms (national anthems, marching songs), more contemporary ceremonials, such as various receptions and state celebrations, use a broad specter of musical and other means of expression as part of the contemporary language of diplomacy [2]. So this is a process of combining tradition, symbolizing national identity, with the contemporary, symbolizing the future. The above stated combination of elements as an efficient recipe to increase popular support can often be seen in diplomatic practices of various statesmen.

An interesting example of one such combination was the enthronement of the new Dutch king Willem-Alexander in 2013, which almost went awry at first glance, but in the end turned to his advantage. First the media [3] practically tore the official crowning to pieces as soon as

the lyrics were published, claiming that the lyrics are daft. Even the fact that this popular ballad was supposed to be carried out by some local celebrities did not help. A petition was also launched in the Netherlands as part of the general dislike of the song. After the inauguration ceremony the situation changed rapidly in favor of the new king, because he also went to the concert of the world famous and very popular Dutch DJ Armin van Buuren with the Royal Concertgebouw Orchestra with his wife and children [4]. Joining tradition (symbolized by the symphony orchestra) and popular music (in form of electronic music) turned out to be a great success, especially because it was supported with somewhat populist statements, which the king gave in his ceremonial speech after the inauguration, where he also talked about how he should be addressed: »I don't care, people can address me as they wish, as long as it makes them feel good.« [5].

The current President of the Republic of Slovenia Borut Pahor has been using similar principles lately, in general keeping the formal framing of the ceremonial, but "softening" and popularizing it when this is possible, often helping in this process himself. A popular rock band performed at the award ceremony for *Jabolko navdiha (The apple of inspiration)*[1], which was awarded to the drummer of the band Elvis Jackson Marko Soršak - Soki for his contribution to child music literacy. They were joint on stage by the president himself: "Pahor the all-rounder joined the band Big Foot Mama on stage and played the song *Nisem več s tabo* with them. He played the drums with drumsticks given to him by the drummer of the band Elvis Jackson, Marko Soršak - Soki.« [6].

The former US president Barack Obama went even one step further towards popularizing the protocol, as he gave an iPod to the Queen of the United Kingdom Elizabeth II (a political figure personifying tradition) as part of the traditional protocol act of exchanging gifts in 2009. On the iPod were photos of her visit to Washington and Virginia and also 40 popular Broadway songs, among them *The King and I*, *West Side Story* and *Dreamgirls* [6]. With this gesture he was innovative in combining a photo album (a normal gift for such occasions) and a standard music storage medium (CD) in a product of American technology that symbolizes looking to the future and patriotism.

3. Police orchestra of the Republic of Slovenia as the official protocol orchestra

The Slovene Police Orchestra was established in 1948 and has been active to this day under different names, political regimes and state regulations, performing in formal state circumstances. Since the independence of the Republic of Slovenia in 1991 it has also officially become the state protocol orchestra and has ever since had a significant role in Slovene State Protocol. After gaining its independence, Slovenia had to create the foundations of a new state protocol and thereby define the role and the repertoire of the protocol orchestra during ceremonial events [7].

Protocol events, which are based on an established ceremonial with the corresponding music forms, are mostly performed by the Police Orchestra. During such events the

[1] Jabolko navdiha is an award, given by the President of the Republic of Slovenia at a ceremonial, similar to a presidential commendation.

orchestra usually appears and performs together with the Guard of Honour of the Slovene Armed Forces. When united, the two formations are officially addressed as the Honorary Unit of the Republic of Slovenia [8].
Most standard in terms of the musical form and at the same time the most frequently performed musical pieces by the Police Orchestra are: anthems, marches, mourning songs and solo performances of trumpeters. These are being regularly used in standard protocol events such as: welcome receptions with military honours, inspections of the Guard of Honour, wreath laying ceremonies, receptions, etc [8].
State celebrations present a wider and above all more versatile field of creative performing options for the Police Orchestra, where the repertoire of the orchestra is not limited to the usual standard musical literature [2].

4. Music of state celebrations

At the more relaxed events, among which the cultural programs of state celebrations are the most expressive, there are basically only few (but important) restrictions – the principles of moderation, adequacy and appropriateness.
The latter (cultural parts of state celebrations) vary and are characterized by, among other factors, different producing and directing approaches to how the event is structured, which defines the role of music as a structural element of each individual celebration. This also defines the work of the music composer or author, as the concept of the celebration determines, if a certain composition or piece will be performed in the original or as an adaptation, and if the music is serving as the background or central element of the event. In any case the music at state celebration events can be comprehensively presented only in the context of the other structural elements, which applies not only to state celebrations, but to protocol music in general, which actually categorizes it as a musical genre [2].

5. The crucial meaning of the performative context for the protocol music genre

Considering the fact that music is »neutral« in its original form and something we all share, it gets its connotation only when performed with a specific background, having a role in various situations or becoming part of the collective memory. In an example from WWII, given by Jessica Gienow-Hecht [9], a decorated US pilot had supposedly refused to bomb a city, in which Beethoven was born and educated. In reference to music as a universal language, Kathleen M. Higgins [9] is of the opinion that we all, regardless our differences and the diversity of our music, sound human.
In the first place, protocol music needs to be performed in certain objective circumstances (location, music cast, etc.) for being able to impact the listener. Furthermore, the intensity of its message is substantially defined by the context in which it is being performed. The term context should be understood as a social, emotional or ambiental category which has the capacity to determine the quality of the musical experience.
A very indicative example of the stated theory can be a musical piece originally performed by an Oberkrainer musical band. The chosen musical example can reach into entirely different emotional range of the listener if it's being performed in the Oberkrainer context (typical

musical cast, instruments, outfit of the performers and environment) in comparison with a situation, in which just the music itself is being extracted and installed into an entirely different context, for example a state celebration. In such case, the originally »mocking« character of the musical piece transforms into something entirely different, perhaps even solemn and glamorous as the context of state celebrations actually is [2].

In certain cases, it is not the ceremonial that dictates the music, but the other way around, which means that certain music can become some sort of »parastatal protocol element« in certain circumstances. A picturesque example of the above is the Slovenian »local patriotic« song *Vstajenje Primorske*[2]. This composition is considered a sort of unofficial anthem among the people of the Primorska region and often evokes stronger emotions than the official national anthem, as the audience often stand up when it is played, place their right hand on their hearts and sing the lyrics in unison. As Felicity Laurence [9] states, music can be a strong instrument of propaganda. Primarily in such cases as the above mentioned composition, caution is needed so patriotism does not turn into nationalism, political incitement or a way of dividing people.

In the context of sports, which (this applies very much to Slovenia) can unify a nation, the danger of misuse for propaganda is slightly smaller. The song *Slovenija gre naprej*[3] for instance, became an informal anthem of the Slovenia national football team. The song still evokes feelings of unity and patriotism in its most positive form.

6. Conclusion

Music in the function of or as a protocol element represents one of the building blocks of an individual protocol event or ceremonial. It is music that cannot exist by itself and cannot fulfill its function by itself, but has its practical function and conveys a message only within the protocol framework. Therefore, its artistic value can only be discussed within its context. At the same time, it is music that is absolutely and inseparably tied to the event; it is subject to the event in a way and supports it. After all, fanfares cannot truly exist without a ruler and there in no real point in state celebration without an audience.

References

1. Kušej NG, Glasba kot protokolarni element, Protokol. 2016. Muzikološki zbornik. 2021; 53:267-268, http://bos.zrc-sazu.si/cgi/a03.exe?name=sskj_testa&expression=protokol&hs=1.
2. Kušej NG, Glasba kot protokolarni element. Master's degree thesis. Ljubljana, Filozofska fakulteta, Oddelek za muzikologijo, 2016.

[2] The song *»Vstajenje Primorske,«* was set to music and adapted by Rado Simoniti in 1968 for the celebration of the 25th anniversary of the general rebellion in the Primorska region at the fall of fascism.

[3] The song *»Slovenija gre naprej«* was written in 2000 by Zoran Predin, Peter Lovšin and Vlado Kreslin for the European football championship in Belgium and the Netherlands.

3. MMC RTV Slovenija. 2013a. »Foto: ‘‘Naj živi kralj!’’ Viljem Aleksander je ustoličen.« Accessed on 10 June 2021, https://www.rtvslo.si/svet/foto-naj-zivi-kralj-viljem-aleksander-je-ustolicen/307797.
4. A State of Trance. 2013. »King and Queen of The Netherlands surprise Armin van Buuren.« Accessed on 10 June 2021, http://www.astateoftrance.com/news/king-and-queen-of-the-netherlands-surprise-armin-van-buuren/.
5. 24ur.com. 2013. »Nizozemska kljub kritikam ostaja pri pesmi za ustoličenje kralja.« Accessed on 10 June 2021, http://www.24ur.com/ekskluziv/zanimivosti/nizozemska-kljub-kritikam-ostaja-pri-pesmi-za-ustolicenje-kralja.html.
6. MMC RTV Slovenija. 2015. »Foto: Koncert v predsedniški palači – za bobni pa Borut Pahor.« Accessed on 10 June 2021, http://www.rtvslo.si/zabava/druzabna-kronika/foto-koncert-v-predsedniski-palaci-za-bobni-pa-borut-pahor/362775.
7. Kolenc T, Od Godbe ljudske milice do protokolarnega orkestra: 50 let delovanja Policijskega orkestra. 1999, Ministrstvo za notranje zadeve, Urad za javno varnost, Ljubljana.
8. Kušej NG, Private archive of the amployee of the Protocol of the Republic of Slovenia.
9. Ahrendt R, Ferraguto M, Mahiet D, . 2014. »Introduction.« In Music and Diplomacy from the Early Modern Era to the Present, edited by Rebekah Ahrendt, Mark Ferraguto and Damien Mahiet, 1–16. New York: Palgrave Macmillan.

Research

The role of painting in the life and works of Fyodor Mikhailovich Dostoevsky

Prelovšek Anita*
*anita.prelovsek@gmail.com

Abstract
This article, as a contribution to the bicentenary of the birth of Fyodor Mikhailovich Dostoevsky, describes the way in which the art of painting was important for the writer's life, mentioning his favourite paintings and describing how they and the art of painting in general are reflected in his works. Especially during the years he spent abroad, Dostoevsky was a regular visitor to art galleries. In St Petersburg, he frequently went to the Ermitage and visited exhibitions of new works by Russian painters. He also published two articles containing his critical opinions about exhibitions he visited in Russia. In its last part, the article briefly quotes some modern examples of painting or drawing relating to the life and work of Dostoevsky.

---

1. Introduction

Dostoevsky admired all forms of art, included painting. He was a regular visitor to the Ermitage and attended the exhibitions of paintings organized every year in the Academy of Arts in St Petersburg, where he was informed about new works by the most important Russian painters. He expressed his opinions about exhibitions in two articles, published in his *Diary of a Writer*. During his stays abroad (1867-71), he was a keen patron of galleries in European cities such as Dresden, Basle, Florence, Venice and Bologna. He had his favourite painters and paintings which he never tired of seeing again and again. He retained the impressions that examples of the visual art made on him and used them to depict some of the characters, scenes, feelings and philosophical ideas in his novels and short stories. In some of his works he also makes explicit mention of certain paintings.

2. Dostoevsky's favourite paintings and their place in his works

2.1. Paradise on Earth

Coastal landscape with Acis and Galatea (**Figure 1**), a work by Claude Lorrain, a French painter of the baroque era, was for Dostoevsky a representation of a paradise on Earth. He was particularly fond of it, mentioning it three times in his works: in his novels *The Raw Youth* and *The Possessed (The Devils)* and also in *The Dream of a Ridiculous Man, a short story*.

The painting represents an episode from an ancient Greek mythological story used by Ovid in Metamorphoses. It tells the story of Galatea, a sea nymph (the first of the fifty Nereids), who refused the attentions of the cyclops Polyphemus and fell in love with Acis. When Polyphemus saw Galatea in the arms of Acis, he killed his rival with a rock, who after his death transformed himself into a river [1].

Claude Lorrain,[4] who spent much of his life in Italy, where he was inspired by its nature and art, was famous for painting landscapes and portraying mythological or biblical subjects. In this painting, he depicts an idyllic landscape on the seashore, where Acis and Galatea are enjoying their love. The beauty of nature surrounds the protagonists, who are hidden from the eyes of Polyphemus. On the right side of the painting, on one of the rocks above the shore, we can see the jealous Polyphemus playing on a flute. This is a typical romantic topic showing an idyllic landscape, where everything is in harmony, a pastoral scene par excellence, from which all troubles and the final catastrophe seem far removed.

[4] He was born under the name Claude Gellée, taking the pseudonym Claude Lorrain because of his being born in the Duchy of Lorraine [2].

Figure 1. Claude Lorrain: Coastal landscape with Acis and Galatea (1657) [3].

Dostoevsky named this painting »The Golden Age«. A hero from the novel *The Raw Youth,* Versilov, gives it this title and says he saw it in his dreams, though not as a painting but as a reality, the picture serving as a description of a paradise [4].
The same description of a Garden of Eden on Earth that appeared in *The Raw Youth* (1875) was originally intended to replace the chapter »At Tikhon's« that had been censored[5] out of a previous novel, *The Possessed (The Devils)* (1872).

»A corner of the Greek Archipelago; blue caressing waves, islands and rocks; fertile shore, a magic vista on the horizon, the appeal of the setting sun – no words could describe it. Here was the cradle of European man, here were the first scenes of the mythological world, here its green paradise. … Here had once lived a beautiful race. They rose and went to sleep happy

[5] In this chapter the hero, Stavrogin, confesses to the monk Tikhon the sin he has committed, abusing a vulnerable young girl. The chapter had been censored by Mikhail Katkov, editor of The Russian Messenger, where the novel was first published. In modern editions of *The Possessed (The Devils)* this chapter is usually included (as a Chapter 9 in the second part of the novel or as an appendix) [6]. It has also been published separately, as in the celebrated translation by S. S. Koteliansky and Virginia Woolf [5].

and innocent; they filled the woods with their joyful songs; the great abundance of their virgin powers went out into love and into simple happiness. The sun bathed these islands and sea in its beams, rejoicing in its beautiful children. Wonderful dream, splendid illusion! A dream the most incredible of all that had ever been dreamt, but upon it the whole of mankind has lavished all its powers throughout history; for this men have died on the cross and their prophets have been killed; without this, nations will not live and are unable even to die. I lived through all these feelings in my dream; I do not know what exactly I dreamt about, but the rocks, the sea, and the slanting rays of the setting sun – all these seemed to be still visible to me, when I woke and opened my eyes, fort he first time in my life, found them full of tears. A feeling of happiness, until then unfamiliar to me, went through my whole heart, even painfully. […]« [5].

A painting by Claude Lorrain also has the same function of depicting a paradise on Earth in the short story *The Dream of a Ridiculous Man* (1877):

I came to stand on this other earth, in the bright light of a sunny day, lovely as paradise. I was standing, it seems, on one of those islands which on our earth make up the Greek archipelago, or somewhere on the coast of the mainland adjacent to that archipelago. Oh, everything was exactly as with us, but seemed everywhere to radiate some festivity and a great, holy, and finally attained triumph. The gentle emerald se splashed softly against the shores and kissed them with love - plain, visible, almost conscious. Tall, beautiful trees stood in all the luxury of their flowering, and their numberless leaves, I was convinced, greeted me with their soft, gentle sound, as if uttering words of love. The grass glittered with bright, fragrant flowers. Flocks of birds flew about in the air and, fearless of me, landed on my shoulders and arms, joyfully beating me with their dear, fluttering wings. And finally I got to see and know the people of that happy earth. They came to me themselves, they surrounded me, kissed me. Children of the sun, children of their sun - oh, how beautiful they were! Never on earth have I seen such beauty in man. Maybe only in our children, in their first years, can one find a remote, though faint, glimmer of that beauty. The eyes of these happy people shone with clear brightness. Their faces radiated reason and a sort of consciousness fulfilled to the point of serenity, yet they were mirthful faces; a childlike joy sounded in the words and voices of these people. Oh, at once, with the first glance at their faces, I understood everything, everything! This was the earth undefiled by the fall, the people who lived on it had not sinned, they lived in the same paradise in which, according to the legends of all mankind, our fallen forefathers lived, with the only difference that the whole earth here was everywhere one and the same paradise. These people, laughing joyfully, crowded around me and caressed me; they took me with them and each of them wished to set me at ease. Oh, they didn't ask me about anything, but it seemed to me as if they already knew everything, and wished quickly to drive the torment from my face. [7].

2.2. The Ideal of Beauty

Dostoevsky felt very highly of the art of Raphael Sanzio and considered his *Sistine Madonna* (**Figure 2**) to be the best work of this renaissance master [8].

This vast oil painting (265 cm x 196 cm) represents Maria holding in her arms a baby Christ surrounded by St Barbara and St Sixtus. At the bottom of the painting there are two cherubs with wings [9]. Today these two cherubs are the most famous part of the painting, being represented on a range of souvenirs and objects. It was commissioned in 1512 by Pope Julius for the basilica of San Sisto in Piacenza, and in 1754, it was sold to a Polish king and taken to Dresden. During the Second World War, it was saved from the bombing of the city and removed to Moscow. Until 1955 it had been exposed in the Pushkin State Museum of Fine Arts and then returned to Dresden [10].

This picture became one of the most famous representations of the Madonna. Numerous European and Russian intellectuals and artists expressed their enthusiasm about it, among them Dostoevsky. In his novel *The Possessed (The Devils)* Dostoevsky named the Sistine Madonna *»Queen of Queens, that ideal of humanity«* [11]. As Dostoevsky's wife Anna Grigorevna writes in her memoirs, during their stay in Dresden they visited the gallery and Dostoevsky, of all of the exposition rooms, immediately took her to the one displaying the Sistine Madonna. This painting was for him »the highest manifestation of the human genius« and »he was able to stand in front of this picture for hours and hours, moved to tears« [8].[6] Dostoevsky's contemporaries testify that the writer loved this painting so much that a copy of it always hung above his bed in his apartment in St Petersburg [13].

[6] For example, in an article about this painting, the Russian poet Vasily Zhukovsky (1783-1852) mentions »a genius of pure beauty« [12].

Figure 2. Raphael: Sistine Madonna (1513-14) [9]

From September 1868 to May 1869, Dostoevsky and his wife spent nine months in Italy. First they settled for two months in Milan, where Dostoevsky was a keen admirer of the great cathedral [8]. Their next stop was Florence, where Dostoevsky had already been before. As Anna Grigorevna Dostoevskaya wrote, Dostoevsky had fond memories of this city, especially because of its artistic treasures. He was enthusiastic about the cathedral, the church of Santa Maria del Fiore and the baptistery with its famous Ghiberti door. As Anna Grigorevna writes, he couldn't take his eyes of it and was fond of saying that if he were to become rich, he would buy photos of those doors, even full-size, so that he could put them in the room where he worked, so he could enjoy looking at them [8]. In Florence, they were living near the Palazzo Pitti, which they visited more than once, so that they had an opportunity to see and admire another important Raphael Madonna, the *Madonna della Sedia*.[7]

[7] Maria sitting on a chair with the baby Christ and John the Baptist nearby. This circular-shaped oil painting (tondo), commissioned by an unknown person, had been the property of the Medici family [14].

Figure 3. Raphael: Madonna della Sedia (1513-14) [14]

In her memoirs, Dostoevsky's wife also mentions another Raphael painting, *Saint John the Baptist,* which they could see in the Uffizi gallery. She also mentions the marble statue of Venus de' Medici by the Greek sculptor Cleomenes, which Dostoevsky considered to be a »work of genius« [8]. In the Pinacoteca Nazionale in Bologna, Dostoevsky could finally see Raphael's *Saint Cecilia* (**Figure 4**), a reproduction of which he had seen before. According to his wife, he »glowed with pleasure« when he saw it.

The last stop on their Italian journey was Venice, where they spent several days, Dostoevsky admiring the church of St Mark and the Palazzo Ducale, enchanted by their architecture, mosaics and paintings [8].

Figure 4. Raphael: St Cecilia (1514-17) [15]

Figure 5. Cleomenes: Venus de' Medici (1st century B. C.) [16].

2.3. Death and Religion

Another very important painting in the life and works of Dostoevsky is *The Body of the Dead Christ in the Tomb* by Hans Holbein the Younger (**Figure 6**). Dostoevsky saw it in 1867, when on a journey from Baden-Baden to Geneva he and his wife made a one-day stop in Basle in order to see this painting in the museum of art there [7]. Dostoevsky had probably read about it in Nikolai Karamzin's *Letters of a Russian Traveller* [12] or, as his wife reported, somebody had told him about it [8] or maybe he had even seen a reproduction of it.

The painting made an extraordinary impression on Dostoevsky; he stood in front of it for a long time and became so upset that his wife was worried that he risked suffering an epileptic fit [8].[8]

Figure 6. Hans Holbein the Younger: The Body of the Dead Christ in the Tomb (1520-22) [18].

This painting played an important part in the novel *The Idiot.* Prince Myshkin mentions it for the first time in Chapter 5: *»When I was in Basle I saw a picture […] it struck me very forcibly.«* [19].

In the second part of the novel, in Chapter 4, at the home of Rogozhin, among other paintings of landscapes and portraits there is also a copy of Hans Holbein's The Death of Christ*: »Yes—that's a copy of a Holbein, said the prince, looking at it again, and a good copy, too, so far as I am able to judge. I saw the picture abroad, and could not forget it […]«* And then, because Christ's body is not beautified by the artist, the prince exclaims: *»Why, a man's faith might be ruined by looking at that picture!«* [20].

This tempera and oil on limewood painting is large (30.5 cm x 200 cm). The dead body is depicted very realistically; it has three wounds in its hand, feet and side, and the eyes and

[8]The French writer Stendhal (Marie-Henri Beyle) (1783-1842) described a kind of physical sensation provoked by the beauty of art, writing about it in his impressions of his travels in Italy (1816) entitled *Rome, Naples et Florence.* In the twentieth century this sensation became known as »Stendhal syndrome« [17].

mouth are open. Dostoevsky used this image of a dead body in *The House of the Dead* when describing the death of Mikhailov, a prisoner in a penitentiary hospital [21].

In *The Idiot* (Chapter 6 of the first part) mention is made of another famous painting, by Hans Holbein the Younger*, Darmstadt Madonna* (**Figure7**). Dostoevsky saw a copy of it in the Dresden gallery which was in his time more famous than the original, being what came to be called the Dresden Madonna, attributed to Bartholomäus Sarburgh and dated later, around 1635-37. At that time it was considered to be an original work by Hans Holbein the Younger [23].

»You too, Alexandra Ivanovna, have a very lovely face; but I think you may have some secret sorrow. Your heart is undoubtedly a kind, good one, but you are not merry. There is a certain suspicion of 'shadow' in your face, like in that of Holbein's Madonna in Dresden.« [19].

Figure 7. Hans Holbein the Younger: Darmstadt Madonna (1526-28) [22]

3. The Principle of »Painting« in Dostoevsky's Narrative Art

Realistic descriptions in Dostoevsky's literary works were not only based on recollections of real paintings that Dostoevsky saw in galleries. The writer was also capable of producing in his imagination such descriptions of the visible world as if he himself had painted a picture with the words in front of him. According to L. P. Grossman in his article »Poetics of Dostoevsky. Painting of Dostoevsky«, his representation of the world seen with our eyes is very rich and colourful in its literary creativity. He liked to observe and collect a variety of small things and to enjoy their diversity [24].[9]

[9] For example, in Semipalatinsk, where he was stationed when on military service and living in far from luxurious conditions, he collected old things like rings, coins, jewellery and tiny little objects made of different materials, demonstrating his passionate attraction to pleasant material things [24].

As Grossman says, in Dostoevsky's novels we can always sense this meticulous attention to »painterly« details in his description of everyday life and nature, but he represents them as consisting of »quick brush strokes«.

Grossman makes the point that representations of landscapes are few and far between in Dostoevsky's works. In his first novel, *Poor Folk,* he depicts impressions and memories of the landscape of the village of Chermashnya, where he spent his childhood. In his later works, the descriptions of landscapes became sparser, but there are some exceptions. One, for example, as Grossman suggests, is the view of a Siberian landscape in *The House of the Dead, or*, for instance, the beautiful romantic view of a waterfall described by prince Myshkin in *The Idiot* (in Chapter 5 of the first part), which resembles a painting [24]:

»*There was a waterfall near us, such a lovely thin streak of water, like a thread but white and moving. It fell from a great height, but it looked quite low, and it was half a mile away, though it did not seem fifty paces. I loved to listen to it at night, but it was then that I became so restless. Sometimes I went and climbed the mountain and stood there in the midst of the tall pines, all alone in the terrible silence, with our little village in the distance, and the sky so blue, and the sun so bright, and an old ruined castle on the mountain-side, far away. I used to watch the line where earth and sky met, and longed to go and seek there the key of all mysteries, thinking that I might find there a new life, perhaps some great city where life should be grander and richer—and then it struck me that life may be grand enough even in a prison.*« [19].

As Grossman also testifies, Dostoevsky pays much attention to the physical depiction of his heroes. The description of his last female heroine, Grushenka in *The Brothers Karamazov,* is long and in sharp contrast with other descriptions of people, where he preferred not to describe every little detail as in a photo. His descriptions reveal instantaneous impressions and »quick brush strokes«. Grossman also notes that Dostoevsky often uses a »Rembrandt effect«, meaning that scenes take place in the dim light of a candle [19].

Dostoevsky fully understood the basic principle of art as being a very accurate observation and contemplation of life. His feeling, as voiced through the mouth of Prince Myshkin in *The Idiot,* was: *»[…] I know nothing about painting. It seems to me one only has to look, and paint what one sees.«* [19].

4. Dostoevsky and Russian Painting. Criticism of pictures at exhibitions

Dostoevsky always made a great effort to keep abreast of new trends in Russian literature and art in general. At the exhibitions of paintings organized every year by the St Petersburg Art Academy, he was able to see new works by the leading Russian painters. He wrote and published two articles about these exhibitions in which he expressed his critical opinion about the works on display.

In the first such article, entitled A*cademy of Arts Exhibition for the year 1860-61* [25], he analyses the paintings of Valery Jacobi and Vasily Perov.[10] As he says at the outset, the picture that visitors liked the most of all at the exhibition was Jacobi's *The Prisoner's Rest* (**Figure 8**), for which the painter had been awarded the highest prize the Academy had to offer, a gold medal.

Figure 8. Valery I. Jacobi: The Prisoner's Rest (1861) [26]

Dostoevsky praises Jacobi's undoubted talent, emphasizing his realism as if we were seeing a scene in a photo or in a mirror, but possession of this skill alone is far from real art. Art demands »something else, bigger, larger, deeper« [25]. Similarly, as in the words of Prince Myshkin quoted above in *The Idiot,* Dostoevsky here too expresses his belief that a real artist »be it in a painting or in a story or in a musical piece, has to be seen personally; he reveals himself involuntarily, even if he doesn't want to, with all his opinions, his character and his

[10] Vasily Perov in 1872 painted the most famous portrait of Dostoevsky. Dostoevsky's wife Anna Grigorevna spoke highly of the painter, who came to their house every day for one week to see her husband's different facial expressions caused by his different emotional states. Anna Grigorevna called it »a moment of Dostoevsky's creating«. The portrait had been made in reply to a request by P. M. Tretyakov, the owner of the Moscow Tretyakov Gallery [8].

general mindset« [25]. Further, Dostoevsky criticises some of the details depicted, doing it with conviction and a knowledge of the subject that derive from his own personal experience. In parallel with a story by Pliny the Elder, in which a shoemaker criticized the shoes in a painting by the great painter of antiquity, Apelles, Dostoevsky gave reasons to justify his critical remarks. He reproaches the painter for having painted a ring on the hand of a deceased convict, then for having painted a thief stealing a ring; further, he claims that other convicts would never calmly watch from the sidelines taking in the interesting scene of an officer examining the dead man, adding that he painted shackles without leather pads under them. Who would know better than Dostoevsky that convicts cannot possess property, that a thief cannot steal a ring, because everyone else would like to steal such a treasure, that all convicts would gather round to watch an officer examining a dead man, and that shackles cannot be worn at all unless fitted with leather pads.

Similarly, writing about the exhibition in 1875, [27] he reproaches a painting by Nikolai Ge, *The Last Supper* (**Figure 9**)*,* which was due to be sent to the Vienna exhibition, for being too unrealistic, embodying the high gospel theme in the guise of genre painting. Christ should be presented not as an ordinary man, but as a God - just as on Orthodox icons [27]. [11]

Dostoevsky worries that in Vienna Russian painting would not be understood at all, even the beautiful emotional, typical Russian landscapes of Arkhip Kuindzhi (**Figure 10**), for example, being unlikely to strike a chord with the Germans.

[11] In his journalism and letters, Dostoevsky several times expressed his opinion on the art of icon painting. In 1880, in a letter to a collector of old icons, E. Opochinin, he stated very clearly that for him an icon is a mediator between man and God [13].

Figure 9. Nikolai Ge: Last Supper (1863) [28]

Figure 10. Arkhip Kuindzhi: On a Valaam Island (1873) [29]

In 1878, at the sixth exhibition of Russian realist painters – »Peredvizhniki« (»The Wanderers«) a painting by Ivan Kramskoj,[12] *The Contemplator* (**Figure 11**), was displayed. In *The Brothers Karamazov* (Chapter 6, entitled »Smerdyakov«, of the third book, first part) Dostoevsky uses this painting to describes Smerdyakov, (the illegitimate son of Fyodor Karamazov and lackey and assassin):

»The artist Kramskoy has one amazing painting which is called "Contemplator": it shows the forest in winter, and in the woods, on the road, in a ragged frock and straw shoes a lost man is standing absolutely by himself; he is standing there as if lost in thought, but he is not really thinking, he is "contemplating" something. If you could just push him, he would flinch and looked at you as if just woken up but not understanding anything.« [30].

Dostoevsky sees in him a type of man, frequently encountered, who only observes, it being impossible to guess what is hidden in the mind of this gloomy and pensive face. He could become a saint or commit something dreadful.

[12] Dostoevsky and Ivan Kramskoy (1837- 87) were friends and remained in contact for many years by correspondence [31].

Figure 11. Ivan Kramskoy: The Contemplator (1876) [30]

Dostoevsky was portrayed (**Figure 12**) by Vasily Perov - the author of genre paintings and psychological portraits of his famous contemporaries.

Figure 12. Vasily Perov: Portrait of F. M. Dostoevsky (1872) [32]

5. Dostoevsky's life and work in contemporary visual depictions

Dostoevsky was widely read throughout the world, and a particular example of the interest shown in him in many foreign couintries is to be found in Japan, where several Japanese adaptations of his works to the native Japanese culture were published, including some comic cartoons.

A Japanese comic publication, manga, was even created in 1953, based on Dostoevsky's *Crime and Punishment* (**Figure 13**). Its author was a Japanese so-called »Godfather of manga«, Osamu Tezuka (1928–89). In 2000, these comics were translated into Russian and exposed in the Dostoevsky's museum in St Petersburg [33].

Figure 13. Osamu Tezuka: Crime and Punishment (1953) [33]

Also in America there are a few comics based on *Crime and Punishment.* In one of them (from the year 2009) (**Figure 14**), Raskolnikov is transformed into Batman [34].

Figure 14. Dostoevsky Comics — Crime and Punishment (2009) Artist: Robert Sikoryak [34]

In February 2016, an unusual exhibition was set up in the Museum of Dostoevsky Literature in Omsk. The artists who painted the works on display, showing portraits of Dostoevsky and views of the old city of Omsk, were today's prisoners in Omsk, accused of serious crimes. The exhibitions also contained models of the buildings of the forced labour camp in which Dostoevsky was a prisoner from 1849 to 1853. This event, organized under a leitmotiv of the famous quote from Dostoevsky's *Idiot*: »Beauty will save the world« celebrated the 195th anniversary of Dostoevsky's birth and the three-hundredth anniversary of the founding of the city of Omsk [35].

References

1. Philibert, M. Dictionnaire des Mythologies. Manchecourt: Maxi – poche références. 2000.
2. Claude Lorrain. Internet source: https://en.wikipedia.org/wiki/Claude_Lorrain Accessed on 25 April 2021.
3. Landscape with Acis and Galatea. Internet source: https://commons.wikimedia.org/wiki/File:Claude_Lorrain_-_Landscape_with_Acis_and_Galatea_-_Google_Art_Project.jpg Accessed on 25 April 2021.
4. Dostoevsky, F. Izpoved mladega človeka. Ljubljana: DZS, 1979.
5. Dostoevsky, F. Translated by S. S. Koteliansky and Virginia Woolf. Stavrogin's Confession and The Plan of the Life of a Great Sinner. Hogarth press, Paradise Road, Richmond 1922.
6. Demons (Dostoevsky novel). Internet source: https://en.wikipedia.org/wiki/Demons_(Dostoevsky_novel) Accessed on 27 April 2021.
7. Dostoevsky, F. The Dream of a Ridiculous Man. A Fantastic Story. Internet source: http://www.holybooks.com/ Accessed on 18 April 2021.
8. Dostoevskaya, A. Življenje z genijem (Spomini). Kranj: Zelolepo, 2007.
9. Sistine Madonna. Internet source: https://en.wikipedia.org/wiki/Sistine_Madonna Accessed on 25 April 2021.
10. Sistine Madonna. Internet source: http://www.raphael-sanzio.com/sistine-madonna/ Accessed on 25 April 2021.
11. Dostoevsky, F. 1916. The Possessed (The Devils). Translation by Constance Garnett. Internet source: https://fb2bookfree.com/uploads/files/2020-06/1591542278_the-possessed-the-devils-by-fyodor-dostoyevsky.pdf Accessed on 22 April 2021.
12. Русский поэт Василий Жуковский о "Сикстинской Мадонне" Рафаэля 3 March 2018. Internet source: https://kinohit.mirtesen.ru/blog/43929257869/Russkiy-poet-Vasiliy-Zhukovskiy-o-Sikstinskoy-Madonne-Rafaelya Accessed on 25 April 2021.
13. Valchak, D. Д. Вальчак. «Сикстинская Мадонна», «Мертвый Христос» и икона Богоматери: Ф. М. Достоевский о религиозной живописи и иконописи Internet source: http://www.den-za-dnem.ru/page.php?article=2161 Accessed on 7 April 2021.
14. Madonna della sedia. Internet source: https://en.wikipedia.org/wiki/Madonna_della_seggiola Accessed on 25 April 2021.
15. The Ectasy of St. Cecilia (Raphael). Internet source: https://en.wikipedia.org/wiki/The_Ecstasy_of_St._Cecilia_(Raphael) Accessed on 25 April 2021.
16. Venere de' Medici. Internet source: https://www.uffizi.it/opere/venere-dei-medici Acessed on 25 April 2021.

17. Stendhal syndrom. Internet source: https://en.wikipedia.org/wiki/Stendhal_syndrome Accessed on 27 April 2021.
18. The Body of the Dead Christ in the Tomb. Internet source: https://en.wikipedia.org/wiki/The_Body_of_the_Dead_Christ_in_the_Tomb Accesed on 25 April 2021.
19. Dostoevsky, F. The Idiot. Freeditorial. Internet source: https://freeditorial.com/en/books/the-idiot--5 Accessed on 22 April 2021.
20. Dostoevsky, F. The Idiot. Internet source: http://www.gutenberg.org/files/2638/2638-h/2638-h.htm Accessed on 27 April 2021.
21. Dostoevsky, F. 1914. The House of the Dead or Prison Life in Siberia. Ernes Rhys Editor. Gutenberg EBook. Internet source: https://www.gutenberg.org/files/37536/37536-h/37536-h.htm#Page_194 25 September 2011. Accessed on 18 April 2021.
22. Darmstadt Madonna. Internet source: https://en.wikipedia.org/wiki/Darmstadt_Madonna Accessed on 1st May 2021.
23. Bader, L. Artists versus art historians? Conflicting interpretations in the Holbein controversy. Internet source: https://arthistoriography.files.wordpress.com/2018/11/bader.pdf Accessed on 1 May 2021.
24. Grossman, L. Гроссман Л. П.: Поэтика Достоевского. Живопись Достоевского. Internet source: http://dostoevskiy-lit.ru/dostoevskiy/kritika/grossman-poetika-dostoevskogo/grossman-poetika-dostoevskogo-zhivopis.htm Accessed on 7 April 2021.
25. Dostoevsky, F. Выставка в Академии художеств за 1860-61 год. Internet source: http://russian-literature.org/tom/410545 Т. 19. Статьи и заметки, 1861. Институт русской литературы (Пушкинский Дом) Российской Академии наук. Академические собрания сочинений. Электронная библиотека. Accessed on 18 April 2021.
26. Valery Jacobi. Internet source: https://en.wikipedia.org/wiki/Valery_Jacobi Accessed on 25 April 2021.
27. Dostoevsky, F. Translation: Borut Kraševec. Dnevnik pisatelja 2. Izbor publicističnih besedil. Ljubljana: Beletrina 2007.
28. Last Supper (Ge). Internet source: https://en.wikipedia.org/wiki/Last_Supper_(Ge) Accessed on: 30 April 2021.
29. Arkhip Kuindzhi. On a Valaam Island. Internet source: https://www.wikiart.org/en/arkhip-kuindzhi/on-a-valaam-island-1873 Accessed on 30 April 2021.
30. Ivan Kramskoy. Contemplator. Internet source: https://todiscoverrussia.com/ivan-kramskoy-contemplator/ Accessed on 1 May 2021.

31. Kulagina, A. Любимые картины Достоевского. Шедевры русской и мировой живописи в творчестве писателя. Internet source: https://diletant.media/articles/45257000/ 18 June 2019. Accessed on 1 May 2021.
32. Vasily Perov. Portrait of F. M. Dostoevsky. Internet source: https://en.wikipedia.org/wiki/File:Vasily_Perov_-_%D0%9F%D0%BE%D1%80%D1%82%D1%80%D0%B5%D1%82_%D0%A4.%D0%9C.%D0%94%D0%BE%D1%81%D1%82%D0%BE%D0%B5%D0%B2%D1%81%D0%BA%D0%BE%D0%B3%D0%BE_-_Google_Art_Project.jpg Accessed on 30 April 2021.
33. Японский комикс по "Преступлению и Наказанию" Достоевского. Internet source: https://zen.yandex.ru/media/id/5ab5e8628309055286b2abf1/iaponskii-komiks-po-prestupleniiu-i-nakazaniiu-dostoevskogo-5b915e0446f39d00aa6727a5 12 September 2018. Accessed on 1 May 2021.
34. Mani Jha, A. Raskolnikov rises: Batman makes everything better. Internet source: https://www.sundayguardianlive.com/books/387-raskolnikov-rises-batman-makes-everything-better 25 July 2015. Accessed on 1 May 2021.
35. ГТРК Омск. Омские заключенные воссоздали острог времен Достоевского. Internet source: https://www.youtube.com/watch?v=RHq8LGjQ2x0 10 February 2021. Accessed on 18 April 2021.

Reflection

The wanishing memory of the bourgeois world in Rožna dolina and Mirje districts in Ljubljana, Slovenia

Romolo Anna[1,*], Kralj-Iglič Veronika[1]

University of Ljubljana, Faculty of Health Sciences, Laboratory of Clinical Biophysics

*annaromolo@gmail.com

Abstract

The urbane ambient reflects historical, ethnological and social status of the inhabitants. Moreover, it exhibits the relation of those who plan the development, to the cultural heritage. Tradition presents the link of those who presently occupy the space with those who have lived in it before. Once destroyed, it can never be restored. Pieces of evidence indicate that the city of Ljubljana, Slovenia has hundreds years tradition, including the bourgeois lifestyle. Corresponding to the latter, in some districts of the city, villas embedded in gardens can be seen, of which some are still well preserved. However, others are being replaced by modern buildings which promote a different concept that is consistent with higher profit of the present owners. The aim of this contribution is to observe the present state of the villas in the district of Rožna dolina and Mirje, including those that are being subjected to decay and eradication.

1. Peak of the bourgeois life in Ljubljana in the 20.th century

At the beginning of 20th century, the majority of inhabitants of Slovenia were farmers and workers [1]. The bourgeois class was minor as regards number, however, it had a leading role in the society. It has developed from the urban society into a privileged group, which had an important impact on common matters. Besides outlining the values of work, money, education and family, this class has achieved courtesy in relationships and lifestyle that promoted well being, including all forms of culture.

Creation of an ambient is an important part of well being. The Carniola Construction Company (founded in 1873) started building houses for the rich in Ljubljana in 1889. These objects were constructed mostly in Vrtača, Prešernova cesta and Erjavčeva cesta [2] (**Figure 1**).

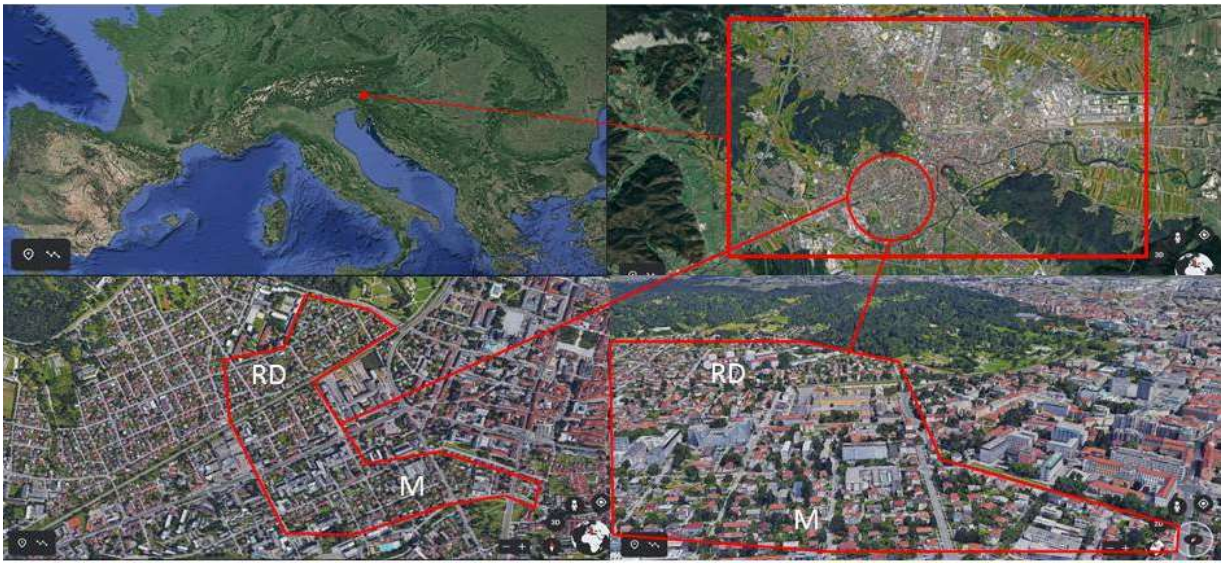

Figure 1. The position and the morphology of the city of Ljubljana, Slovenia. The marked areas refer to the district with bourgeois villas and gardens. RD: the district called "Rožna dolina", M: the district called "Mirje". The images were downloaded from Google Earth, June 23, 2021.

Construction was interrupted by the Ljubljana earthquake in 1995, but it continued, in particular with the support of Ivan Hribar who became the mayor of Ljubljana in 1896. Ivan Hribar was a polititian – a representative of Carniola within the Austro-Hungarian empire (Carniolan Provincial Deputy, Member of the Austrian National Assembly) and after the breakdown of the empire – the representative of Slovenia within the Monarchy Yugoslavia. He is known for his contribution to urban development, architectural and urban renovation, and introduction of many infrastructural innovations that meant an important step towards a modern provincial capital and construction of a large number of nationally important buildings. Also, he was involved in banking and investments.

Hribar was re-elected the mayor of Ljubljana several times before he was succeeded by Ivan Tavčar. Deep involvement in investments is hinted in the memories of Ivan Hribar [3]: "Dr. Tavčar acknowledges in the journal "Slovene nation" that someone has intervened at the Ministry of finance aiming at exclusion of certain Ljubljana Credit Bank officers from the

military service; he got the answer from the person in charge: “Die Hribarbank möge meinethalben ihre Bureaux schliesen.” Readers might have asked themselves why dr. Tavčar has published this article that regards Ljubljana Credit Bank since it is of little interest to the public. I think there could be many reasons such as to show a ridicule of the person in charge at the Ministry of Finance; that the board justifies to the public why dr. Tavčar was elected instead of me; that he himself shows the impact of war loans issued by banks; to strike me.” And then: “He (Tavčar) had transformed the Hribar Bank - where myself founding it he at the public meeting described as a sin - into dr. Tavčar Bank, as he made himself elected its president.”

Hribar considered the economic, urbanistic and infrastructure point of view of the development of the city of Ljubljana in which he involved the contribution of industrious rich people. In urbanistic and architecture planning he connected with Maks Fabiani and Josip Costaperaria [4,5]. Costaperaria studied architecture and art in Wienna. At first he collaborated with Maks Fabiani. He supervised the construction of the public building National House in Trieste designed by Fabiani in 1901-1904. Costaperaria designed a multifunctional public pallace called Ljubljanski dvor for merchant, business, social and residential activities and included also the cinema hall [6]. Besides being an architect of the mayor Hribar, he collaborated with the families von Pongratz and Auersperg. He was a member of the Rotary club Ljubljana, other societies and cultural circles. With his modernistic views he oposed the views of then acknowledged architect Jože Plečnik.

As reviewed in [7], the district of Rožna dolina was sparsely inhabited before the earthquake, but its development has accelerated within the reconstruction urbanization plan of Maks Fabiani after the earthquake and continued on. Luxorious houses for the rich were built and surrounded by large gardens. The bourgeois construction of the Rožna dolina was concentrated mainly in the northern part along the streets Cesta na Rožnik and Večna pot. In the green belt around the new city center, residential settlements were emerging. In Rožna dolina, in Mirje, between Poljanska and Streliška streets, in Kodeljevo and behind Bežigrad, most of the villas and larger single-family houses were built for wealthy citizens (**Figures 2-7**). The plots were subdivided with street nets, and the newly designed neighborhoods were mostly one-storey villas, modeled on the construction of single-family houses, outlined at the end of the 19th century by the Vienna Cottage Verein Society. They were covered with roofs of the prescribed slope with a predetermined layout on the land with landscaped gardens and shaped appearance of fences, which ran exactly along the building line and formed a closed street facade line. Thus, the appearance of the new neighborhoods was tidy and beautiful, regardless of the diverse artistic ideas expressed on the facades. In addition to the high quality of living, the value of the prestigious residential neighborhoods formed at that time was also the beauty of them [7].

Figure 2. Villas in Mirje district. The full yellow circles indicate the villas that were already demolished and replaced by apartment houses. The empty circles mark the objects that are intended for demolition. The images were downloaded from Google Earth, June 23, 2021.

Figure 3. Villas in Groharjeva ulica (Mirje district). A and B: No. 8 in Figure 2, D: No. 9 in Figure 2.

The majority of construction activity of the luxorious villas was still very conventional in style as the ideals of historicism were strongly rooted. The villas ressembled mansions with towers and balconies, facade ornaments or visible wooden frameworks. However, architect Josip Costaperaria has designed modernistic villas that became popular amindst the costumers as well as apartment buildings. The reconstruction plan of the "Vila Zlatica" [7]

which belonged to Ivan Hribar's daughter Zlatica includes detailed description of the object, of its historical and social background and of about 3000 m^2 garden which consisted of two parts divided by the stream. Boxwood, hedges of hornbeams, various shrubs such as currants and gooseberries, fruit trees, terracotta flowers - roses, imported from the Netherlands tulips and daffodils, wisteria, geraniums and dahlias were grown. They had so much fruit and berries that they also sold it (pears of various kinds, plums, apples, strawberries, currants, raspberries), as well as hay [7].

Figure 4. A: Villas in Mirje. B: Wiew from behind the Roman wall (No. 10 in Figure 2).

Figure 5. Villas in Mirje district. A,B,D,E: Teslova ulica (A,B: No.4, D: No.5, E: No.2 in Figure 2).

Figure 6. Villas in Mirje district (Jamova ulica) (Nos. 3, 6 and 7 in **Figure 2**).

2. Dawn of the bourgeois life in Ljubljana after WW II

Jealousy and hatred for the privileged ones have played an important role in features leading to WW I and II. As things have turned out in Yugoslavia which was at the time after WW 2 the official state at the territory of Ljubljana, bourgeoisie was not in favor of the party in power. The social middle class that originated from cities has been viewed as an idle class which owes its well being to the exploited workers and farmers. By the laws from 1946, all private enterprises have been nationalized [8]. In 1958, the Yugoslav state, established after World War II, launched the third nationalisation campaign for nationalization of construction land and residential and commercial buildings. The law indicated the compensation to the owners, but it was not always performed. Jewish capital in Slovenia was already subject to confiscation under German and Italian occupation in WW II, and this continued also after the war on the basis of proclaiming them enemies due to their German origin. The villa at Levstikova 31 was owned by Feliks and Klara Moskovič who were taken to the Auschwitz extermination camp where they and their daughter died [9]. Their son died as an Italian partisan [9]. The late Felix Moskovič was accused by the Yugoslav communist authorities of

collaborating with the Gestapo for which all his property was confiscated in 1946 [9]. The authorities also confiscated property of some Jews who, after the formation of the Jewish state in 1948, opted for Israel or they moved there. The confiscated villas (e.g. Ebenspanger, Mergenthaler, Pollak) were then occupied by the members of the new authorities [10].

Figure 7. Villas in Rožna dolina district (A: The Dukić villa).

In the post WW II time, the architectural work connected with bourgeoisie was marginalized and the work of architects (e.g. Costaperaria and some others) was not mentioned. It was only some years ago that this work has initiated to be presented [4,5], but has not yet been given a proper place in the tradition of the Slovene architecture. After the fall of the Yugoslavia and the change to democratic organization, the denationalization law had returned the property to the owners or to their heirs. However, many of the owners have already died or have lost their social and economic status and cannot restore it even today [11]. That is why each of these old houses and villas, with their former and increasingly rare

old inhabitants and together with house objects and gardens, have special testimonial and ethnological values, values regarding health and nature protection (high biological diversity, beneficial microclimate) and socio-economic value (contribution to the identity of the habitants and to the beauty and history of the city) [11].

3. The seeds of decline lie in economic laws

The Slovenian writer Ivan Mrak (1906-1986) who has thoroughly and ingeniously portrayed bourgeois life in Ljubljana in the first part of the 20. th century has described the decline of traditional values after the WW I due to economic reasons in his book Ivan O.; the chapter entitled: The world of new people [12]. The main character is describing his father, the "Roman", a wealthy innkeeper and a gentleman, facing the appearance of newly rich after the WW I:

"In the beginning of the world war my father has bought an oversized amount of wine. I think he invested his entire capital as much as it was available to him; he even indebted himself. As soon as it was heard that there is going to be a war with Italy, he hastily sold the whole supply for a quarter of the initial price. That was the first mortal blow to his property. After the war – due to inflation – the second blow.

In a moment, he was faced with the fact that he must start anew. The man lived honorably. The effort of his hands was blessed. And overnight, all those who were nothing just yesterday (he did not even return their flattery greetings – not that he looked down on them because they were poor – but because of their lowly ways) – all these have found themselves with lots of money. Now they have houses, properties. He knows what from. The folks know too, they whisper, but deeply greet the newly rich. He despises all that. He could have gained in similar ways if he wanted to, but he loathes such ways. These newly rich, war profiteers and second hand merchants sit around in his inn, course and present themselves with bloat. The ever-drunk Dolfe whose wife has been coming in rages to my mother for the soup, today owns a two-story house, a carriage and horses. My father does not shake hands with any of these. He despises their pomp and screaming wealth.

The sophisticated fabrics have all been taken by servant girls and footmen. Should he teach them the finery of vinery? Their throats are too rough. The vines that he holds in his cellar are too subtle for this nobility. Instead, cheap wines are gaining popularity in Ljubljana. He finds them rough and vulgar. But since they are cheap they can be bought in almost all restaurants and inns. Who would drink the ones from Štajerska which are too expensive? The newly rich have shown the conceited Roman his power and worth. For them wine is wine. They find no difference and they acknowledge none. Why would a man drink the expensive ones from Štajerska when the fashionable ones are so devilishly cheap?

The father is more and more tired every day. He retreats more and more to his chambers. He visits guests more and more seldom. He feels that the time has overturned. He bitterly finds that what subject to natural laws should be found at the bottom, has swam to the top.

That the money has overwhelmed everyone and that the idea that the man is for the money and not the other way around, has overcome everything."
Economical reasons seem timeless. The villas and the gardens are a potential source of profit, in this particular at the account of eradication of houses and gardens for building apartment houses which can occupy considerably larger area and attain considerably larger volumes than the original ones. Laws that pose bounds to the wish for profit allow considerable changes in the concept of building and lifestyle of the former districts of beauty and sophistication.
When the tradition is considered, there is a question whether it is better to conserve and restaurate or tear down and build new. There are multiple criteria to take into account:

- The condition of the building as regards its stability
- A possibility of tearing down a part of the building, complement it with a new part and integrate the parts
- If it is necessary to tear down the building, it could be thought how to construct the new building to fit into the existing ambient and its tradition
- Conservation of the original area of the building and of the garden
- Using the same material or parts of the building (e.g. decorations, fences) in restauration and the same colors

The planning could take into account the possibilities that the evidences from the past are conserved and not destroyed, as every building carries a message for the existing and future population. It is a part of the local history as well as of the architecture [13]. By treasuring good tradition and its conservation we express our relation to the wholistic approach to space and past and present residents.
However, some villas have already been demolished (marked with full yellow circles in **Figure 2**) or are intended to be (marked with empty yellow circles in **Figure 2** and shown in **Figure 3C**) [14]. Already being missed is a small but exquisite villa at Teslova 12 that was a property of the family Šantel: amindst them, the acknowledged painters Avgusta Šantel and her children Saša, Avgusta and Henrika. The villa was surrounded by a garden with distinguisged flowers, in particular roses that covered the whole façade, and various fruit trees.

References

1. Kejžar K, Družabno življenje ljubljanskih meščanov v prvi polovici 20. Stoletja kot vsebina pri pouku družbe, Thesis. University of Ljubljana, Pedagogical Faculty, Ljubljana, 2016
2. https://www.odprtehiseslovenije.org/fabianijeva-ljubljana-brezplacna-knjiga/
3. Ivan Hribar, Moji spomini II del. Slovenska matica 1984, pp. 247.
4. Zupančič B, Pozzetto M, Josip Costaperaria in ljubljansko moderno meščanstvo. KUD Polis, Ljubljana, 2004.
5. Zupančič B, Usode ljubljanskih stavb in ljudi, KUD Polis, Ljubljana 2007.

6. Josip Costaperaria. http://sokultura.si/wp/mesto-kultur/josip-costaperaria/
7. Klančar V, Konservatorski načrt Vile Zlatica, Mestna občina Ljubljana, Ljubljana, Slovenia.
8. https://www.kamra.si/mm-elementi/item/jugoslovanski-zakon-o-nacionalizaciji-iz-leta-1946.html
9. https://www.casnik.si/kaksna-je-resnicna-usoda-moskoviceve-vile/
10. Podbersič R, Mestna zaplembena komisija v Ljubljani plenila lastnino Judov, Časnik, maj 2017, https://www.casnik.si/aktualnim-polemikam-ob-rob/
11. Zorko I, Kruta usoda naselbinske dediščine prve polovice 20. Stoletja. Outsider, 2021, https://outsider.si/ira-zorko-kruta-usoda-naselbinske-dediscine-prve-polovice-20-stoletja/
12. Mrak I, Ivan O. Prešernova družba, 1991, pp:62-64.
13. Deu Ž, Odprta vrata: Stara vila – občutje udobja, varnosti in doma, http://www.deloindom.si/rustikalni/odprta-vrata-stara-vila-obcutje-udobja-varnosti-doma

Iglič A, Načrtno uničevanje slovenske meščanske stavbne dediščine v Ljubljani ter gradnja nadomestnih betonskih kocka- in kvadro-blokov, Demokracija, nov. 2020

Research

Postural sway on inclined surfaces

Rugelj Darja*

University of Ljubljana, Faculty of Health Sciences, Biomechanical Laboratory, Slovenia

*darja.rugelj@zf.uni-lj.si

Abstract

Professional and recreational activities are often performed on inclined surfaces, which can thus influence postural stability. The purpose of the present study was to evaluate the influence of three different surface inclinations (7, 13 and 19 degrees, toes up) on postural sway during quiet standing and to define the inclination that is already steep enough to influence postural stability. The group consisted of young healthy college students, 6 males and 15 females, with an average age of 22.5 (3.2) years. The average height and weight were 169.9 (9.5) cm and 62.6 (11.3) kg, respectively. Postural sway was measured using a force platform, and four postural variables were selected for analysis. The results show that the mean velocity of the center of pressure, its medio-lateral and antero-posterior path, and the sway area increased with the increase in the angle of inclination. There was a significant increase of the sway for the 19-degree toe up position for all sway variables evaluated ($p < 0.01$). These results suggest decreased postural stability when standing on an inclined surface, which is dependent on the angle of inclination of the surface and was greatest when participants approached the available passive range of their ankle joint motion. These results are of importance when considering the safety of individuals working on inclined surfaces.

1. Introduction

The work environment in a variety of occupations requires standing on inclined slopes. Typically roofers, lumbers and firefighters in mountainous regions. In an environment that is challenging for postural control, there is an increased risk of losing balance and possibly falling. Loss of balance has been reported to be the leading precipitating factor leading to a fall in the construction work environment [1]. Injuries are the second leading cause of lost work time in the 20-60 age group, which is the active working population (NIJZ).

In addition to work, people engage in various recreational activities that require maintaining balance on inclined surfaces. For example, a survey of the Slovenian population found that 14.6 per cent of people in the 20-65 age group hike and climb mountains in their leisure time [2]. Mountain climbing is also popular among individuals in advanced age groups [3]. The most common types of injuries among recreational hiking and mountaineering include sprains, strains and soft tissue injuries (28%), with ankle sprains being the most commonly reported type of injury (74%)[4]. Therefore, there is a need to investigate the postural stability issues associated with different slope inclinations and define the inclination that is already steep enough to affect postural stability and therefore poses a potential risk for loss of balance. When the support surface is very steep, such as 26 degrees, the kinematics of the whole body changes to adapt to the degree of inclination of the support surface [5] and alters postural stability. Available research reports focus on two directions of inclined surfaces: one experimental condition with toes up and the other with toes down [6,7]. Previous reports of postural sway on inclined surfaces investigated toe elevation in the range of 5 degrees [8], 8.5 degrees [7], 10 degrees [6], 14 degrees [9], 26 degrees [10], and up to 34 degrees [11].

Regardless of the angle of inclination of the support surface, the authors report its influence on postural response, including postural sway. During outdoor activities, the degree of inclination varies. Therefore, we decided to investigate the dependence of postural sway at four different surface inclinations. However, we wanted to exclude the contribution of knee flexion to postural sway because subjects tilt their bodies forward and flex their knees during standing or walking [12] on very steep surfaces, which changes body kinematics. Therefore, the surface inclinations were within the average available range of motion of ankle dorsiflexion. The aim of the present study was to investigate the influence of four different surface inclinations (0, 7, 13, 19 degrees, toes up) on postural sway and to define the smallest inclination that is already steep enough to influence postural stability. We hypothesized that the magnitude of the center of pressure (CoP) variation depends on the angle of the surface inclination and consequently on the degree of dorsiflexion in the ankle joint and the degree of stretching of the calf muscle.

2. Methods

2.1 Participants

Twenty-one healthy college students, with no known history of musculo-skeletal injury requiring medical treatment or a neurological history, participated in this study. The average age (± SD) of the participants was 22.5 (3.2) years. The average height and mass were 169.9 (9.5) cm and 62.6 (11.3) kg, respectively. The group consisted of 6 male and 15 female participants. The Slovenian National Medical Ethics Committee approved the study and participants provided written informed consent prior to participation.

2.2 Procedure

Each participant stood on a level surface and on three different surfaces with an inclination of 7, 13 and 19 degrees, all in toe-up orientation. The inclined surfaces were realized by wooden blocks on which the participants stood during the experiments (**Figure 1**). The wooden blocks were 40 cm wide and 30 cm long, and their height at the highest point ranged from 3.5 cm, 7 cm to 10.7 cm, thus forming inclined surfaces of 7, 13 and 19 degrees. Participants were instructed to stand as still as possible on the wooden blocks placed on the Kistler 9286 force platform AA (Kistler, Winthertur, Switzerland) with their feet together, arms at their sides, and facing a point marked on the wall approximately 3 m away. The first measurement was taken on level surface, followed by 7, 13 and 19 degrees of surface inclination. The last, control condition, took place again on the level surface. Thus, all participants were tested in five consecutive trials, each lasting 60 seconds. Between trials, there was a one-minute rest in a seated position. Data were collected at a sampling rate of 50 Hz. The raw data were further analyzed using a specially developed software [13].

Figure 1. Experimental set up for postural sway measurements on an inclined surface.

2.3 Calculation

Data analysis was performed using web-based software developed specifically for our stabilometric measurements [13]. Analysis of the stabilometric data began with smoothing the recorded CoP positions in the medio-lateral and antero-posterior directions using Gaussian averages over 3 adjacent points. Four sway parameters were chosen for this analysis: (1) medio-lateral (2) and antero-posterior path lengths, (3) mean velocity, and (4) the sway area. Test-retest reliability of the system was established for young and elderly persons [14].

2.4 Statistical analysis

The Statistical Package for Social Sciences (SPSS 26, SPSS Inc., Chicago, IL USA) was used for statistical analysis. For the stabilometric data, one-way ANOVA was calculated using LSD (Least significant difference) post hoc test. The significance level was set at $p < 0.05$.

3. Results

The descriptive values of the group average for the four selected postural sway variables at different inclinations are shown in **Table 1.** Four participants were unable to maintain their knees in an extended position while standing on a 19 degree slope, and all of their sway parameters deviated more than 1 and 2 standard deviations from the group average. Therefore, the results of these participants were excluded from the analysis of the 19-degree toe-off position. One-way repeated measures ANOVA for the selected sway parameters showed a significant effect of surface inclination on mean velocity ($F = 3.965$, $p = 0.005$), total medio-lateral path length ($F = 2.926$, $p = 0.025$), and total antero-posterior path length ($F = 3.505$, $p = 0.010$), while sway area did not differ significantly between the different surface inclinations ($F = 1.521$, $p = 0.202$). Post-hoc tests were calculated relative to the level ground standing and showed a significant difference between the level surface and the 19 degree inclination for mean velocity ($p = 0.002$), total medio-lateral path length ($p = 0.015$), total antero-posterior path length ($p = 0.002$), and sway area ($p = 0.025$).

Regression analysis showed a linear relationship between surface inclination and postural sway variables:CoP mean velocity increased by 0.014 cm/s per degree of inclination ($R^2 = 0.87$), antero-posterior path length increased by 0.38 cm per degree of inclination ($R^2 = 0.89$), medio-lateral path length increased by 0.51 cm per degree of inclination ($R^2 = 0.63$), and sway area increased by 0.08 cm2 per degree ($R^2 = 0.99$) (**Figure 2**).

Repeatability obtained by comparing the two no inclination conditions and an LSD post-hoc test showed no significant differences for all sway variables at p between $p = 0.652$ for sway area and $p = 1$ for medio-lateral sway.

Table 1. Average values and their standard deviations for the five variables calculated for all surface inclinations. The significant difference compared to the level ground condition is bolted ($p < 0.01$).

	Level	7 degrees toes-up	13 degrees toes-up	19 degrees toes-up	Control
Mean velocity (cm/s)	1.01 ± 0.21	1.02 ± 0.21	1.13 ± 0.28	**1.27 ± 0.29**	1.01 ± 0.22
ML path length(cm)	45.14 ± 9.51	46.16 ± 9.75	48.16 ± 9.21	**52.53 ± 8.70**	42.90 ± 8.53
AP path length (cm)	31.50 ± 8.23	41.34 ± 7.57	37.30 ± 15.38	**43.27 ± 14.76**	33.59 ± 9.94
Sway area (cm^2)	2.99 ± 1.71	3.64 ± 2.09	3.98 ± 2.45	**4.56 ± 2.52**	3.36 ± 1-76

ML medio-lateral, AP antero-posterior

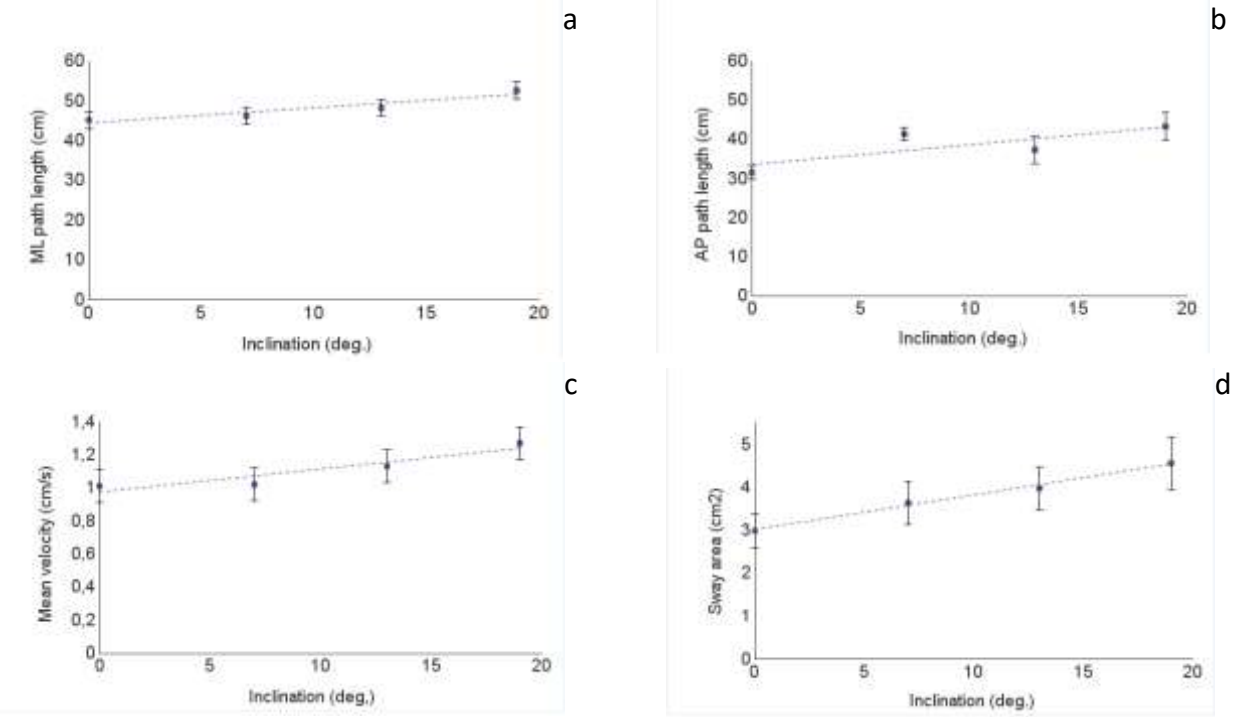

Figure 2. Medio-lateral (a) antero-posterior path length (b), mean velocity (c) and sway area (d) are plotted as a function of the inclination of the support surface.

4. Discusion

In the present study, the aim was to identify the toe-up inclination at which immediate increase of postural sway was observed. The inclined surface varied in angles from level to 7, 13, and 19 degrees toe-up. The results show a gradual increase in postural sway with statistically significant effect of inclination on postural sway at 19 degrees toe up. These results suggest that the degree of slope affects the magnitude of postural sway. In the present study, small slope inclinations (7 and 14 degrees) resulted in a non-significant increase of the CoP variables. These results are consistent with those of [9], where the response of CoP was measured at 14 degrees toe up and no effect on postural sway was found. Similar to our study, participants were also asked to keep their knees in an extended position. When participants stood at 26 [11] or 25 degrees toe up [15], an increase in medio-lateral sway was noted. Therefore, based on the current research and previous research, we can conclude that toe up at 20 degrees of tilt results in an increased amount of postural sway.

Our maximum inclination was chosen to require approximately the average passive range of motion (ROM) of dorsiflexion in the ankle joint, which is 20 degrees [16]. Interestingly, we found that even some young participants were unable to maintain their knees in an extended position while standing on a 19 degree toe contact patch, which is consistent with Soucie et al., (2011) [17] who later reported lower values of passive ROM (17.3 degrees for females and 16.3 degrees for males) for a group of young individuals. Therefore, four of our participants had to be excluded from the analysis of the 19-degree toe-off position because they were unable to maintain a straight knee position. The study results show that increasing the upward toe tilt towards the limits of the passive ROM of the ankle joint leads to increased postural sway. While lesser dorsiflexion did not result in a significant incerase of postural sway. A linear relationship was particularly pronounced for mean velocity of the CoP (R^2=0.99) and antero-posterior path length (R^2=0.89). Mean velocity is one of the most sensitive indicators of the multiple variables of postural sway [18,19] and is often used as the main variable in stabilometric measurements.

Changes in the length and tension of muscles, tendons, and other soft tissue extensions can temporarily alter proprioception, which may contribute to instability [20]. With prolonged standing on inclined surfaces, the proprioceptive system adapts, such that persons who rely primarily on proprioceptive afferent flow to establish their frame of reference tend to maintain the forward inclined position after returning to standing on a flat support surface [8]. Subjects exposed to 26 degrees of incline for up to 2 hours were unstable compared to standing on a flat surface [10]. Additionally, proprioceptive systems can be negatively affected by muscular fatigue due to the decrease in muscle function and decreased activation of muscular mechanoreceptors [21], as fatigued muscles are unable to produce and maintain the desired force output, and in addition, fatigue also negatively affects proprioceptive systems. Increased inclination alone significantly increased electromiographic activity in the tibialis anterior muscle [22]. However, ankle muscle fatigue could not be the

explanation for the present results, as the duration of exposure to the inclined surface was 60 seconds for each incline and a total of five minutes for each participant, with rest periods in between. However, in recreational walking or occupational activities on inclined surfaces, muscle fatigue may be induced by prolonged activities that are not necessarily of high intensity. Fatigue can be induced at intensities less than 15% of maximal voluntary contraction if the duration is sufficiently long (1 - 8 hours) [23]. With fatigue, the latency of a response may be increased, which can adversely affect both normal and reactive emergency control to a perturbation [24]. In addition, local ankle muscle fatigue is known to result in a significant increase in antero-posterior sway and mean velocity [25].
Challenging environments such as rooftops, working on sloping terrain on hillsides such as firefighters, loggers, mountain climbers, or recreational hikers walking on inclined and uneven trails increase the risk of balance loss and potential injury. During the above activities, the slope of the support surface can vary from slightly steep to very steep, resulting in variable foot and ankle flexion position and muscle activity requirements. The slope of the supporting surface of more than 20 degrees seems to be the one at which postural stability decreases significantly. In addition to the slope of the hill, it is reasonable to expect the combined effect on postural stability of different surface slopes along with the effect of the additional load in the form of professional equipment or a backpack, which can reach up to 29% of body weight [5]. The contribution of additional load carried on the back showed a linear increase in postural instability when carrying a backpack with 12, 21 and 30 kg load [26]. Carrying an external load potentially increases the risk of falling, regardless of age, physical fitness, or the purpose of carrying the load, be it duty or leisure.

The limitation of the present study is a relatively small number of participants and a non-randomized order of trials with gradual increase in slope. However, the control measurement as the final measurement confirms that the change in the magnitude of postural sway is a result of the different slopes. Further research is needed to combine the three risk factors for postural destabilization: surface slope, added load, and age.
In conclusion results show the increase in postural sway when participants stood on three progressively inclined surfaces. The increase was observed at all inclinations, with postural sway increasing the most when participants stood near the available passive range of motion at the ankle. These results are of importance when considering the safety of individuals working on inclined surfaces or recreational hikers of various ages.

Acknowledgements
Authors acknowledge support of ARRS, grant P3-0388.

References

1. Wade C, Davis J, Weimar WH, Balance and exposure to an elevated sloped surface. Gait Posture. 2014; 39(1):599-605. doi: 10.1016/j.gaitpost.2013.09.017
2. Pori M, Sila B, S katerimi športnorekreativnimi dejavbnostmi se Slovenci najraje ukvarjamo? Šport. 2010; LVII (1-2):105-107.
3. Pori M, Pori P, Sila B, Ali starost vpliva na izbor najbolj priljubljenih športnih rekreativnih dejavnosti? Šport. 2010, LVII (1-2), 112-114.
4. Lobb B, Load carriage for fun. Appl Erg. 2004; 35:541-547. doi: 10.1016/j.apergo.2004.06.006
5. Dutt-Mazumder A, Challis J, Newell K, Maintenance of postural stability as a function of tilted base of support. Human Movement Science. 2016; 48: 91-101. doi:10.1016/j.humov.2016.04.010
6. Sasagawa S, Ushiyama J, Masani K, Kouzaki M, Kanehisa H, (). Balance control under different passive contributions of the ankle extensiors: quiet standing on inclined surfaces. Exp Brain Res, 2009; 196:537-544. doi:10.1007/s00221-009-1876-4
7. Garkavenko W, Gorkovenko AV, Kolosova EV, Korneyev VV, Melnichouk AV, Vasilenko DA, Modification of stabilogram during upright standing posture under conditions of inclines of the supporting surface. Neurophysiol. 2012; 44:132-137. doi: 10.1007/s11062-012-9279-8
8. Kluzik JO, Horak FB, Peterka RJ, Differences in preffered reference frames for postural orientation shown by after-effects of stance on an inclined surface. Exp Brain Res. 2005; 162:474-489. doi:10.1007/s00221-004-2124-6
9. Mezzarane RA, Kohn AF, Control of upright stance over inclined surface. Experimental Brain Research. 2007; 180:377-388. doi: 10.1007/s00221-007-0865-8
10. Wade C, Davis J, Postural sway following prolonged exposure to an inclined surface. Saf Sci. 2009; 47:652-568. doi:10.1016/j.ssci.2008.09.002
11. Simeonov P, Hsiao H, Hendricks S, Effectiveness of vertical reference for reducing postural instability on inclined and compliant surfaces at elevation. Applied Ergonomics. 2009; 40:353-361. doi:10.1016/j.apergo.2008.11.007
12. Leroux A, Fung J, Barbeau H, Postural adaptation to walking on inclined surfaces: I. Normal strategies. Gait Posture. 2002; 15:64-74. doi:10.1016/s0966-6362(01)00181-3
13. Sevšek F, Rugelj D. StabDat V 3.0. Faculty of health sciences, Ljubljana. 2020. http://manus.zf.uni-lj.si/stabdat
14. Rugelj D, Hrastnik A, Sevšek F, Vauhnik R, Reliability of modified sensory interaction test as measured with force platform. Med Biol Eng Comput. 2015; 53(6):525–534. doi: 10.1007/s11517-015-1259-x
15. King AC, Patton J, Dutt-Mazumder A, Newell KM, Center-of-pressure dynamics of upright standing as a function of sloped surfaces and vision. Neurosc Letters. 2020; 737:135334. doi: 10.1016/j.neulet.2020.135334

16. Palmer ML, Epler ME, Clinical Assessment Procedures in Physical Therapy. New York Philadelphia, J.B. Lippincont Co. 1990.
17. Soucie JM, Wang C, Forstyh A, Funk S, Denny M, Roach KE, Range of motion measurements: reference values and a database for comparison studies. Haemophilia. 2011; 17:500-507. doi:10.1111/j.1365-2516.2010.02399.x
18. Raymakers JA, Samson MM, Verhaar HJJ, The assessment of body sway and the choice of the stability parameter(s). Gait Posture. 2005; 21:48-58. doi: 10.1016/j.gaitpost.2003.11.006
19. Doyle TLA. Dugan EL, Humphries B, Newton RU, Discriminating between elderly and young using fractal dimension analysis of centre of pressure. Int J Med Sci. 2004; 1(1): 11-20. doi:10.7150/ijms.1.11
20. Breloff SP, Wade C, Waddell DE, Lower extremity kinematics of cross-slope roof walking. Appl Erg. 2019; 75:134-142. doi: 10.1016/j.apergo.2018.09.013
21. Vuillerme N, Forestier N, Nougier V, Attentional demands and postural sway: the effect on the calf muscles fatigue. Med Scie Sports Exercise. 2002; 169(2):1907-1912. doi: 10.1097/00005768-200212000-00008
22. Lu ML, Kincl L , Lowe B, Succop P, Bhattacharya A, Muscular activity of lower limb muscles associated with working on inclined surfaces. Ergonomics. 2015; 58:278-290. doi:10.1080/00140139.2014.968634
23. Davidson BS, Madigan ML, Nussbaum MA, Effects of lumbar fatigue rate on postural sway. Eur J Appl Physiol. 2004; 93:183-189. doi:10.1007/s00421-004-1195-1
24. Johnston RB, Howard ME, Cawley PW, Losse GM, Effect of lower extremity muscular fatigue on motor control performance. Med Sci Sport Exercise. 1998; 30(12):1703-1707. doi:10.1097/00005768-199812000-00008
25. Gimmon Y, Riemer R, Oddsson L, Melzer I, The effect of plantar flexor muscle fatigue on postural control. J Electromyog Kinesiol. 2011; 21(6):922-928. doi: 10.1016/j.jelekin.2011.08.005
26. Rugelj D, Sevšek F, The effect of load mass and its placement on postural sway. Applied Ergonomics. 2011; 42(6):860-866. doi:10.1016/j.apergo.2011.02.002